ISSN 2307-8960 (online)

World Journal of *Clinical Cases*

World J Clin Cases 2019 May 26; 7(10): 1093-1241

Published by Baishideng Publishing Group Inc

World Journal of Clinical Cases

Contents

Semimonthly Volume 7 Number 10 May 26, 2019

ORIGINAL ARTICLE

Retrospective Cohort Study

Retrospective Study

Observational Study

CASE REPORT

Contents

World Journal of Clinical Cases

Volume 7 Number 10 May 26, 2019

World Journal of Clinical Cases
Volume 7 Number 10 May 26, 2019

Contents

NAME OF JOURNAL
World Journal of Clinical Cases

ISSN
ISSN 2307-8960 (online)

LAUNCH DATE
April 16, 2013

FREQUENCY
Semimonthly

EDITORS-IN-CHIEF
Dennis A Bloomfield, Sandro Vento

EDITORIAL BOARD MEMBERS
https://www.wjgnet.com/2307-8960/editorialboard.htm

EDITORIAL OFFICE
Jin-Lei Wang, Director

PUBLICATION DATE
May 26, 2019

INSTRUCTIONS TO AUTHORS
https://www.wjgnet.com/bpg/gerinfo/204

GUIDELINES FOR ETHICS DOCUMENTS
https://www.wjgnet.com/bpg/GerInfo/287

GUIDELINES FOR NON-NATIVE SPEAKERS OF ENGLISH
https://www.wjgnet.com/bpg/gerinfo/240

PUBLICATION MISCONDUCT
https://www.wjgnet.com/bpg/gerinfo/208

ARTICLE PROCESSING CHARGE
https://www.wjgnet.com/bpg/gerinfo/242

STEPS FOR SUBMITTING MANUSCRIPTS
https://www.wjgnet.com/bpg/GerInfo/239

ONLINE SUBMISSION
https://www.f6publishing.com

World Journal of Clinical Cases

Submit a Manuscript: https://www.f6publishing.com

World J Clin Cases 2019 May 26; 7(10): 1093-1102

DOI: 10.12998/wjcc.v7.i10.1093

ISSN 2307-8960 (online)

ORIGINAL ARTICLE

Retrospective Cohort Study

Impact of perioperative transfusion in patients undergoing resection of colorectal cancer liver metastases: A population-based study

Bo Long, Zhen-Nan Xiao, Li-Hua Shang, Bo-Yan Pan, Jun Chai

ORCID number: Bo Long (0000-0002-4659-1948); Zhen-Nan Xiao (0000-0001-6752-9791); Li-Hua Shang (0000-0003-1833-3762); Bo-Yan Pan (0000-0001-9016-5551); Jun Chai (0000-0002-0833-9127).

Author contributions: Long B conceptualized and designed the study, analyzed and interpreted the data, drafted the manuscript, and approved the final manuscript; Xiao ZN acquired the data, drafted the manuscript, and approved the manuscript; Shang LH collected the data, performed statistical analysis, and approved the manuscript; Pan BY acquired the data, guaranteed the integrity of the entire study, revised the study, and approved the final manuscript; Chai J conceptualized and designed the study, analyzed and interpreted the data, and approved the final manuscript.

Conflict-of-interest statement: The authors disclose no conflicts of interests.

Bo Long, Zhen-Nan Xiao, Li-Hua Shang, Bo-Yan Pan, Jun Chai, Department of Anesthesiology, Shengjing Hospital, China Medical University, Shenyang 110004, Liaoning Province, China

Bo-Yan Pan, Department of Anesthesiology, Shenyang Women's and Children's Hospital, Shenyang 110011, Liaoning Province, China

Corresponding author: Jun Chai, MD, PhD, Department of Anesthesiology, Shengjing Hospital, China Medical University, No. 36, Sanhao Street, Shenyang 110004, Liaoning Province, China. chaij@sj-hospital.org
Telephone: +86-24-23892617
Fax: +86-24-23892617

Abstract

BACKGROUND

Perioperative allogeneic blood transfusion is associated with poorer outcomes.

AIM

To identify the factors that were associated with perioperative transfusion and to examine the impact of perioperative transfusion in patients undergoing resection of colorectal cancer (CRC) liver metastases.

METHODS

The United States National Inpatient Sample (NIS) database was searched for patients with CRC who received surgery for liver metastasis. Linear and logistic regression analyses were performed.

RESULTS

A total of 2018 patients were included, and 480 had a perioperative transfusion. Emergency admission (adjusted odds ratio [aOR] = 1.42; 95%CI: 1.07-1.87), hepatic lobectomy (aOR = 1.76; 95%CI: 1.42-2.19), and chronic anemia (aOR = 2.62; 95%CI: 2.04-3.35) were associated with increased chances of receiving a transfusion, but receiving surgery at a teaching hospital (aOR = 0.75; 95%CI: 0.58-0.98) was associated with a decreased chance of receiving a transfusion. Receiving a perioperative transfusion was significantly associated with increased in-hospital mortality (aOR = 3.38; 95%CI: 1.57-7.25), and increased overall postoperative complications (aOR = 1.67; 95%CI: 1.31-2.13), as well as longer length of hospital stay

CONCLUSION

Patients with an emergency admission, hepatic lobectomy, chronic anemia, and who have surgery at a non-teaching hospital are more likely to receive a

Manuscript source: Invited manuscript

Received: February 3, 2019
Peer-review started: February 6, 2019
First decision: March 5, 2019
Revised: March 24, 2019
Accepted: May 1, 2019
Article in press: May 1, 2019
Published online: May 26, 2019

P-Reviewer: Bang YJ, Saner F
S-Editor: Ma YJ
L-Editor: Wang TQ
E-Editor: Wu YXJ

perioperative transfusion. Patients with CRC undergoing surgery for hepatic metastases who receive a perioperative transfusion are at a higher risk of in-hospital mortality, postoperative complications, and longer length of hospital stay.

Key words: Colorectal cancer; Liver metastasis; Perioperative blood transfusion; Intraoperative blood loss; National inpatient sample

Core tip: Among patients undergoing resection of colorectal cancer liver metastases, those with an emergency admission, hepatic lobectomy, chronic anemia, and undergoing surgery at a non-teaching hospital are more likely to receive a perioperative transfusion. Furthermore, patients who receive a perioperative transfusion are at a higher risk of in-hospital mortality, postoperative complications, and longer length of hospital stay.

Citation: Long B, Xiao ZN, Shang LH, Pan BY, Chai J. Impact of perioperative transfusion in patients undergoing resection of colorectal cancer liver metastases: A population-based study. *World J Clin Cases* 2019; 7(10): 1093-1102
URL: https://www.wjgnet.com/2307-8960/full/v7/i10/1093.htm
DOI: https://dx.doi.org/10.12998/wjcc.v7.i10.1093

INTRODUCTION

The use of allogeneic blood transfusion during surgery has improved outcomes and saved countless lives. However, blood transfusion is not without risk. Risks of a blood transfusion include allergic reactions, infectious diseases, acute or delayed hemolytic reaction, and transfusion-related immune modulation (TRIM)[1]. Furthermore, studies have linked perioperative allogeneic blood transfusions with poorer outcomes such as increased postoperative complications and mortality[2,3].

Patients with malignancies undergoing surgery are frequently anemic or the anticipated blood loss during surgery may be large, and as such the transfusion threshold is relatively low. However, a number of studies have shown that a perioperative transfusion is associated with poorer oncological outcomes, such as cancer recurrence[4-8]. While the pathophysiological mechanism is not entirely clear, it is thought to be related to an altered immune response as a result of TRIM which changes the body' surveillance for malignant cells.[3]

Colorectal cancer (CRC) is potentially curative by surgery. Patients with a metastatic disease confined to the liver also have the potential for a curative surgery such as hepatic lobectomy or hepatic metastectomy[6]. However, these patients are at an increased risk for a perioperative transfusion, and thus the effect of a transfusion on surgical and oncological outcomes is an area of study. A number of studies have indicated that patients with CRC undergoing colon resection and/or surgical treatment of liver metastasis who receive a perioperative allogeneic transfusion have increased mortality, reduced overall survival, reduced disease free survival, more postoperative complications, and longer length of hospital stay[4,9-12]. Studies, however, have not been consistent in all of their findings.

Thus, the purpose of this study was to use a United States nationwide population-based database to identify factors associated with transfusing blood, and to examine the impact of perioperative transfusion in patients undergoing resection of CRC liver metastases. Analysis of the impact of perioperative transfusion in this population may help to assess the significance of appropriate blood management measures and transfusion avoidance strategies.

MATERIALS AND METHODS

Data source

Data for this population-based study were extracted from the United States Nationwide Inpatient Sample (NIS) database. The NIS was developed as part of the United States Healthcare Cost and Utilization Project (HCUP), which is sponsored by

the Agency for Healthcare Research and Quality. The NIS represents a 20% sample of inpatient admissions from the 45 states that participate in the program. The NIS database contains over 100 clinical and nonclinical data elements from approximately 8 million hospital stays each year. Data available include primary and secondary diagnoses, primary and secondary procedures, admission and discharge status, patient demographic information, expected payment source, length of hospital stay, and hospital characteristics. The present study did not require either Institutional Review Board approval or informed consent by the study subjects because the NIS data are de-identified. We obtained permission to access the research data files of the HCUP program (certificate number, HCUP- 1M44EVV39), and the data use agreement for the NIS from the HCUP Project was followed.

Study population and definitions

We first identified patients in the 2005 to 2014 NIS database who had a partial hepatectomy (ICD-9: 50.22) and/or hepatic lobectomy (ICD-9: 50.3). From this population, we identified patients with liver metastases (ICD-9: 197) from CRC (ICD-9: 153; 154.1, 154.8).

Patients with a history of blood transfusion (V58.2) or coagulopathy (CM_COAG) were excluded. Finally, the eligible patients were divided into two groups: those who received a perioperative transfusion (ICD-9: 99.0) and those who did not.

Dependent variables

Length of hospital stay (LOS) was defined using (LOS_X), and in-hospital mortality was defined using (DIED). In addition, patients with one of the following postoperative complications were recognized as positive with respect to overall postoperative complications: infection (ICD-9: 998.59); intra-abdominal abscess (ICD-9: 567.22); infected post-operative seroma (ICD-9: 998.51); wound dehiscence (ICD-9: 998.31, 998.32); urinary tract infection (UTI) (ICD-9: 595.0, 996.64, 997.5); pulmonary complications, including pulmonary embolus and pneumonia (ICD-9: 415.11, 997.31, 997.32, 997.39); deep vein thrombosis (DVT) (ICD-9: 451.11, 451.19, 451.2, 451.81, 451.82, 451.83, 451.84, 451.89, 451.9, 453.4, 453.41, 453.42, 997.2); postoperative myocardial infarction (ICD-9: 997.1, 410.0-410.9, 998.0); sepsis (ICD-9: 995.91); ascites (ICD-9: 789.5); acute liver failure (ICD-9: 570); and other digestive system complications (ICD-9: 997.49).

Independent variables

Patient demographic characteristics (age, sex, and race) and data of income status, type of admission, insurance status, hospital bed size, hospital location, hospital teaching status, and hospital region were collected from the NIS database. The following potential confounding variables were also examined with data extracted for the NIS database: hepatic precondition, primary tumor site, extent of liver resection, laparoscopic procedure, robotic-assisted procedure, and comorbidities (chronic anemia, congestive heart failure, chronic pulmonary disease, diabetes, hypertension, obesity, and renal failure). The definition of comorbidities used in this study was based on the NIS database. Variables CM_ANEMDEF and CM_BLDLOSS were used for chronic anemia. Variables CM_CHF and CM_CHRNLUNG were used for congestive heart failure and chronic pulmonary disease, respectively. Variables CM_DM and CM_DMCX were used for diabetes. Variable CM_HTN_C was used for hypertension. CM_OBESE and CM_RENLFAIL were used for obesity and renal failure, respectively.

Statistical analysis

Statistical review of the present study was performed by a biomedical statistician. Descriptive statistics were used to present patient demographic and clinical characteristics and hospital data, and are presented as unweighted counts and weighted percentages. Data were weighted according to recommendations from the Healthcare Cost and Utilization Project (HCUP), using three variables for weights (DISCWT), stratum (NIS_STRATUM), and cluster (HOSPID) to produce national estimates. Chi-square tests were performed to examine associations between characteristics and perioperative transfusion. To illustrate that patients who received a perioperative transfusion would have a greater risk of mortality and postoperative complications, and longer length of stay as reported in other studies[10], we estimated the association between perioperative transfusion and mortality, postoperative complications, and length of stay by linear regression and logistic regression. Significant findings in baseline demographic, clinical, and hospital characteristics were selected and input into multivariate models. Finally, univariate and multivariate logistic regressions were performed to examine associations between perioperative transfusion and clinical outcomes and comorbidities with adjustment for

demographic characteristics and hospital characteristics. Two-sided *P*-values < 0.05 were considered statistically significant. All statistical analyses were performed with SAS version 9.4 (Windows NT version, SAS Institute, Inc., Cary, NC, United States).

RESULTS

Study population

A total of 27269 patients who had a partial hepatectomy and/or hepatic lobectomy were initially identified in the 2005-2014 HCUP-NIS database. Of them, 3305 patients had liver metastases and CRC. After excluding patients with coagulopathy and a history of blood transfusion (n = 237), and patients who lacked data of length of hospital stay (n = 1050), 2018 patients were included in the study analysis (Figure 1). G*Power was used to calculate the number of samples required, which revealed that the present study required at least 150 subjects, so the sample size of this study is sufficient. In addition, after applying weights, the analytic sample size was equivalent to a population-based sample size of 9991 individuals.

Patient demographic and clinical characteristics

The mean patient age was 59.75 years, with 1532 patients below the age of 70 (Table 1). Of the 2018 patients, 480 had a perioperative transfusion, while 1538 did not. The non-transfusion group and the perioperative transfusion group were significantly different in age, sex, type of admission, insurance status, primary tumor site, extent of liver resection, chronic anemia, congestive heart failure, hypertension, bed size of hospital, and teaching status of hospital. A higher proportion of perioperative transfusion patients also had their primary tumor site in the colon (*vs* rectum) (83.59%), compared with patients who did not have a transfusion (77.64%). More patients with transfusions had hepatic lobectomies (29.81%), when compared to patients who did not have transfusions (21.60%). Comorbidities were also more prevalent in patients who had a perioperative transfusion, especially for the comorbidities of chronic anemia (36.37% *vs* 15.87%), congestive heart failure (5.02% *vs* 2.31%), and hypertension (46.32% *vs* 40.43%). Patients who had a transfusion were more likely to be in medium sized hospitals (21.12% *vs* 15.15%) and non-teaching hospitals (27.64% *vs* 18.46%).

Factors associated with perioperative transfusion

In order to identify the factors that were associated with perioperative transfusion, logistic regression models were performed (Table 2). Univariate logistic regression analysis found that perioperative transfusion was significantly associated with age, sex, type of admission, insurance status, primary tumor site, extent of liver resection, comorbidities, and teaching status of the hospital. Patients who were 70 years of age and above had a 1.5-times higher risk of getting a perioperative transfusion as compared to patients who were younger than 70 (95%CI: 1.19-1.88). Female patients had a 1.31-times higher risk of getting a perioperative transfusion as opposed to male patients (95%CI: 1.08-1.58). Patients who had an emergency admission had a 1.9-times higher risk of getting a perioperative transfusion than patients who had an elective admission (95%CI: 1.45-2.50). Patients who had a hepatic lobectomy had increased odds for perioperative transfusion as compared to patients who had a partial hepatectomy (OR = 1.54, 95%CI: 1.24-1.91). Furthermore, patients with chronic anemia, congestive heart failure, and hypertension had 2.98, 2.20, and 1.27 higher risks, respectively, of receiving a perioperative transfusion as compared to patients who did not have these conditions.

In contrast, compared to users of Medicare/Medicaid, patients who had private insurance (OR = 0.65; 95%CI: 0.53-0.80) or were self-paid (OR = 0.49; 95%CI: 0.29-0.85) had a lower chance of receiving a perioperative transfusion. Patients whose primary tumor site was located in the rectum had a lower risk of having a perioperative transfusion compared to patients with a primary colon tumor (OR = 0.67; 95%CI: 0.52-0.87). Patients at teaching hospitals had a lower risk of receiving a perioperative transfusion than those at non-teaching hospitals (OR = 0.59; 95%CI: 0.46-0.76).

Multivariate logistic regression analysis found that only four factors retained their significant association with perioperative transfusion: emergency admission (aOR = 1.42; 95%CI: 1.07-1.87), hepatic lobectomy (aOR = 1.76; 95%CI: 1.42-2.19), chronic anemia (aOR = 2.62; 95%CI: 2.04-3.35), and teaching hospital (aOR = 0.75; 95%CI: 0.58-0.98).

Influence of perioperative transfusion on clinical outcomes

The frequencies of postoperative complications in the non-transfusion and perioperative transfusion group are shown in Table 3. Of the 2018 included patients,

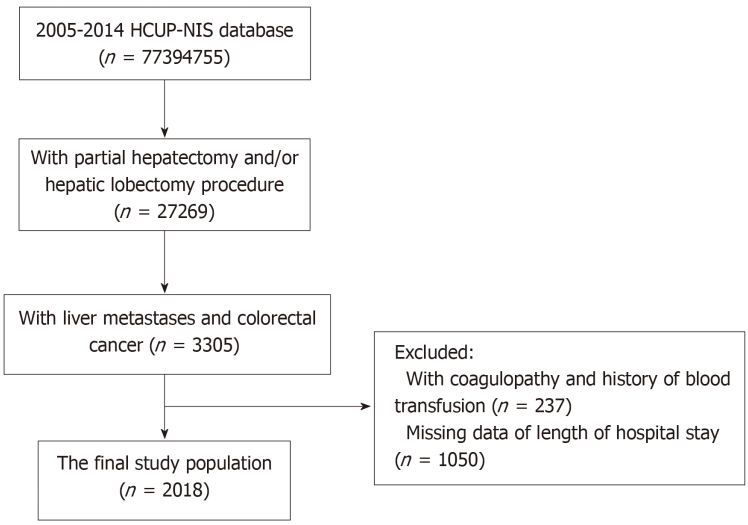

Figure 1 Flow chart of study population.

338 had postoperative complications, with approximately one-third of infections (*n* = 108). The results of association analysis between perioperative transfusion and clinical outcomes are shown in Table 4. Both univariate and multivariate linear regression models revealed significant associations between perioperative transfusion and length of hospital stay (univariate: β = 2.01, standard error [SE] = 0.37; multivariate: β = 1.51, SE = 0.36). These results indicate that perioperative transfusion was associated with an increased length of hospital stay after adjustment for sex, type of admission, chronic anemia, congestive heart failure, hypertension, and hospital size.

The univariate logistic regression model showed significant associations between perioperative transfusion and in-hospital mortality (OR = 4.42; 95%CI: 2.05-9.51), and overall postoperative complications (OR = 1.69; 95%CI: 1.33-2.15). After adjustment for age, type of admission, extent of liver resection, and hypertension, multivariate analysis showed a significant association between perioperative transfusion and in-hospital mortality (aOR = 3.38; 95%CI: 1.57-7.25). After adjustment for congestive heart failure and hypertension, multivariate analysis indicated a significant association between perioperative transfusion and overall postoperative complications (aOR = 1.67; 95%CI: 1.31-2.13).

DISCUSSION

The results of this study using data from the United States NIS showed that significant risk factors for receiving a perioperative transfusion were emergency admission, hepatic lobectomy, and chronic anemia, while having surgery at a teaching hospital was associated with a lower risk of receiving a transfusion. In addition, for patients with CRC undergoing surgery for hepatic metastasis, perioperative transfusion was significantly associated with greater in-hospital mortality, a higher rate of postoperative complications, and longer length of hospital stay.

The results of this study have confirmed the results of other studies of CRC, and are consistent with studies that have shown perioperative transfusions are associated with poorer outcomes in patients with lung cancer undergoing resection[8], and patients with gastric cancer undergoing curative surgeries[7]. Importantly, this study identified factors associated with receiving a transfusion, which may assist in identifying patients in whom more intensive management may help to avoid a transfusion and thus obtain a better outcome.

It has become clear that perioperative allogeneic blood transfusions are associated with worse outcomes in patients with CRC who receive surgery. A recent systematic review and meta-analysis by Acheson *et al*[4] included approximately 21000 CRC patients, of whom 58% received a transfusion. The analysis revealed that allogeneic blood transfusion was significantly associated with increased all-cause mortality, cancer-related mortality, combined recurrence-metastasis-death, postoperative infection, surgical re-intervention, and longer length of hospital stay. Studies of patients who undergo surgery for CRC liver metastases have provided similar results.

A recent meta-analysis by Lyu *et al*[9] examined the outcomes of patients who received a hepatectomy for CRC metastasis. The analysis included 10621 patients, and

Table 1 Characteristics of the study population (unweighted *n* = 2018, weighted *n* = 9991)

	Total	No transfusion	Perioperative transfusion	*P*-value[1]
	n = 2018	*n* = 1538	*n* = 480	
Demographic data				
Age				
<70 yr	1532 (76.04)	1195 (77.88)	337 (70.12)	0.0004[a]
≥70 yr	486 (23.96)	343 (22.12)	143 (29.88)	
Sex				
Male	1112 (55.10)	870 (56.59)	242 (50.32)	0.01[a]
Female	903 (44.90)	665 (43.41)	238 (49.68)	
Race				
White	1251 (76.29)	955 (76.94)	296 (74.22)	0.10
Black	175 (10.53)	121 (9.63)	54 (13.32)	
Hispanic	115 (7.07)	86 (7.04)	29 (7.16)	
Asian/Pacific	55 (3.32)	40 (3.21)	15 (3.62)	
Others	46 (2.80)	39 (3.16)	7 (1.68)	
Household income				
Q1	484 (24.34)	355 (23.59)	129 (26.90)	0.14
Q2	473 (23.79)	369 (24.34)	104 (22.06)	
Q3	471 (23.93)	372 (24.89)	99 (20.87)	
Q4	541 (27.93)	400 (27.22)	141 (30.16)	
Type of admission				
Elective	1676 (83.35)	1311 (85.59)	365 (76.12)	<0.0001[a]
Emergency	338 (16.65)	224 (14.41)	114 (23.88)	
Insurance status				
Medicare/Medicaid	877 (43.31)	628 (40.62)	249 (51.97)	<0.0001[a]
Private including HMO	1027 (51.05)	816 (53.25)	211 (43.95)	
Self-pay/no charge/other	114 (5.65)	94 (6.13)	20 (4.07)	
Clinical data				
Hepatic precondition				
No	1967 (97.41)	1494 (97.07)	473 (98.52)	0.24
Steatosis/fibrosis	44 (2.23)	38 (2.52)	6 (1.29)	
Cirrhosis	7 (0.36)	6 (0.41)	1 (0.19)	
Primary tumor site				
Colon	1595 (79.04)	1194 (77.64)	401 (83.59)	0.003[a]
Rectum	423 (20.95)	344 (22.36)	79 (16.40)	
Extent of liver resection				
Partial hepatectomy	1541 (76.46)	1204 (78.39)	337 (70.19)	<0.0001[a]
Hepatic lobectomy	477 (23.54)	334 (21.60)	143 (29.81)	
Laparoscopic procedure				
No	1971 (97.64)	1498 (9737.)	473 (98.52)	0.15
Yes	47 (2.36)	40 (2.63)	7 (1.48)	
Robotic-assisted				
No	2010 (99..59)	14532 (99.59)	478 (99.56)	0.91
Yes	8 (0.41)	6 (0.40)	2 (0.43)	
Comorbidity				
Chronic anemia	422 (20.71)	247 (15.87)	175 (36.37)	<0.0001[a]
Congestive heart failure	59 (2.95)	35 (2.31)	24 (5.02)	0.002[a]
Chronic pulmonary disease	188 (9.26)	135 (8.72)	53 (11.02)	0.12
Diabetes	293 (14.32)	221 (14.16)	72 (14.84)	0.70
Hypertension	848 (41.82)	625 (40.43)	223 (46.32)	0.02[a]
Obesity	118 (5.85)	89 (5.80)	29 (6.02)	0.86
Renal failure	39 (1.89)	30 (1.936)	9 (1.79)	0.86
Hospital data				

Hospital bed size				
Small	212 (10.21)	162 (10.28)	50 (9.97)	0.007[a]
Medium	327 (16.58)	227 (15.15)	100 (21.12)	
Large	1453 (73.22)	1125 (74.56)	328 (68.91)	
Location of hospital				
Rural	77 (3.71)	62 (3.89)	15 (3.14)	0.34
Urban	1915 (96.29)	1452 (96.10)	463 (96.87)	
Teaching status of hospital				
Non-teaching	419 (20.65)	284 (18.46)	135 (27.64)	<0.0001[a]
Teaching	1573 (79.35)	1230 (81.54)	343 (72.36)	
Region of hospital				
Northeast	437 (22.65)	351 (23.79)	86 (18.97)	0.11
Midwest	480 (23.71)	360 (23.27)	120 (25.11)	
South	737 (35.65)	566 (35.99)	171 (34.53)	
West	364 (17.98)	261 (16.94)	103 (21.39)	

Data are presented as unweighted counts (weighted proportion). Percentages may not add up to 100% due to missing data. Q1: 0-25th percentile; Q2: 26th to 50th percentile; Q3: 51st to 75th percentile; Q4: 76th to 100th percentile.
[1]χ^2 test.
[a]$P < 0.05$, non-transfusion group *vs* transfusion group.

the authors found that transfused patients had higher overall morbidity (OR = 1.98), higher mortality (OR = 4.13), longer hospital stays (OR = 4.43), reduced overall survival (RR = 1.24), and reduced disease-free survival (RR = 1.38). Another recent meta-analysis by Bennet *et al*[2] also reported that a transfusion in patients undergoing liver resection was associated with postoperative complications and decreased cancer survival.

The American College of Surgeons National Surgical Quality Improvement Program reviewed approximately 27000 cases of CRC surgery, of which 14% had blood transfusions[6]. They found that transfusions were associated with increased mortality (OR = 1.78), morbidity (OR = 2.38), length of hospital stay (mean difference 3.5 d), pneumonia (OR = 2.70), and surgical site infection (OR = 1.45). Interestingly, they found that the effect was dose dependent; patients who received a greater amount of transfused blood were more likely to have adverse events. Another study also reported that in patients undergoing hepatic resection for CRC metastasis, the operative mortality rate was 2.5% for patients who received one or two units of blood, 11.1% for those who received more than two units, and only 1.2% for those who did not receive a transfusion[10].

Other studies have also examined factors associated with receiving a transfusion. The aforementioned American College of Surgeons study found that predictors of a blood transfusion were hematocrit < 38%, open surgery, proctectomy, low platelet count, American Society of Anesthesiologists class IV or V, total colectomy, metastatic cancer, emergency surgery, ascites, and infection[6]. Schiergens *et al*[11] also examined factors associated with having a transfusion and found that female sex, preoperative anemia, major intraoperative blood loss, and major postoperative complications were independently associated with the necessity of a transfusion. The authors also reported that a perioperative transfusion was independently associated with earlier disease recurrence. An earlier study that examined 480 consecutive patients who underwent hepatic resection reported that a preoperative hemoglobin level below 12.5 g/dL, largest tumor more than 4 cm, exposure of the vena cava, an associated procedure, and cirrhosis were associated with the need for a transfusion[13]. The authors used these data to develop a transfusion risk score (TRS), and in a validation set, the area under the receiver operating characteristic curve was 0.89. A still earlier study demonstrated that prothrombin rate and the size of the liver resection were independently correlated with receiving a blood transfusion in patients with liver tumors undergoing resection[14].

Although it appears clear that perioperative blood transfusions are associated with worse surgical and oncological outcomes, the exact reasons remain to be determined. Current evidence suggests that TRIM, a complex immunological condition that results in transient immunosuppression, is involved[1,3].

In addition to identifying factors associated with receiving a perioperative transfusion, efforts have been made to reduce the need for allogenic blood transfusions. Bui *et al*[15] examined "blood saving strategies" such as administration of aprotinin, low CVP anesthesia, use of the Pringle maneuver, and ultrasonic dissection

Table 2 Associations between perioperative transfusion and factors of interest

	OR (95%CI)	aOR (95%CI)
Age		
<70 yr	1	1
≥70 yr	1.50 (1.19, 1.88)	1.10 (0.83, 1.47)
Sex		
Male	1	1
Female	1.31 (1.08, 1.58)	1.19 (0.97, 1.45)
Type of admission		
Elective	1	1
Emergency	1.90 (1.45, 2.50)	1.42 (1.07, 1.87)
Insurance status		
Medicare/Medicaid	1	1
Private including HMO	0.65 (0.53, 0.80)	0.78 (0.60, 1.01)
Self-pay/no charge/other	0.49 (0.29, 0.85)	0.56 (0.31, 1.00)
Primary tumor site		
Colon	1	1
Rectum	0.67 (0.52, 0.87)	0.86 (0.66, 1.14)
Extent of liver resection		
Partial hepatectomy	1	1
Hepatic lobectomy	1.54 (1.24, 1.91)	1.76 (1.42, 2.19)
Comorbidity		
Chronic anemia	2.98 (2.34, 3.80)	2.62 (2.04, 3.35)
Congestive heart failure	2.20 (1.32, 3.69)	1.57 (0.91, 2.68)
Hypertension	1.27 (1.03, 1.57)	1.10 (0.88, 1.37)
Bed size of hospital		
Small	1	1
Medium	1.43 (1.00, 2.04)	1.26 (0.85, 1.86)
Large	0.95 (0.69, 1.30)	0.92 (0.65, 1.30)
Teaching status of hospital		
Non-teaching	1	1
Teaching	0.59 (0.46, 0.76)	0.75 (0.58, 0.98)

OR: Odds ratio; aOR: Adjusted OR; CI: Confidence interval. Numbers in bold indicate statistical significance ($P < 0.05$).

in patients undergoing hepatic resection and reported that blood saving strategies decreased the estimated blood loss from a mean of 4500 mL to 1000 mL. Another study showed that preoperative autologous blood donation reduced the need for transfusion of homologous blood, as well as reducing the overall complication rate[16].

There are both strengths and limitations to this study. An important strength of the study is that it included a relatively large representative sample of patients from the United States, despite the relative rarity of the procedure. However, diagnoses were identified based on ICD-9 codes only, and coding errors and misclassifications might exist. In addition, the severities of the comorbidities were not known, as that information is not available in the database, and thus may confound the results. As a retrospective observational study, only associations can be demonstrated; causation cannot be determined. The primary aim of this study was to determine factors associated with a perioperative blood transfusion, and the findings may help surgeons and anesthetists anticipate the need for blood products during surgery. Examination of the long-term clinical and oncological outcomes was beyond the scope of this study.

In summary, patients with an emergency admission, hepatic lobectomy, chronic anemia, and who have surgery at a teaching hospital are more likely to receive a perioperative transfusion. Patients with CRC undergoing surgery for hepatic metastases who receive a perioperative transfusion are at a higher risk of in-hospital mortality, postoperative complications, and longer length of hospital stay.

Table 3 Characteristics of patients stratified by postoperative complications

	Total	No transfusion	Perioperative transfusion
	n = 2018	*n* = 1538	*n* = 480
Overall postoperative complications	338 (16.67)	229 (11.31)	109 (5.36)
Infection	108 (5.36)	67 (3.31)	41 (2.05)
Intra-abdominal abscess	45 (2.19)	27 (1.30)	18 (0.89)
Infected post-operative seroma	5 (0.26)	4 (0.22)	1 (0.05)
Wound dehiscence	27 (1.31)	21 (1.02)	6 (0.29)
UTI	32 (1.59)	26 (1.29)	6 (0.30)
Pulmonary complications	41 (2.05)	21 (1.04)	20 (1.00)
DVT	26 (1.29)	18 (0.90)	8 (0.39)
Postoperative myocardial infarction	58 (2.88)	42 (2.10)	16 (0.78)
Sepsis	30 (1.44)	23 (1.09)	7 (0.34)
Ascites	65 (3.20)	43 (2.13)	22 (1.07)
Acute liver failure	14 (0.70)	10 (0.49)	4 (0.21)
Other digestive system complications	17 (0.81)	14 (0.67)	3 (0.14)

Data are presented as unweighted counts (weighted proportion). Percentages may not add up to 100% due to missing data. DVT: Deep vein thrombosis; UTI: Urinary tract infection.

Table 4 Associations between perioperative transfusion and length of hospital stay, in-hospital mortality, and postoperative complications

	Univariate	Multivariate
Linear regression	B ± SE	B ± SE
Length of stay	2.01 ± 0.37	1.51 ± 0.36[1]
Logistic regression	OR (95%CI)	aOR (95%CI)
In-hospital mortality	4.42 (2.05, 9.51)	3.38 (1.57, 7.25)[2]
Overall postoperative complications	1.69 (1.33, 2.15)	1.67 (1.31, 2.13)[3]

[1]Multivariate analysis was adjusted for sex, type of admission, chronic anemia, congestive heart failure, hypertension, and bed size of hospital;
[2]Multivariate analysis was adjusted for age, type of admission, extent of liver resection, and hypertension;
[3]Multivariate analysis was adjusted for congestive heart failure and hypertension. β: Estimate; SE: Standard error; OR: Odds ratio; aOR: Adjusted OR; CI: Confidence interval. Numbers in bold indicate statistical significance ($P < 0.05$).

ARTICLE HIGHLIGHTS

Research background

Since perioperative allogeneic blood transfusion is associated with poorer outcomes, the risk of blood transfusion is high, including allergic reactions, infectious diseases, acute or delayed hemolytic reaction, and transfusion-related immune modulation. Previous studies have shown that perioperative allogeneic blood transfusion was associated with poor outcomes, such as increased postoperative complications and mortality. Patients with malignant tumors undergoing surgery often showed anemia. The amount of blood loss during surgery may be large, so the blood transfusion threshold is relatively low.

Research motivation

The use of allogeneic blood transfusion during surgery can improve outcomes and save countless lives. However, blood transfusions have higher risks, such as allergic reactions, infectious diseases, acute or delayed hemolysis, and transfusion-related immune regulation.

Research objectives

Based on above motivation, the study was designed to determine factors associated with perioperative blood transfusions and to examine the effects of perioperative blood transfusions on patients with colorectal cancer (CRC) metastasis undergoing liver resection.

Research methods

A total of 2018 patients were included from The United States National Inpatient Sample database, of whom 480 had a perioperative transfusion. Comorbidities such as chronic anemia, congestive heart failure, chronic pulmonary disease, diabetes, hypertension, obesity, and renal

failure were used.

Research results

Emergency admission, hepatectomy, and chronic anemia were significantly positively associated with the chance of receiving a blood transfusion, but there was a significant negative correlation between the chances of undergoing surgery and receiving blood transfusions at teaching hospitals. Perioperative blood transfusions were significantly associated with increased in-hospital mortality, overall increase in postoperative complications, and prolonged hospital stay.

Research conclusions

The results of this study demonstrated that in addition to hepatic lobectomy, emergency admission, chronic anemia, and surgery at a non-teaching hospital are more likely to receive a perioperative transfusion. In addition, the study provides an initial hit that patients with liver metastases who undergo perioperative transfusion are at a higher risk of hospital mortality, postoperative complications, and longer hospital stays.

Research perspectives

Based on this study, patients with liver metastasis who undergo tumor resection have a higher chance of receiving a blood transfusion, and a higher risk of hospital mortality. In future studies, it is worthwhile to continue to study the impact of liver resection area and extent on mortality in CRC patients.

REFERENCES

1 **Cata JP**, Wang H, Gottumukkala V, Reuben J, Sessler DI. Inflammatory response, immunosuppression, and cancer recurrence after perioperative blood transfusions. *Br J Anaesth* 2013; **110**: 690-701 [PMID: 23599512 DOI: 10.1093/bja/aet068]

2 **Bennett S**, Baker LK, Martel G, Shorr R, Pawlik TM, Tinmouth A, McIsaac DI, Hébert PC, Karanicolas PJ, McIntyre L, Turgeon AF, Barkun J, Fergusson D. The impact of perioperative red blood cell transfusions in patients undergoing liver resection: a systematic review. *HPB (Oxford)* 2017; **19**: 321-330 [PMID: 28161216 DOI: 10.1016/j.hpb.2016.12.008]

3 **Velásquez JF**, Cata JP. Transfusions of blood products and cancer outcomes. *Rev Esp Anestesiol Reanim* 2015; **62**: 461-467 [PMID: 25896733 DOI: 10.1016/j.redar.2015.02.013]

4 **Acheson AG**, Brookes MJ, Spahn DR. Effects of allogeneic red blood cell transfusions on clinical outcomes in patients undergoing colorectal cancer surgery: a systematic review and meta-analysis. *Ann Surg* 2012; **256**: 235-244 [PMID: 22791100 DOI: 10.1097/SLA.0b013e31825b35d5]

5 **Kaneko M**, Sasaki S, Ishimaru K, Terai E, Nakayama H, Watanabe T. The impact of perioperative allogeneic blood transfusion on survival in elderly patients with colorectal cancer. *Anticancer Res* 2015; **35**: 3553-3558 [PMID: 26026124]

6 **Halabi WJ**, Jafari MD, Nguyen VQ, Carmichael JC, Mills S, Pigazzi A, Stamos MJ. Blood transfusions in colorectal cancer surgery: incidence, outcomes, and predictive factors: an American College of Surgeons National Surgical Quality Improvement Program analysis. *Am J Surg* 2013; **206**: 1024-32; discussion 1032-3 [PMID: 24296103 DOI: 10.1016/j.amjsurg.2013.10.001]

7 **Sun C**, Wang Y, Yao HS, Hu ZQ. Allogeneic blood transfusion and the prognosis of gastric cancer patients: systematic review and meta-analysis. *Int J Surg* 2015; **13**: 102-110 [PMID: 25486261 DOI: 10.1016/j.ijsu.2014.11.044]

8 **Luan H**, Ye F, Wu L, Zhou Y, Jiang J. Perioperative blood transfusion adversely affects prognosis after resection of lung cancer: a systematic review and a meta-analysis. *BMC Surg* 2014; **14**: 34 [PMID: 24884867 DOI: 10.1186/1471-2482-14-34]

9 **Lyu X**, Qiao W, Li D, Leng Y. Impact of perioperative blood transfusion on clinical outcomes in patients with colorectal liver metastasis after hepatectomy: a meta-analysis. *Oncotarget* 2017; **8**: 41740-41748 [PMID: 28410243 DOI: 10.18632/oncotarget.16771]

10 **Kooby DA**, Stockman J, Ben-Porat L, Gonen M, Jarnagin WR, Dematteo RP, Tuorto S, Wuest D, Blumgart LH, Fong Y. Influence of transfusions on perioperative and long-term outcome in patients following hepatic resection for colorectal metastases. *Ann Surg* 2003; **237**: 860-9; discussion 869-70 [PMID: 12796583 DOI: 10.1097/01.SLA.0000072371.95588.DA]

11 **Schiergens TS**, Rentsch M, Kasparek MS, Frenes K, Jauch KW, Thasler WE. Impact of perioperative allogeneic red blood cell transfusion on recurrence and overall survival after resection of colorectal liver metastases. *Dis Colon Rectum* 2015; **58**: 74-82 [PMID: 25489697 DOI: 10.1097/DCR.0000000000000233]

12 **Gruttadauria S**, Saint Georges Chaumet M, Pagano D, Marsh JW, Bartoccelli C, Cintorino D, Arcadipane A, Vizzini G, Spada M, Gridelli B. Impact of blood transfusion on early outcome of liver resection for colorectal hepatic metastases. *J Surg Oncol* 2011; **103**: 140-147 [PMID: 21259247 DOI: 10.1002/jso.21796]

13 **Pulitanò C**, Arru M, Bellio L, Rossini S, Ferla G, Aldrighetti L. A risk score for predicting perioperative blood transfusion in liver surgery. *Br J Surg* 2007; **94**: 860-865 [PMID: 17380562 DOI: 10.1002/bjs.5731]

14 **Mariette D**, Smadja C, Naveau S, Borgonovo G, Vons C, Franco D. Preoperative predictors of blood transfusion in liver resection for tumor. *Am J Surg* 1997; **173**: 275-279 [PMID: 9136779 DOI: 10.1016/S0002-9610(96)00400-X]

15 **Bui LL**, Smith AJ, Bercovici M, Szalai JP, Hanna SS. Minimising blood loss and transfusion requirements in hepatic resection. *HPB (Oxford)* 2002; **4**: 5-10 [PMID: 18333146 DOI: 10.1080/136518202753598672]

16 **Nagino M**, Kamiya J, Arai T, Nishio H, Ebata T, Nimura Y. One hundred consecutive hepatobiliary resections for biliary hilar malignancy: preoperative blood donation, blood loss, transfusion, and outcome. *Surgery* 2005; **137**: 148-155 [PMID: 15674194 DOI: 10.1016/j.surg.2004.06.006]

World Journal of Clinical Cases

Submit a Manuscript: https://www.f6publishing.com

World J Clin Cases 2019 May 26; 7(10): 1103-1110

DOI: 10.12998/wjcc.v7.i10.1103

ISSN 2307-8960 (online)

ORIGINAL ARTICLE

Retrospective Study

Analysis of 24 patients with Achenbach's syndrome

Fatih Ada, Ferit Kasimzade

ORCID number: Fatih Ada (0000000269535906); Ferit Kasimzade (0000000336463181).

Author contributions: Ada F designed and performed the research and wrote the paper; Kasimzade F provided clinical advice and contributed to the analysis.

Institutional review board statement: This study was reviewed and approved by the Local Ethics Committee of the Sivas Cumhuriyet University.

Informed consent statement: All patients gave informed consent.

Conflict-of-interest statement: The authors declare that they have no conflict-of-interests.

Data sharing statement: No additional data are available.

Manuscript source: Unsolicited manuscript

Received: January 15, 2019

Peer-review started: January 15,

Fatih Ada, Department of Cardiovascular Surgery, Sivas Cumhuriyet University School of Medicine, Sivas 58140, Turkey

Ferit Kasimzade, Department of Cardiovascular Surgery, Turkiye Yuksek Ihtisas Training and Research Hospital, Ankara 06100, Turkey

Corresponding author: Fatih Ada, PhD, Assistant Professor, Cardiovascular Surgeon, Department of Cardiovascular Surgery, Sivas Cumhuriyet University School of Medicine, Merkez, Sivas 58140, Turkey. drfatihada@gmail.com
Telephone: +90-346-2191010

Abstract

BACKGROUND

Achenbach's syndrome is a rare condition, and the etiology is unknown. It is most commonly seen in the volar plate of the hand distal interphalangeal joint. Patients diagnosed with Achenbach's syndrome in cardiovascular surgery clinic were retrospectively compared with the literature.

AIM

To investigate the symptoms, findings, sociodemographic conditions, and laboratory data of patients diagnosed with Achenbach's syndrome.

METHODS

The study is a retrospective review of 24 patients diagnosed with Achenbach's syndrome at Afyonkarahisar State Hospital between March 2015 and November 2016, at Sivas Numune Hospital between November 2016 and November 2017, and at Cumhuriyet University Cardiovascular Surgery Department between November 2017 and November 2018. In the study, demographic characteristics of the patients, signs and symptoms of the disease, and laboratory data were analyzed retrospectively.

RESULTS

The cohort consisted of 83.33% female patients and 16.67% male patients. The disease was most commonly located in the index finger of the right hand. All of the patients complained of bruising and pain. No pathologic findings were present in the laboratory results. According to these results, it can be concluded that Achenbach syndrome is most commonly seen in the right index finger of middle-aged female patients.

CONCLUSION

Further research is needed to clarify Achenbach's syndrome and to develop a diagnosis and treatment algorithm. As the awareness of this syndrome increases, large amounts of data will be obtained. According to current knowledge,

2019
First decision: March 10, 2019
Revised: April 29, 2019
Accepted: May 1, 2019
Article in press: May 1, 2019
Published online: May 26, 2019

P-Reviewer: Huang Y
S-Editor: Dou Y
L-Editor: Filipodia
E-Editor: Xing YX

Achenbach's syndrome is not among the known causes of mortality or morbidity. However, it is unknown whether it is seen in brain or other vital organs.

Key words: Achenbach's syndrome; Blue thumb; Digital hematoma; Digital hemorrhage; Hand; Pulse oximeter

Core tip: The etiology of Achenbach's syndrome is not clearly known. This disease is often seen on the volar surface of fingers. Blue-colored finger and sudden onset pain are the most common symptoms. No morbidity and mortality have been reported in this syndrome. However, there is little awareness of the disease. This study showed that this syndrome is most commonly seen in the index finger of middle-aged female patients. Further studies are needed to explain Achenbach's syndrome pathogenesis and to define a diagnostic and therapeutic algorithm.

Citation: Ada F, Kasimzade F. Analysis of 24 patients with Achenbach's syndrome. *World J Clin Cases* 2019; 7(10): 1103-1110
URL: https://www.wjgnet.com/2307-8960/full/v7/i10/1103.htm
DOI: https://dx.doi.org/10.12998/wjcc.v7.i10.1103

INTRODUCTION

The etiology of Achenbach's syndrome, which is often encountered in the cardiac surgery clinics, yet forgotten during the diagnostic process, is not clearly known. This rare syndrome is frequently neglected in the diagnostic process because the disease does not clearly result in any mortality or morbidity, and therefore it is ignored. However, we are convinced that as the studies on this subject increase (such as studies to enlighten if this syndrome is a precursor to more serious illnesses or to reveal what happens in the vascular bed), the awareness about the disease will also increase. Achenbach's syndrome is typically characterized by a digital hematoma and bruising that begins suddenly and painfully in one or several fingers and decreases within hours or days. There are no known risk factors such as trauma, drug use, bleeding disorder, or rheumatologic disease associated with the etiology of the syndrome. The disease was named after German doctor Achenbach as it was first diagnosed by him[1]. We retrospectively analyzed the data of 24 patients with Achenbach's syndrome in our study and compared with the literature.

MATERIALS AND METHODS

The study is a retrospective analysis of 24 patients diagnosed with Achenbach's syndrome at Afyonkarahisar State Hospital between March 2015 to November 2016, at Sivas Numune Hospital between November 2016 to November 2017, and at Sivas Cumhuriyet University Cardiovascular Surgery Department between November 2017 to November 2018. It was approved by the local ethics committees. Written consent forms were obtained from all patients. Patient information was obtained from patient cards and the hospital registry system. The anamnesis of the patients was carefully taken and the physical examinations were made to identify vascular and other pathological diseases. Subsequently, arterial and venous Doppler scans of the extremity veins, complete blood counts (to diagnose bleeding disorders), international normalized ratio, prothrombin time, and activated partial thromboplastin time tests were requested. Biochemical parameters were studied. Oxygen saturation was measured at the fingertips of the patients by pulse oximetry. Patients who did not use anticoagulants or antiaggregants in their history, normal Doppler ultrasonographic findings, normal pulse oximeter values, and no laboratory abnormalities were evaluated as Achenbach's syndrome. Patients were treated with analgesics (if necessary), mucopolysaccharidepolysulphate containing cream or gel, cold applications, and just advised to rest the diseased hand. After 2 wk of treatment, it was observed that the patients did not have any complaints.

RESULTS

In total, 24 patients were studied retrospectively. Of these, 83.33% of the patients were female (n = 20) and 16.67% were male (n = 4). The mean age was 47.91 ± 11.72. As a result, it was concluded that this syndrome was seen in middle ages and occurs in females five times more than males. None of the patients had received anticoagulation and antiplatelet treatment. The arterial and venous Doppler findings showed no pathology. Only 16.67% of the patients were smokers and none of them had a history of alcohol use. A summary of the demographic data of the patients can be found in Table 1.

In the patients' laboratory data, the mean number of platelets was 246.95 (PLT × 10^3/μL), the mean international normalized ratio was 1.05, the mean prothrombin time was 11.79 min, and the mean activated partial thromboplastin time was 29.54 min. Unlike other studies, we used a pulse oximeter in the differential diagnosis of arterial ischemia or digital ischemia, and we did not observe oxygenation impairment in the pulse oximetry that would suggest ischemia in any of the patients (Table 2).

When the symptoms and the location of the syndrome were examined, all the patients had pain and bruising in the affected area. The swelling was 54.1% and the paresthesia was 37.5%. The mean number of episodes was 3.04. When the affected area and finger were considered, the most common regions were right hand (54.1%) and index finger (33.3%) (Table 3). Herein, it can be concluded that the disease is most commonly seen at the right hand index fingers of middle-aged females.

DISCUSSION

There are few publications on Achenbach's syndrome in the literature. However, the scarcity of these publications is not due to the rareness of the disease. Our clinical observations suggest that the disease is more common than generally thought. Although a large proportion of patients were referred to cardiac surgery clinics, some were referred to other departments such as family medicine, dermatology, internal medicine, hematology, rheumatology, plastic surgery, and orthopedics, or the patients were directed to these departments from cardiac surgery clinics.

In the absence of a known essential cause, Achenbach's syndrome is characterized by an acute pain and numbness in the fingers. In addition to these complaints, swelling and paresthesia can be observed. In our study, all the patients had complaints of pain and bruising, yet swelling and paresthesia were present in only some of them. In the literature, two cases were identified in which the location of the disease was not the fingers. One of these cases was recurrent subconjunctival hemorrhage in the eye while the other was located in the wrist[2,3].

Although the etiology of Achenbach's syndrome is unknown, Singer has hypothesized that in some patients increased capillary resistance and vascular fragility may trigger this disease even in a minimal trauma[4]. It has also been reported that acrocyanosis, gastrointestinal diseases, migraines, and biliary diseases may be related to the etiology of the disease[5]. Kämpfen *et al*[6] have proposed the etiology of vasospasm through a case in which ergotamine was used due to migraine. It has been suggested that Achenbach's syndrome may be associated with Raynaud's syndrome and Chilblain's disease in the secondary data gathered from Carpentier *et al*[7]. In the same study, this syndrome was found to be associated with tobacco use, alcohol consumption, and estrogen therapy while no relationship was observed with body mass index, education level, marital status, occupation, vibration, and trauma. Achenbach's syndrome is 2-7 times more common in middle-aged women than in men[8-10]. Although the most common location of the disease varies in the sources, it has been observed more frequently in the middle and index fingers[7]. Achenbach's syndrome is generally episodic[11,12]. In our study, the average number of episodes was 3.04, and the most common finger was the index finger (Figures 1 and 2).

Physical examination and anamnesis have a major role in the diagnosis of Achenbach's syndrome. Laboratory and imaging techniques may be required for differential diagnosis (Table 4). However, in suspected cases, these methods should be used and unnecessary invasive procedures should be avoided[6,13]. Because of the possibility of mistaking the syndrome with many vascular, hematologic, dermatologic, and rheumatologic diseases, some laboratory and imaging methods might be required (such as complete blood count, coagulation factors, c-reactive protein, blood lipid level, and arterial and venous Doppler ultrasonography of the concerned extremity)[8,11,14]. In the literature, biopsies were performed for lesions in two cases[8,15]. In one of these cases, the epidermis showed hyperkeratosis and parakeratosis. In the other case, amorphous, eosinophilic amyloid deposition in the

Table 1 Demographic data of patients

Variable	*n* or mean ± SD	% or min-max
Age	47.91 ± 11.72	21-67
Female	20	83.33
Male	4	16.67
Family history	1	4.1
Bruising elsewhere	2	8.3
Diabetes	3	12.5
Hypertension	7	29.1
Smoking	4	16.6
Alcohol	0	-
Antiplatelet use	0	-
Anticoagulant use	0	-
Pathology in arterial duplex ultrasonography	0	-
Pathology in venous duplex ultrasonography	0	-

min: Minimum; max: Maximum.

stroma and fibrin accumulation was observed. In both cases, no pathology was detected in microvascular structures. Capillaroscopy examination was not necessary for diagnosis, but Khaira *et al*[9] performed capillaroscopy in 11 patients, and no pathology was detected. Frerix *et al*[16] showed capillary hemorrhage in one case. Arterial and venous Doppler ultrasonography is a good non-invasive choice for evaluating the vascular bed[17]. No arterial or venous pathology was found in the Doppler ultrasonography in any of the studies performed.

Upon suspicion of arterial microembolism, invasive imaging methods can be used to investigate the origin of the microemboli[18]. While in the case reported by Weinberg *et al*[11], no pathology was observed in the upper extremity angiography, in the case of Robertson *et al*[19], slow flow was observed in the digital arteries. There are studies in which transthoracic echocardiography was used in the diagnosis of arterial embolism, and no cardiogenic embolic source had been found in these studies[10,11]. In our study, oxygen saturation was measured at the diseased fingertip by pulse oximetry in order to possibly detect microemboli. No abnormal oxygen saturation, which would suggest ischemia or embolism, was found in any of the patients. Achenbach's syndrome should be considered in the differential diagnosis of symptoms similar to Raynaud's syndrome with clinical episodic digital ischemia[20]. The rheumatologic aspect of the syndrome has been further investigated in case reports, but no rheumatologic relationship has been found other than Achenbach's syndrome associated with rheumatoid arthritis reported by Manappallil *et al*[8,21,22].

Nowadays, many patients now refer to hospitals by searching their symptoms from the internet, from written and visual media, and from social media. This situation forces physicians not only to diagnose and treat, but also to help reduce the anxiety caused by incorrect or incomplete information. Patients with Achenbach's syndrome who refer to the clinics are in urgent expectation thinking that there is a blockage of the blood vessels or a blood clot in the finger. For this reason, the unwarranted concerns of the patients should be eliminated properly. There are many different opinions in the general treatment of the disease. Some of these views suggest that there is no need for treatment because of the benign course of the disease and that only follow-up is sufficient[10,23,24]. On the other hand, there are publications in which treatment includes sargegrelate hydrochloride, acetylsalicylic acid 81 mg, long-acting diprimadol, heparin, or isosorbidedinitrate[8,11,19]. Though the etiology was unknown, if a bleeding point was definite, we did not apply anticoagulant, antiplatelet, or vasodilator treatments unless there was another compulsory indication. When necessary, patients were treated with analgesics, or with cream or gel containing mucopolysaccharidepolysulphate; occasionally cold applications were applied or the patient was advised to rest the diseased hand. After 2 wk of treatment, it was observed that the patients did not have any complaints.

Today we know very little about this syndrome. Further studies on the disease is important because we know that the disease is on the fingers, the palmar surface, the ankle, and the eye, but we do not know whether the brain and other vital organs have the same bleeding and hematoma[7]. Due to Achenbach's syndrome, a probable hemorrhage or hematoma in the brain and other vital organs would be life

Table 2 Laboratory data of patients

Parameter	mean (min-max)	Reference range
White blood cell, × 10^3/μL	7.84 (4.2-13.4)	4-11
Red blood cell, × 10^6 /μL	5.07 (3.8-6.4)	4.6-6.2
Hemoglobin, g/dL	15.06 (11.4-19.2)	14-18
Hematocrit, %	45.62 (34.2-57)	42-52
Platelets, × 10^3/μL	246.95(152-356)	150-400
International normalized ratio	1.05 (0.82-1.18)	0.8-1.2
Prothrombin time, s	11.79 (10.8-12.8)	10.7-13.0
Active partial thromboplastin time, s	29.54 (24-36)	22-36.9
C-reactive protein, mg/L	4.18 (0.8-8.4)	0-8
Sedimentation, mm/h	13.45 (2-24)	0-24
Low density lipoprotein, mg/dL	130.83 (48-184)	< 160
Triglycerides, mg/dL	150.37 (36-252)	< 203
Pulse oximeter, SpO%	96.8 (94-100)	95-100

min: Minimum; max: Maximum.

threatening, so the disease should be further investigated.

In conclusion, there is no doubt that many new studies will be done as the awareness of Achenbach's syndrome increases. The etiology and prognosis of the disease is still a mystery. It is of great importance to know whether the syndrome is seen in the brain and vital organs. However, it is relieving to know that there is no proven mortality or morbidity of the disease and that the course of the disease is benign.

Table 3 Achenbach's syndrome symptoms and location features

Symptom / location	*n* or mean	% or min-max
Swollen	13	54.1
Pain	24	100
Paresthesia	9	37.5
Bruising	24	100
Mean episode count	3.04	1-6
Thumb	4	16.6
Index finger	8	33.3
Middle finger	7	29.1
Ring finger	3	12.5
Little finger	1	4.1
Other, Palmar, wrist, *etc*	1	4.1
Right hand	13	54.1
Left hand	11	45.8

min: Minimum; max: Maximum.

Table 4 Differential diagnoses

Differential diagnosis	
Raynaud's syndrome or phenomenon	Thoracic outlet syndrome
Spontaneous digital venous thrombosis	Trauma
Gardner-Diamond syndrome	Collagen vascular disease
Atherosclerosis	Buerger disease
Takayasu arteritis	Ulnar artery thrombosis
Giant cell arteritis	Radial artery thrombosis
Aneurysmal disease producing emboli	Microemboli
Vibration-induced injury	Polycythemia
Cold injury	Cryoglobulinemia
Dermatitis artefacta	Spontaneous rupture of the vincula
Acute limb ischemia	Chilblain's disease
Acrocyanosis	Acrorygosis

Figure 1 The bruising is located on the right hand ring finger.

Figure 2 The bruising is located on the right hand index finger.

ARTICLE HIGHLIGHTS

Research background

Achenbach's syndrome is often characterized by a sudden onset of pain and bruising in the fingers. The etiology and clinical course of this syndrome are unknown. In fact, this syndrome is seen commonly in the clinic, but the lack of a known morbidity and mortality lead to a neglect of diagnosis and treatment. In our retrospective study from different centers, detailed data were obtained about Achenbach's syndrome.

Research motivation

Achenbach's syndrome is rarely diagnosed but is commonly seen in clinical practice. As the awareness of the syndrome increases, it will be revealed that it is seen much more than it was once thought.

Research objectives

In this study, we aimed to determine the symptoms, laboratory values, and clinical characteristics of patients with Achenbach's syndrome. It was aimed to compare the obtained data with the current literature.

Research methods

Twenty-four patients who were diagnosed with Achenbach's syndrome in different centers between 2016 and 2018 were retrospectively evaluated. The sociodemographic data, laboratory values, and clinical characteristics of the patients were compared with the literature.

Research results

In this study, patients diagnosed with Achenbach's syndrome were retrospectively evaluated, and 83.33% of the patients were female. This rate was 5 times higher than male patients. There was no pathology in the bleeding profiles of the patients. No pathology was detected by pulse oximetry of the bruising finger in any patient. All patients had pain and bruising of their fingers. The most frequently affected side was the upper right extremity and the index finger.

Research conclusions

The bruising in the fingers was not characterized by impaired circulation and oxygenation. Therefore, we hypothesized the syndrome is a venous disease. Although the most common place of this syndrome is the fingers, the condition of the brain and other vital organs is unknown. Achenbach's syndrome needs an algorithm for diagnosis and treatment.

Research perspectives

Achenbach's syndrome should be kept in mind if a patient suddenly has a bruised finger. An algorithm should be created for diagnosis and treatment of Achenbach's syndrome. Other features of the Achenbach's syndrome should be revealed in a multidisciplinary approach.

REFERENCES

1 **Achenbach W**. Paroxysmal hematoma of the hand. *Medizinische* 1958; **52**: 2138-2140 [PMID: 13622116]
2 **Young B**, Okera S. Recurrent subconjunctival haemorrhage in Achenbach's syndrome. *Clin Exp Ophthalmol* 2018; **46**: 965-966 [PMID: 29700952 DOI: 10.1111/ceo.13314]
3 **Huikeshoven M**, de Priester JA, Engel AF. A case of spontaneous wrist haematoma in Achenbach syndrome. *J Hand Surg Eur Vol* 2009; **34**: 551-552 [PMID: 19675046 DOI: 10.1177/1753193409103731]
4 **Sınger R**. On the symptoms and diagnosis of finger apoplexy (paroxysmal hematoma of the hand). *Wien Klin Wochenschr* 1962; **74**: 741-743 [PMID: 13977617]
5 **Layton AM**, Cotterill JA. A case of Achenbach's syndrome. *Clin Exp Dermatol* 1993; **18**: 60-61 [PMID:

8440056 DOI: 10.1111/j.1365-2230.1993.tb00970.x]
6 **Kämpfen S**, Santa DD, Fusetti C. A painful blue thumb: a case of Achenbach's syndrome. *EJVES Extra* 2005; **10**: 84-85 [DOI: 10.1016/j.ejvsextra.2005.07.004]
7 **Carpentier PH**, Maricq HR, Biro C, Jiguet M, Seinturier C. Paroxysmal finger haematoma--a benign acrosyndrome occurring in middle-aged women. *Vasa* 2016; **45**: 57-62 [PMID: 26986711 DOI: 10.1024/0301-1526/a000496]
8 **Takeuchi H**, Uchida HA, Okuyama Y, Wada J. Acute idiopathic blue fingers: a young man with Achenbach's syndrome. *BMJ Case Rep* 2016; **2016**: 10.1136/bcr-2016-214491 [PMID: 27090544 DOI: 10.1136/bcr-2016-214491]
9 **Khaira HS**, Rittoo D, Vohra RK, Smith SR. The non-ischaemic blue finger. *Ann R Coll Surg Engl* 2001; **83**: 154-157 [PMID: 11432130]
10 **Cowen R**, Richards T, Dharmadasa A, Handa A, Perkins JM. The acute blue finger: management and outcome. *Ann R Coll Surg Engl* 2008; **90**: 557-560 [PMID: 18701013 DOI: 10.1308/003588408X318237]
11 **Weinberg I**, Jaff MR. Spontaneous blue finger syndrome: a benign process. *Am J Med* 2012; **125**: e1-e2 [PMID: 22195537 DOI: 10.1016/j.amjmed.2011.05.007]
12 **Yamada T**. Achenbach's syndrome in an elderly woman. *J Gen Fam Med* 2018; **19**: 65-66 [PMID: 29600134 DOI: 10.1002/jgf2.158]
13 **Kordzadeh A**, Caine PL, Jonas A, Rhodes KM, Panayiotopolous YP. Is Achenbach's syndrome a surgical emergency? A systematic review. *Eur J Trauma Emerg Surg* 2016; **42**: 439-443 [PMID: 26669687 DOI: 10.1007/s00068-015-0610-0]
14 **Harper CM**, Waters PM. Acute idiopathic blue finger: case report. *J Hand Surg Am* 2013; **38**: 1980-1982 [PMID: 24021741 DOI: 10.1016/j.jhsa.2013.07.022]
15 **Watchorn RE**, Babu S, Lewis F, Calonje E, Taibjee SM. Paroxysmal purple palmar macules with a rare aetiology. *Clin Exp Dermatol* 2017; **42**: 561-563 [PMID: 28543701 DOI: 10.1111/ced.13101]
16 **Frerix M**, Richter K, Müller-Ladner U, Hermann W. Achenbach's syndrome (paroxysmal finger hematoma) with capillaroscopic evidence of microhemorrhages. *Arthritis Rheumatol* 2015; **67**: 1073 [PMID: 25546651 DOI: 10.1002/art.39003]
17 **Sidhu MS**, Ahmad Z, Jose RM. A case of non-ischaemic blue finger and toe. *Eur J Plast Surg* 2015; **38**: 165-166 [DOI: 10.1007/s00238-014-1040-7]
18 **Gaines PA**, Swarbrick MJ, Lopez AJ, Cleveland T, Beard J, Buckenham TM, Belli AM, Kessel D. The endovascular management of blue finger syndrome. *Eur J Vasc Endovasc Surg* 1999; **17**: 106-110 [PMID: 10063403 DOI: 10.1053/ejvs.1998.0704]
19 **Robertson A**, Liddington MI, Kay SP. Paroxysmal finger haematomas (Achenbach's syndrome) with angiographic abnormalities. *J Hand Surg Br* 2002; **27**: 391-393 [PMID: 12162986 DOI: 10.1054/jhsb.2001.0726]
20 **Yetkin U**, Gürbüz A. Current Approach To Raynaud's Phenomenon. *Turk Gogus Kalp Dama* 2002; **10**: 56-62
21 **Manappallil RG**, Jayaraj J. Blue Finger Syndrome: An Unusual Presentation of Rheumatoid Arthritis. *J Clin Diagn Res* 2017; **11**: OD06-OD07 [PMID: 28658830 DOI: 10.7860/JCDR/2017/25300.9784]
22 **Hayta SB**, Guner R. A case with acute idiopathic blue finger. *CMJ* 2017; **39**: 635-636 [DOI: 10.7197/223.v39i31705.347465]
23 **Yamamoto Y**, Yamamoto S. Achenbach's Syndrome. *N Engl J Med* 2017; **376**: e53 [PMID: 28657879 DOI: 10.1056/NEJMicm1610146]
24 **Mintz J**, Mintz BL, Jaff MR, editors. Atlas of Clinical Vascular Medicine. e-book: John Wiley & Sons, Ltd; 2013; 82-83 [DOI: 10.1002/9781118618189.ch41]

World Journal of Clinical Cases

Submit a Manuscript: https://www.f6publishing.com

World J Clin Cases 2019 May 26; 7(10): 1111-1121

DOI: 10.12998/wjcc.v7.i10.1111

ISSN 2307-8960 (online)

ORIGINAL ARTICLE

Retrospective Study

Risk factors and clinical responses of pneumonia patients with colistin-resistant *Acinetobacter baumannii-calcoaceticus*

Hande Aydemir, Hande Idil Tuz, Nihal Piskin, Guven Celebi, Canan Kulah, Furuzan Kokturk

ORCID number: Hande Aydemir (0000-0002-1650-7573); Hande İdil Tüz (0000-0003-4483-0906); Nihal Piskin (0000-0002-5963-592X); Guven Celebi (0000-0003-4035-6864); Canan Kulah (0000-0001-9926-3422); Furuzan Kokturk (0000-0002-2580-7770).

Author contributions: Aydemir H and Tuz HI contributed together to this work; Aydemir H, Piskin N and Celebi G designed research; Aydemir H, Tuz HI and Kulah C performed research; Kokturk F analyzed data; and Aydemir H wrote the paper.

Institutional review board statement: This study was approved by the ethics committee of Zonguldak Bulent Ecevit University Teaching and Research Hospital.

Informed consent statement: Patients were not required to give informed consent statement for this study due to the suggestion of ethical committee of our hospital. We did not use any personal data. The data which was used for this study is available from our hospital's computer system. But written informed consent forms were taken for the agreement to treatment of pan-drug resistant *Acinetobacter baumannii* infections from patients or legal representatives.

Conflict-of-interest statement: All authors declare no conflicts of interest related to this article.

Data sharing statement: The datasets used and/or analyzed during this study available from

Hande Aydemir, Hande Idil Tuz, Nihal Piskin, Guven Celebi, Department of Infectious Diseases and Clinical Microbiology, Zonguldak Bulent Ecevit University, Faculty of Medicine, Zonguldak 67100, Turkey

Canan Kulah, Department of Microbiology, Zonguldak Bulent Ecevit University, Faculty of Medicine, Zonguldak 67100, Turkey

Furuzan Kokturk, Department of Biostatistics, Zonguldak Bulent Ecevit University, Faculty of Medicine, Zonguldak 67100, Turkey

Corresponding author: Hande Aydemir, MD, Associate Professor, Department of Infectious Diseases and Clinical Microbiology, Zonguldak Bulent Ecevit University, Faculty of Medicine, Bülent Ecevit Üniversitesi Tıp fakültesi, Enfeksiyon hastalıkları A. D, Zonguldak 67100, Turkey. drhaydemir@yahoo.com
Telephone: +90-538-3712756
Fax: +90-372-2610264

Abstract

BACKGROUND

Nosocomial infections with carbapenem-resistant *Acinetobacter baumannii-calcoaceticus* complex (ABC) strains are great problem for intensive care units. ABC strains can develop resistance to all the antibiotics available. Carbapenem resistance is common and colistin resistance is rare in our country. Knowing the risk factors for colistin resistance is important since colistin seems to be the only remaining therapeutic option for the patients with pneumonia due to extensively drug resistant ABC for our country.

AIM

To investigate the comparison of clinical responses and outcomes between pneumonia patients with colistin-susceptible and -resistant *Acinetobacter sp.* Strains.

METHODS

During the study period, 108 patients with pneumonia due to colistin-susceptible strains and 16 patients with colistin-resistant strains were included retrospectively. Continuous variables were compared with the Mann-Whitney U test, and categorical variables were compared using Pearson's chi-square test or Fisher's Exact chi-square test for two groups. A binary logistic regression model was developed to identify the potential independent factors associated with colistin resistance in patients with colistin-resistant strains.

the corresponding author on reasonable request.

Manuscript source: Unsolicited manuscript

Received: February 10, 2019
Peer-review started: February 12, 2019
First decision: April 18, 2019
Revised: April 24, 2019
Accepted: May 1, 2019
Article in press: May 1, 2019
Published online: May 26, 2019

P-Reviewer: Tulkens PM, Porfyridis I
S-Editor: Dou Y
L-Editor: A
E-Editor: Xing YX

RESULTS

High Acute Physiology and Chronic Health Evaluation II scores (OR = 1.9, 95%CI: 1.4-2.7; $P < 0.001$) and prior receipt of teicoplanin (OR = 8.1, 95%CI: 1.0-63.3; $P = 0.045$) were found to be independent risk factors for infection with colistin-resistant *Acinetobacter sp*. Different combinations of antibiotics including colistin, meropenem, ampicillin/sulbactam, amikacin and trimethoprim/sulfamethoxazole were used for the treatment of patients with colistin-resistant strains. Although the median duration of microbiological cure ($P < 0.001$) was longer in the colistin-resistant group, clinical ($P = 0.703$), laboratory ($P = 0.277$), radiological ($P = 0.551$), microbiological response ($P = 1.000$) and infection related mortality rates ($P = 0.603$) did not differ between the two groups. Among the patients with infections due to colistin-resistant strains, seven were treated with antibiotic combinations that included sulbactam. Clinical (6/7) and microbiological (5/7) response rates were quite high in these patients.

CONCLUSION

The optimal therapy regimen is unclear for colistin-resistant *Acinetobacter sp*. infections. Although combinations with sulbactam seems to be more effective in our study patients, data supporting the usefulness of combinations with sulbactam is very limited.

Key words:*Acinetobacter baumannii*; Colistin; Ventilator-associated pneumonia

Core tip:*Acinetobacter baumannii-calcoaceticus* complex (ABC) may cause serious infections. As *Acinetobacter* species are resistant to many antimicrobials, treatment options for them are extremely limited. Knowing risk factors is important for colistin resistance since colistin seems to be the only remaining therapeutic option for the patients with pneumonia due to extensively drug resistant ABC. We aimed to investigate the risk factors for colistin resistance in ABC strains isolated from the patients with ventilator associated pneumonia (VAP). We also compared clinical response and the outcome between VAP patients due to colistin susceptible and resistant *Acinetobacter sp*. strains. Furthermore, different treatment combinations were evaluated.

Citation: Aydemir H, Tuz HI, Piskin N, Celebi G, Kulah C, Kokturk F. Risk factors and clinical responses of pneumonia patients with colistin-resistant *Acinetobacter baumannii-calcoaceticus*. *World J Clin Cases* 2019; 7(10): 1111-1121
URL: https://www.wjgnet.com/2307-8960/full/v7/i10/1111.htm
DOI: https://dx.doi.org/10.12998/wjcc.v7.i10.1111

INTRODUCTION

Acinetobacter baumannii-calcoaceticus complex (ABC) consists of Gram-negative round, rod-shaped bacteria that may cause serious hospital acquired infections. As *Acinetobacter species* (*sp*.) are simultaneously resistant to many antimicrobial agents, treatment options are extremely limited. Colistin is known as the most active therapeutic agent against extensively drug resistant (XDR) *Acinetobacter sp*. infections. Currently, besides its toxicities, the use of this agent is limited by the resistance of *Acinetobacter sp*. strains[1,2]. As shown in the literature, colistin-resistance has been reported worldwide[2]. The first colistin-resistant *Acinetobacter sp*. isolate was notified from the Czech Republic in 1999 by Vincent *et al*[3]. The highest rate of colistin-resistance was reported from Asia followed by Europe and other regions of the world[2]. Furthermore, in a surveillance study conducted in United States hospitals, it was reported that 5.3% of all *Acinetobacter sp*. strains were resistant to colistin[4]. Per the limited reported data, colistin resistance in ABC strains is rare in our country[5,6], with most of our isolates resistant to carbapenems but susceptible to colistin[7,8]. Knowledge of the risk factors is important for colistin resistance, since colistin appears to be the only remaining therapeutic option for patients with pneumonia due to XDR ABC. Combination therapy is a common strategy because of the in vitro synergistic

effect of antimicrobials against XDR ABC infections[9]. Although a few researches have studied the *in-vitro* activity of antimicrobial combinations against colistin-resistant *Acinetobacter sp*. isolates[10,11], these studies were not supported by clinical trials. Limited reported data are available about the clinical response and outcome of nosocomial pneumonia caused by colistin-resistant ABC (CRABC)[12,13]. In this study, we aimed to investigate the risk factors for colistin resistance in ABC strains isolated from patients with ventilator-associated pneumonia (VAP). We also compared clinical response and outcome between VAP patients due to colistin susceptible and resistant *Acinetobacter sp*. strains. Furthermore, different treatment combinations were evaluated in patients with VAP caused by CRABC.

MATERIALS AND METHODS

This comparative, retrospective, single-center study was conducted between January 2015 and April 2018 in the Zonguldak Bulent Ecevit University Hospital, a 416 bed adult tertiary care center with 49 adult intensive care unit beds. This study was approved by the ethics committee of the hospital. The following were included: patients aged ≥ 18 years who were diagnosed with VAP and whose culture and antimicrobial susceptibility results indicated infection with CRABC or colistin-susceptible ABC (CSABC), and patients who were within 48 h of the onset of VAP. Exclusion criteria included the following: (1) Patients who had polymicrobial cultures; (2) Patients who acquired different infection with another microorganism; (3) Patients who were transferred from different center under antibiotic treatment; (4) Patients who died within 3 d of antimicrobial therapy; and (5) Patients who were colonized with ABC without symptoms and signs of an infection. Resistance to imipenem and meropenem was defined as carbapenem resistance[14].

VAP diagnoses were made when the onset of the signs, and symptoms of pneumonia occurred 48 h after the initiation of mechanical ventilation[15]. These signs and symptoms included new or increased infiltrate on chest X-ray and two or more of the following: hyperthermia or hypothermia (> 38 ˚C or < 35.5 ˚C), white blood cell count > 12000 cells/mm^3 or < 4000 cells/mm^3, and purulent bronchial secretion. ABC strains were isolated from cultures of tracheal aspirates (TA) and/or bronchoalveolar lavages. ABC was considered to be the causative agent if the TA culture yielded >10^6 colony forming units (cfu)/mL of the organism[15,16]. TA specimens having > 25 polymorphonuclear leucoytes and ≤ 10 epithelial cells on the Gram stain were cultured. Blood cultures were taken routinely from patients who were diagnosed with VAP. The infectious disease (ID) specialist followed-up daily and evaluated patients to determine treatment durations. Patients were treated with broad-spectrum antimicrobials when the diagnosis of pneumonia was established. The initial antimicrobial regimens were modified within 2 d as soon as the susceptibilities of ABC strains became available. The total length of ICU stay was defined as the number of days hospitalized in this unit until death, discharge or transfer to another unit. Patients who fulfilled the following criteria were considered to have a clinical response: (1) Resolution of high fever or hypothermia with fever between 36-38 ˚C; (2) Reduction of tracheal secretion or the absence of purulence, with polymorphonuclear neutrophil counts < 25 cells/mm^3 in Wright stain smears of the tracheal secretion; (3) Improvement of hypoxemia, a PaO_2/FiO_2 ratio (the ratio of partial pressure of arterial O_2 to the fraction of inspired O_2) > 240, or elimination of the need for mechanical ventilation; and (4) Partial or complete resolution of respiratory crackles was observed[15,16,17]. The study patients were followed by the ID specialist until death or discharge. Bronchial secretion cultures were taken at the time of VAP diagnosis, before initial antibiotic therapy and after 3rd, 5th-7th and 10th d of treatment and when the treatment duration was completed.

If subsequent cultures (blood and TA) were negative for ABC, then patients were considered to have a microbiological response to antibiotic treatment. If a clinical response was achieved but the microorganism could not be eradicated from the cultures, the antibiotic regimen was stopped and the patient was thought to be colonized. The normalization of white blood cell counts (4000-10000 cells/mm^3), a decrease in the sedimentation rate, or a 40% decrease of the beginning CRP levels were defined as laboratory response. Disappearance of consolidation and absence of parapneumonic effusion on chest radiography were considered to be a radiological response to antibiotic treatment[17]. Death under the antibiotic treatment of infection or death occurring when the signs and symptoms of pneumonia were present, or death due to septic shock was considered as VAP-related mortality[15].

Isolation and identification of Acinetobacter sp. from cultures

Isolation and identification of ABC were performed by conventional techniques and confirmed by the BBL Crystal enteric/nonfermenter identification system (Becton Dickinson, United States). Susceptibility to antibiotics was determined by the standard disk diffusion method and interpreted according to the Clinical Laboratory Standards Institute (CLSI)[18]. Resistance to imipenem and meropenem was verified by determination of the minimal inhibitory concentrations (MICs) with E-tests (AB Biodisk, Sweden)[18]. The MICs of colistin were determined using the broth microdilution method according to CLSI recommendations. Standard powder form colistin sulphate (Sigma Chemical Co.) was stored at 2-8 ˚C until use. The stock solutions and serial twofold dilutions (to at least double the MIC) were prepared according to CLSI recommendations and in-house prepared panels of concentrations of 0.125–512 mg/mL were used. The breakpoints for colistin resistance were defined by CLSI recommendations (≤ 2 mg/mL for susceptible and ≥ 4 mg/mL for resistant)[18].

Molecular typing

Molecular typing was performed on 16 colistin-resistant isolates by the arbitrary primer polymerase chain reaction (AP-PCR) typing method.

Isolation of genomic DNA

Strains were grown overnight on MacConkey agar plates at 37 °C, and the growth from approximately one-quarter of a plate was resuspended in 180 μL of distilled water. Following this, 200 μL buffer solution (0.01 mol Tris-Cl, pH 7.8, 0.005 mol EDTA, and 0.5% SDS) and 20 μL proteinase K (1 mg/mL) was added. The mixture was incubated for 2 h at 55 °C followed by conventional phenol-chloroform extraction[19]. The DNA concentration was measured by UV absorbance at A_{260}.

AP-PCR

AP-PCR was performed using M13 and DAF4 primers[20]. Amplification products were electrophoresed on 2% agarose gel with ethidium bromide and were visualized under UV illumination. Strains belonging to the same clones showed identical DNA profiles.

Statistical analysis

The statistical review of the study was performed by a biomedical statistician. Statistical analysis was performed with SPSS 19.0 software (SPSS Inc., United Stated). The distribution of data was determined by the Shapiro-Wilk test. Continuous variables were expressed as the median (min-max); categorical variables were expressed as frequency and percent. Continuous variables were compared with the Mann-Whitney *U* test, and categorical variables were compared using Pearson's chi-square test or Fisher's exact chi-square test for two groups. A binary logistic regression model was developed to identify the potential independent factors associated with colistin resistance in patients with VAP due to ABC strains. Statistically significant and/or clinically relevant variables [APACHE II scores (Acute Physiology and Chronic Health Evaluation), duration of mechanical ventilation before diagnosis, prior use of colistin, prior receipt of carbapenems, prior receipt of ampicillin/sulbactam, prior receipt of piperacillin/tazobactam, prior receipt of fluoroquinolones, prior receipt of teicoplanin, and total parenteral nutrition (TPN)] were entered into the multivariate logistic regression model with 95% confidence intervals (CIs) calculated as estimators. When *P* values were < 0.05, they were accepted to be statistically significant.

RESULTS

During the study period, 124 patients with VAP due to CRABC and CSABC met the inclusion criteria. Patients' underlying medical conditions, previous antimicrobial usage and clinical characteristics were summarized in Table 1. The median age of patients infected with CSABC (74.0 ± 18-91) was significantly older than the patients with CRABC (59.5 ± 18-86) (P = 0.022). The ratio of male patients with VAP due to CRABC (81.3%) was significantly higher than male patients with CSABC (46.3%) (P = 0.019). Prior colistin (P = 0.001) and TPN (P = 0.030) usages were more common in the CRABC group than CSABC group. Although there was no statistically significant difference between the SOFA (Sequential Organ Failure Assessment) scores (P = 0.546) of the two groups on the day of VAP diagnosis, the difference in the APACHE II scores (P < 0.001) at time of ICU admission was statistically significant. The median APACHE II scores were higher in the CRABC group (22.5 ± 17-28) than in the CSABC group (12.0 ± 5-22). Although the median duration of microbiological cure (P < 0.001)

was longer in CRABC group, clinical (P = 0.703), laboratory (P = 0.277), radiological (P = 0.551) and microbiological response (P = 1.000) rates did not differ between the two groups. Although the crude in-hospital mortality (71/108, 65.7%, P = 0.058) and VAP-related mortality (45/108, 41.7%, P = 0.603) rates were higher in the CSABC group, the differences were not statistically significant. Using multivariate analysis, prior receipt of teicoplanin (OR = 8.1, 95%CI: 1.0-63.3; P = 0.045) and high APACHE II scores (OR = 1.9; 95%CI: 1.4-2.7; P < 0.001) were found to be independent risk factors for resistance to colistin. Clinical characteristics, antibiotic treatments and responses to treatment of the patients with VAP due to CRABC are shown in Table 2 and Table 3.

In the CSABC group, antibiotic combinations of 106 patients (98.1%) included colistin. Nephrotoxicity occurred in 38 (35.8%), and antibiotic dosage was adjusted in 32 (30.2%) cases. In the CRABC group, 12 of 16 patients (75%) were treated with colistin. Four patients (33.3%) developed nephrotoxicity during colistin treatment, and dosage was adjusted in these cases.

Sixteen of 124 (12.9%) isolated *Acinetobacter sp*. strains were resistant to colistin, and 108 of these isolates were susceptible to colistin. Only 7 of 108 (6.5%) colistin-susceptible strains were also susceptible to carbapenems (imipenem and/or meropenem). Ten (62.5%) of the colistin-resistant strains were resistant to all antibiotics tested, and all of them were resistant to carbapenems. The phenotypes of the CRABC isolates are shown in Table 4. Four different phenotypes were detected in these strains. Phenotype 1 isolates were resistant to all tested antibiotics. Phenotype 2 isolates were susceptible to tobramycin which is not available in our country; and while phenotype 3 isolates were susceptible to gentamicin, phenotype 4 isolates were susceptible to trimethoprim/sulfamethoxazole. Six isolates showed elevated colistin MICs (256 μg/mL to ≥ 512 μg/mL). AP-PCR analysis was performed on 16 CRABC isolates. AP-PCR fingerprinting yielded two types. Type 1 included 13 isolates, while type 2 included 3 isolates. Genotypes were not correlated to the phenotypes.

DISCUSSION

In recent years, carbapenem resistance seemed to be the primary barrier to treating infections with *Acinetobacter sp*. strains. Although colistin was a longstanding antimicrobial agent and not preferred due to side effects, it was reintroduced to clinical practice as a treatment of last resort because of the emergence of carbapenem-resistant Gram-negative pathogens including *Acinetobacter sp*. strains[1]. Clinicians have begun to use colistin more commonly due to an increase in carbapenem resistance in multidrug-resistant microorganisms, including *Acinetobacter sp*. Today, the emergence of colistin resistance and salvage therapies in *Acinetobacter sp*. infections are widely-studied topics in many countries[2,10,21,22]. *Acinetobacter sp*. strains are one of the most common pathogens in ICUs in our country[6]. The dissemination of resistance to carbapenems and recent resistance to colistin are major problems for our country and the world. In the literature, mechanical ventilation, hemodialysis[23], prior receipt of carbapenems and fluoroquinolones[24] and high SOFA score[25] were found to be independent risk factors for carbapenem resistant *Acinetobacter* infections. However, limited data is available about the risk factors for colistin-resistant *Acinetobacter sp*. infections. In a recently published study, prior use of colistin (OR = 155.95, 95%CI: 8.00-3041.98), carbapenems (OR = 12.84, 95%CI: 1.60-103.20) and a high Simplified Acute Physiology Score (OR = 1.10, 95%CI: 1.01-1.22) were found to be risk factors for VAP due to pan-drug resistant *A. baumannii*[25]. In our study, high APACHE II scores and prior teicoplanin receipt were found to be independent risk factors for colistin resistance. In another recently published multicenter study conducted in our country, prior carbapenem and fluoroquinolone usage was found to increase the risk of infection with colistin-resistant Gram-negative microorganisms. Their study population included not only colistin-resistant *A. baumannii* but also *Klebsiella pneumonia* and *Pseudomonas aeruginosa*[12]. In our study, finding that prior receipt of teicoplanin was an independent risk factor for colistin resistance may be worth exploring further, as a recent study found that teicoplanin appeared to enhance the activity of colistin in a mouse model. Although the authors suggested that the combination of colistin and teicoplanin may improve the therapy of multiresistant *A. baumannii* infection, this may lead to further infection due to colistin-resistant strains[26].

The mortality rate was higher in patients with multidrug resistant *Acinetobacter* strains. A systematic review of observational studies that included over 2500 patients with infection due to either carbapenem susceptible or resistant *Acinetobacter* strains found that the overall mortality rate was 33%, and, in this study, carbapenem resistance was found to increase mortality (pooled odds ratio 2.22, 95%CI: 1.66-2.98).

Table 1 Demographic data and clinical characteristics of patients with ventilator-associated pneumonia due to colistin-resistant and colistin-susceptible *Acinetobacter baumannii- calcoaceticus complex*

Variable	Total, *n* = 124	CRABC group, *n* = 16	CSABC group, *n* = 108	*P*-value
Male sex (%)	63 (50.8)	13 (81.3)	50 (46.3)	0.019
Age, med ± (min-max)	73.0 ± (18-91)	59.5 ± (18-86)	74.0 ± (18-91)	0.022
Comorbidity				
Diabetes mellitus (%)	35 (28.2)	5 (31.5)	30 (27.8)	0.771
Chronic renal failure (%)	11 (8.9)	0 (0.0)	11 (10.2)	0.356
Chronic obstructive lung disease (%)	33 (26.6)	4 (25.0)	29 (26.9)	1.000
Hypertension (%)	57 (46.0)	8 (50.0)	49 (45.4)	0.938
Congestive heart failure (%)	25 (20.2)	4 (25.0)	21 (19.4)	0.738
Malignity (%)	30 (24.2)	2 (12.5)	28 (25.9)	0.353
Cerebrovascular disease (%)	24 (19.4)	1 (6.3)	23 (21.3)	0.305
Trauma (%)	8 (6.5)	3 (18.8)	5 (4.6)	0.066
Operation (%)	24 (19.4)	2 (12.5)	22 (20.4)	0.735
Immunosuppression (%)	9 (7.3)	1 (6.3)	8 (7.4)	1.000
Obesity (%)	12 (9.7)	3 (18.8)	9 (8.3)	0.186
Duration of mechanical ventilation before diagnosis, med ± min-max	11 ± (2-450)	12 ± (4-50)	11 ± (2-450)	0.872
Total length of ICU stays, med ± min-max	45.5 ± (5-540)	49.0 ± (11-305)	43.0 ± (5-540)	0.685
Central venous catheterization (%)	67 (54.0)	9 (56.3)	58 (53.7)	1.000
Urethral catheterization (%)	114 (91.9)	14 (87.5)	100 (92.6)	0.616
Total parenteral nutrition (%)	21 (16.9)	6 (37.5)	15 (13.9)	0.030
Prior receipt of colistin (%)	11 (8.9)	6 (37.5)	5 (4.6)	0.001
Prior receipt of carbapenems (%)	68 (54.8)	10 (62.5)	58 (53.7)	0.696
Prior receipt of linezolid (%)	6 (4.8)	1 (6.3)	5 (4.6)	0.571
Prior receipt of ampicillin/sulbactam (%)	19 (15.3)	1 (6.3)	18 (16.7)	0.462
Prior receipt of flouroquinolones (%)	51 (41.1)	5 (31.3)	46 (42.6)	0.556
Prior receipt of teicoplanin (%)	25 (20.2)	6 (37.5)	19 (17.6)	0.091
Prior receipt of piperacillin/tazobactam (%)	19 (15.3)	1 (6.3)	18 (16.7)	0.462
Prior receipt of ceftriaxone (%)	9 (7.3)	0 (0.0)	9 (8.3)	0.603
Presence of bacteremia (%)	3 (2.4)	2 (12.5)	1 (0.9)	0.044
APACHE II scores, med ± min-max	14. 0 ± (5-28)	22.5 ± (17-28)	12.0 ± (5-22)	< 0.001
SOFA scores, med ± min-max	9.0 ± (3-20)	9 ± (7-18)	9 ± (3-20)	0.546
Clinical response (%)	71 (61.3)	11 (68.8)	65 (60.2)	0.703
Laboratory response (%)	82 (66.1)	13 (81.3)	69 (63.9)	0.277
Radiological response (%)	65 (52.4)	10 (62.5)	55 (52.9)	0.551
Microbiological response (%)	67 (54.0)	9 (56.3)	58 (53.7)	1.000
Duration of microbiological cure, med ± (min-max)	4 ± (2-10)	6 ± (3-10)	3 ± (2-7)	<0.001
In-hospital mortality (%)	77 (62.1)	6 (37.5)	71 (65.7)	0.058
VAP-related mortality (%)	50 (40.3)	5 (31.3)	45 (41.7)	0.603

VAP: Ventilator associated pneumonia; CRABC: Colistin resistant *Acinetobacter baumannii-calcoaceticus* complex; CSABC: Colistin susceptible *Acinetobacter baumannii-calcoaceticus* complex; APACHE: High Acute Physiology and Chronic Health Evaluation; SOFA: Sequential Organ Failure Assessment.

Since the patients with carbapenem-resistant infection were more likely to have severe comorbid diseases, or to receive inappropriate empiric antibiotic therapy, these were likely confounding variables that lead tan an increased mortality[27].

In our study, our strains were mostly carbapenem resistant (only seven isolates were susceptible to carbapenems). The median duration of microbiological cure was longer in patients with VAP due to CRABC. Although VAP-related mortality and in-hospital mortality rates were lower in the CRABC group, the differences were not statistically significant. We also did not find statistically significant differences in clinical, laboratory, radiological or microbiological responses between the two groups. In a recently published clinical trial, data from 266 patient isolates were evaluated (214 CSABC and 52 CRABC). Patients with colistin-resistant isolates had lower rates of mechanical ventilation. After adjusting for variables associated with mortality, they found a significantly lower mortality rate among patients with CRABC[28]. In our

Table 2 Clinical characteristics and antibiotic treatment combinations of patients with ventilator-associated pneumonia due to colistin-resistant *Acinetobacter baumannii - calcoaceticus complex* (part 1)

	Patients' number with ventilator associated pneumonia due to colistin-resistant *Acinetobacter baumannii-calcoaceticus complex*							
Isolate number of patients	1	2	3	4	5	6	7	8
Culture location	TA	BAL	TA	TA	TA	BAL	TA	BAL
Phenotype of isolate	1	1	1	1	1	1	1	2
MIC of isolate	8	> 256	4	6	4	> 256	> 256	> 256
Treatment	1	1	1	1	2	3	2	2
Clinical response	Yes	Yes	No	No	Yes	Yes	No	Yes
Laboratory response	Yes	Yes	No	Yes	Yes	Yes	Yes	Yes
Radiological response	Yes	Yes	No	No	Yes	Yes	No	Yes
Microbiological response	Yes	Yes	No	No	Yes	Yes	Yes	Yes
VAP-related mortality	No	No	Yes	No	No	No	Yes	No

Treatment 1: meropenem + colistin, Treatment 2: meropenem + ampicillin/sulbactam, Treatment 3: colistin + amikacin. MIC: Minimum inhibitory concentration; VAP: Ventilator-associated pneumonia; BAL: Bronchoalveolar lavage; TA: Tracheal aspirate.

study, although the mortality rate did not statistically differ between the patients with CSABC and CRABC, the VAP-related mortality rate for all study patients was quite high.

In clinical trials, a combination of antimicrobials is frequently preferred for treatment of *Acinetobacter sp*. infections. Although it seems that an appropriate approach is to cover resistant strains before antimicrobial susceptibility testing is available, there are no clear clinical data supporting this strategy. However, some studies suggest combination therapy may improve the outcome of infections with resistant *Acinetobacter sp*. strains[29-31]. Treatment of patients with pan-drug-resistant strains is a major emerging problem for clinicians. Combination therapies including ampicillin/sulbactam, carbapenems, minocycline, tigecycline, rifampicin and vancomycin might be administered to patients with pan-drug-resistant strains as a salvage therapy[2,10]. In our study, different combinations of colistin, meropenem, sulbactam, amikacin and trimethoprim/sulfamethoxazole were used for treatment of patients with CRABC as salvage therapies. The combination of meropenem and colistin, and the combination of meropenem and ampicillin/sulbactam, were the most commonly used regimens. Seven patients were treated with meropenem and colistin. Microbiological (2/7) and clinical (3/7) response rates were very low with this treatment. The meropenem and ampicillin/sulbactam combination was administered to four patients. Microbiological eradication and clinical response were obtained from three of them. Among the VAP patients with CRABC, seven were treated with antibiotic combinations including sulbactam. Clinical (6/7) and microbiological (5/7) response rates were quite high in these patients. Although it is difficult to draw a firm conclusion about the optimal antibiotic treatment due to the small sample size of our CRABC group, combinations including sulbactam seem to yield better clinical response and microbiological eradication.

Limitations

Our study has some limitations including that it was a retrospective study with a small sample size for the colistin-resistant group and the difficulty in the diagnosis of VAP and in the evaluation of the outcomes in critically ill patients with comorbidities.

Conclusions

We found a high APACHE II score and usage of teicoplanin to be risk factors for colistin resistance. No data are available for the optimal therapy regimen for resistant strains. Various antibiotic combinations might be given to patients with infections due to CRABC as salvage therapies. Among colistin-resistant group, the clinical responses were better with antibiotic combinations including sulbactam. As very limited data to support the usefulness of combination therapies with sulbactam is available, management in these patients should be individualized, and further comparative clinical studies are needed to identify optimal treatment regimens.

Table 3 Clinical Characteristics and Antibiotic treatment combinations of patients with ventilator-associated pneumonia due to colistin-resistant *Acinetobacter baumannii - calcoaceticus complex* (part 2)

Variables	Patients' number with ventilator associated pneumonia due to colistin-resistant *Acinetobacter baumannii-calcoaceticus complex*							
Isolate number of patients	9	10	11	12	13	14	15	16
Culture location	TA	TA	TA	TA	TA	TA	BAL	TA
Phenotype of isolate	3	4	3	1	1	4	4	1
MIC of isolate	> 256	32	> 256	16	6	8	24	4
Treatment	4	5	1	1	2	7	6	1
Clinical response	Yes	Yes	No	Yes	Yes	Yes	Yes	No
Laboratory response	Yes	Yes	No	Yes	Yes	Yes	Yes	No
Radiological response	Yes	Yes	No	Yes	No	Yes	Yes	No
Microbiological response	Yes	Yes	No	No	No	No	Yes	No
VAP related mortality	No	No	Yes	No	Yes	No	No	Yes

Treatment 1: meropenem + colistin, Treatment 2: meropenem + ampicillin/sulbactam, Treatment 4: colistin + ampicillin/sulbactam + trimethoprim/sulfamethoxazole, Treatment 5: colistin + ampicillin/sulbactam, Treatment 6: meropenem + trimethoprim/sulfamethoxazole, Treatment 7: meropenem + sulbactam + trimethoprim/sulfamethoxazole. MIC: Minimum inhibitory concentration; VAP: Ventilator-associated pneumonia; BAL: Bronchoalveolar lavage; TA: Tracheal aspirate.

Table 4 Phenotypes of colistin-resistant *Acinetobacter sp.* isolates

Isolate number of patients	AN	CN	TOB	SAM	STX	IPM	MEM	CAZ	CIP	TZP
1	R	R	R	R	R	R	R	R	R	R
2	R	R	R	R	R	R	R	R	R	R
3	R	R	R	R	R	R	R	R	R	R
4	R	R	R	R	R	R	R	R	R	R
5	R	R	R	R	R	R	R	R	R	R
6	R	R	R	R	R	R	R	R	R	R
7	R	R	R	R	R	R	R	R	R	R
8	R	R	S	R	R	R	R	R	R	R
9	R	S	R	R	R	R	R	R	R	R
10	R	R	R	R	S	R	R	R	R	R
11	R	S	R	R	R	R	R	R	R	R
12	R	R	R	R	R	R	R	R	R	R
13	R	R	R	R	R	R	R	R	R	R
14	R	R	R	R	S	R	R	R	R	R
15	R	R	R	R	S	R	R	R	R	R
16	R	R	R	R	R	R	R	R	R	R

CO: Colistin; AN: Amikacin; CN: Gentamicin; TOB: Tobramycin; TE: Tetracycline; IPM: Imipenem; LEV: Levofloxacin; SXT: Trimetoprim-sulfamethoxazole; CIP: Ciprofloxacin; MEM: Meropenem; PIP: Piperacillin; TZP: Piperacillin-tazobactam; FEP: Sefepim; CAZ: Ceftazidim; SAM: Sulbactam-ampicillin; R: Resistant; S: Susceptible.

ARTICLE HIGHLIGHTS

Research background

Acinetobacter species are simultaneously resistant to many antimicrobial agents, and treatment options are extremely limited. Although colistin appears to be the only remaining therapeutic option for extensively-resistant *Acinetobacter* infections, colistin resistance in *Acinetobacter* strains has been reported worldwide. Knowledge of the risk factors is important for colistin resistance. This study highlights risk factors of colistin resistance and salvage therapies in *Acinetobacter sp*. Infections.

Research motivation

Infections with resistant *Acinetobacter* strains were found to be associated with high mortality

rates. Combination therapies were commonly recommended since resistance could develop during therapies. The main goals for control of multidrug-resistant *Acinetobacter* should be early recognition, knowing risk factors, aggressive control of spread of the resistant strains. The problem for treatment of nosocomial infections with extensively- or pandrug-resistant *Acinetobacter* strains may be solved in future with development of new antimicrobial agents targeting these resistant strains.

Research objectives

In our study we evaluated the clinical responses and the outcomes of ventilator-associated pneumonia (VAP) patients with resistant *Acinetobacter* strains. The risk factors for colistin resistance were also investigated.

Research methods

Between January 2015 and April 2018, 108 patients with VAP due to colistin-susceptible strains and 16 patients with colistin-resistant strains were included in this study retrospectively. These two groups were compared for the age, sex, comorbidities, prior receipt of antibiotics, mortality rates, APACHE II and SOFA scores, duration of microbiological cure and the clinical, laboratory, radiological, and microbiological responses. Mann-Whitney *U* test was used to compare continuous variables whereas Pearson's χ^2 test or Fisher's Exact χ^2 test was used to compare the categorical variables. The potential independent risk factors for infection with colistin resistant strains were identified by using a binary logistic regression model.

Research results

The median duration of microbiological cure ($P < 0.001$) was longer in colistin-resistant group. Clinical ($P = 0.703$), laboratory ($P = 0.277$), radiological ($P = 0.551$), microbiological response ($P = 1.000$) and infection related mortality rates ($P = 0.603$) did not differ between patients with pneumonia due to colistin-resistant and colistin-susceptible strains. Independent risk factors for pneumonia with colistin-resistant *Acinetobacter* strains were found to be high APACHE II scores (OR = 1.9, 95%CI: 1.4-2.7; $P < 0.001$) and prior receipt of teicoplanin (OR = 8.1, 95%CI: 1.0-63.3; $P = 0.045$). Different combination of antibiotic regimens included colistin, meropenem, ampicillin/sulbactam, amikacin and trimetoprim/sulfamethoxazole were given to patients with colistin-resistant strains. Among patients with infection due to colistin-resistant strains, seven of them were treated with antibiotic combinations included sulbactam. Clinical (6/7) and microbiological (5/7) response rates were quite high in these patients. Very limited data is available for the optimal therapy regimens of infections with pandrug-resistant *Acinetobacter* strains. Individual treatment combinations may be given to the patients with infection due to colistin-resistant *Acinetobacter* strains.

Research conclusions

High APACHE II scores and prior teicoplanin usage were found to be the risk factors for pneumonia due to colistin resistant *Acinetobacter* strains. Statistically significant difference was not found between the mortality rates of the patients with colistin-susceptible and colistin-resistant strains. Combination antibiotic regimens including sulbactam seemed to be more useful. Further prospective studies are needed to evaluate the optimal therapy regimens. As prior usage of teicoplanin was found to be an independent factor for colistin resistance, patients should be carefully treated with teicoplanin empirically.

Research perspectives

Prospective randomized-controlled studies investigating optimal therapy regimens or new antimicrobials targeting colistin resistant *Acinetobacter* strains are needed. Risk factors for colistin resistance should be well known and strict prevention and control methods should be used in intensive care units.

REFERENCES

1 **Rossi F**, Girardello R, Cury AP, Di Gioia TS, Almeida JN, Duarte AJ. Emergence of colistin resistance in the largest university hospital complex of São Paulo, Brazil, over five years. *Braz J Infect Dis* 2017; **21**: 98-101 [PMID: 27832961 DOI: 10.1016/j.bjid.2016.09.011]

2 **Clark NM**, Zhanel GG, Lynch JP. Emergence of antimicrobial resistance among Acinetobacter species: a global threat. *Curr Opin Crit Care* 2016; **22**: 491-499 [PMID: 27552304 DOI: 10.1097/MCC.0000000000000337]

3 **Vincent JL**, Rello J, Marshall J, Silva E, Anzueto A, Martin CD, Moreno R, Lipman J, Gomersall C, Sakr Y, Reinhart K; EPIC II Group of Investigators. International study of the prevalence and outcomes of infection in intensive care units. *JAMA* 2009; **302**: 2323-2329 [PMID: 19952319 DOI: 10.1001/jama.2009.1754]

4 **Chuang YC**, Sheng WH, Li SY, Lin YC, Wang JT, Chen YC, Chang SC. Influence of genospecies of Acinetobacter baumannii complex on clinical outcomes of patients with acinetobacter bacteremia. *Clin Infect Dis* 2011; **52**: 352-360 [PMID: 21193494 DOI: 10.1093/cid/ciq154]

5 **Evren E**. Cesitli Klinik Orneklerden Izole Edilen Coklu Ilaca Direncli Acinetobacter baumannii Suslarinin Imipenem, Meropenem, Kolistin, Amikasin ve Fosfomisin Duyarliliklari. *GMJ* 2013; **24**: 1-4 [DOI: 10.12996/gmj.2013.01]

6 **Naldan ME**, Coşkun MV, Ünal O, Karasahin O, Vural MK. Evaluation of Gram-negative bacilli isolated from patients in intensive care units. *Turk J Intense Care* 2017; **15**: 117-123 [DOI: 10.4274/tybd.15238]

7 **Ogutlu A**, Guclu E, Karabay O, Utku AC, Tuna N, Yahyaoglu M. Effects of Carbapenem consumption on the prevalence of Acinetobacter infection in intensive care unit patients. *Ann Clin Microbiol Antimicrob*

2014; **13**: 7 [PMID: 24405720 DOI: 10.1186/1476-0711-13-7]
8 **Cakirlar FK**, Ciftci IH, Gonullu N. OXA-type Carbapenemases and Susceptibility of Colistin and Tigecycline Among Carbapenem-Resistant Acinetobacter Baumannii Isolates from Patients with Bacteremia in Turkey. *Clin Lab* 2015; **61**: 741-747 [PMID: 26299073 DOI: 10.7754/Clin.Lab.2014.141116]
9 **Shojaei L**, Mohammadi M, Beigmohammadi MT, Doomanlou M, Abdollahi A, Feizabadi MM, Khalili H. Clinical response and outcome of pneumonia due to multi-drug resistant Acinetobacter baumannii in critically ill patients. *Iran J Microbiol* 2016; **8**: 288-297 [PMID: 28149487]
10 **Leite GC**, Oliveira MS, Perdigão-Neto LV, Rocha CK, Guimarães T, Rizek C, Levin AS, Costa SF. Antimicrobial Combinations against Pan-Resistant Acinetobacter baumannii Isolates with Different Resistance Mechanisms. *PLoS One* 2016; **11**: e0151270 [PMID: 26998609 DOI: 10.1371/journal.pone.0151270]
11 **Hong DJ**, Kim JO, Lee H, Yoon EJ, Jeong SH, Yong D, Lee K. In vitro antimicrobial synergy of colistin with rifampicin and carbapenems against colistin-resistant Acinetobacter baumannii clinical isolates. *Diagn Microbiol Infect Dis* 2016; **86**: 184-189 [PMID: 27475960 DOI: 10.1016/j.diagmicrobio.2016.07.017]
12 **Yilmaz GR**, Dizbay M, Guven T, Pullukcu H, Tasbakan M, Guzel OT, Tekce YT, Ozden M, Turhan O, Guner R, Cag Y, Bozkurt F, Karadag FY, Kartal ED, Gozel G, Bulut C, Erdinc S, Keske S, Acikgoz ZC, Tasyaran MA. Risk factors for infection with colistin-resistant gram-negative microorganisms: a multicenter study. *Ann Saudi Med* 2016; **36**: 216-222 [PMID: 27236394 DOI: 10.5144/0256-4947.2016.216]
13 **Oliva A**, Cipolla A, Vullo V, Venditti M, Mastroianni CM, Falcone M. Clinical and in vitro efficacy of colistin plus vancomycin and rifampin against colistin-resistant Acinetobacter baumannii causing ventilator-associated pneumonia. *New Microbiol* 2017; **40**: 205-207 [PMID: 28675246]
14 **Peleg AY**, Seifert H, Paterson DL. Acinetobacter baumannii: emergence of a successful pathogen. *Clin Microbiol Rev* 2008; **21**: 538-582 [PMID: 18625687 DOI: 10.1128/CMR.00058-07]
15 **Garnacho-Montero J**, Ortiz-Leyba C, Jiménez-Jiménez FJ, Barrero-Almodóvar AE, García-Garmendia JL, Bernabeu-Wittell M, Gallego-Lara SL, Madrazo-Osuna J. Treatment of multidrug-resistant Acinetobacter baumannii ventilator-associated pneumonia (VAP) with intravenous colistin: a comparison with imipenem-susceptible VAP. *Clin Infect Dis* 2003; **36**: 1111-1118 [PMID: 12715304 DOI: 10.1086/374337]
16 **Motaouakkil S**, Charra B, Hachimi A, Nejmi H, Benslama A, Elmdaghri N, Belabbes H, Benbachir M. Colistin and rifampicin in the treatment of nosocomial infections from multiresistant Acinetobacter baumannii. *J Infect* 2006; **53**: 274-278 [PMID: 16442632 DOI: 10.1016/j.jinf.2005.11.019]
17 **American Thoracic Society**. Infectious Diseases Society of America. Guidelines for the management of adults with hospital-acquired, ventilator-associated, and healthcare-associated pneumonia. *Am J Respir Crit Care Med* 2005; **171**: 388-416 [PMID: 15699079 DOI: 10.1164/rccm.200405-644ST]
18 **Clinical and Laboratory Standards Institute**. Performance standards for antimicrobials susceptibility testing; 24th informational supplement. Approved standard M100-S24. Wayne, PA: CLSI; 2014.
19 **Welsh J**, McClelland M. Characterization of pathogenic microorganisms by genomic fingerprinting used arbitrarily primed PCR. In: Persing HD, Smith TF, Tenover FC, White TJ, editors. Diagnostic molecular microbiology: principles and applications. Washington, DC: American Society for Microbiology 1993; 595-602
20 **Grundmann HJ**, Towner KJ, Dijkshoorn L, Gerner-Smidt P, Maher M, Seifert H, Vaneechoutte M. Multicenter study using standardized protocols and reagents for evaluation of reproducibility of PCR-based fingerprinting of Acinetobacter spp. *J Clin Microbiol* 1997; **35**: 3071-3077 [PMID: 9399496]
21 **Qureshi ZA**, Hittle LE, O'Hara JA, Rivera JI, Syed A, Shields RK, Pasculle AW, Ernst RK, Doi Y. Colistin-resistant Acinetobacter baumannii: beyond carbapenem resistance. *Clin Infect Dis* 2015; **60**: 1295-1303 [PMID: 25632010 DOI: 10.1093/cid/civ048]
22 **Nowak J**, Zander E, Stefanik D, Higgins PG, Roca I, Vila J, McConnell MJ, Cisneros JM, Seifert H, MagicBullet Working Group WP4. High incidence of pandrug-resistant Acinetobacter baumannii isolates collected from patients with ventilator-associated pneumonia in Greece, Italy and Spain as part of the MagicBullet clinical trial. *J Antimicrob Chemother* 2017; **72**: 3277-3282 [PMID: 28961773 DOI: 10.1093/jac/dkx322]
23 **Dizbay M**, Tunccan OG, Sezer BE, Hizel K. Nosocomial imipenem-resistant Acinetobacter baumannii infections: epidemiology and risk factors. *Scand J Infect Dis* 2010; **42**: 741-746 [PMID: 20500117 DOI: 10.3109/00365548.2010.489568]
24 **Vitkauskiene A**, Dambrauskiene A, Cerniauskiene K, Rimdeika R, Sakalauskas R. Risk factors and outcomes in patients with carbapenem-resistant Acinetobacter infection. *Scand J Infect Dis* 2013; **45**: 213-218 [PMID: 23113773 DOI: 10.3109/00365548.2012.724178]
25 **Inchai J**, Liwsrisakun C, Theerakittikul T, Chaiwarith R, Khositsakulchai W, Pothirat C. Risk factors of multidrug-resistant, extensively drug-resistant and pandrug-resistant Acinetobacter baumannii ventilator-associated pneumonia in a Medical Intensive Care Unit of University Hospital in Thailand. *J Infect Chemother* 2015; **21**: 570-574 [PMID: 26026660 DOI: 10.1016/j.jiac.2015.04.010]
26 **Cirioni O**, Simonetti O, Pierpaoli E, Barucca A, Ghiselli R, Orlando F, Pelloni M, Trombettoni MM, Guerrieri M, Offidani A, Giacometti A, Provinciali M. Colistin enhances therapeutic efficacy of daptomycin or teicoplanin in a murine model of multiresistant Acinetobacter baumannii sepsis. *Diagn Microbiol Infect Dis* 2016; **86**: 392-398 [PMID: 27712928 DOI: 10.1016/j.diagmicrobio.2016.09.010]
27 **Lemos EV**, de la Hoz FP, Einarson TR, McGhan WF, Quevedo E, Castañeda C, Kawai K. Carbapenem resistance and mortality in patients with Acinetobacter baumannii infection: systematic review and meta-analysis. *Clin Microbiol Infect* 2014; **20**: 416-423 [PMID: 24131374 DOI: 10.1111/1469-0691.12363]
28 **Dickstein Y**, Lellouche J, Dalak Amar MB, Schwartz D, Nutman A, Daitch V, Yahav D, Leibovici L, Skiada A, Antoniadou A, Daikos GL, Andini R, Zampino R, Durante-Mangoni E, Mouton JW, Friberg LE, Benattar YD, Bitterman R, Neuberger A, Carmeli Y, Paul M; AIDA study group. Treatment outcomes of colistin and carbapenem-resistant Acinetobacter baumannii infections: an exploratory subgroup analysis of a randomized clinical trial. *Clin Infect Dis* 2018 [PMID: 30462182 DOI: 10.1093/cid/ciy988]
29 **Özvatan T**, Akalın H, Sınırtaş M, Ocakoğlu G, Yılmaz E, Heper Y, Kelebek N, İşçimen R, Kahveci F. Nosocomial Acinetobacter pneumonia: Treatment and prognostic factors in 356 cases. *Respirology* 2016; **21**: 363-369 [PMID: 26635315 DOI: 10.1111/resp.12698]
30 **Rigatto MH**, Vieira FJ, Antochevis LC, Behle TF, Lopes NT, Zavascki AP. Polymyxin B in Combination with Antimicrobials Lacking In Vitro Activity versus Polymyxin B in Monotherapy in Critically Ill

Patients with Acinetobacter baumannii or Pseudomonas aeruginosa Infections. *Antimicrob Agents Chemother* 2015; **59**: 6575-6580 [PMID: 26259799 DOI: 10.1128/AAC.00494-15]

31 **Wood GC**, Hanes SD, Croce MA, Fabian TC, Boucher BA. Comparison of ampicillin-sulbactam and imipenem-cilastatin for the treatment of acinetobacter ventilator-associated pneumonia. *Clin Infect Dis* 2002; **34**: 1425-1430 [PMID: 12015687 DOI: 10.1086/340055]

World Journal of Clinical Cases

Submit a Manuscript: https://www.f6publishing.com

World J Clin Cases 2019 May 26; 7(10): 1122-1132

DOI: 10.12998/wjcc.v7.i10.1122

ISSN 2307-8960 (online)

ORIGINAL ARTICLE

Observational Study

Diagnostic value of two dimensional shear wave elastography combined with texture analysis in early liver fibrosis

Zhao-Cheng Jian, Jin-Feng Long, Yu-Jiang Liu, Xiang-Dong Hu, Ji-Bin Liu, Xian-Quan Shi, Wei-Sheng Li, Lin-Xue Qian

ORCID number: Zhao-Cheng Jian (0000-0003-0159-507X); Jin-Feng Long (0000-0001-7929-8433); Yu-Jiang Liu (0000-0002-4007-4413); Xiang-Dong Hu (0000-0001-5496-6685); Ji-Bin Liu (0000-0003-2979-9162); Xian-Quan Shi (0000-0002-7424-0360); Wei-Sheng Li (0000-0002-0961-1559); Lin-Xue Qian (0000-0001-7116-0608).

Author contributions: All authors helped to perform the research; Jian ZC manuscript writing, performing procedures and data analysis; Long JF contribution to writing the manuscript, performing experiments, and data analysis; Liu YJ and Hu XD contribution to performing experiments; Liu JB contribution to writing the manuscript; Shi XQ and Li WS contribution to data analysis; Qian LX manuscript writing, drafting conception and design, performing experiments, and data analysis.

Institutional review board statement: This study was reviewed and approved by the Ethics Committee of Beijing Friendship Hospital, Capital Medical University.

Informed consent statement: Patient's informed consent was obtained before the study,though the clinical data used in this study were anonymous.

Conflict-of-interest statement: All authors declare no conflicts-of-interest related to this article.

Zhao-Cheng Jian, Yu-Jiang Liu, Xiang-Dong Hu, Xian-Quan Shi, Wei-Sheng Li, Lin-Xue Qian, Department of Ultrasound, Beijing Friendship Hospital, Capital Medical University, Beijing 100050, China

Zhao-Cheng Jian, Jin-Feng Long, Medical Imaging Center, Affiliated Hospital of Weifang Medical University, Weifang 261031, Shandong Province, China

Ji-Bin Liu, Institute of Ultrasound, Thomas Jefferson University Hospital, Philadelphia, PA 19107, United States

Corresponding author: Lin-Xue Qian, MD, Chief Doctor, Department of Ultrasound, Beijing Friendship Hospital, Capital Medical University, No. 95 Yongan Road, Xicheng District, Beijing 100050, China. qianlinxue2002@163.com
Telephone: +86-13562645007
Fax: +86-10-63138576

Abstract

BACKGROUND

Staging diagnosis of liver fibrosis is a prerequisite for timely diagnosis and therapy in patients with chronic hepatitis B. In recent years, ultrasound elastography has become an important method for clinical noninvasive assessment of liver fibrosis stage, but its diagnostic value for early liver fibrosis still needs to be further improved. In this study, the texture analysis was carried out on the basis of two dimensional shear wave elastography (2D-SWE), and the feasibility of 2D-SWE plus texture analysis in the diagnosis of early liver fibrosis was discussed.

AIM

To assess the diagnostic value of 2D-SWE combined with textural analysis in liver fibrosis staging.

METHODS

This study recruited 46 patients with chronic hepatitis B. Patients underwent 2D-SWE and texture analysis; Young's modulus values and textural patterns were obtained, respectively. Textural pattern was analyzed with regard to contrast, correlation, angular second moment (ASM), and homogeneity. Pathological results of biopsy specimens were the gold standard; comparison and assessment of the diagnosis efficiency were conducted for 2D-SWE, texture analysis and their combination.

Data sharing statement: No additional data are available.

STROBE statement: The authors have read the STROBE Statement—checklist of items, and the manuscript was prepared and revised according to the STROBE Statement—checklist of items.

Manuscript source: Unsolicited manuscript

Received: February 2, 2019
Peer-review started: February 2, 2019
First decision: March 10, 2019
Revised: March 19, 2019
Accepted: April 8, 2019
Article in press: April 9, 2019
Published online: May 26, 2019

P-Reviewer: Chamberlain MC, Gilbert MR, Jones G
S-Editor: Wang JL
L-Editor: A
E-Editor: Wu YXJ

RESULTS

2D-SWE displayed diagnosis efficiency in early fibrosis, significant fibrosis, severe fibrosis, and early cirrhosis (AUC > 0.7, $P < 0.05$) with respective AUC values of 0.823 (0.678-0.921), 0.808 (0.662-0.911), 0.920 (0.798-0.980), and 0.855 (0.716-0.943). Contrast and homogeneity displayed independent diagnosis efficiency in liver fibrosis stage (AUC > 0.7, $P < 0.05$), whereas correlation and ASM showed limited values. AUC of contrast and homogeneity were respectively 0.906 (0.779-0.973), 0.835 (0.693-0.930), 0.807 (0.660-0.910) and 0.925 (0.805-0.983), 0.789 (0.639-0.897), 0.736 (0.582-0.858), 0.705 (0.549-0.883) and 0.798 (0.650-0.904) in four liver fibrosis stages, which exhibited equivalence to 2D-SWE in diagnostic efficiency ($P > 0.05$). Combined diagnosis (PRE) displayed diagnostic efficiency (AUC > 0.7, $P < 0.01$) for all fibrosis stages with respective AUC of 0.952 (0.841-0.994), 0.896 (0.766-0.967), 0.978 (0.881-0.999), 0.947 (0.835-0.992). The combined diagnosis showed higher diagnosis efficiency over 2D-SWE in early liver fibrosis ($P < 0.05$), whereas no significant differences were observed in other comparisons ($P > 0.05$).

CONCLUSION

Texture analysis was capable of diagnosing liver fibrosis stage, combined diagnosis had obvious advantages in early liver fibrosis, liver fibrosis stage might be related to the hepatic tissue hardness distribution.

Key words: Elastography; Two-dimensional shear wave; Texture analysis; Liver fibrosis, Staging

Core tip: This study explored the diagnostic value of texture analysis in early liver fibrosis in patients with chronic hepatitis B on the basis of two dimensional shear wave elastography. It demonstrated that texture analysis was capable of diagnosing liver fibrosis, combined diagnosis had obvious advantages in early liver fibrosis, and the liver fibrosis stage might be related to the spatial heterogeneity of hepatic tissue hardness distribution.

Citation: Jian ZC, Long JF, Liu YJ, Hu XD, Liu JB, Shi XQ, Li WS, Qian LX. Diagnostic value of two dimensional shear wave elastography combined with texture analysis in early liver fibrosis. *World J Clin Cases* 2019; 7(10): 1122-1132
URL: https://www.wjgnet.com/2307-8960/full/v7/i10/1122.htm
DOI: https://dx.doi.org/10.12998/wjcc.v7.i10.1122

INTRODUCTION

Liver fibrosis is an important stage in the development of chronic hepatitis B. Its progression can be halted or even reversed by early diagnosis, dynamic assessment and effective treatment. Identification of the fibrosis stage is thus an essential requisite for timely diagnosis and therapy[1]. Liver biopsy is considered the gold standard for diagnosis of cirrhosis and staging of fibrosis; however, biopsy is an invasive procedure the clinical application of which is restrained due to poor patient compliance and sampling error[2,3]. Hence, an accurate and non-invasive method to determine fibrosis stage is urgently required in the clinic. Ultrasound elastography is rapidly advancing and is becoming an important clinical measure for the detection of liver fibrosis stage[4].This is demonstrated by the clinical guidelines published by the European Federation of Societies for Ultrasound in Medicine and Biology[5] and World Federation for Ultrasound in Medicine and Biology[6]. At present, transient elastography (TE) and two dimensional shear wave elastography (2D-SWE) are hot topics. This is demonstrated by previous studies[7,8] involving the diagnosis of liver fibrosis which focused on significant liver fibrosis (≥ F2), whereas less has been reported regarding the diagnosis of early liver fibrosis (F1). In this study, on the basis of 2D-SWE in patients with chronic hepatitis B, the textural features of the designated elastic image were derived from gray-level co-occurrence matrix (GLCM) built by

texture analysis software. These results were compared with pathological results of liver biopsies and statistical analyses were conducted to explore the feasibility of 2D-SWE plus texture analysis in the diagnosis of early liver fibrosis stage.

MATERIALS AND METHODS

Subjects

This study recruited patients with chronic hepatitis B who were scheduled for percutaneous liver biopsy at Beijing Friendship Hospital, Capital Medical University (Beijing, China) between September 2016 and September 2017 and included 20 males and 26 females with ages ranging from 15-71 years (mean age of 45.1 ± 13.5 years). Exclusion criteria were patients in whom elastography failed or biopsy specimens didn't meet the quality requirements for pathological diagnosis. This study was reviewed and approved by the Ethical Committee of Beijing Friendship Hospital, Capital Medical University. All patients or their guardians signed the informed consent.

Instruments and methods

Instruments and parameter set-up: SuperSonic Imagine Aixplorer ultrasound system(Aixplore®, SuperSonic Imagine, Ain-en-Provence, France) was used with parameters as follows: SC6-1 convex lens probe and probe frequency of 1-6 MHz; image depth of 8 cm, image enlargement to 120%; elastography sampling frame at 4 cm × 3 cm; region of interest (ROI) of 15 ± 2 mm; elastic measurement scale of 40 kPa; 2D image elastic images arrayed up and down, elastography sampling frame was placed on the image center.

Ultrasonography: Eight hours of fasting was ordered before ultrasonography. Patients were in the supine position with right upper limb lifted to increase the width of the intercostal space. On the right intercostal space, the right lower sections of the anterior or posterior liver lobe was selected and the probe was properly pressed to clearly display the image while avoiding large intrahepatic ducts. The upper edge of the elastography sampling frame was positioned about 1 cm below the liver capsule. Patients were asked to hold breathing for 3-5 s under the condition of calm respiration. The 2D-SWE mode was switched on and images were frozen upon stabile elastic images followed by storage of raw images and measurement and documentation of the mean values (kPa) within ROI. The criteria for elastography failure were: the color filling defect in the elastography sampling frame exceeded half area or the minimum value in ROI was zero. Each patient was measured 3 times, and 3 raw images (for subsequent texture analysis) were stored to yield 3 values of the Young's modulus and the mean value was calculated as well. All patients were examined by the same senior clinician who specialized in ultrasound for more than 5 years and was expert at ultrasound elastography. Data collection was performed by the same clinician as well.

Texture analysis: Texture analysis software (SSI_Toll_Tsinghua, Tsinghua, Beijing, China) was used to delineate the filling area (without filling the defect area) on the raw elastic image. The textural features of the designated area were derived *via* constructing a GLCM. In addition, 4 sets of indexes were acquired from 4 different angles (0°, 45°, 135°, and 180°) including contrast, correlation, angular second moment (ASM), and homogeneity. The mean values were calculated. Figure 1 illustrates the analysis process. Each patient was measured 3 times, and the individual mean values of contrast, correlation, ASM, and homogeneity were calculated.

Percutaneous liver biopsy: Ultrasound-guided liver biopsy was performed in all patients. The elastography sampling frame region was the biopsy target, and liver tissue of 1.5-2.5 cm length was collected using a 16G biopsy needle (MG1522, Bard, Murray Hill, New Jersey, USA). Under a microscope, more than 10 complete portal areas were collected, and specimens with fractured liver tissue were excluded. Needle biopsies were made 2-3 times for each patient, and collected tissues were fixed in formaldehyde solution prior to sectioning, HE staining, reticular fiber and Masson staining. Diagnosis was made jointly by 2 senior pathologists who reviewed the slides blinded. Liver fibrosis was staged to F0-F4 according to the METAVIR scoring system: F0 referred to no fibrosis; F1 referred to star-shaped enlargement of the portal area but without a fibrous septum; F2 referred to star-shaped enlargement of the portal area with a few fibrous septa; F3 referred to the presence of abundant fibrous septa but without pseudo-lobule formation; F4 referred to numerous fibrous septa with pseudo-lobule formation.

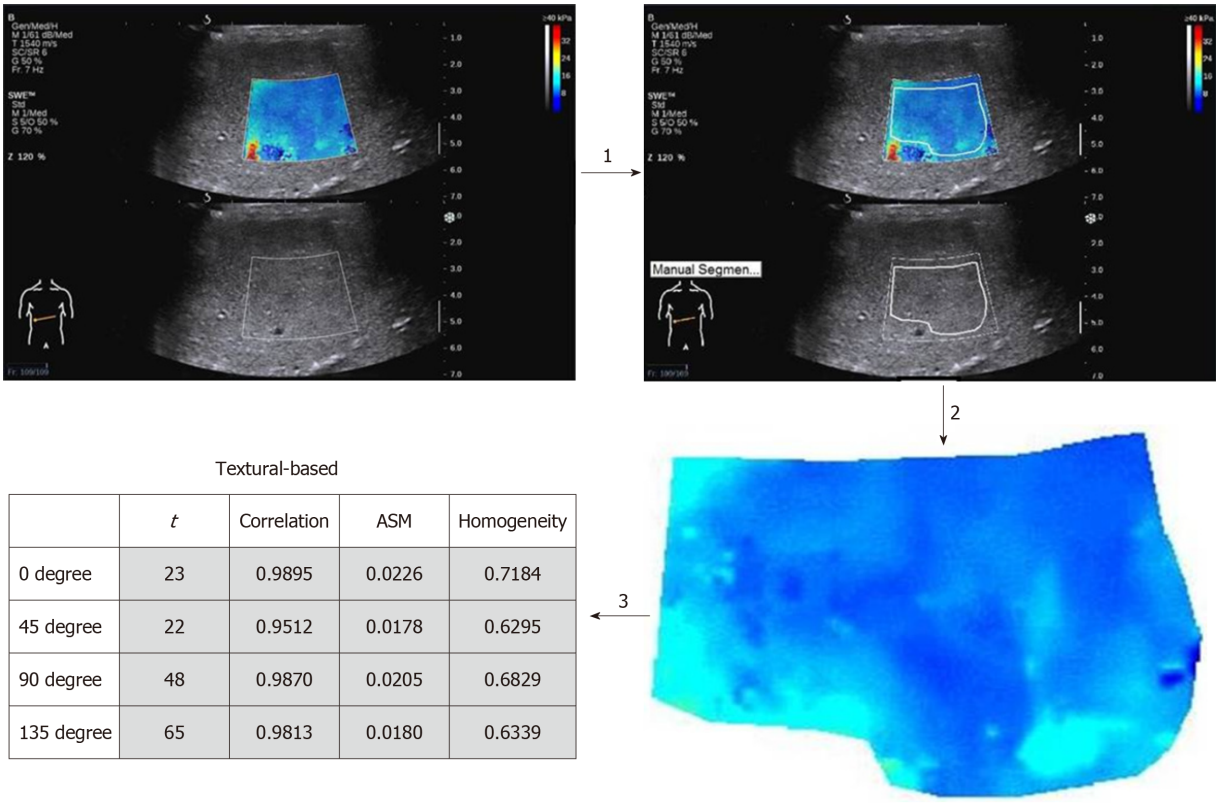

Textural-based

	t	Correlation	ASM	Homogeneity
0 degree	23	0.9895	0.0226	0.7184
45 degree	22	0.9512	0.0178	0.6295
90 degree	48	0.9870	0.0205	0.6829
135 degree	65	0.9813	0.0180	0.6339

Figure 1 Texture analysis process. Step 1, texture analysis software was used to delineate the filling area (without filling defect area) on the raw elastic image, avoiding vascular and biliary cavities. Step 2, a texture analysis image was generated. Step 3, 4 sets of indexes were acquired from 4 different angles (0°, 45°, 135°, and 180°), including contrast, correlation, angular second moment, and homogeneity. ASM: Angular second moment.

Grouping and inter-group comparisons: Based on the pathological results of liver biopsies, all eligible patients were allocated into different groups of liver fibrosis stages: early liver fibrosis group (≥ F1), significant fibrosis group (≥ F2), severe fibrosis group (≥ F3), and early cirrhosis group (F4). Inter-group comparisons were made accordingly as: F0 *vs* F1-4; F0-1 *vs* F2-4; F0-2 *vs* F3-4; F0-3 *vs* F4. Totally, statistical analyses were conducted for 4 groups to test the diagnosis efficiency of the aforementioned results in liver fibrosis stage.

Statistical analysis

Statistical analysis was conducted with SPSS 20.0 software (Version 20.0, SPSS Inc., Chicago, IL, USA) and MedCalc statistical software (Version 18.6, MedCalc software, Ostend, Belguim). Data were expressed by median and range, and a Mann-Whitney U test was adopted for making comparison between two independent groups, while Spearman's rank correlation coefficient was used to evaluate the correlation of individual variables with pathological stages. Predictive value (PRE) of combined diagnosis was calculated based on a logistic regression model. In addition, receiver operating characteristic (ROC) curves were plotted, followed by calculation of the area under the ROC curves (AUC) with 95%CI. Diagnostic efficacy was considered when AUC was greater than 0.7. Intra-group AUC comparisons for different variables were analyzed by Hanley and McNeil's method. The threshold value for diagnosis was determined by the highest critical point of Youden's index (YI). Intra-class correlation coefficients (ICC) were adopted to assess consistency in diagnosis, with ICC > 0.75 defined as a good consistency. $P < 0.05$ was considered statistically significant.

RESULTS

Pathological diagnosis

As shown in Table 1, among 46 patients, 44 cases were ultimately enrolled into this study. Two cases were excluded: one case due to failure of 2D-SWE (patient had poor compliance with breathing instruction which rendered filling the ROI less than 50%); the other case was due to fracture of liver biopsy tissue - patient rejected repeated

biopsy.

In 44 cases with complete data, pathological stages encompassed: F0 in 15 cases, F1 in 9 cases, F2 in 9 cases, F3 in 5 cases, and F4 in 6 cases.

Correlation of individual detection results with pathological stage and inter-group comparisons

Rank correlation: Rank correlation analysis displayed: pathological fibrosis stage was statistically correlated with the values of Young's modulus, contrast and homogeneity (r value of 0.659, 0.710 and -0.498, respectively, $P < 0.01$ for all indexes); no significant correlation was detected between pathological fibrosis stage and correlation or ASM (r values of -0.210 and -0.323, respectively).

Inter-group comparison for individual variables: As shown in Table 2, statistical differences were found in all inter-group comparisons for the values of Young's modulus, contrast and homogeneity ($P < 0.05$).

Comparing diagnosis efficiency of liver fibrosis stage

As shown in Figure 2, ROC curves for each group were constructed for 2D-SWE, contrast, correlation, ASM, homogeneity, and PRE of combined diagnosis, respectively. The diagnosis efficiency of each index was analyzed as well.

Diagnosis efficiency of 2D-SWE: 2D-SWE displayed diagnosis efficiency in early liver fibrosis (≥ F1), significant liver fibrosis (≥ F2), severe liver fibrosis (≥ F3), and early cirrhosis (F4) (AUC > 0.7, $P < 0.05$), with respective AUC of 0.823 (0.678-0.921), 0.808 (0.662-0.911), 0.920 (0.798-0.980) and 0.855 (0.716-0.943), and with cutoff values of 5.967, 8.667, 11.033 and 13.000 kPa. Table 3 shows sensitivity and specificity results.

Diagnosis efficiency of texture analysis: Contrast and homogeneity illustrated diagnosis efficiency in all stages of liver fibrosis (AUC > 0.7, $P < 0.05$). AUC of contrast in early liver fibrosis (≥ F1), significant liver fibrosis (≥ F2), severe fibrosis (≥ F3), and early cirrhosis (F4) groups were 0.906 (0.779-0.973), 0.835 (0.693-0.930), 0.807 (0.660-0.910), 0.925 (0.805-0.983); AUC of homogeneity in all stages of liver fibrosis were 0.789 (0.639-0.897), 0.736 (0.582-0.858), 0.705 (0.549-0.883), 0.798 (0.650-0.904) respectively. No significant differences were observed in all comparisons with 2D-SWE ($P > 0.05$). Table 3 presents cut-off values, sensitivity, and specificity.

Correlation and ASM showed poor diagnosis efficiency with the exception of ASM, which had diagnostic ability in the early cirrhosis group (AUC > 0.7, $P < 0.05$).

Diagnosis efficiency for combined diagnosis: PRE of combined diagnosis displayed efficiency in all stages of liver fibrosis (AUC > 0.7, $P < 0.01$). AUC in early liver fibrosis (≥ F1), significant liver fibrosis (≥ F2), severe fibrosis (≥ F3), and early stage of cirrhosis (F4) groups were 0.952 (0.841-0.994), 0.896 (0.766-0.967), 0.978 (0.881-0.999) and 0.947 (0.835-0.992), respectively. The combined diagnosis showed higher diagnosis efficiency over 2D-SWE in early liver fibrosis ($P < 0.05$), whereas no significant differences were observed in other comparisons ($P > 0.05$).The cut-off values, sensitivity, and specificity are listed in Table 3.

Assessment of consistency in individual detection results

Raw images of two measurements were randomly selected out of the F0 group, followed by consistency assessment in 2D-SWE and textural variables (contrast, correlation, ASM, homogeneity). ICC values were 0.88, 0.98, 0.97, 0.99and 0.99 (more than 0.75), respectively, indicating a good consistency in various detection results.

DISCUSSION

In recent years, the non-invasive detection technology of liver fibrosis has developed rapidly, especially the ultrasound elastography technology. Significant liver fibrosis and early liver cirrhosis were the focus of previous studies[9,10], which are considered as important markers of disease progression and initiation of treatment. However, hepatitis B virus DNA and alanine aminotransferase level are the main basis for the initiation of antiviral therapy of chronic hepatitis B patients[11,12], The diagnosis of liver fibrosis stage is more important as a means of disease monitoring and therapeutic effect evaluation, so the diagnosis of early liver fibrosis particularly important. Hepatic fibrosis is a dynamic process in which early liver fibrosis indicates the transition from quantitative to qualitative changes of the disease, and indicates that patients require more active monitoring and treatment. In view of this, the ultrasound elastography was combined with the application of texture analysis in this study in order to make progress in the diagnosis of early liver fibrosis.

Table 1 Distribution of patients with liver fibrosis

Pathological stage	Gender		Mean age (yr)
	Male	Female	
F0	7	8	36.8 ± 11.1
F1	6	3	39.8 ± 14.9
F2	3	6	52.4 ± 8.6
F3	2	3	49.4 ± 8.1
F4	2	4	59.3 ± 9.3

Ultrasound-based elastography technology as currently used widely in clinical applications are mainly TE and 2D-SWE. In clinical practice, TE is adopted universally[13], which manifests satisfactory diagnostic value to liver fibrosis stage[14,15]. Nonetheless, because TE is unable to display 2D sonography in real-time, the intrahepatic duct system could interfere with detection, and the measurement accuracy could be affected by the ribs, gas, ascites, and thick subcutaneous fat[16]. A previous study reported that failure of TE detection resulted in unreliable measurements that accounted for 16.3%[17]. 2D-SWE can detect the transmission speed of shear waves and generate images *via* super speed image processing technology that produces color elastic images of target tissue. The severity of liver fibrosis is quantified by Young's modulus. It avoids partial defects of TE and shows appropriate diagnosis efficiency[18,19] and reproducibility[9,20]. Our study revealed that the cutoff value of 2D-SWE was 8.667, 11.033, and 13.000 kPa in significant liver fibrosis (≥ F2), severe fibrosis (≥ F3), and early stage of cirrhosis (F4), respectively, while the sensitivity/specificity was accordingly 90.0%/58.3%, 90.9%/90.9%, and 83.3%/86.8%, which presents a stable diagnosis efficiency. Given that no liver function or other factors were taken into account for eligible patients enrolled in this study, our results were slightly divergent from previous studies[9,18-20]. Even though 2D-SWE can overcome some drawbacks associated with TE, the advantages of high sampling range, universal feasibility, and real-time 2D imaging also impose poor diagnosis efficiency in liver fibrosis. In this study, 2D-SWE illustrated some diagnostic value in liver fibrosis with low YI which was only 0.533, but with high-sensitivity and low specificity. It failed to meet the clinical requirements for diagnosis of early liver fibrosis.

Texture analysis is a process of extracting texture feature parameters by certain image processing techniques to obtain a quantitative or qualitative description of the texture. In previous ultrasound elastography studies, texture analysis has demonstrated advantages in the identification of carotid vulnerable plaques, thyroid and breast nodules[21,22]. In the 2D-SWE inspection, the elastic image is obtained by gray-scale coding of the information of Young's modulus. This study attempts to characterize the texture by extracting the spatial distribution of grayscale *via* creating a GLCM[23,24] and thereby reflecting the spatial statistical properties of Young's modulus. Then, combined with the Young's modulus value and the pathological results of liver fibrosis, the application value of texture features in the diagnosis of liver fibrosis was analyzed. Textural features encompass contrast, correlation, ASM, and homogeneity. Contrast refers to measurements of local variations in the image; correlation means the linear correlation of gray levels in the image; ASM reflects the order of gray levels in the image; homogeneity, which is also called inverse torque, represents measurement of proximity between element and the diagonal in GLCM and reflects uniformity of the image[25]. In our study, contrast was positively correlated with liver fibrosis stage, while homogeneity was negatively correlated with liver fibrosis stage. As the degree of liver fibrosis increased, contrast increased and homogeneity decreased, which is consistent with the intuitive features of the obtained image. In the diagnosis of liver fibrosis in all stages, both features have independent diagnosis efficiency (AUC > 0.7, $P < 0.05$), but there is no statistically difference from 2D-SWE. Whereas, correlation and ASM showed limited diagnosis efficiency. Therefore, we believe that it is feasible to obtain and analyze the textural features quantified based on the GLCM, and to take it as a diagnosis index for liver fibrosis stage; contrast and homogeneity harbor potency as an independent index for diagnosis of liver fibrosis stage. Furthermore, It can be inferred that the liver fibrosis patients with the progress of the disease, the overall hardness of the liver tissue increases, while the imbalance of liver tissue hardness distribution is also increasing, that is, the spatial heterogeneity of the hardness distribution is more obvious, the

Table 2 Comparison of two dimensional shear wave elastography and textural features in different groups (Median, Range)

Comparison		2D-SWE	*P*-value	Contrast	*P*-value	Correlation	*P*-value	ASM	*P*-value	Homogeneity	*P* value
F0 *vs* F1-4 (≥ F1)	F0	5.97 (4.07-11.03)	0.001	1.51 (0.44-6.69)	< 0.001	0.97 (0.79-0.99)	0.72	0.056 (0.015-0.87)	0.087	0.76 (0.64-0.97)	0.002
	F1-4	10.63 (6.40-44.87)		8.39 (1.39-200.76)		0.96 (0.67-0.99		0.043 (0.003-0.33)		0.54 (0.33-0.87)	
F0-1 *vs* F2-4 (≥ F2)	F0-1	7.78 (4.07-17.43)	< 0.001	2.66 (0.44-19.64)	< 0.001	0.97 (0.79-0.99)	0.041	0.05 (0.015-0.87)	0.11	0.69 (0.59-0.97)	0.007
	F2-4	11.94 (6.4-44.87)		11.78 (1.39-200.76)		0.94 (0.66-0.98)		0.034 (0.003-0.33)		0.61 (0.33-0.87)	
F0-2 *vs* F3-4 (≥ F3)	F0-2	9.03 (4.07-17.43)	< 0.001	3.39 (0.44-27.43)	0.002	0.96 (0.79-0.99)	0.23	0.049 (0.012-0.87)	0.11	0.68 (0.50-0.97)	0.044
	F3-4	14.97 (9.00-44.87)		14.86 (1.39-200.76)		0.94 (0.67-0.98)		0.030 (0.003-0.33)		0.59 (0.33-0.87)	
F0-3 *vs* F4 (F4)	F0-3	9.42 (4.07-22.23)	0.004	3.69 (0.44-67.49)	< 0.001	0.96 (0.74-0.99)	0.29	0.05 (0.012-0.87)	0.018	0.68 (0.50-0.97)	0.018
	F4	17.30 (9.00-44.87)		90.43 (9.34-200.76)		0.93 (0.67-0.98)		0.019 (0.003-0.094)		0.50 (0.33-0.69)	

2D-SWE: Two dimensional shear wave elastography; ASM: Angular second moment.

stage of liver fibrosis may be heavier.

PRE arose from combinatorial diagnosis and exerted optimal performance in the diagnosis of liver fibrosis stage (AUC > 0.7, $P < 0.05$). Compared with the above independent factors in all groups, ROC curve of PRE was more proximal to the left upper corner, while AUC is the greatest value. Combination of 2D-SWE with textural analysis could more accurately reflect liver tissue hardness when the former reflects the absolute elastic modulus values in the region of interest, while the latter reflects the spatial distribution of the elastic modulus in the selected region. Statistical analysis showed that the combined diagnosis of early liver fibrosis was superior to 2D-SWE ($P < 0.05$).

Our study demonstrated that combination of 2D-SWE with texture analysis could effectively improve diagnosis efficiency peculiarly for early liver fibrosis with chronic hepatitis B. Nonetheless, this study contains some drawbacks: on one hand, the sample size was limited, though the feasible of texture analysis in diagnosis of liver fibrosis was conformed, the diagnosis model of liver fibrosis related texture analysis has not yet been established; on the other hand, hepatitis B virus DNA level, liver function and other factors weren't stratified. In particular, alanine aminotransferase, which is very important in the diagnosis and treatment of liver fibrosis with chronic hepatitis B, is not included in this study and may affect the stability of the result. In future studies, more effort should be directed to increasing sample size and simultaneously to comprehensive analysis of relevant indexes. Doing this should provide a novel and effective clinical measure for the non-invasive examination of liver fibrosis, especially of early liver fibrosis.

Table 3 Receiver operating characteristic curve analysis of various indicators in diagnosing pathological stages of liver fibrosis

		2D SWE	Contrast	Correlation	ASM	Homogeneity	PRE
F0 *vs* F1-4 (≥ F1)	AUC (95%CI)	0.823 (0.678-0.921)	0.906 (0.779-0.973)	0.533 (0.377-0.685)	0.659 (0.500-0.795)	0.789 (0.639-0.897)	0.952 (0.841-0.994)[1]
	P	< 0.0001	< 0.0001	0.735	0.09	< 0.0001	< 0.0001
	YI	0.533	0.697	0.195	0.363	0.448	0.761
	Cutoff	> 5.967	> 2.726	≤ 0.899	≤ 0.0940	≤ 0.632	> 0.591
	TPR (%)	100.0	89.7	13.8	89.7	44.8	82.8
	TNR (%)	53.3	80.0	66.7	46.7	100.0	93.3
F0-1 *vs* F2-4 (≥ F2)	AUC (95%CI)	0.808 (0.662-0.911)	0.835 (0.693-0.930)	0.680 (0.523-0.813)	0.641 (0.482-0.780)	0.736 (0.582-0.858)	0.896 (0.766-0.967)
	P	< 0.0001	< 0.0001	0.0267	0.0936	0.0023	< 0.0001
	YI	0.483	0.567	0.358	0.258	0.508	0.767
	Cutoff	> 8.667	> 7.391	≤ 0.973	≤ 0.0350	≤ 0.617	> 0.440
	TPR (%)	90.0	65.0	90.0	55.0	55.0	85.0
	TNR (%)	58.3	91.7	45.8	70.8	95.8	91.7
F0-2 *vs* F3-4 (≥ F3)	AUC (95%CI)	0.920 (0.798-0.980)	0.807 (0.660-0.910)	0.624 (0.465-0.765)	0.663 (0.504-0.798)	0.705 (0.549-0.883)	0.978 (0.881-0.999)
	P	< 0.0001	0.0002	0.21	0.107	0.0392	< 0.0001
	YI	0.818	0.546	0.273	0.363	0.485	0.939
	Cutoff	> 11.033	> 8.385	≤ 0.938	≤ 0.0330	≤ 0.587	> 0.124
	TPR (%)	90.9	72.7	54.6	63.6	54.6	100.0
	TNR (%)	90.9	81.8	72.7	72.7	93.9	93.9
F0-3 *vs* F4 (F4)	AUC (95%CI)	0.855 (0.716-0.943)	0.925 (0.805-0.983)	0.638 (0.480- 0.777)	0.796 (0.648-0.902)	0.798 (0.650-0.904)	0.947 (0.835-0.992)
	P	< 0.0001	< 0.0001	0.272	0.0058	0.0058	< 0.0001
	YI	0.702	0.790	0.377	0.597	0.561	0.807
	Cutoff	> 13.000	> 8.385	≤ 0.938	≤ 0.030	≤ 0.587	> 0.383
	TPR (%)	83.3	100.0	66.7	83.3	66.7	83.3
	TNR (%)	86.8	79.0	71.1	76.3	89.5	97.4

[1]There is statistically significance when compared with two dimensional shear wave elastography group ($P < 0.05$).
PRE: Predictive value of combined diagnosis; AUC: The area under the ROC curve; YI: Youden index; Cutoff: The diagnostic cut-off point; TPR: The true positive rate; TNR: The true negative rate.

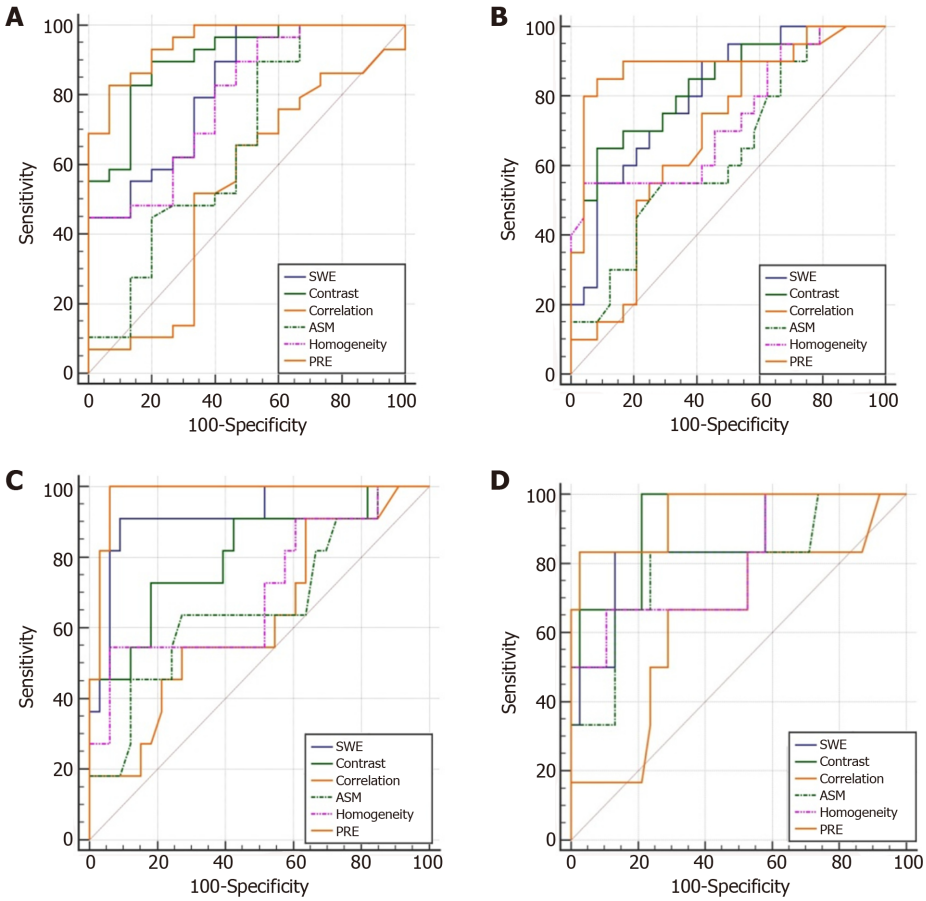

Figure 2 Receiver operating characteristic curves. A: F0 *vs* F1-4 (≥ F1); B: F0-1 *vs* F2-4 (≥ F2); C: F0-2 *vs* F3-4 (≥ F3); D: F0-3 *vs* F4 (F4). SWE: Shear wave elastography; ASM: Angular second moment; PRE: Predictive value.

ARTICLE HIGHLIGHTS

Research background

Two dimensional shear wave elastography (2D-SWE) has been widely used in non-invasive diagnosis of liver fibrosis due to its non-invasiveness, reproducibility and high accuracy. However, it is not effective in the diagnosis of early liver fibrosis and it is not completely replaceable with liver biopsy; therefore, how to further improve the diagnostic efficacy of 2D-SWE examination on liver fibrosis staging is a clinically urgent problem. Texture analysis has always been a hotspot of image analysis, and texture analysis of medical images has also been achieved good results in the diagnosis and treatment of many diseases. But there are few studies on texture analysis for ultrasound elastic images currently. The combination of the two is expected to improve the diagnostic efficacy of liver fibrosis, especially early liver fibrosis in patients with chronic hepatitis B.

Research motivation

In order to improve the efficacy of non-invasive diagnosis of early liver fibrosis in patients with chronic hepatitis B, the information of elastic images obtained by 2D-SWE examination should be fully applied. This study intends to use the texture analysis software to deeply analyze the elastic images and obtain the spatial distribution information of elastic modulus, meanwhile, combined with the Young's modulus value to diagnose the liver fibrosis. It will provide a new idea and method for the diagnosis of liver fibrosis in patients with chronic hepatitis B.

Research objectives

The objective of this study was to find a non-invasive, reproducible, and accurate method for the diagnosis of early liver fibrosis caused by chronic hepatitis B. The study demonstrated that combination of 2D-SWE with texture analysis can effectively improve the diagnostic efficacy of early liver fibrosis, which provides theoretical support for the application of texture analysis in the diagnosis of early liver fibrosis in patients with chronic hepatitis B, and it also provides a possibility for non-invasive diagnosis to gradually replace the liver tissue biopsy.

Research methods

Based on the 2D-SWE examination, this study applied texture analysis software (SSI) to obtain the mean values at different angles of four texture patterns (contrast, correlation, ASM and

homogeneity). Take pathological results of biopsy specimens as the gold standards to orderly test: comparison and assessment of the diagnosis efficiency conducted for 2D-SWE, contrast, correlation, ASM, homogeneity and their combination. The feasibility of 2D-SWE combined texture analysis in the diagnosis of liver fibrosis was discussed by analyzing the spatial distribution characteristics of elastic modulus, and combined with the application of Young's modulus value.

Research results

The study demonstrated that contrast and homogeneity have separated diagnostic efficacy in the diagnosis of liver fibrosis in patients with chronic hepatitis B. The AUC values of each group in the combined diagnosis are improved compared with the separated diagnosis of each index. The combined diagnosis showed higher diagnosis efficiency over 2D-SWE in early liver fibrosis. This study is the first to apply the texture analysis of elastic images to the non-invasive diagnosis of liver fibrosis, and confirmed the value of contrast and homogeneity in the diagnosis of liver fibrosis, and found that combined diagnosis can improve the diagnostic efficacy of early liver fibrosis. In the further study, it is necessary to continue to explore the influence of different angles on the diagnostic performance of texture features and the feasibility of combined application with other liver fibrosis diagnostic prediction models.

Research conclusions

The main conclusions of this study are as follows: (1) Texture analysis of elastic images can be applied in the diagnosis of liver fibrosis with chronic hepatitis B, in which the diagnostic efficacy of contrast and homogeneity is comparable to 2D-SWE, but correlation and ASM showed poor diagnosis efficiency; (2) Combined diagnosis (2D-SWE plus texture analysis) can effectively improve the diagnostic efficacy of liver fibrosis in patients with chronic hepatitis B, especially in the diagnosis of early liver fibrosis, combined diagnostic efficacy is better; and (3) The staging of liver fibrosis in chronic hepatitis B may be related to the spatial heterogeneity of liver tissue hardness distribution. The more spatial heterogeneity of hardness distribution, the more severe the degree of liver fibrosis.

Research perspectives

This study confirmed that the post-processing of elastic images can further improve the diagnostic value of ultrasound-elastic images for liver fibrosis. However, the sample size of this study is small, and other diagnostic indicators related to liver fibrosis have not been combined. A robust diagnosis model of liver fibrosis has not yet been established. In the follow-up study, while optimizing the texture analysis, the sample size will be expanded, and other liver fibrosis diagnostic methods may be combined to establish a non-invasive diagnostic model for early liver fibrosis with higher efficacy.

REFERENCES

1 **Lefton HB**, Rosa A, Cohen M. Diagnosis and epidemiology of cirrhosis. *Med Clin North Am* 2009; **93**: 787-799, vii [PMID: 19577114 DOI: 10.1016/j.mcna.2009.03.002]

2 **Bedossa P**, Dargère D, Paradis V. Sampling variability of liver fibrosis in chronic hepatitis C. *Hepatology* 2003; **38**: 1449-1457 [PMID: 14647056 DOI: 10.1016/j.hep.2003.09.022]

3 **Kose S**, Ersan G, Tatar B, Adar P, Sengel BE. Evaluation of Percutaneous Liver Biopsy Complications in Patients with Chronic Viral Hepatitis. *Eurasian J Med* 2015; **47**: 161-164 [PMID: 26644763 DOI: 10.5152/eurasianjmed.2015.107]

4 **Bamber J**, Cosgrove D, Dietrich CF, Fromageau J, Bojunga J, Calliada F, Cantisani V, Correas JM, D'Onofrio M, Drakonaki EE, Fink M, Friedrich-Rust M, Gilja OH, Havre RF, Jenssen C, Klauser AS, Ohlinger R, Saftoiu A, Schaefer F, Sporea I, Piscaglia F. EFSUMB guidelines and recommendations on the clinical use of ultrasound elastography. Part 1: Basic principles and technology. *Ultraschall Med* 2013; **34**: 169-184 [PMID: 23558397 DOI: 10.1055/s-0033-1335205]

5 **Dietrich CF**, Bamber J, Berzigotti A, Bota S, Cantisani V, Castera L, Cosgrove D, Ferraioli G, Friedrich-Rust M, Gilja OH, Goertz RS, Karlas T, de Knegt R, de Ledinghen V, Piscaglia F, Procopet B, Saftoiu A, Sidhu PS, Sporea I, Thiele M. EFSUMB Guidelines and Recommendations on the Clinical Use of Liver Ultrasound Elastography, Update 2017 (Long Version). *Ultraschall Med* 2017; **38**: e16-e47 [PMID: 28407655 DOI: 10.1055/s-0043-103952]

6 **Ferraioli G**, Filice C, Castera L, Choi BI, Sporea I, Wilson SR, Cosgrove D, Dietrich CF, Amy D, Bamber JC, Barr R, Chou YH, Ding H, Farrokh A, Friedrich-Rust M, Hall TJ, Nakashima K, Nightingale KR, Palmeri ML, Schafer F, Shiina T, Suzuki S, Kudo M. WFUMB guidelines and recommendations for clinical use of ultrasound elastography: Part 3: liver. *Ultrasound Med Biol* 2015; **41**: 1161-1179 [PMID: 25800942 DOI: 10.1016/j.ultrasmedbio.2015.03.007]

7 **Li Y**, Huang YS, Wang ZZ, Yang ZR, Sun F, Zhan SY, Liu XE, Zhuang H. Systematic review with meta-analysis: the diagnostic accuracy of transient elastography for the staging of liver fibrosis in patients with chronic hepatitis B. *Aliment Pharmacol Ther* 2016; **43**: 458-469 [PMID: 26669632 DOI: 10.1111/apt.13488]

8 **Feng JC**, Li J, Wu XW, Peng XY. Diagnostic Accuracy of SuperSonic Shear Imaging for Staging of Liver Fibrosis: A Meta-analysis. *J Ultrasound Med* 2016; **35**: 329-339 [PMID: 26795041 DOI: 10.7863/ultra.15.03032]

9 **Leung VY**, Shen J, Wong VW, Abrigo J, Wong GL, Chim AM, Chu SH, Chan AW, Choi PC, Ahuja AT, Chan HL, Chu WC. Quantitative elastography of liver fibrosis and spleen stiffness in chronic hepatitis B carriers: comparison of shear-wave elastography and transient elastography with liver biopsy correlation. *Radiology* 2013; **269**: 910-918 [PMID: 23912619 DOI: 10.1148/radiol.13130128]

10 **Jiang H**, Zheng T, Duan T, Chen J, Song B. Non-invasive in vivo Imaging Grading of Liver Fibrosis. *J Clin Transl Hepatol* 2018; **6**: 198-207 [PMID: 29951365 DOI: 10.14218/JCTH.2017.00038]

11 **Caviglia GP**, Abate ML, Pellicano R, Smedile A. Chronic hepatitis B therapy: available drugs and treatment guidelines. *Minerva Gastroenterol Dietol* 2015; **61**: 61-70 [PMID: 25323305]
12 **Vallet-Pichard A**, Pol S. Hepatitis B virus treatment beyond the guidelines: special populations and consideration of treatment withdrawal. *Therap Adv Gastroenterol* 2014; **7**: 148-155 [PMID: 25057295 DOI: 10.1177/1756283X14524614]
13 **Jeong JY**, Kim TY, Sohn JH, Kim Y, Jeong WK, Oh YH, Yoo KS. Real time shear wave elastography in chronic liver diseases: accuracy for predicting liver fibrosis, in comparison with serum markers. *World J Gastroenterol* 2014; **20**: 13920-13929 [PMID: 25320528 DOI: 10.3748/wjg.v20.i38.13920]
14 **Chon YE**, Choi EH, Song KJ, Park JY, Kim DY, Han KH, Chon CY, Ahn SH, Kim SU. Performance of transient elastography for the staging of liver fibrosis in patients with chronic hepatitis B: a meta-analysis. *PLoS One* 2012; **7**: e44930 [PMID: 23049764 DOI: 10.1371/journal.pone.0044930]
15 **Dong DR**, Hao MN, Li C, Peng Z, Liu X, Wang GP, Ma AL. Acoustic radiation force impulse elastography, FibroScan®, Forns' index and their combination in the assessment of liver fibrosis in patients with chronic hepatitis B, and the impact of inflammatory activity and steatosis on these diagnostic methods. *Mol Med Rep* 2015; **11**: 4174-4182 [PMID: 25651500 DOI: 10.3892/mmr.2015.3299]
16 **Kanamoto M**, Shimada M, Ikegami T, Uchiyama H, Imura S, Morine Y, Kanemura H, Arakawa Y, Nii A. Real time elastography for noninvasive diagnosis of liver fibrosis. *J Hepatobiliary Pancreat Surg* 2009; **16**: 463-467 [PMID: 19322509 DOI: 10.1007/s00534-009-0075-9]
17 **Cassinotto C**, Lapuyade B, Mouries A, Hiriart JB, Vergniol J, Gaye D, Castain C, Le Bail B, Chermak F, Foucher J, Laurent F, Montaudon M, De Ledinghen V. Non-invasive assessment of liver fibrosis with impulse elastography: comparison of Supersonic Shear Imaging with ARFI and FibroScan®. *J Hepatol* 2014; **61**: 550-557 [PMID: 24815876 DOI: 10.1016/j.jhep.2014.04.044]
18 **Guibal A**, Renosi G, Rode A, Scoazec JY, Guillaud O, Chardon L, Munteanu M, Dumortier J, Collin F, Lefort T. Shear wave elastography: An accurate technique to stage liver fibrosis in chronic liver diseases. *Diagn Interv Imaging* 2016; **97**: 91-99 [PMID: 26655870 DOI: 10.1016/j.diii.2015.11.001]
19 **Zeng J**, Liu GJ, Huang ZP, Zheng J, Wu T, Zheng RQ, Lu MD. Diagnostic accuracy of two-dimensional shear wave elastography for the non-invasive staging of hepatic fibrosis in chronic hepatitis B: a cohort study with internal validation. *Eur Radiol* 2014; **24**: 2572-2581 [PMID: 25027837 DOI: 10.1007/s00330-014-3292-9]
20 **Mancini M**, Salomone Megna A, Ragucci M, De Luca M, Marino Marsilia G, Nardone G, Coccoli P, Prinster A, Mannelli L, Vergara E, Monti S, Liuzzi R, Incoronato M. Reproducibility of shear wave elastography (SWE) in patients with chronic liver disease. *PLoS One* 2017; **12**: e0185391 [PMID: 29023554 DOI: 10.1371/journal.pone.0185391]
21 **Huang C**, Pan X, He Q, Huang M, Huang L, Zhao X, Yuan C, Bai J, Luo J. Ultrasound-Based Carotid Elastography for Detection of Vulnerable Atherosclerotic Plaques Validated by Magnetic Resonance Imaging. *Ultrasound Med Biol* 2016; **42**: 365-377 [PMID: 26553205 DOI: 10.1016/j.ultrasmedbio.2015.09.023]
22 **Bhatia KS**, Lam AC, Pang SW, Wang D, Ahuja AT. Feasibility Study of Texture Analysis Using Ultrasound Shear Wave Elastography to Predict Malignancy in Thyroid Nodules. *Ultrasound Med Biol* 2016; **42**: 1671-1680 [PMID: 27126245 DOI: 10.1016/j.ultrasmedbio.2016.01.013]
23 **Haralick R**, Shanmuga K, Dinstein I. Textural Features for Image Classification. *IEEE Trans Syst Man Cybern* 1973; **3**: 610-621
24 **Valckx FM**, Thijssen JM. Characterization of echographic image texture by cooccurrence matrix parameters. *Ultrasound Med Biol* 1997; **23**: 559-571 [PMID: 9232765]
25 **Huang C**, He Q, Huang M, Huang L, Zhao X, Yuan C, Luo J. Non-Invasive Identification of Vulnerable Atherosclerotic Plaques Using Texture Analysis in Ultrasound Carotid Elastography: An In Vivo Feasibility Study Validated by Magnetic Resonance Imaging. *Ultrasound Med Biol* 2017; **43**: 817-830 [PMID: 28153351 DOI: 10.1016/j.ultrasmedbio.2016.12.003]

World Journal of Clinical Cases

Submit a Manuscript: https://www.f6publishing.com

World J Clin Cases 2019 May 26; 7(10): 1133-1141

DOI: 10.12998/wjcc.v7.i10.1133

ISSN 2307-8960 (online)

CASE REPORT

Selective dorsal rhizotomy in cerebral palsy spasticity - a newly established operative technique in Slovenia: A case report and review of literature

Tomaz Velnar, Peter Spazzapan, Zoran Rodi, Natasa Kos, Roman Bosnjak

ORCID number: Tomaz Velnar (0000-0002-6283-4348); Peter Spazzapan (0000-0002-5278-7947); Zoran Rodi (0000-0002-6283-43X2); Natasa Kos (0000-0002-1515-813X); Roman Bosnjak (0000-0001-7565-0989).

Author contributions: Velnar T, Spazzapan P, Rodi Z, Kos N and Bosnjak R contributed equally to this work; Velnar T, Spazzapan P, Rodi Z, Kos N and Bosnjak R designed research; Velnar T and Spazzapan P performed research; Rodi Z, Kos N and Bosnjak R analyzed data; and Velnar T, Spazzapan P, Rodi Z, Kos N and Bosnjak R wrote the paper.

Informed consent statement: Informed consent to publish was obtained from the patient.

Conflict-of-interest statement: The authors declare that they have no competing interests.

CARE Checklist (2016) statement: The authors have read the CARE Checklist (2016), and the manuscript was prepared and revised according to the CARE Checklist (2016).

Tomaz Velnar, Peter Spazzapan, Roman Bosnjak, Department of Neurosurgery, University Medical Centre Ljubljana, Ljubljana 1000, Slovenia

Tomaz Velnar, AMEU-ECM Maribor, Ljubljana 1000, Slovenia

Zoran Rodi, Department of Neurophysiology, University Medical Centre Ljubljana, Ljubljana 1000, Slovenia

Natasa Kos, Medical Rehabilitation Unit, University Medical Centre Ljubljana, Ljubljana 1000, Slovenia

Corresponding author: Tomaz Velnar, MD, PhD, Assistant Professor, Doctor, Department of Neurosurgery, University Medical Centre Ljubljana, Zaloska 7, Ljubljana 1000, Slovenia. tvelnar@hotmail.com
Telephone: +00-386-15223250

Abstract

BACKGROUND

Spasticity affects a large number of children, mainly in the setting of cerebral palsy, however, only a few paediatric neurosurgeons deal with this problem. This is mainly due to the fact that until 1979, when Fasano has published the first series of selective dorsal rhizotomy (SDR), neurosurgeons were able to provide such children only a modest help. The therapy of spasticity has made a great progress since then. Today, peroral drugs, intramuscular and intrathecal medicines are available, that may limit the effects of the disease. In addition, surgical treatment is gaining importance, appearing in the form of deep brain stimulation, peripheral nerve procedures and SDR. All these options offer the affected children good opportunities of improving the quality of life.

CASE SUMMARY

A 15-year old boy is presented that was surgically treated for spasticity as a result of cerebral palsy. Laminotomy at L1 level was performed and L1 to S1 nerve roots were isolated and divided in smaller fascicles. Then, the SDR was made.

CONCLUSION

We describe a patient report and surgical technique of SDR that was performed in Slovenia for the first time.

Key words: Cerebral palsy; Spasticity; Selective dorsal rhizotomy; Operation; Case report

Manuscript source: Invited manuscript

Received: November 15, 2018
Peer-review started: November 16, 2018
First decision: January 12, 2019
Revised: April 23, 2019
Accepted: May 1, 2019
Article in press: May 2, 2019
Published online: May 26, 2019

P-Reviewer: Chowdhury FH, Vaudo G, Yang XJ
S-Editor: Dou Y
L-Editor: A
E-Editor: Xing YX

Core tip: Spasticity affects a large number of children, mainly in the setting of cerebral palsy. The therapy of spasticity has made a great progress. Today, peroral drugs, intramuscular and intrathecal medicines are available. In addition, surgical treatment is gaining importance. We describe a patient report and surgical technique of SDR that was performed in Slovenia for the first time and successfully introduced in the clinical practice.

Citation: Velnar T, Spazzapan P, Rodi Z, Kos N, Bosnjak R. Selective dorsal rhizotomy in cerebral palsy spasticity - a newly established operative technique in Slovenia: A case report and review of literature. *World J Clin Cases* 2019; 7(10): 1133-1141
URL: https://www.wjgnet.com/2307-8960/full/v7/i10/1133.htm
DOI: https://dx.doi.org/10.12998/wjcc.v7.i10.1133

INTRODUCTION

Spasticity is a motor disorder characterized by an increase in muscle tone that interferes with the mobility and therefore affects the quality of life[1]. Spasticity, which results from the unbalanced factors that act on rising and lowering the muscle tone, is the result of an abnormal increase and irritability of myotactic reflexes and depends on the speed of movement. Although spasticity is evident in various diseases that affect muscle tone, such as idiopathic or secondary forms, mainly in connection with dystonia or atethosis, it is most commonly associated with cerebral palsy, which affects 2 to 3 children in 1000 people[2]. The spasticity in cerebral palsy is not evident immediately at birth. On the contrary, it usually becomes pronounced only after the first year of life. The treatment of spasticity is important to reduce the muscle tone, improve the quality of life and reduce pain and deformations. It has two objectives: to reduce the efferent impulses that stimulate muscles and rise the abnormal muscle tone [with surgical procedures such as selective dorsal rhizotomy (SDR)] or increase the inhibitory activity on the muscle tone (with the action of drugs such as baclofen)[2-4].

Spasticity typically affects some muscle groups more than others[3]. In the clinical picture of a child with a cerebral palsy, muscular rigidity, tiredness, muscle pain and cramps are evident. The pain and muscle cramps are particularly pronounced in the nocturnal hours. In time, the spasticity may also lead to the deformations of the skeleton, such as luxations and subluxations of the hip and ankle joints. Additionally, upper limbs are almost always affected to some degree. The most affected are abductors and flexors. This is evident in patients with spastic paraparesis, who are standing on the toes with flexed hips and knees and internal rotation of lower limbs[4-6].

Clinically, spasticity is described according to the affected limbs as spastic tetraparesis, spastic diplegia (or paraparesis), spastic haemy- and monoparesis[2,4]. The most used evaluation scale for spasticity is Ashworth Scale (and very similar Modified Ashworth Scale), which determinates the degree of spasticity (Table 1). Spasticity can also affect paraspinal muscles, but this disorder is not included in the above classification. The motor function, which may also be severely affected due to the spasticity of the muscles, is classified according to the Gross Motor Function Classification System (GMFCS) (Table 2)[4-6].

There are many forms of spasticity treatment. The aim is to reduce the degree of spasticity, rather than cure it completely[7]. The treatment encompasses many modalities that include oral medications, intramuscular injections of intrathecal medications, physiotherapy and orthopaedic procedures and even neurosurgical operations[8]. One of the options includes SDR. It is a neurosurgical procedure with the aim of reducing spasticity and improving mobility in children with cerebral palsy suffering from lower extremity spasticity[9-11]. The technique involves a selective division of the lumbosacral sensory rootlets with the aid of intraoperative neurophysiological monitoring. The SDR represents a valuable surgical option especially for young patients with bilateral spastic cerebral palsy with the objective of improving lower limb function[10].

A proper form of treatment should be therefore proposed by a multidisciplinary team with experience in each of these therapies that assesses the patients. The most important factor in predicting the SDR performance is not so much a sample of

Table 1 The Ashworth scale for classification of the degree of spasticity

SCORE- Degree of spasticity	DESCRIPTION
0	No increase in muscle tone.
1	Slight increase in tone giving a catch when the limb was moved in flexion or extension.
2	More marked increase in tone but limb easily flexed.
3	Considerable increase in tone - passive movement difficult.
4	Limb rigid in flexion or extension.

neurophysiological monitoring, acquired during the operation, but the correct preoperative selection of the patient[12]. Choosing the correct patient for SDR is therefore of utmost importance and requires a comprehensive evaluation. Ideal patients for SDR are children between 4 and 8 years of age, with spastic paraparesis, which impedes their pattern of walking. Such patients usually have preserved strength in the lower extremities and only rare contractions. Unfortunately, only few children with cerebral palsy fulfil these requirements, in clinical practice less than 5%[13-15].

Although SDR has been efficacious in treating spastic patients, many clinicians are not well aware of the procedure, its indications and expected outcomes due to the limited number of centres performing this procedure[10,16]. In this article, the authors describe the SDR technique in the management of spastic diplegia in a child with cerebral palsy that was performed in Slovenia for the first time and has been introduced in the neurosurgical practice.

CASE PRESENTATION

Chief complaints

A 15-year old boy was admitted to the neurosurgery department for SDR. He was experiencing severe and painful muscle cramps and the increased muscle tone prevented him from normal walking and sitting.

History of present illness

A 15-year old boy was admitted to the neurosurgery department for SDR. He was born prematurely at the gestational age of 35 wk and postnatally sustained an intraventricular haemorrhage, grade 2. Later on, he was recovering well. There were no signs of hydrocephalus and he was regularly followed-up at paediatric neurology and physiatry. He was cognitively intact. After one year, an increased muscle tone was observed and he was included into a rehabilitation programme. A spastic diplegia started to develop and the muscle tone has increased progressively. For many years, the physiatric, orthopaedic and medicamentous care sufficed to counterbalance the spasticity, however, due to deformations and shortage of hamstrings and calf muscles he needed an orthopaedic intervention. At the age of 15, he was referred to the neurosurgeon as a result of increasing spasticity and difficulties in walking, sitting and numerous muscle cramps in lower extremities.

History of past illness

No past illnesses were documented in the new-born or mother.

Personal and family history

Unremarkable.

Physical examination upon admission

At the examination, the cranial nerves and upper extremities were functioning normally. In the lower extremities, however, spasticity was evident and the muscle tone was rated at 4, according to the Modified Ashworth Scale and to 3 according to the GMFCS. The spastic gait was evident as was the scissor-pattern walk. The sphincters were unaffected. After initial neurosurgical evaluation, a multidisciplinary team assessed and discussed possible treatment options. For muscle tone reduction, the SDR was recommended.

Laboratory examinations

Laboratory examinations were within the normal range. The haemostasis was normal, as was the blood count and the biochemistry test.

Table 2 The Gross Motor Function Classification System

SCORE- Level of spasticity	DESCRIPTION
Level I	Walks well in all settings. Balance and speed may be limited compared with children developing normally.
Level II	Walks in most settings but may have difficulty walking long distances or with balance. May utilise personal or environmental mobility aids to climb stairs.
Level III	Walks with the use of hand-held mobility aids such as K-walkers in most indoor settings. Uses wheeled mobility for longer distance travel.
Level IV	Utilises wheeled mobility aids in most settings (either attendant-propelled or powered) and requires assistance to transfer.
Level V	Transported in wheelchairs in all settings and has limited to no antigravity head, trunk and limb control.

Imaging examinations

No special imaging was required for the surgical treatment. The level L1 was marked with x-rays intraoperatively for the location of conus medullaris.

FINAL DIAGNOSIS

The final diagnosis was consistent with the spasticity as a result of cerebral palsy.

TREATMENT

After initial anaesthesiological preparation, the boy was placed prone on the operating table. The neuromonitoring for dermatomes and myotomes L2 to S2 was attached. The level L1 was marked with X-rays for the location of conus medullaris. A laminotomy L1 followed and the dural sac was exposed. With the ultrasound, the location of the conus and cauda was determined and these structures were clearly seen (Figure 1). Under the operating microscope, the dura was cut in the median line and the arachnoid dissected. The conus was exposed, surrounded by the spinal roots and left and right roots were separated. On the left side, L1 root was identified anatomically, exiting from the neuroformanen. The root is composed of three fascicles, with the most ventral one being motor and the two caudal ones sensory. These two fascicles were then separated from the motor part and one of these two rootlets was coagulated and cut, so as to disconnect 50% of the fibres (Figure 2).

Disconnection of the lower roots then followed. First, the groove separating the motor and sensory roots was identified anatomically and electrophysiologically (Figure 3). The motor roots trigger the EMG potential when touched with an instrument, on the contrary to the sensory roots. Then, the sensory roots from L2 to S2 were separated from other structures with an elastic cloth (4cm × 1.5cm). The limit between S2 and S3 roots was anatomically recognized, since the S3 roots are smaller and thinner than the S2. The L2 root, which is located most laterally, was then isolated and confirmed with the electrophysiology. This root was again separated from others with a fine cotton patty and divided into four fascicles with a fine blunt microdiscector (Figure 4). Neurophysiologically the most abnormally active fascicles were coagulated and disconnected (Figure 5). The root L2 was then placed separately from other lower lumbar and sacral roots. The same procedure was exerted on roots L3 to S1. The number of fascicles was various, ranging from four to seven, and two-thirds of them were cut, specifically those with an abnormal electrophysiological response. The S2 root required a special attention. It was divided in two fascicles and the potential of the pudendal action potential was explored. Here, part of the fascicle with lower electrophysiological sphincter activity was cut. An identical procedure was repeated on the right side.

A meticulous intradural haemostasis followed and the dura was closed with a running suture. The lamina was positioned and attached on the place with sutures and the wound was closed in layers.

OUTCOME AND FOLLOW-UP

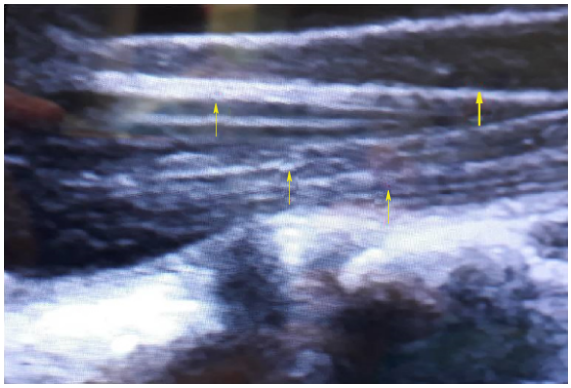

Figure 1 The conus medullaris and caud equina as seen on transdural ultrasound (US) examination. The conus is hypoechogenic on US (thick arrow) and the cauda is hyperechogenic (thin arrows).

After the operation, the patient was transferred to the neurosurgical intensive care and the next day onto the ward. The muscle tone was reduced in a day after surgery, as was the strength in the lower extremities. It was not reduced to such extent, however to prevent the patient from walking. No motor deficits were observed and the sphincter control was intact. The pain subsided gradually in as well as the muscle cramps in the lower extremities. The physiotherapy started gradually after the established protocol from the first day to the discharge, first with passive and then with active exercises, gait control and walking. A special emphasis was put into verticalisation, initially sitting on the wheelchair and then progressive training of proper walking. The patient did not experienced difficulties during this part of rehabilitation.

Ten days after the operation he was discharged to specialised rehabilitation institute for further treatment. The Ashworth Scale and the GMFCS at the discharge were both rated at 2. The neurosurgical examination was planned after on month and the general condition improved markedly. The boy was able to walk independently, the muscle tone was lower (Modified Ashowrth Scale and the GMFCS were 2). No sensory and sphincter disturbances were reported. Next neurosurgical evaluation has been planned after three and six months, as well as continuous physiatric assessment.

DISCUSSION

Spasticity in cerebral palsy is still a great challenge for patients and clinicians treating them, despite the advances in medical care, rehabilitation medicine and surgical techniques. The dorsal rhizotomy as an option for spasticity treatment is not new, as it has been practiced for over 100 years[3-5,17]. First described in 1908 by Sherrington and later developed and performed also by Foerster, early surgical procedures were effective in reducing spasticity. Despite favourable results on muscle tone, they were associated with significant postoperative morbidity as a result of sensory loss and ataxia, which occurred in the total section of lumbar sensory roots (usually section encompassed the L2 to S1 roots). This has led to a temporary omission of the technique for several decades, until in 1979, Fasano described the selective section of the lumbar sensory roots, known as SDR. Here, only those fascicles were disconnected that were causing a permanent and pathological contraction of the muscle during the neurophysiological stimulation[7]. Later, Peacock defined the significance of the pathological response to the electrophysiological irritation of the dorsal fascicle even more precisely. Since then, various modifications of the original surgical technique have been described. Currently, SDR is one of most commonly performed ablative treatment procedures for spasticity in cerebral palsy in children. Technical advancements over the last two decades have helped to reduce the invasiveness of the procedure even more[17-19].

In Slovenia, the SDR has been performed for the first time in October 2017 and since then it was introduced in the regular paediatric neurosurgical activity. Until then, the children with spasticity due to the cerebral palsy were referred for surgical treatment to other centres abroad that performed this operation, most commonly to St. Louis, Missouri, United States. The initial evaluation and medical treatment were done in the Slovenian rehabilitation institute, as well as the postoperative and late rehabilitation, eventual orthopaedic corrections and continuous physiotherapy. The neurosurgical technique that was used in our patient was the same as already

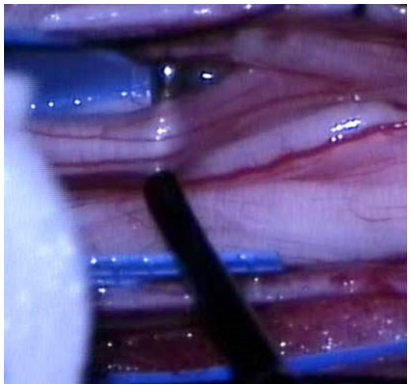

Figure 2 The exposure and isolation of the L1 root. The root is composed of three fascicles, which will be subsequently separated. The motor fascicle will be spared, as will be one of the two sensory fascicles. The electrophysiological probe can be seen (right) and the cotton patty (left), which is used for isolation of the L1 root from other nerves.

described in detail by Sindou *et al*[20]. The laminotomy at L1 level offers an unobstructed view to the end part of the conus and the cauda and the identification of the sensory roots that need to be divided, monitored and cut, namely the roots form L1 to S2 bilaterally. The SDR can also be performed through a larger laminotomy, from L1 to S1. Using this approach each dorsal root can be recognized at the correspondent neuroforamen. This wide laminotomy offers a good view but. However, it may compromise the stability of the spine and with time lead to scoliosis[20,21]. In our case, the bone fragment was sutured in place at the end of the operation to prevent possible instability.

Monitoring is of vital importance and helps the surgeons to confirm the radix that is going to be cut[22]. Normally, each sensory root is divided into 4 to 8 rootlets, each of them is monitored and those evoking the most abnormal response in the muscles are cut, which is usually about 70% of the rootlets. It is particularly important to spare the innervation of the sphincters and care must be taken during the operation not to damage these nerves. The pudendal action potential is of great usefulness for recognition of these rootlets[19-24].

The spasticity in cerebral palsy is the most common indication for SDR[10,19-25]. This diagnosis may be set when a child at a certain age does not achieve a normal motor development (*e.g.*, head lifting, sitting, standing and walking). The gait and posture are inappropriate with an increased muscle tone. In the initial phase, the muscles are loose, with spasticity occurring later. In the early childhood, the typical signs of cerebral palsy may not be evident and the spasticity may occur later, usually after 6 mo of age. In general, the symptoms may be diverse, ranging from almost undetectable clumsiness to severe disability. Typical symptoms, regardless of type, include abnormal muscle tone, balance disorders and abnormally lively tendon reflexes, often accompanied by involuntary movements. The walk is unstable, usually scissor pattern of walking may be observed or walking on toes. As a result of increased muscle tone, the deformation of bones and joints may also occur, worsening the mobility[10,13]. Cerebral palsy can also be accompanied with epileptic seizures, apraxia, sensory disorders and disturbances in sphincter control. Pain, which occurs in combination with a spastically elevated muscular tone, abnormal posture and hardened joints, can often be associated with these symptoms. In the spastic form of the cerebral palsy, which is the most common, the muscular tone is extremely elevated and the tendon reflexes are very pronounced. Muscle contractions may sometimes be provoked by an unexpected hearing or visual stimulus. Joint contractions worsen the general condition and improve to deformations and pain. Swallowing and speech disorders are not uncommon in this type of cerebral palsy[18-24].

According to the affected limbs and spasticity, the cerebral palsy may be divided into a paraplegic, diplegic and tetraplegic type. The paraplegic form is most often the result of a reduced blood supply to the child's brain in the third trimester of pregnancy. Rarely diagnosed at birth, it usually manifests at the age of 6 months. It is this type that is most suitable for the SDR, as was also the case in our patient[7,26].

The management of cerebral palsy is complex and therefore requires a multidisciplinary approach, which should be tailored for individual cases. As the SDR is one of ablative surgical therapies with irreversible properties, preoperative assessment and decision making for the operation are critical[22,27]. Not all patients with cerebral palsy suffering from spasticity need treatment. The highest success has been

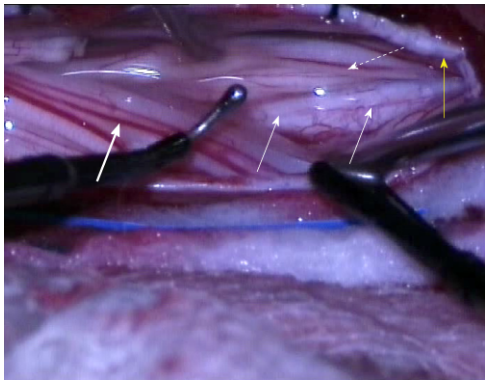

Figure 3 The intraoperative separation of motor and sensory roots and the identification of the groove that divides the roots anatomically. The electrophysiological probe can be seen in place (right) as well as the groove on conus medullaris, separating the both groups of roots (thin arrows). The thick arrow indicates sensory roots and the dotted arrow indicates motor roots. The yellow arrow indicates the dural rim, held in place by tack-up sutures.

observed in patients with Modified Ashworth grades 2 and 3. In low degrees of spasticity, the daily activities are not disturbed to such degree, that the operation would bring a relief, as it is with high grades. The goals of the treatment include improvement of child's functional state, especially the pattern of walking; facilitate the everyday care, to prevent the appearance of contractures and deformations and the onset of pain. The SDR is mostly suitable for children with spastic diplegia who are potential ambulators[27,28]. When choosing the best possible treatment, the main considerations include the age of the child and the goals for the improvement of the general condition. When considering the age, the SDR is ideal procedure from 4 to 8 years, as the growth and brain myelinization is almost complete during this time. Rarely, the indication for SDR is justified after 15 years of age, since it is difficult to strengthen the muscles and alter the pattern of walking after the surgery. Though, recent articles have showed a positive effect on spasticity also in more severely affected patients (Modified Ashworth Scale 4 and 5)[29,30]. After the SDR, persistent deformations and tendons should be corrected by appropriate orthopaedic surgery. The motivation of the child and parents is a fact that always must to be considered before the surgery[26-29].

Because of pronounced spasticity and ambulatory inability, we have decided to treat the spastic diplegia in our patient, despite his age. However, after the SDR, the treatment of patients is not completed[5,6]. The spasticity immediately after the operation declines and the muscle strength deteriorates, thus worsening the condition transiently. This usually lasts for approximately three weeks[13]. During this time, paraesthesia and burning or painful sensations tin extremities can be noted. Gradually, they disappear, the muscle tone clearly lowers and the pattern of walking improves. In our patient, the spasticity was reduced immediately and dropped from Modified Ashworth grade 4 to 2. There was neither paraesthesia or pain reported nor sphincter worsening.

In the post-operative phase, the rehabilitation plays an essential role, supplemented by possible corrective orthopaedic interventions. Due to the inhibitory effect on ascendant interneurons, also the spasticity of the upper limbs can be reduced and the effect on bladder control can be improved, as well as the general functioning[13,24].

The operation in our patient was successful and the recovery was smooth. In the future, more patents with spastic diplegia will be included into the multidisciplinary programme for spasticity treatment, employing the SDR technique, thus improving the life of cerebral paralysis patients.

CONCLUSION

The SDR is an efficient surgical technique for reducing spasticity, especially in young children with spastic diplegia as a result of cerebral palsy. The technique requires meticulous neuromonitoring during the operation and continuous child rehabilitation with long-term follow-up. The treatment outcome of the SDR is long-lasting and the side effects with careful surgery are minimal.

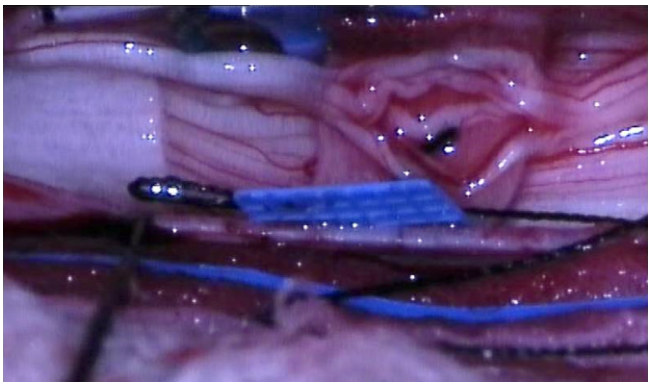

Figure 4 The separation of the sensory roots with an elastic cloth. This root was again separated from others and divided into fascicles with a fine blunt microdisector.

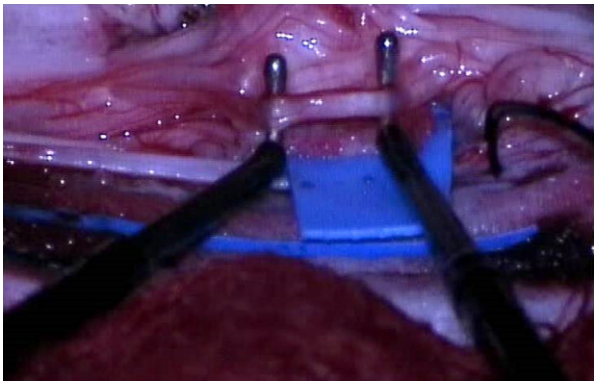

Figure 5 The separation of the root into fascicles and electrophysiological monitoring for confirmation with both probes in place before the fascicle disconnection.

REFERENCES

1 **Lieber RL**, Roberts TJ, Blemker SS, Lee SSM, Herzog W. Skeletal muscle mechanics, energetics and plasticity. *J Neuroeng Rehabil* 2017; **14**: 108 [PMID: 29058612 DOI: 10.1186/s12984-017-0318-y]

2 **O'Shea TM**. Diagnosis, treatment, and prevention of cerebral palsy. *Clin Obstet Gynecol* 2008; **51**: 816-828 [PMID: 18981805 DOI: 10.1097/GRF.0b013e3181870ba7]

3 **Nahm NJ**, Graham HK, Gormley ME, Georgiadis AG. Management of hypertonia in cerebral palsy. *Curr Opin Pediatr* 2018; **30**: 57-64 [PMID: 29135566 DOI: 10.1097/MOP.0000000000000567]

4 **D'Aquino D**, Moussa AA, Ammar A, Ingale H, Vloeberghs M. Selective dorsal rhizotomy for the treatment of severe spastic cerebral palsy: efficacy and therapeutic durability in GMFCS grade IV and V children. *Acta Neurochir (Wien)* 2018; **160**: 811-821 [PMID: 29116382 DOI: 10.1007/s00701-017-3349-z]

5 **Roberts A**, Stewart C, Freeman R. Gait analysis to guide a selective dorsal rhizotomy program. *Gait Posture* 2015; **42**: 16-22 [PMID: 25979183 DOI: 10.1016/j.gaitpost.2015.04.004]

6 **Roberts A**. Surgical management of spasticity. *J Child Orthop* 2013; **7**: 389-394 [PMID: 24432100 DOI: 10.1007/s11832-013-0512-9]

7 **Grunt S**, Fieggen AG, Vermeulen RJ, Becher JG, Langerak NG. Selection criteria for selective dorsal rhizotomy in children with spastic cerebral palsy: a systematic review of the literature. *Dev Med Child Neurol* 2014; **56**: 302-312 [PMID: 24106928 DOI: 10.1111/dmcn.12277]

8 **Graham D**, Aquilina K, Mankad K, Wimalasundera N. Selective dorsal rhizotomy: current state of practice and the role of imaging. *Quant Imaging Med Surg* 2018; **8**: 209-218 [PMID: 29675362 DOI: 10.21037/qims.2018.01.08]

9 **Sitthinamsuwan B**, Nunta-Aree S. Ablative neurosurgery for movement disorders related to cerebral palsy. *J Neurosurg Sci* 2015; **59**: 393-404 [PMID: 26635190]

10 **Farmer JP**, Sabbagh AJ. Selective dorsal rhizotomies in the treatment of spasticity related to cerebral palsy. *Childs Nerv Syst* 2007; **23**: 991-1002 [PMID: 17643249 DOI: 10.1007/s00381-007-0398-2]

11 **Engsberg JR**, Park TS. Selective dorsal rhizotomy. *J Neurosurg Pediatr* 2008; **1**: 177; discussion 178-177; discussion 179 [PMID: 18352759 DOI: 10.3171/PED/2008/1/3/177]

12 **Oki A**, Oberg W, Siebert B, Plante D, Walker ML, Gooch JL. Selective dorsal rhizotomy in children with spastic hemiparesis. *J Neurosurg Pediatr* 2010; **6**: 353-358 [PMID: 20887108 DOI: 10.3171/2010.7.PEDS09318]

13 **Langerak NG**, Lamberts RP, Fieggen AG, Peter JC, Peacock WJ, Vaughan CL. Functional status of patients with cerebral palsy according to the International Classification of Functioning, Disability and Health model: a 20-year follow-up study after selective dorsal rhizotomy. *Arch Phys Med Rehabil* 2009; **90**: 994-1003 [PMID: 19480876 DOI: 10.1016/j.apmr.2008.11.019]

14 **Park TS**, Liu JL, Edwards C, Walter DM, Dobbs MB. Functional Outcomes of Childhood Selective

Dorsal Rhizotomy 20 to 28 Years Later. *Cureus* 2017; **9**: e1256 [PMID: 28649479 DOI: 10.7759/cureus.1256]
15 **Park TS**, Edwards C, Liu JL, Walter DM, Dobbs MB. Beneficial Effects of Childhood Selective Dorsal Rhizotomy in Adulthood. *Cureus* 2017; **9**: e1077 [PMID: 28401027 DOI: 10.7759/cureus.1077]
16 **Park TS**, Johnston JM. Surgical techniques of selective dorsal rhizotomy for spastic cerebral palsy. Technical note. *Neurosurg Focus* 2006; **21**: e7 [PMID: 16918228]
17 **Aquilina K**, Graham D, Wimalasundera N. Selective dorsal rhizotomy: an old treatment re-emerging. *Arch Dis Child* 2015; **100**: 798-802 [PMID: 25670404 DOI: 10.1136/archdischild-2014-306874]
18 **Narayanan UG**. Management of children with ambulatory cerebral palsy: an evidence-based review. *J Pediatr Orthop* 2012; **32** Suppl 2: S172-S181 [PMID: 22890458 DOI: 10.1097/BPO.0b013e31825eb2a6]
19 **Lynn AK**, Turner M, Chambers HG. Surgical management of spasticity in persons with cerebral palsy. *PM R* 2009; **1**: 834-838 [PMID: 19769917 DOI: 10.1016/j.pmrj.2009.07.016]
20 **Sindou MP**, Simon F, Mertens P, Decq P. Selective peripheral neurotomy (SPN) for spasticity in childhood. *Childs Nerv Syst* 2007; **23**: 957-970 [PMID: 17605016 DOI: 10.1007/s00381-007-0399-1]
21 **Steinbok P**, Hicdonmez T, Sawatzky B, Beauchamp R, Wickenheiser D. Spinal deformities after selective dorsal rhizotomy for spastic cerebral palsy. *J Neurosurg* 2005; **102**: 363-373 [PMID: 15926386 DOI: 10.3171/ped.2005.102.4.0363]
22 **Tilton A**. Management of spasticity in children with cerebral palsy. *Semin Pediatr Neurol* 2009; **16**: 82-89 [PMID: 19501336 DOI: 10.1016/j.spen.2009.03.006]
23 **Steinbok P**. Selective dorsal rhizotomy for spastic cerebral palsy: a review. *Childs Nerv Syst* 2007; **23**: 981-990 [PMID: 17551739 DOI: 10.1007/s00381-007-0379-5]
24 **Kothbauer KF**, Deletis V. Intraoperative neurophysiology of the conus medullaris and cauda equina. *Childs Nerv Syst* 2010; **26**: 247-253 [PMID: 19904544 DOI: 10.1007/s00381-009-1020-6]
25 **Gump WC**, Mutchnick IS, Moriarty TM. Selective dorsal rhizotomy for spasticity not associated with cerebral palsy: reconsideration of surgical inclusion criteria. *Neurosurg Focus* 2013; **35**: E6 [PMID: 24175866 DOI: 10.3171/2013.8.FOCUS13294]
26 **Mittal S**, Farmer JP, Al-Atassi B, Gibis J, Kennedy E, Galli C, Courchesnes G, Poulin C, Cantin MA, Benaroch TE. Long-term functional outcome after selective posterior rhizotomy. *J Neurosurg* 2002; **97**: 315-325 [PMID: 12186459 DOI: 10.3171/jns.2002.97.2.0315]
27 **Abou Al-Shaar H**, Imtiaz MT, Alhalabi H, Alsubaie SM, Sabbagh AJ. Selective dorsal rhizotomy: A multidisciplinary approach to treating spastic diplegia. *Asian J Neurosurg* 2017; **12**: 454-465 [PMID: 28761524 DOI: 10.4103/1793-5482.175625]
28 **Dudley RW**, Parolin M, Gagnon B, Saluja R, Yap R, Montpetit K, Ruck J, Poulin C, Cantin MA, Benaroch TE, Farmer JP. Long-term functional benefits of selective dorsal rhizotomy for spastic cerebral palsy. *J Neurosurg Pediatr* 2013; **12**: 142-150 [PMID: 23713680 DOI: 10.3171/2013.4.PEDS12539]
29 **Nemer McCoy R**, Blasco PA, Russman BS, O'Malley JP. Validation of a care and comfort hypertonicity questionnaire. *Dev Med Child Neurol* 2006; **48**: 181-187 [PMID: 16483393 DOI: 10.1017/S0012162206000405]
30 **Ingale H**, Ughratdar I, Muquit S, Moussa AA, Vloeberghs MH. Selective dorsal rhizotomy as an alternative to intrathecal baclofen pump replacement in GMFCS grades 4 and 5 children. *Childs Nerv Syst* 2016; **32**: 321-325 [PMID: 26552383 DOI: 10.1007/s00381-015-2950-9]

World Journal of Clinical Cases

Submit a Manuscript: https://www.f6publishing.com

World J Clin Cases 2019 May 26; 7(10): 1142-1148

DOI: 10.12998/wjcc.v7.i10.1142

ISSN 2307-8960 (online)

CASE REPORT

Invasive myxopapillary ependymoma of the lumbar spine: A case report

Tadej Strojnik, Tatjana Bujas, Tomaz Velnar

ORCID number: Tadej Strojnik (0000-0003-1152-2368); Tatjana Bujas (0000-0002-6283-4453); Tomaz Velnar (0000-0002-6283-4348).

Author contributions: Strojnik T, Bujas T and Velnar T contributed equally to this work; Strojnik T designed the research; Bujas T and Velnar T performed the research; Bujas T and Velnar T analysed the data; and Strojnik T, Bujas T and Velnar T wrote the paper. No supportive foundations.

Informed consent statement: Patient consent obtained.

Conflict-of-interest statement: The authors declare that they have no competing interests.

CARE Checklist (2016) statement: The guidelines of the "CARE Checklist - 2016: Information for writing a case report has been adopted.

Manuscript source: Invited manuscript

Tadej Strojnik, Department of Neurosurgery, University Medical Centre Maribor, Maribor 2000, Slovenia

Tadej Strojnik, Faculty of Medicine, University of Maribor, Maribor 2000, Slovenia

Tatjana Bujas, Department of Pathology, University Medical Centre Maribor, Maribor 2000, Slovenia

Tomaz Velnar, Department of Neurosurgery, University Medical Centre Ljubljana, Ljubljana 1000, Slovenia

Corresponding author: Tomaz Velnar, MD, PhD, Assistant Professor, Doctor, Department of Neurosurgery, University Medical Centre Ljubljana, Zaloska 7, Ljubljana 1000, Slovenia. tvelnar@hotmail.com
Telephone: +00-386-15223250

Abstract

BACKGROUND

Myxopapillary ependymomas are rare spinal tumours. Although histologically benign, they have a tendency for local recurrence.

CASE SUMMARY

We describe a patient suffering from extra- and intradural myxopapillary ependymoma with perisacral spreading. He was treated with subtotal resection and postoperative radiation therapy. After treatment, he experienced slight sphincter disorders and lumboischialgic pain with no motor or sensory disturbances. Eight months later, a tumour regression was documented. The patient is still followed-up regularly.

CONCLUSION

Lumbar myxopapillary ependymomas may present with lumbar or radicular pain, similar to more trivial lesions. Magnetic resonance imaging (MRI) is the primary modality for diagnosis. The treatment aim is to minimize both tumour and therapy-related morbidity and to involve different treatment modalities.

Key words: Myxopapillary ependymoma; Spinal tumour; Surgery; Lumbar pain; Case report

Core tip: Myxopapillary ependymomas are rare spinal tumours. They may present with

Received: December 29, 2018
Peer-review started: December 29, 2018
First decision: March 10, 2019
Revised: April 23, 2019
Accepted: May 2, 2019
Article in press: May 2, 2019
Published online: May 26, 2019

P-Reviewer: Coskun A, Afzal M
S-Editor: Dou Y
L-Editor: Filipodia
E-Editor: Wu YXJ

spinal or radicular pain, similar to more trivial lesions. The treatment aim is to minimize both tumour and therapy-related morbidity. We present a patient with extra- and intradural mixopapillary ependymoma with perisacral spreading.

Citation: Strojnik T, Bujas T, Velnar T. Invasive myxopapillary ependymoma of the lumbar spine: A case report. *World J Clin Cases* 2019; 7(10): 1142-1148
URL: https://www.wjgnet.com/2307-8960/full/v7/i10/1142.htm
DOI: https://dx.doi.org/10.12998/wjcc.v7.i10.1142

INTRODUCTION

The spinal cord can be affected by various tumours, including ependymomas[1]. More frequently encountered intracranially, these are rare malignancies that arise from the cells lining the ventricles and the central canal of the spinal cord. The current hypothesis of tumour formation is that these lesions originate from the extrusion of ependymal cells before neural tube closure[2].

There are many histological types that differ in clinical course and mode of treatment. In the spinal cord, two locations of ependymomas have been described, namely intradural and extradural[3]. Intradurally, spinal ependymomas most commonly occur as intramedullary lesions throughout the entire spinal cord and represent 40% to 60% of spinal cord tumours in adults[2]. The intradural extramedullary location is very rare, with the exception of tumours arising from the lumbosacral region, such as filum terminale, cauda equine and conus medullaris[2-4]. These exhibit histological features of myxopapillary ependymomas [World Health Organization (WHO) grade I][2]. Extradurally, ependymomas occur in the sacrum, presacral tissues or even in subcutaneous tissues over the sacrum. These two tumour locations lead to different management strategies. In both, gross-total resection is the treatment of choice when feasible[3]. However, there is still not a standard therapeutic principle for this disease[5]. The role of radiation therapy has not been adequately studied for either tumour location[3].

We present a patient with a slowly growing myxopapillary ependymoma located intra- and extradurally, involving the sacrum and infiltrating the lumbar and sacral nerves. Treatment of such extensive extra- and intradural myxopapillary epenymoma with perisacral spreading presented a great challenge.

CASE PRESENTATION

Chief complaints

A 51-year old male was admitted to the neurosurgical department on August 2014 due to a planned operation of an extensive intradural tumour with perispinal spreading.

History of present illness

First signs and symptoms were noticed approximately seven years before the admission, when he complained about lumboischialgic pain involving both legs. No other difficulties were reported by the patient at that time, and his neurological condition was intact.

History of past illness

No past illnesses were documented.

Personal and family history

Personal and family history was unremarkable.

Physical examination upon admission

During the neurological examination, the patient complained of lumbar and radicular pain and occasional difficulties with micturition and defecation. There were no abnormalities in neurological function, except for slightly decreased sensory function in the right L5 and S1 dermatomes. Sphincter control was intact.

Laboratory examinations

Laboratory examinations were within the normal range. Haemostasis was normal, as was the blood count and the biochemistry test. Tumour marker levels were not increased.

Imaging examinations

Diagnostic imaging in 2007, which included X-rays and magnetic resonance imaging (MRI), revealed only slight degenerative changes in the lumbar spine, according to the neuroradiological report, although the tumour growth was already visible from the L4 to S2 level (Figure 1). The neuroradiological report did not document any signs of neoplastic lesions, and the patient was not referred to the neurosurgeon. The pain was remitting and relapsing, but no neurological symptoms were reported by the patient. In July 2014, an MRI was performed again due to constant lumbar and radicular pain. On that occasion, an extensive tumorous lesion was seen intramedullary, extending from the Th11 level and invading the conus medullaris. The tumour encompassed the entire sacral and lumbar canal to the S2 level, invading the vertebrae and spreading to perispinal muscles. Contrast homogenously enhanced the tumour (Figure 2). The radiological working diagnosis was paraganglioma or ependymoma.

FINAL DIAGNOSIS

The working diagnosis was set according to the radiological characteristics, classifying the expansive lesion as a paraganglioma or ependymoma. The final diagnosis, according to the histological features, confirmed that the tumour was a myxopapillary ependymoma.

TREATMENT

Due to the extensiveness of the lesion, surgical treatment with tumour reduction was recommended. A laminectomy on the L4 to S1 levels was performed, and a partial reduction was made under electrophysiological monitoring. The tumour tissue was brownish to purple, adherent, vividly vascularised and covering the entire dorsal aspect of the sacral bone, invading the vertebral laminae and bodies, the spinal canal extradurally and extending through the dura into the subdural space and medulla. The lower lumbar and sacral nerves were also affected, and no clear dissection was possible. Due to such extensive infiltration, a radical excision was not possible. The dura was approximated as best as possible and covered with a lyophilised dural patch, collagen sponge and fibrin glue.

OUTCOME AND FOLLOW-UP

The postoperative course was uneventful. No neurological deterioration was observed. According to the histological examination, the tumour was a myxopapillary ependymoma (Figure 3). After the recovery, oncological treatment with irradiation was recommended. The patient received 56 Greys in 28 fractions and was followed-up with an oncologist and neurosurgeon every 4 mo. No further growth was recognised by control MRI imaging (Figure 4). The patient experienced slight sphincter disorders and lumboischialgic pain with no motor or sensory disturbances. After 8 mo, a tumour regression was documented. The patient is still followed-up regularly.

DISCUSSION

Myxopapillary ependymoma was first reported by Kernohan in 1932 as a subtype of ependymoma[6]. These are rare spinal tumours in children and adults, although more frequent in the former. Although histologically considered benign tumours (WHO grade I) with long survival rates, they exhibit a tendency for local recurrence. Additionally, aggressive behaviour has also been described and may lead to dissemination through cerebrospinal fluid and even systemic metastases[7-9]. The intradural ependymomas, especially those in the lumbosacral region, exhibit the potential for spreading throughout the central nervous system (commonly referred to as CNS), whereas extradural tumours are more frequently associated with extraneural metastases[3].

In the lumbosacral region, the majority of ependymomas arise from the intradural filum terminale. Histologically, myxopapillary ependymomas comprise the majority

Figure 1 The first magnetic resonance imaging of the lumbosacral spine in 2007 showing only slight degenerative changes.

of cases. At gross examination, they are often well-encapsulated, soft, vascular and lobular or sausage-shaped masses[3,10]. They may grow quite large, filling and expanding the spinal canal[11,12]. Extradural ependymomas are very rare and arise around or in the sacrum[3]. Our patient had the tumour in both locations, intra- and extradurally, due to such extensive tumour growth and spreading to the perisacral tissues.

The diagnosis of a spinal tumour requires a high level of suspicion, which is based upon the clinical signs and symptoms, as well as spine-directed MRI. Both a complete neurological examination and MRI are equally important to precisely delineate the disease[3,13]. Ependymomas may present with lumbar or radicular pain, weakness and urinary symptoms[14]. However, many patients have a long history of nonspecific complaints prior to the clinical presentation, owing to a slow growth of the myxopapillary ependymoma. Therefore, the diagnosis is often delayed[15]. The symptoms usually consist of pain during walking, frequently located in the calves, which is rapidly relieved by stooping, sitting or otherwise adopting a flexed posture of the hips, and recurs on attempting to walk again. These symptoms may mimic lumbar disc herniation, lumbar spinal stenosis or other spinal tumours[5]. Our patient had a non-specific presentation with lumboishialgic pain in both legs, first reported seven years before surgery. Consequently, when a patient presents with long prodromal and nonspecific lower extremity symptoms, neuroradiological re-evaluation is suggested.

The clinical and radiographic findings of spinal lesions are not specific enough to identify a myxopapillary ependymoma. Differential diagnosis should take into account some other more frequent extramedullary tumours in this region, including schwannomas, meningiomas or dermoid tumours, as well as degenerative lesions. MRI is the primary modality for imaging spinal neoplasms and of vital importance in making the diagnosis. It may uncover spinal or paraspinal neoplasms, as well as unusual degenerative conditions[2]. MRI is helpful in identifying the extent of the tumour and its relationship with intraspinal structures, as well as the eventual bone destruction and invasion of the surrounding soft tissues[10]. The key point of diagnosis is the pathological result[5].

The treatment aim is to minimize both tumour and therapy-related morbidity. Usually, it encompasses different modalities[9,14]. It generally involves surgical treatment with or without adjuvant radiotherapy, which is most commonly used in patients with subtotal resection of intradural ependymomas, local recurrence or CNS dissemination. Although the effect of adjuvant radiotherapy is significant in younger patients, the data supporting the use of radiation therapy for extradural ependymomas are lacking, and there is no substantial role for chemotherapy in tumour treatment, except in children in an effort to delay radiation. The surgical methods include gross total removal, piecemeal total removal and subtotal removal. When possible, a complete resection is made, which is associated with decreased recurrence rates and improvement in performance score, especially in older patients[3,5,7,9,16]. The grossly encapsulated tumours could be removed intact. Indeed, en block rather than piecemeal resection should be performed, since the latter has been associated with higher recurrence rates[17]. However, when the lesion is large or unencapsulated or infiltrates and adheres to the nerve roots, the piecemeal total removal could be adopted[3,5]. When the conus medullaris and cauda equina are involved with the tumour, gross-total resection can be obtained in 43% to 59% of cases[17,18]. Under electrophysiological monitoring, we performed subtotal removal of

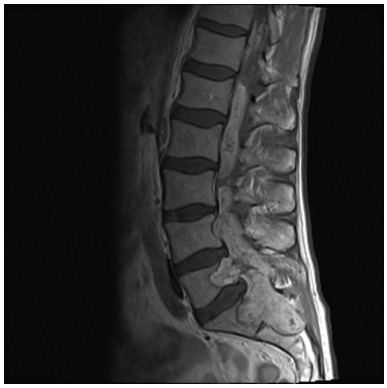

Figure 2 An extensive tumorous lesion was seen in 2014, located intramedullary, extending from the Th11, invading the conus medullaris and encompassing the entire sacral and lumbar canal to the S2 level, invading the vertebrae and spreading to perispinal muscles. Homogenous contrast enhancement is evident.

the tumour in this case. There was no postoperative neurological deficit caused by piecemeal partial removal of the intra- and extradural parts. As a result of subtotal tumour resection, postoperative radiation therapy was necessary. Although there was no evidence of a dose-response relationship between the amount of radiation and tumour progression, most authorities recommend radiation doses in the range of 40 Gy to 50 Gy[19]. Our patient received 56 Gy in 28 fractions. At the follow-up, a good outcome was observed.

The prognosis of ependymomas depends on many factors, such as tumour location, histology, stage of the disease and the extent of surgical resection. This is particularly important for myxopapillary tumours that occur in the lumbar spine[7]. Despite the risk for local recurrence and CNS dissemination, the prognosis for intradural lumbosacral ependymomas is good, with a 10-year survival rate of 90%. On the other hand, the extradural location bears worse prognosis, which is better for dorsal sacral tumours than presacral tumours[3]. In our case, a partial tumour resection was achieved and postoperative radiation therapy of the spinal cord was effective. After 8 mo, tumour regression was documented by MRI. The patient had an uneventful clinical course and has been regularly followed up for over 18 mo after the surgery.

CONCLUSION

Many factors may influence the prognosis of myxopapillary ependymomas of the lumbar spine. Despite the risk of tumour recurrence and CNS dissemination, the prognosis of lumbosacral ependymomas is usually good. As the disease may present with signs and symptoms similar to more trivial lesions, a high level of clinical suspicion is necessary.

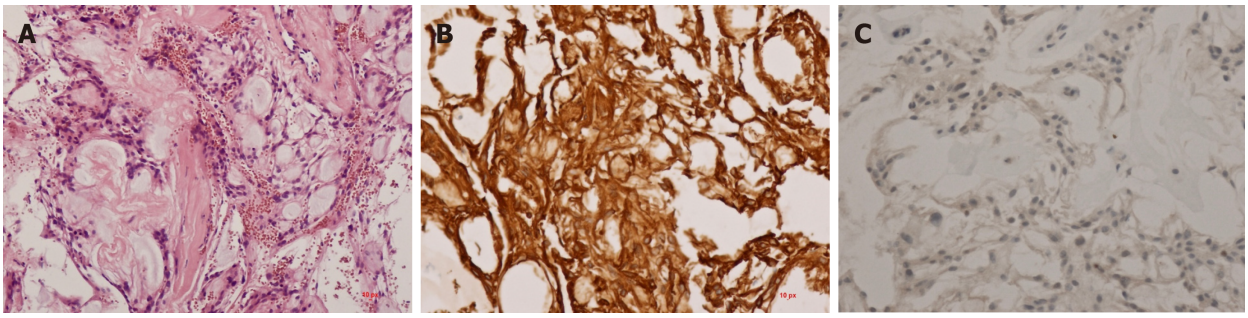

Figure 3 Histological examination results. A: Myxopapillary ependymomas display a variable papillary architecture with cuboid to elongated glial cells radially arranged in myxoid stroma with a central blood vessel; B: The tumour cells are immunoreactive for vimentin and GFAP; C: Immunoreactivity for cytokeratins is typically absent.

Figure 4 The control magnetic resonance imaging showing no progression of the tumour.

ACKNOWLEDGEMENTS

We thank Dr. Irena Strojnik for technical assistance in preparing the manuscript and Dr. Kristina Gornik Kramberger for providing microphotography of the tumour.

REFERENCES

1 **Vera-Bolanos E**, Aldape K, Yuan Y, Wu J, Wani K, Necesito-Reyes MJ, Colman H, Dhall G, Lieberman FS, Metellus P, Mikkelsen T, Omuro A, Partap S, Prados M, Robins HI, Soffietti R, Wu J, Gilbert MR, Armstrong TS; CERN Foundation. Clinical course and progression-free survival of adult intracranial and spinal ependymoma patients. *Neuro Oncol* 2015; **17**: 440-447 [PMID: 25121770 DOI: 10.1093/neuonc/nou162]

2 **Morselli C**, Ruggeri AG, Pichierri A, Marotta N, Anzidei M, Delfini R. Intradural Extramedullary Primary Ependymoma of the Craniocervical Junction Combined with C1 Partial Agenesis: Case Report and Review of the Literature. *World Neurosurg* 2015; **84**: 2076.e1-2076.e6 [PMID: 26210708 DOI: 10.1016/j.wneu.2015.07.027]

3 **Fassett DR**, Schmidt MH. Lumbosacral ependymomas: a review of the management of intradural and extradural tumors. *Neurosurg Focus* 2003; **15**: E13 [PMID: 15323470 DOI: 10.3171/foc.2003.15.5.13]

4 **Sevick RJ**, Wallace CJ. MR imaging of neoplasms of the lumbar spine. *Magn Reson Imaging Clin N Am* 1999; **7**: 539-553, ix [PMID: 10494534]

5 **Al-Habib A**, Al-Radi OO, Shannon P, Al-Ahmadi H, Petrenko Y, Fehlings MG. Myxopapillary ependymoma: correlation of clinical and imaging features with surgical resectability in a series with long-term follow-up. *Spinal Cord* 2011; **49**: 1073-1078 [PMID: 21647167 DOI: 10.1038/sc.2011.67]

6 **Koeller KK**, Shih RY. Intradural Extramedullary Spinal Neoplasms: Radiologic-Pathologic Correlation. *Radiographics* 2019; **39**: 468-490 [PMID: 30844353 DOI: 10.1148/rg.2019180200]

7 **Moynihan TJ**. Ependymal tumors. *Curr Treat Options Oncol* 2003; **4**: 517-523 [PMID: 14585232 DOI: 10.1007/s11864-003-0052-5]

8 **Plans G**, Brell M, Cabiol J, Villà S, Torres A, Acebes JJ. Intracranial retrograde dissemination in filum terminale myxopapillary ependymomas. *Acta Neurochir (Wien)* 2006; **148**: 343-6; discussion 346 [PMID: 16362177 DOI: 10.1007/s00701-005-0693-1]

9 **Feldman WB**, Clark AJ, Safaee M, Ames CP, Parsa AT. Tumor control after surgery for spinal myxopapillary ependymomas: distinct outcomes in adults versus children: a systematic review. *J Neurosurg Spine* 2013; **19**: 471-476 [PMID: 23971762 DOI: 10.3171/2013.6.SPINE12927]

10 **Shors SM**, Jones TA, Jhaveri MD, Huckman MS. Best cases from the AFIP: myxopapillary ependymoma of the sacrum. *Radiographics* 2006; **26** Suppl 1: S111-S116 [PMID: 17050509 DOI:

10.1148/rg.26si065020]
11 **Moelleken SM**, Seeger LL, Eckardt JJ, Batzdorf U. Myxopapillary ependymoma with extensive sacral destruction: CT and MR findings. *J Comput Assist Tomogr* 1992; **16**: 164-166 [PMID: 1729299]
12 **Biagini R**, Demitri S, Orsini U, Bibiloni J, Briccoli A, Bertoni F. Osteolytic extra-axial sacral myxopapillary ependymoma. *Skeletal Radiol* 1999; **28**: 584-589 [PMID: 10550537 DOI: 10.1007/s002560050624]
13 **Chamberlain MC**, Tredway TL. Adult primary intradural spinal cord tumors: a review. *Curr Neurol Neurosci Rep* 2011; **11**: 320-328 [PMID: 21327734 DOI: 10.1007/s11910-011-0190-2]
14 **Bandopadhayay P**, Silvera VM, Ciarlini PDSC, Malkin H, Bi WL, Bergthold G, Faisal AM, Ullrich NJ, Marcus K, Scott RM, Beroukhim R, Manley PE, Chi SN, Ligon KL, Goumnerova LC, Kieran MW. Myxopapillary ependymomas in children: imaging, treatment and outcomes. *J Neurooncol* 2016; **126**: 165-174 [PMID: 26468139 DOI: 10.1007/s11060-015-1955-2]
15 **Bagley CA**, Wilson S, Kothbauer KF, Bookland MJ, Epstein F, Jallo GI. Long term outcomes following surgical resection of myxopapillary ependymomas. *Neurosurg Rev* 2009; **32**: 321-34; discussion 334 [PMID: 19221818 DOI: 10.1007/s10143-009-0190-8]
16 **Kukreja S**, Ambekar S, Sharma M, Sin AH, Nanda A. Outcome predictors in the management of spinal myxopapillary ependymoma: an integrative survival analysis. *World Neurosurg* 2015; **83**: 852-859 [PMID: 25108296 DOI: 10.1016/j.wneu.2014.08.006]
17 **Sonneland PR**, Scheithauer BW, Onofrio BM. Myxopapillary ependymoma. A clinicopathologic and immunocytochemical study of 77 cases. *Cancer* 1985; **56**: 883-893 [PMID: 4016681 DOI: 10.1002/1097-0142(19850815)56:4<883::AID-CNCR2820560431>3.0.CO;2-6]
18 **Celli P**, Cervoni L, Cantore G. Ependymoma of the filum terminale: treatment and prognostic factors in a series of 28 cases. *Acta Neurochir (Wien)* 1993; **124**: 99-103 [PMID: 8304078 DOI: 10.1007/BF01401130]
19 **Andoh H**, Kawaguchi Y, Seki S, Asanuma Y, Fukuoka J, Ishizawa S, Kimura T. Multi-focal Myxopapillary Ependymoma in the Lumbar and Sacral Regions Requiring Cranio-spinal Radiation Therapy: A Case Report. *Asian Spine J* 2011; **5**: 68-72 [PMID: 21386949 DOI: 10.4184/asj.2011.5.1.68]

World Journal of Clinical Cases

Submit a Manuscript: https://www.f6publishing.com

World J Clin Cases 2019 May 26; 7(10): 1149-1154

DOI: 10.12998/wjcc.v7.i10.1149

ISSN 2307-8960 (online)

CASE REPORT

Electrohydraulic lithotripsy and rendezvous nasal endoscopic cholangiography for common bile duct stone: A case report

Koichi Kimura, Kensuke Kudo, Tomoharu Yoshizumi, Takeshi Kurihara, Shohei Yoshiya, Yohei Mano, Kazuki Takeishi, Shinji Itoh, Noboru Harada, Toru Ikegami, Tetsuo Ikeda

ORCID number: Koichi Kimura (0000-0003-4116-4135); Kensuke Kudo (0000-0001-8977-9126); Tomoharu Yoshizumi (0000-0002-4497-1816); Takeshi Kurihara (0000-0002-3063-9126); Shohei Yoshiya (0000-0003-4642-5058); Yohei Mano (0000-0001-8365-3194); Kazuki Takeishi (0000-0002-8448-5396); Shinji Itoh (0000-0003-0382-2520); Noboru Harada (0000-0002-6791-7097); Toru Ikegami (0000-0001-5792-5045); Tetsuo Ikeda (0000-0002-1193-6707).

Author contributions: Kimura K was responsible for the study conception, design and drafting of the manuscript; Kudo K, Kurihara T, Yoshiya S, Mano Y, Takeishi K, Itoh S, Harada N, and Ikegami T were responsible for data collection; Yoshizumi T and Ikeda T were responsible for critical revision of the manuscript, and all authors issued final approval for the version to be submitted.

Informed consent statement: Informed written consent was obtained from the patient for publication of this report and any accompanying images.

Conflict-of-interest statement: The authors declare that they have no conflict of interest.

CARE Checklist (2016) statement: The authors have read the CARE Checklist (2016), and the manuscript was prepared and revised according to the CARE Checklist (2016).

Koichi Kimura, Kensuke Kudo, Tetsuo Ikeda, Department of Endoscopy and Endoscopic Surgery, Fukuoka Dental College, Fukuoka 814-0175, Japan

Koichi Kimura, Kensuke Kudo, Tomoharu Yoshizumi, Takeshi Kurihara, Shohei Yoshiya, Yohei Mano, Kazuki Takeishi, Shinji Itoh, Noboru Harada, Toru Ikegami, Tetsuo Ikeda, Department of Surgery and Science, Graduate School of Medical Sciences, Kyushu University, Fukuoka 812-8582, Japan

Corresponding author: Koichi Kimura, MD, PhD, Assistant Professor, Doctor, Surgeon, Department of Endoscopy and Endoscopic Surgery, Fukuoka Dental College, 2-15-1, Tamura, Sawaraku, Fukuoka 814-0175, Japan. kkimura@surg2.med.kyushu-u.ac.jp
Telephone: +81-92-8010411
Fax: +81-92-8010459

Abstract

BACKGROUND

In patients with large stones in the common bile duct (CBD), advanced treatment modalities are generally needed. Here, we present an interesting case of a huge CBD stone treated with electrohydraulic lithotripsy (EHL) by the percutaneous approach and rendezvous endoscopic retrograde cholangiography (ERC) using a nasal endoscope.

CASE SUMMARY

A 91-year-old woman underwent ERC for a symptomatic large CBD stone with a diameter of 50 mm. She was referred to our institution after the failure of lithotomy by ERC, and after undergoing percutaneous transhepatic biliary drainage. We attempted to fragment the stone by transhepatic cholangioscopy using EHL. However, the stones were too large and partly soft clay-like for lithotripsy. Next, we attempted lithotomy with ERC and cholangioscopy by the rendezvous technique using a nasal endoscope and achieved complete lithotomy. No complication was observed at the end of this procedure.

CONCLUSION

Cholangioscopy by rendezvous technique using a nasal endoscope is a feasible and safe endoscopic method for removing huge CBD stones.

Key words: Common bile duct stone; Electrohydraulic lithotripsy; Rendezvous technique; Endoscopic retrograde cholangiography; Nasal endoscop; Case report

Manuscript source: Unsolicited manuscript

Received: February 12, 2019
Peer-review started: February 13, 2019
First decision: March 9, 2019
Revised: March 20, 2019
Accepted: March 26, 2019
Article in press: March 26, 2019
Published online: May 26, 2019

P-Reviewer: de Quadros LG, Friedel D
S-Editor: Dou Y
L-Editor: A
E-Editor: Xing YX

Core tip: Common bile duct (CBD) stones that are very large may require choledochotomy or lithotomy. However, surgery may be contra indicated in very elderly patients, and alternate treatments are required. Recent reports indicate that electrohydraulic lithotripsy (EHL) is an effective treatment for bile duct stones. We used EHL, followed by retrograde cholangiography and the rendezvous technique *via* nasal endoscope to successfully treat an elderly patient with a 50 mm diameter CBD stone.

Citation: Kimura K, Kudo K, Yoshizumi T, Kurihara T, Yoshiya S, Mano Y, Takeishi K, Itoh S, Harada N, Ikegami T, Ikeda T. Electrohydraulic lithotripsy and rendezvous nasal endoscopic cholangiography for common bile duct stone: A case report. *World J Clin Cases* 2019; 7(10): 1149-1154
URL: https://www.wjgnet.com/2307-8960/full/v7/i10/1149.htm
DOI: https://dx.doi.org/10.12998/wjcc.v7.i10.1149

INTRODUCTION

Common bile duct (CBD) stones are identified in up to 12% of patients with bile duct stones and are generally managed with endoscopic retrograde cholangiography (ERC) with endoscopic sphincterotomy (EST) for lithotomy[1]. Unfortunately, up to 15% of all CBD stones cannot be removed using standard techniques, due to the technical difficulty[2]. Extracorporeal shock wave lithotripsy, laser lithotripsy, and balloon sphincteroplasty enable us to manage such complicated cases[3]. Surgical procedures, such as choledochotomy and lithotomy, are performed for cases of endoscopic failure[4]. However, surgical procedures may be contraindicated for very elderly people, such as those over 90 years old, and need careful consideration.

Recently, several reports have shown that electrohydraulic lithotripsy (EHL) is useful as a treatment for bile duct stones[5,6]. This newer procedure has not yet been established as a standard treatment, and only a few reports regarding the endoscopic treatment of bile duct stones have been published. Moreover, some cases are difficult to treat with EHL. Development of endoscopic and noninvasive lithotomy methods that avoid surgical procedures is essential for elderly patients.

Here we present the case of a patient with a huge CBD stone with a diameter of 50 mm that was successfully treated using EHL with transhepatic cholangioscopy, followed by ERC lithotomy and cholangioscopy by the rendezvous technique with a nasal endoscope.

CASE PRESENTATION

Chief complaints

A 91-year-old woman was admitted to another hospital because of abdominal pain, nausea, vomiting, and jaundice due to cholangitis with CBD stones.

History of present illness

Lithotomy by ERC was unsuccessful due to the large size of the stone. Thereafter, she developed strangulated CBD stones in the papilla of Vater, and underwent percutaneous transhepatic biliary drainage (PTBD) of the left lobe. She was transferred to our hospital afterward for general condition management.

History of past illness

The patient had a history of repeated cholangitis due to CBD stones.

Personal and family history

She had hypertension and dementia. There is no history of her family.

Physical examination upon admission

She had slight jaundice upon admission, but general condition was alomost good.

Laboratory examinations

Laboratory findings indicated thatwhite blood corpuscle was 5900 (reference range

3500-8400), haemoglobin 9.6 g/dL (reference range 11.3-15.2 U/L), albumin 3.0 g/dL (reference range 4.0-5.0 g/dL), aspartate aminotransferase 49 U/L (reference range 13-33 U/L), alanine aminotransferase 97 U/L (reference range 6-30 U/L), alkaline phosphatase 378 U/L (reference range 115-359 U/L), gamma-glutamyl transpeptidase 81 U/L (reference range 10-47 U/L), and C-reactive protein 0.82 mg/dL (reference range < 0.2 mg/dL).

Imaging examinations

Cholangiography revealed a huge CBD stone over 50 mm in diameter (Figure 1).

FINAL DIAGNOSIS

The patient was diagnosed with repeat cholangitis due to CBD stones.

TREATMENT

The single-stage ERC approach was not suitable for the huge CBD stone. We up-sized to a 14 Fr drainage tube and performed cholangioscopy and EHL lithotripsy (SpyGlass™, Boston Scientific Corporation, United States) and ERC. First, EHL was performed with a cholangioscope from the percutaneous route. However, the stone was too large and partly soft clay-like in texture. We scaled down the stone by reducing the periphery with EHL, then performed ERC and EST. After cannulation into the bile duct, which was difficult due to the large periampullary diverticula, we performed the rendezvous technique (Figure 2). Lithotripsy was attempted *via* another crasher catheter (CrasherCatheter PowerCatch™, MTW Endoskopie, Germany). We succeeded in breaking the CBD stone into small pieces in the bile duct, but the stone was too soft and many pieces adhered to the CBD wall. Therefore, we performed direct peroral cholangioscopy by nasal endoscope with the rendezvous technique (Figure 3). The guidewire was inserted from the PTBD route into the papilla of Vater, and was grasped with biopsy forceps *via* the nasal endoscope. The nasal endoscope was then inserted into the CBD along the guidewire. Complete lithotomy was accomplished by nasal endoscope with biopsy forceps and basket catheter (MiniCatch™, MTW Endoskopie, Germany).

OUTCOME AND FOLLOW-UP

There is no recurrence of CBD stones after treatment for one year.

DISCUSSION

Trikudanathan *et al*[2] reported that in approximately 10%-15% of patients, managing biliary stones becomes hard due to hardships in accessing the bile duct (periampullary diverticula, gastrointestinal reconstructive surgery), a large number or size of stones (diameter > 15 mm), misshapen shaped stones, or location of the stones. In this case, the large diameter of the stone, its soft clay-like texture, and large parapapillary diverticula made it hard to accomplish complete lithotomy. Recently, various techniques for the treatment of intractable CBD stones have been reported. In 1982, Riemann *et al*[7] first introduced mechanical lithotripsy with baskets. Mechanical lithotripsy is currently the most widely used technique for fragmentation of stones and is routinely the first approach to fragment CBD stones with great advantages that are simplicity and cost-effectiveness. However, this procedure cannot be adapted to stones larger than the size of the basket, and hard and densely calcified stones resist mechanical fragmentation, resulting in an extraction failure with standard baskets.

EHL consists of a bipolar lithotripsy probe that discharges sparks with the aid of a charge generator in an aqueous medium. The sparks generated under water generate high-frequency hydraulic pressure waves, the energy of which is absorbed by nearby stones and results in their fragmentation[8]. EHL can be performed under fluoroscopic guidance by direct cholangioscopic vision. Nevertheless, in our case, we could not complete lithotomy by EHL due to the soft clay-like consistency inside the stone. Next, we attempted lithotomy with ERC after scaling down the periphery of the large stone with EHL.

Direct peroral cholangioscopy using an ultra-slim endoscope can be effective in managing patients with retained CBD stones[9]. The most profound disadvantage of

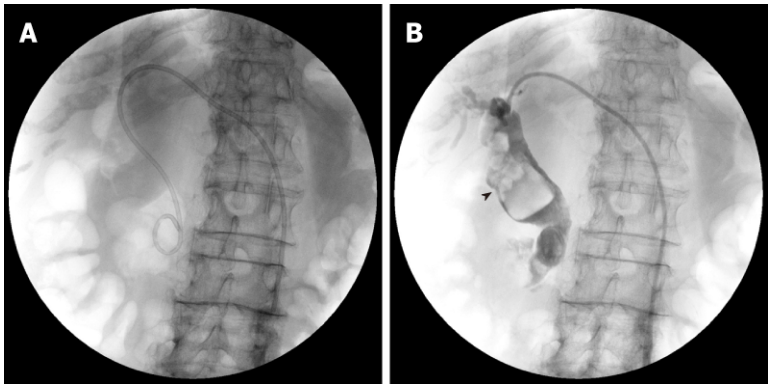

Figure 1 Cholangiography images in percutaneous transhepatic biliary drainage. A: A 6 Fr pig-tail extra drainage tube is inserted; B: Black arrow head shows huge common bile duct stones (over 50 mm).

peroral cholangioscopy, however, is the difficulty associated with traversing the biliary sphincter to gain access to the bile duct. This is mainly due to looping of the ultra-slim upper endoscope in the stomach or in the duodenum. To enhance the success rate of peroral cholangioscopy, specialized accessories or techniques are needed to advance the ultra-slim endoscope into the proximal biliary system[2]. We utilized the rendezvous technique to approach the bile duct by nasal endoscope.

Some studies have reported that the rendezvous technique is useful to easily access the bile duct[6,10,11]. When performing the rendezvous technique, we were easily able to access the CBD by grasping the guidewire inserted from the PTCD route using biopsy forceps.

The nasal endoscope was then inserted easily into the CBD, and used to directly visualize the CBD stones. The nasal endoscope has a wide forceps channel that accommodates insertion of biopsy forceps to grasp the guidewire, and the image from the nasal endoscope is clearer than that of the usual cholangioscope. We, therefore, find that it is easier to treat huge CBD stones using the rendezvous technique than the usual peroral cholangioscopy.

CONCLUSION

In this case, the large and soft CBD stone made lithotomy difficult. Moreover, the large parapapillary diverticula made it difficult to cannulate into the papilla of Vater and to complete lithotomy. Therefore, we derived procedures to overcome those challenges.

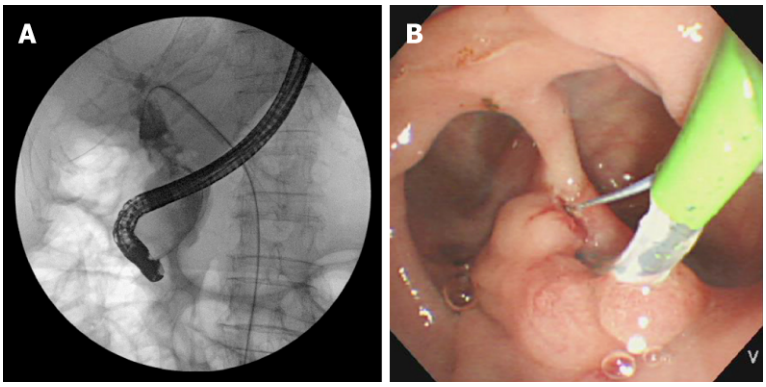

Figure 2 Images of endoscopic retrograde cholangiography and endoscopic sphincterotomy with rendezvous technique. A: Cholangiography image of endoscopic retrograde cholangiography with rendezvous technique; B: Endoscopic image of endoscopic sphincterotomy. Large periampullary diverticula surrounding the papilla of Vater.

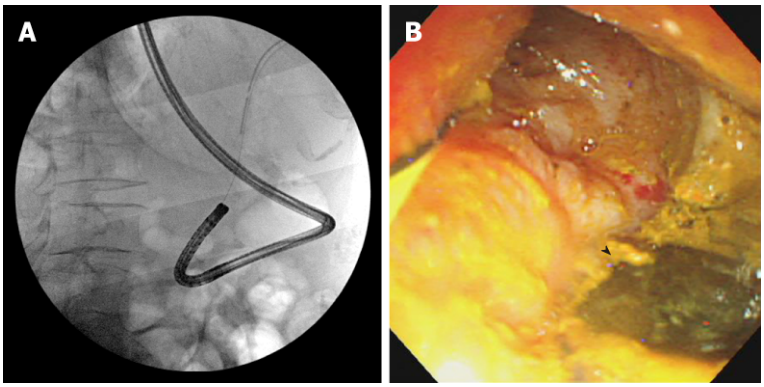

Figure 3 Images of direct peroral cholangioscopy by nasal endoscope with rendezvous technique. A: Cholangiography images of insertion of nasal endoscope in common bile duct (CBD) by rendezvous technique; B: Direct peroral cholangioscopy image by nasal endoscope in CBD. Black arrow head shows adhered stone piece in the CBD wall.

REFERENCES

1 **Freitas ML**, Bell RL, Duffy AJ. Choledocholithiasis: evolving standards for diagnosis and management. *World J Gastroenterol* 2006; **12**: 3162-3167 [PMID: 16718834 DOI: 10.3748/wjg.v12.i20.3162]

2 **Trikudanathan G**, Navaneethan U, Parsi MA. Endoscopic management of difficult common bile duct stones. *World J Gastroenterol* 2013; **19**: 165-173 [PMID: 23345939 DOI: 10.3748/wjg.v19.i2.165]

3 **Li G**, Pang Q, Zhang X, Dong H, Guo R, Zhai H, Dong Y, Jia X. Dilation-assisted stone extraction: an alternative method for removal of common bile duct stones. *Dig Dis Sci* 2014; **59**: 857-864 [PMID: 24254339 DOI: 10.1007/s10620-013-2914-4]

4 **Fang L**, Wang J, Dai WC, Liang B, Chen HM, Fu XW, Zheng BB, Lei J, Huang CW, Zou SB. Laparoscopic transcystic common bile duct exploration: surgical indications and procedure strategies. *Surg Endosc* 2018; **32**: 4742-4748 [PMID: 30298446 DOI: 10.1007/s00464-018-6195-z]

5 **Otsuka Y**, Kamata K, Takenaka M, Minaga K, Tanaka H, Kudo M. Electronic hydraulic lithotripsy by antegrade digital cholangioscopy through endoscopic ultrasound-guided hepaticojejunostomy. *Endoscopy* 2017; **49**: E316-E318 [PMID: 28992640 DOI: 10.1055/s-0043-119971]

6 **Kimura K**, Kudo K, Kurihara T, Yoshiya S, Mano Y, Takeishi K, Itoh S, Harada N, Ikegami T, Yoshizumi T, Ikeda T. Rendezvous Technique Using Double Balloon Endoscope for Removal of Multiple Intrahepatic Bile Duct Stones in Hepaticojejunostomy After Living Donor Liver Transplant: A Case Report. *Transplant Proc* 2019; **51**: 579-584 [PMID: 30879594 DOI: 10.1016/j.transproceed.2018.12.005]

7 **Riemann JF**, Seuberth K, Demling L. Clinical application of a new mechanical lithotripter for smashing common bile duct stones. *Endoscopy* 1982; **14**: 226-230 [PMID: 7140657 DOI: 10.1055/s-2007-1021626]

8 **Seitz U**, Bapaye A, Bohnacker S, Navarrete C, Maydeo A, Soehendra N. Advances in therapeutic endoscopic treatment of common bile duct stones. *World J Surg* 1998; **22**: 1133-1144 [PMID: 9828721 DOI: 10.1007/s002689900532]

9 **Kurihara T**, Yasuda I, Isayama H, Tsuyuguchi T, Yamaguchi T, Kawabe K, Okabe Y, Hanada K, Hayashi T, Ohtsuka T, Oana S, Kawakami H, Igarashi Y, Matsumoto K, Tamada K, Ryozawa S, Kawashima H, Okamoto Y, Maetani I, Inoue H, Itoi T. Diagnostic and therapeutic single-operator cholangiopancreatoscopy in biliopancreatic diseases: Prospective multicenter study in Japan. *World J Gastroenterol* 2016; **22**: 1891-1901 [PMID: 26855549 DOI: 10.3748/wjg.v22.i5.1891]

10 **Noel R**, Arnelo U, Swahn F. Intraoperative versus postoperative rendezvous endoscopic retrograde cholangiopancreatography to treat common bile duct stones during cholecystectomy. *Dig Endosc* 2019; **31**: 69-76 [PMID: 29947437 DOI: 10.1111/den.13222]

11 **Yoshiya S**, Shirabe K, Matsumoto Y, Ikeda T, Soejima Y, Yoshizumi T, Uchiyama H, Ikegami T, Harimoto N, Maehara Y. Rendezvous ductoplasty for biliary anastomotic stricture after living-donor liver transplantation. *Transplantation* 2013; **95**: 1278-1283 [PMID: 23492991 DOI: 10.1097/TP.0b013e31828a9450]

World Journal of Clinical Cases

Submit a Manuscript: https://www.f6publishing.com

World J Clin Cases 2019 May 26; 7(10): 1155-1160

DOI: 10.12998/wjcc.v7.i10.1155

ISSN 2307-8960 (online)

CASE REPORT

F-18 fluorodeoxyglucose positron emission tomography/computed tomography image of gastric mucormycosis mimicking advanced gastric cancer: A case report

Bong-Il Song

ORCID number: Bong-Il Song (0000-0002-3106-6112).

Author contributions: Song BI edited the all manuscript.

Supported by National Research Foundation of Korea (NRF) grant funded by the Korea government (MSIP), No. 2017R1C1B5076640.

Institutional review board statement: This case report was reviewed and approved by the Institutional Review Board of Dongsan Medical Center Keimyung University (IRB No. 2018-04-021).

Informed consent statement: Informed consent was obtained from the patient.

Conflict-of-interest statement: Song BI declare no conflicts of interests.

CARE Checklist (2016) statement: The authors have read the CARE Checklist (2016), and the manuscript was prepared and revised according to the CARE Checklist (2016).

Bong-Il Song, Department of Nuclear Medicine, Dongsan Medical Center, Keimyung University School of Medicine, Daegu 41932, South Korea

Corresponding author: Bong-Il Song, MD, Assistant Professor, Department of Nuclear Medicine, Dongsan Medical Center, Keimyung University School of Medicine, 56 Dalseong-ro, Jung-gu, Daegu 41931, South Korea. song@dsmc.or.kr
Telephone: +82-53-250-7023
Fax: +82-53-250-8695

Abstract

BACKGROUND

Mucormycosis is a very rare fungal infection, and its prognosis is poor. Most common sites of infection are the sinuses, lung, or skin, and gastric involvement is uncommon. The standard antifungal therapy is the treatment of choice for gastric mucormycosis. However, the symptoms of gastric mucormycosis are varied and the early diagnosis is not easy.

CASE SUMMARY

I report a 53-year-old alcoholic man, who was admitted due to epigastric pain. The upper gastrointestinal endoscopy revealed a huge ulcer lesion in the stomach, which was suspected to be gastric cancer. F-18 fluorodeoxyglucose positron emission tomography/computed tomography (F-18 FDG PET/CT) showed diffusely intense FDG uptake at the ulcer lesion of the stomach, and several enlarged hypermetabolic lymph nodes were noted at the left gastric chain. Although, endoscopy and F-18 FDG PET/CT findings suggested advanced gastric cancer with regional lymph node metastases, there was no cancer cells in the biopsy results and multiple fungal hyphae were noted in the periodic acid-Schiff stained image.

CONCLUSION

He was diagnosed with gastric mucormycosis and successfully underwent amphotericin B and posaconazole treatment.

Key words: F-18 fluorodeoxyglucose; Positron emission tomography; Mucormycosis; Amphotericin B; Gastric cancer; Case report

Manuscript source: Unsolicited manuscript

Received: December 29, 2018
Peer-review started: December 29, 2018
First decision: March 10, 2019
Revised: March 21, 2019
Accepted: March 26, 2019
Article in press: March 26, 2019
Published online: May 26, 2019

P-Reviewer: Eleftheriadis NP, Tsolakis AV
S-Editor: Dou Y
L-Editor: A
E-Editor: Wu YXJ

Core tip: Gastric mucormycosis is very rare, and there have been no reports on the F-18 fluorodeoxyglucose positron emission tomography/computed tomography (F-18 FDG PET/CT) finding of gastric mucormycosis. Since, endoscopic findings of gastric mucormycosis reveal ulcer margin with inflammatory/necrotic debris and hemorrhagic clots, F-18 FDG PET/CT of gastric mucormycosis reveal increased FDG uptake in the infected site. Additionally, reactive enlarged hypermetabolic lymph nodes in the perigastric chain could be observed. In this regard, it was difficult to differentiate gastric mucormycosis and gastric cancer by endoscopic findings and radiologic examinations. Therefore, careful consideration of clinical manifestations and precise diagnosis are necessary for optimal treatment of gastric mucormycosis.

Citation: Song BI. F-18 fluorodeoxyglucose positron emission tomography/computed tomography image of gastric mucormycosis mimicking advanced gastric cancer: A case report. *World J Clin Cases* 2019; 7(10): 1155-1160
URL: https://www.wjgnet.com/2307-8960/full/v7/i10/1155.htm
DOI: https://dx.doi.org/10.12998/wjcc.v7.i10.1155

INTRODUCTION

Mucormycosis is a life-threatening angioinvasive infection caused by fungi in the order Mucorales. It has the characteristic of invading the blood vessels; thus, the prognosis is known to be very poor. Like other fungal infections, patients with mucormycosis may have several predisposing factors associated with immunosuppressive conditions such as diabetes or long-term corticosteroid use. Additionally, several studies reported that chronic alcoholism can be one of the important predisposing conditions[1].

The three common sites of mucormycosis are the sinuses (39%), lung (24%), and skin (19%). Mucormycosis less commonly occurs in the gastrointestinal (GI) tract (about 7%)[2]. In the GI tract, mucormycosis most commonly affects the stomach followed by the colon and ileum[2]. Pathogens are known to be acquired by ingestion of contaminated foods.

The treatment for gastric mucormycosis is amphotericin B, posaconazole, and adjuvant surgical removal of the "fungal ball". The mortality rate is known to be extremely high, which is about 85%[3]. One of the major causes of gastric mucormycosis mortality is extremely delayed diagnoses; only 25% of patients with GI mucormycosis are diagnosed before death. Recently, several studies emphasized the importance of early diagnosis, which can affect the treatment direction and improve prognosis[4].

It is difficult to diagnose gastric mucormycosis because confirmation is possible only through histologic examination. In addition, some cases have been misdiagnosed as cancer during the initial screening due to their radiologic and endoscopic similarities. Several studies have reported the detection of mucormycosis in other organs using F-18 fluorodeoxyglucose positron emission tomography/computed tomography (F-18 FDG PET/CT); however, there have been no reports on the F-18 FDG PET/CT finding of gastric mucormycosis. We present an interesting case of a 53-year-old man who underwent F-18 FDG PET/CT and were initially suspected with advanced gastric cancer but finally confirmed as gastric mucormycosis.

CASE PRESENTATION

Chief complaints

A 53-year-old man presented with a 1-wk history of epigastric pain. He also had complaints of bloody vomitus and melena.

History of present illness

Three weeks prior to this hospital admission, abdominal discomfort and nausea had developed. He had visited the local hospital and received conservative treatment. However, the symptoms were not relieved after medication. A week ago, epigastric pain had developed, and he had vomited reddish blood on the day before admission. For further evaluation, the patient was transferred to this hospital.

History of past illness
He had no history of surgery and past medical history.

Personal and family history
The patient had a history of severe alcohol abuse and a 20 pack-year history of smoking. Otherwise, there were no special circumstances in family history.

Physical examination upon admission
The physical examination revealed no palpable abdominal mass or signs of peritoneal irritation. His blood pressure was 153/120 mmHg, and pulse rate was 115/min. He appeared chronically ill.

Laboratory examinations
The laboratory testing showed a normal white blood cell count, blood glucose, creatinine, coagulation profile, and serum electrolytes except low hemoglobin was present with a level of 10.5 g/dL (normal range: 13.5-17.5 g/dL).

Imaging examinations
The patient's upper GI endoscopy revealed diffuse erythema and edema of the gastric wall. Furthermore, a huge ulcer was detected in the posterior wall of the lower body (Figure 1), which was suspicious for Borrmann type II gastric cancer; therefore, patient underwent biopsy and additional studies for evaluation. Moreover, the contrast-enhanced abdominal CT showed a huge ulcer within the same lesion with diffuse wall thickening (Figure 2A). The margin of the pancreas was unclear, and multiple enlarged lymph nodes were observed in the left gastric and gastroepiploic chain (Figure 2B).

Because these findings strongly suggested gastric cancer at advanced stage, F-18 FDG PET/CT was performed for further evaluation. In the maximum intensity projection image, there was uneven FDG uptake on the stomach, but no other distant metastasis was seen (Figure 3A). Trans-axial F-18 FDG PET/CT image showed diffusely intense FDG uptake at the ulcer lesion (Figure 3B). In addition, several enlarged hypermetabolic lymph nodes were noted at the left gastric chain (Figure 3C). The clinical impression was gastric cancer with regional lymph node metastases.

However, there were no malignant cells and only severe inflammation was seen in the first biopsy result. The patient underwent secondary endoscopic biopsy for a pathologic confirmation. However, no cancer cells were found, and multiple fungal hyphae were noted in the periodic acid-Schiff (PAS)-stained image. The results indicated mucormycosis based on the characteristics of the hyphae, which showed a 90-degree angle branching with no visible septa (Figure 4).

FINAL DIAGNOSIS
The final diagnosis of the presented case is gastric mucormycosis. Unfortunately, the type of mucormycosis remained undetermined.

TREATMENT
The patient was treated with amphotericin B, given by injection, for 20 d and adjuvant posaconazole for 2 mo.

OUTCOME AND FOLLOW-UP
The follow-up endoscopy finding showed marked improvement of previous infected lesions and only mild redness of the gastric wall was observed (Figure 5). In addition, the follow-up CT showed much-improved state of previous gastric mucormycosis lesion and decreased size and number of previous enlarged lymph nodes (Figure 6). Thereafter, the therapy was terminated without further treatment.

DISCUSSION
With regard to the diagnosis, gastric mucormycosis has no specific finding on radiologic examination. In contrast-enhanced CT image, irregular thickening of the gastric folds can be seen with ulcer forming process[5]. In endoscopic examination,

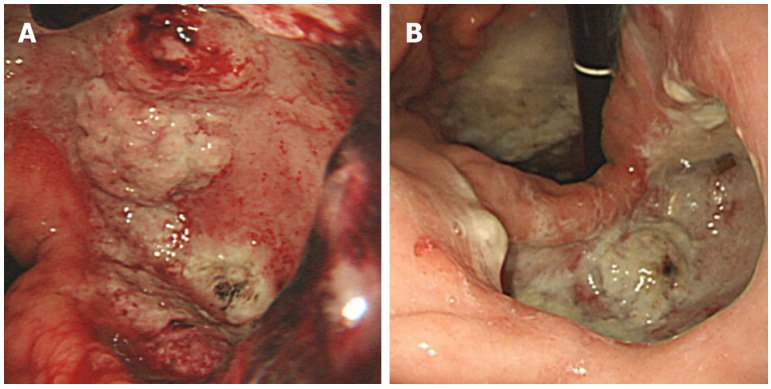

Figure 1 Upper gastrointestinal endoscopy images. This reveals a huge ulcer in the posterior wall of the stomach. The ulcer lesion was suspicious for Borrmann type II gastric cancer.

gastric mucormycosis appears as necrotizing ulcers combined with discoloration or blood clot. Because of the necrotizing tissues, gastric mucormycosis is often misdiagnosed as gastric cancer[6,7].

Diagnostic confirmation of gastric mucormycosis can be made only through histological examination. Fungal infections are best observed in Gomori methenamine silver or PAS stain. The pathologic finding is large and non-septa hyphae with 90-degree angle branching. Additionally, the three subtypes of gastric mucormycosis are detected through histological examination. The first type only exhibits the formation of a colony without invading the surrounding tissue. The second type involves infiltration into the surrounding tissue as a presenting case. Lastly, the third type involves vascular invasion with presence of hyphae in the vessel lumen[8]. The vascular invasion type is frequently associated with poor prognosis.

Although several studies have reported on the F-18 FDG PET/CT findings of patients with mucormycosis, the F-18 FDG PET/CT findings of patients with gastric mucormycosis has not been reported. Increased FDG uptake at the infection focus was noted at the infection site, but there was no specific finding[9]. The F-18 FDG PET/CT finding of gastric mucormycosis in this patient also showed increased FDG uptake at the infection site. Therefore, it was difficult to differentiate gastric mucormycosis and gastric cancer by F-18 FDG PET/CT. However, as the importance of early diagnosis has been increasingly emphasized recently, some studies revealed that F-18 FDG PET/CT can be used to detect active metabolic changes reflecting inflammatory cell activity before the onset of anatomical abnormalities[10]. Furthermore, F-18 FDG PET/CT can give functional information, which can useful for the assessment of the overall therapeutic response[11].

CONCLUSION

The case report suggests that there is no definite method to completely differentiate mucormycosis and malignant tumors using F-18 FDG PET/CT. However, F-18 FDG PET/CT may contribute to the early diagnosis, assessment of disease extent, and evaluation of response to therapy in patients with gastric mucormycosis.

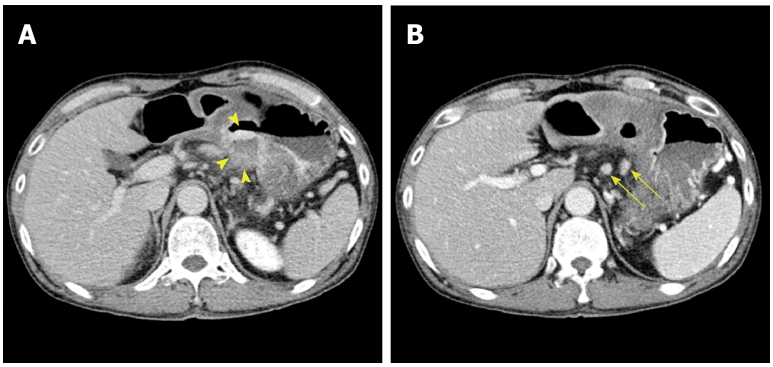

Figure 2 Contrast-enhanced abdominal computed tomography images. A: A huge ulcer lesion with diffuse wall thickening was detected in the posterior wall of the lower body of the stomach (yellow arrow head); B: Multiple enlarged left gastric lymph nodes were noted (yellow arrow).

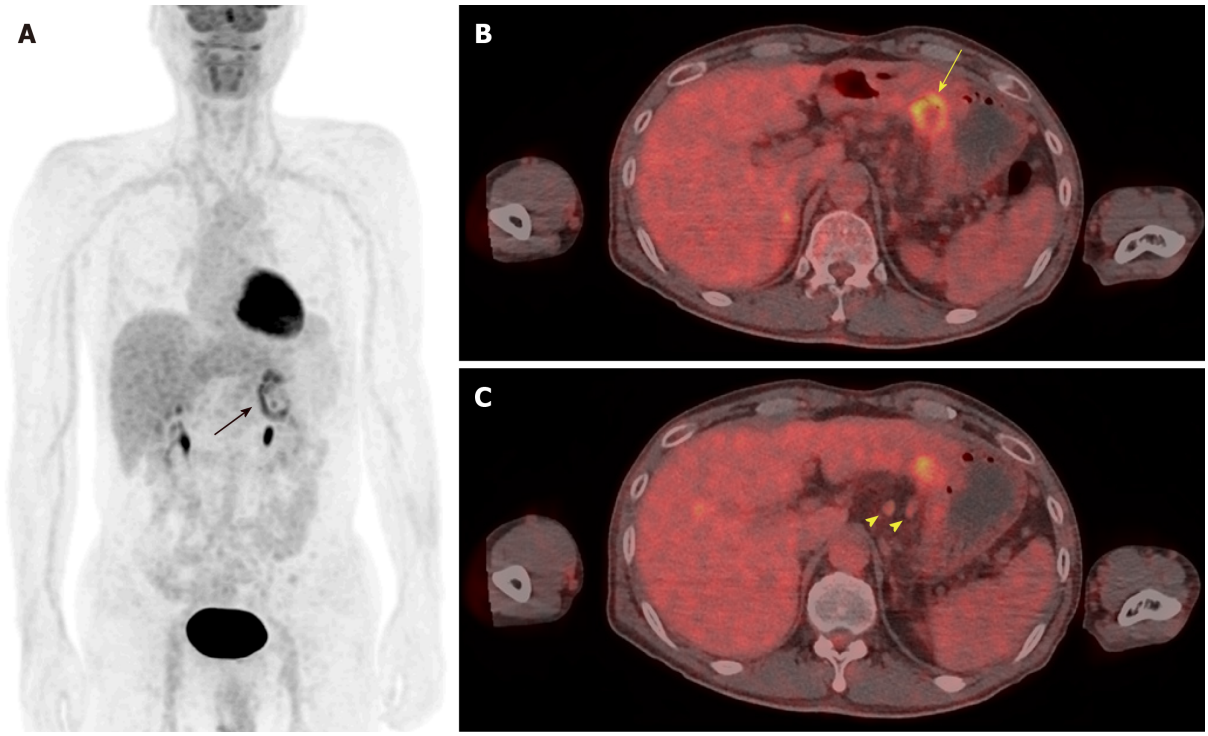

Figure 3 F-18 fluorodeoxyglucose positron emission tomography/computed tomography images. A: The maximum intensity projection image shows uneven uptake on the stomach (black arrow); B: Axial scan shows increased uptake in the posterior wall of the lower body of the stomach (yellow arrow); C: Several enlarged hypermetabolic lymph nodes were seen at the left gastric chain (yellow arrow head).

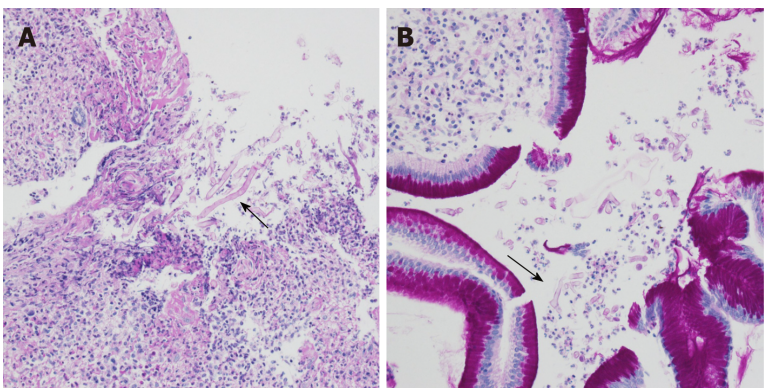

Figure 4 Periodic acid-Schiff stain. A, B: Multiple fungal hyphae with positive periodic acid-Schiff staining were observed (black arrow).

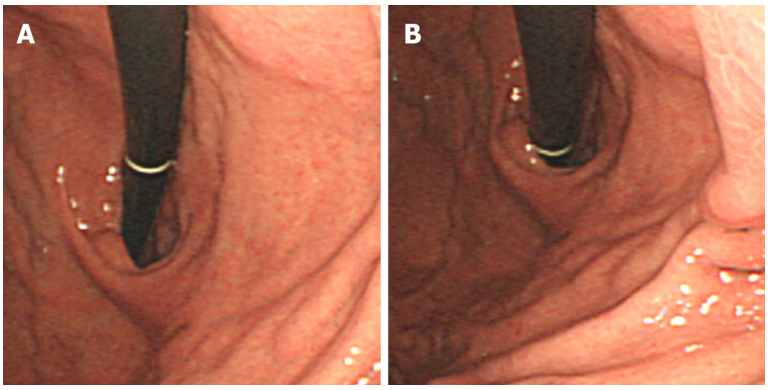

Figure 5 Follow-up upper gastrointestinal endoscopy images. A, B: The follow-up endoscopic finding reveals marked improvement of previous mucormycosis lesion.

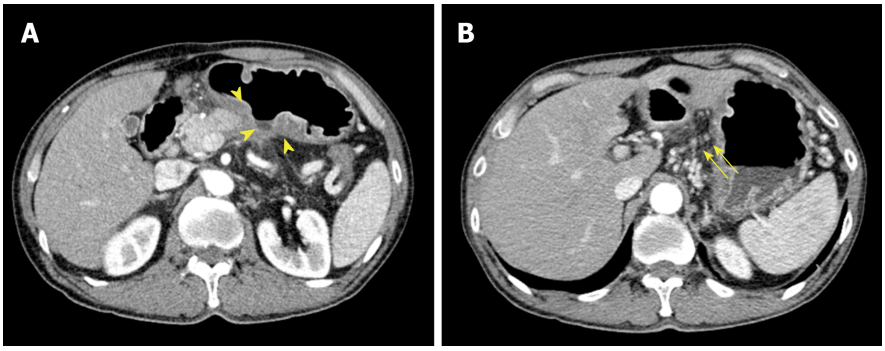

Figure 6 Follow-up contrast-enhanced abdominal computed tomography images. A: Previous mucormycosis lesion in the posterior wall of the lower body of the stomach showed much-improved state (yellow arrow head); B: Only small left gastric lymph nodes was observed (yellow arrow).

REFERENCES

1 **Ho YH**, Wu BG, Chen YZ, Wang LS. Gastric Mucormycosis in an Alcoholic with Review of the Literature. *Tzu Chi Med J* 2007; **19**: 169–172 [DOI: 10.1016/S1016-3190(10)60011-0]

2 **Petrikkos G**, Skiada A, Lortholary O, Roilides E, Walsh TJ, Kontoyiannis DP. Epidemiology and clinical manifestations of mucormycosis. *Clin Infect Dis* 2012; **54** Suppl 1: S23-S34 [PMID: 22247442 DOI: 10.1093/cid/cir866]

3 **Roden MM**, Zaoutis TE, Buchanan WL, Knudsen TA, Sarkisova TA, Schaufele RL, Sein M, Sein T, Chiou CC, Chu JH, Kontoyiannis DP, Walsh TJ. Epidemiology and outcome of zygomycosis: a review of 929 reported cases. *Clin Infect Dis* 2005; **41**: 634-653 [PMID: 16080086 DOI: 10.1086/432579]

4 **Walsh TJ**, Skiada A, Cornely OA, Roilides E, Ibrahim A, Zaoutis T, Groll A, Lortholary O, Kontoyiannis DP, Petrikkos G. Development of new strategies for early diagnosis of mucormycosis from bench to bedside. *Mycoses* 2014; **57** Suppl 3: 2-7 [PMID: 25475924 DOI: 10.1111/myc.12249]

5 **Samet JD**, Horton KM, Fishman EK. Invasive gastric mucormycosis: CT findings. *Emerg Radiol* 2008; **15**: 349-351 [PMID: 18071767 DOI: 10.1007/s10140-007-0689-7]

6 **Thomson SR**, Bade PG, Taams M, Chrystal V. Gastrointestinal mucormycosis. *Br J Surg* 1991; **78**: 952-954 [PMID: 1913115 DOI: 10.1002/bjs.1800780819]

7 **El Hachem G**, Chamseddine N, Saidy G, Choueiry C, Afif C. Successful Nonsurgical Eradication of Invasive Gastric Mucormycosis. *Clin Lymphoma Myeloma Leuk* 2016; **16** Suppl: S145-S148 [PMID: 27521312 DOI: 10.1016/j.clml.2016.02.020]

8 **Feldman M**, Friedman L, Brandt L. *Sleisenger and Fordtran's Gastrointestinal and Liver Disease* 2016; 875

9 **Sharma P**, Mukherjee A, Karunanithi S, Bal C, Kumar R. Potential role of 18F-FDG PET/CT in patients with fungal infections. *AJR Am J Roentgenol* 2014; **203**: 180-189 [PMID: 24951213 DOI: 10.2214/AJR.13.11712]

10 **Altini C**, Niccoli Asabella A, Ferrari C, Rubini D, Dicuonzo F, Rubini G. (18)F-FDG PET/CT contribution to diagnosis and treatment response of rhino-orbital-cerebral mucormycosis. *Hell J Nucl Med* 2015; **18**: 68-70 [PMID: 25679078 DOI: 10.1967/s002449910167]

11 **Liu Y**, Wu H, Huang F, Fan Z, Xu B. Utility of 18F-FDG PET/CT in diagnosis and management of mucormycosis. *Clin Nucl Med* 2013; **38**: e370-e371 [PMID: 23531773 DOI: 10.1097/RLU.0b013e3182867d13]

World Journal of Clinical Cases

Submit a Manuscript: https://www.f6publishing.com

World J Clin Cases 2019 May 26; 7(10): 1161-1168

DOI: 10.12998/wjcc.v7.i10.1161

ISSN 2307-8960 (online)

CASE REPORT

Ultrasound guidance for transforaminal percutaneous endoscopic lumbar discectomy may prevent radiation exposure: A case report

Ming-Bo Zhang, Long-Tao Yan, Shou-Peng Li, Ying-Ying Li, Peng Huang

ORCID number: Mingbo Zhang (0000-0002-7990-3493); Longtao Yan (0000-0002-4518-7396); Shoupeng Li (0000-0002-5675-0068); Yingying Li (0000-0003-4757-9550); Peng Huang (0000-0001-6221-0861).

Author contributions: Zhang MB and Yan LT contributed equally to this work and should be considered co-first authors; Zhang MB and Yan LT reviewed the literature, performed the ultrasound-assisted transforaminal percutaneous endoscopic lumbar discectomy, and contributed to manuscript drafting; Li SP and Li YY reviewed the literature and contributed to data collection; Huang P was responsible for establishment of ultrasound guidance method and the revision of the manuscript; all authors issued final approval for the version to be submitted.

Supported by Clinical Research Support Fund of PLA General Hospital, No. 2018XXFC-18.

Informed consent statement: Written informed consent was obtained from the patient for publication of this report and any accompanying images.

Conflict-of-interest statement: The authors declare that they have no conflict of interest.

CARE Checklist (2016) statement: The authors have read the CARE Checklist (2016), and the manuscript was prepared and revised according to the CARE Checklist (2016).

Ming-Bo Zhang, Shou-Peng Li, Ying-Ying Li, Department of Ultrasound, General Hospital of Chinese PLA, Beijing 100853, China

Long-Tao Yan, Department of Pain, China-Japan Friendship Hospital, Beijing 100029, China

Peng Huang, Department of Orthopedics, General Hospital of Chinese PLA, Beijing 100853, China

Corresponding author: Peng Huang, MD, Associate Professor, Department of Orthopedics, General Hospital of Chinese PLA, No. 28, Fuxing Road, Haidian District, Beijing 100853, China. harryhp@vip.sina.com
Telephone: +86-10-66875503

Abstract

BACKGROUND

Percutaneous endoscopic lumbar discectomy (PELD) has become a mature and mainstream minimally invasive surgical technique for treating lumbar disc herniation (LDH). Repeated fluoroscopy, with more than 30 shots on average, is inevitable to ensure its accuracy and safety. However, exposure to X-rays may pose a threat to human health. We herein report a case of ultrasound (US)-assisted PELD in two levels of LDH to explore a new possibility that can reduce the radiation dose during puncture and cannulation in PELD.

CASE SUMMARY

A 38-year-old man with low back pain and left leg pain for more than 7 years came to our clinic, his symptoms had aggravated for 1 month, and he was diagnosed with L3-4 and L4-5 disc herniations. He received US-guided PELD with good results: His straight leg elevation increased from 40 to 90 degrees after PELD, and his visual analog scale (VAS) and Oswestry Disability Index scores both significantly decreased immediately and 6 mo after PELD. With the guidance of US, he received only two shots of fluoroscopy (fluoroscopic time: 4.4 s; radiation dose: 3.98 mGy). To our knowledge, this is the first case of US-guided puncture and cannulation of PELD for LDH at two levels.

CONCLUSION

US could be used to guide PELD and has the potential to largely reduce radiation than traditional X-ray guidance.

Key words: Ultrasound; Endoscopic lumbar discectomy; Lumbar disc herniation; Radiation; Guidance; Case report

Manuscript source: Unsolicited manuscript

Received: January 13, 2019
Peer-review started: January 14, 2019
First decision: January 30, 2019
Revised: March 1, 2019
Accepted: March 16, 2019
Article in press: March 16, 2019
Published online: May 26, 2019

P-Reviewer: Bazeed MF, Cui XW, Gao BL, Valek V
S-Editor: Ji FF
L-Editor: Wang TQ
E-Editor: Wu YXJ

Core tip: Percutaneous endoscopic lumbar discectomy, a mature and mainstream minimally invasive surgical technique for treating lumbar disc herniation (LDH), needs more than 30 shots of fluoroscopy each level on average, causing a threat to human health. With the help of ultrasound (US) guidance, we report a patient with two levels of LDH who received only two shots to achieve satisfactory results. US guidance has great potential to become an alternative method to reduce radiation largely.

Citation: Zhang MB, Yan LT, Li SP, Li YY, Huang P. Ultrasound guidance for transforaminal percutaneous endoscopic lumbar discectomy may prevent radiation exposure: A case report. *World J Clin Cases* 2019; 7(10): 1161-1168
URL: https://www.wjgnet.com/2307-8960/full/v7/i10/1161.htm
DOI: https://dx.doi.org/10.12998/wjcc.v7.i10.1161

INTRODUCTION

Transforaminal percutaneous endoscopic lumbar discectomy (PELD) has become a mature and mainstream minimally invasive surgical technique for treating lumbar disc herniation (LDH)[1-4]. Fluoroscopy, to ensure the accuracy of puncture and cannulation, is inevitable. However, radiation exposure with X-ray guidance of PELD may be of concern because of its deleterious effects for both patients and surgeons. Therefore, an image guiding system without X-ray is needed to perform PELD. Ultrasound (US) is a real-time dynamic imaging facility with no ionizing radiation. We herein report a case of US-assisted PELD on a 38-year-old man with two levels of LDH at the same time. Our successful experience may contribute to the application of US-guided PELD in the future.

CASE PRESENTATION

A 38-year-old man [height: 174 cm; weight: 74.5 kg; body mass index (BMI): 24.6 kg/m^2] with low back pain and left leg pain for more than 7 years and aggravated symptoms for 1 mo came to our hospital.

History of present and past illness

His previous history and family history were negative. He had lameness on his left leg.

Physical examination

Physical examination showed tenderness and percussion pain radiation to the left leg from the left part of the L4-S1 vertebral spinous processes. Dermal sensation in his left lateral leg and left foot was decreased. Left straight leg raising and strengthening test had positive results (40 degrees).

Imaging examinations

X-ray showed small curvature of the lumbar spine. Computed tomography (CT) and magnetic resonance imaging (MRI) showed L3-4 and L4-5 disc herniations (left margin type) (Figure 1).

FINAL DIAGNOSIS

The patient was diagnosed with LDH of the L3-4 and L4-5 levels (left margin type).

TREATMENT

The patient needed PELD of both L3-4 and L4-5 levels. Institutional approval for PELD was obtained from the ethics committee of our hospital, and the procedure in this study was performed in accordance with the tenets of the Declaration of Helsinki.

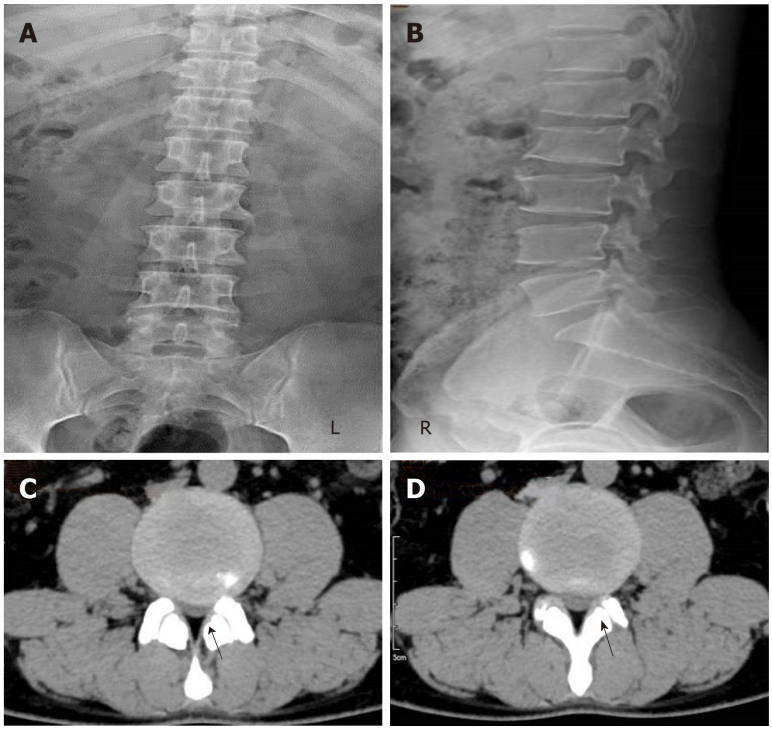

Figure 1 X-ray and computed tomography transverse images of the patient. A and B: X-ray images showing small curvature of the lumbar spine; C: Computed tomography (CT) image suggesting L3-4 disc herniation (black arrow, left margin type); D: CT image suggesting L4-5 disc herniation (black arrow, left margin type).

Written informed consent was obtained from the patient. A portable Mindray M9 US system (Mindray, Shenzhen, China) with a C5-1S convex array transducer (central frequency: 5 MHz) was used in this study. The patient laid in a prone position on a radiolucent table with a pillow under his belly. One US physician with more than 4 years of experience in interventional US performed the US guidance. First, a longitudinal section was used to display the transverse processes, and the lowest transverse process was L5. Second, the probe was rotated by 90 degrees to display the L5 transverse process. The probe was moved upward, and the soft tissue in the intervertebral foramen of L4-5 appeared as a circular hyperechoic zone (HZ), which was located below the facet joint (Figure 2). The auxiliary line on the patient's back skin was drawn at least 9-13 cm away from the midline. Third, the probe was moved to the next highest level to locate the L3-4 intervertebral disc using the same method.

One spinal surgeon with more than 5 years of experience in PELD performed the puncture and cannulation under the guidance of US (Figure 3). The HZ, which was located below the facet joint, was used as the target, and the needle was inserted from the 12 o'clock position to the 3 o'clock position of the HZ. The tip of the 18-gauge spinal needle first touched the facet joint and then slipped into the intervertebral foramen. G-arm X-ray (Whale, Massachusetts, United States) in the anteroposterior and lateral views was used to confirm that the needle tip arrived at the target point. A special instrument set (transforaminal endoscopic surgical system; joimax® GmbH, 102 Karlsruhe, Germany) was applied in the procedure. The guidewire was inserted through the spinal needle, which was removed thereafter. Then, the obturator and reamer were introduced along the guidewire. Finally, the expanders and outer sheath of the endoscope were inserted through the guidewire one after another (Figure 4).

The US-guided puncture lasted 4.5 min (2 min for L3-4 and 2.5 min for L4-5), and the US-guided cannulation lasted 5.5 min (2.5 min for L3-4 and 3 min for L4-5). The positions of the puncture needles and working sheaths were accurate, which was tested by two shots of G-arm fluoroscopy, with a total fluoroscopic time of 4.4 s and a total radiation dose of 3.98 mGy. Partial hypertrophied facetectomy was performed using a 3.0-mm endoscopic lateral bur (drill diameter: 3.0 mm, XISHAN, China) (Figure 5). Then, transforaminal PELD was performed as previously described by Wen *et al*[5].

OUTCOME AND FOLLOW-UP

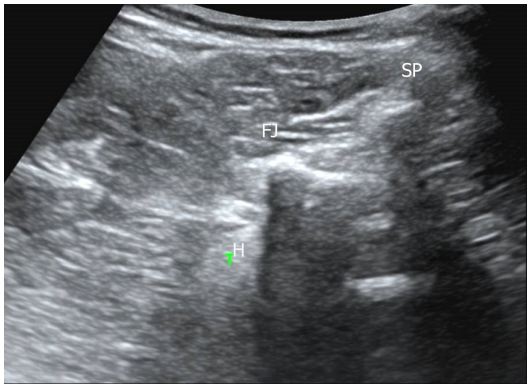

Figure 2 Transverse ultrasound image of the lumbar spine. SP: Spinous process; FJ: Facet joint; HZ: Hyperechoic area.

The operation decompression lasted 82 minutes for two levels (Figure 5B-D), and it was completed with no complications. The patient's straight leg elevation increased from 40 to 90 degrees after PELD (Figure 6). Immediately following PELD, the visual analog scale (VAS) score of his low back pain decreased from 6 to 1, his leg pain score decreased from 8 to 1, and his Oswestry Disability Index (ODI) score decreased from 73 to 11. Videos of the patient's gait immediately after surgery showed a normal and symmetric appearance of the two legs, and the spinal MRI after PELD showed complete decompression of the two levels (Figure 7). The patient was taught a set of waist exercises after the operation to reduce the recurrence of disc herniation after PELD. Follow-up at 6 months after PLED showed that the treatment effect remained the same without recurrence, with the patient showing 90 degrees of straight leg elevation, a VAS of 1 for both low back pain and leg pain, and an ODI of 10. The patient was very satisfied with the treatment, especially with the reduction of radiation.

DISCUSSION

Repeated fluoroscopic scanning is essential for the puncture and cannulation during PELD. Fan *et al*[6] showed that 34.32±4.78 fluoroscopy shots were needed in conventional PELD. They showed that this number was 33.98 ± 2.69 in another group of patients[7]. Patients with more difficult positioning and more treatment levels may receive larger radiation dose, and the same effect will occur in inexperienced surgeons. Fluoroscopic scanning may increase the incidence of malignant tumors, such as thyroid cancer, skin erythema, leukemia and so on[8]. For pregnant women, exposure to X-ray radiation may increase the risk for fetal malformations or developmental abnormalities. High cumulative effective doses also have been found in patients with Crohn's disease[9], cystic fibrosis[10], and end-stage kidney disease[11]. With the guidance of US, the patient in this study received only two shots of fluoroscopy with a low radiation dose of only 3.98 mGy. Future studies with larger samples are needed to validate this technique as an alternative to fluoroscopy.

US has been reported to display intervertebral disc degeneration[12,13] and focal stenosis[14]. It has been used in the guidance of facet joint injections[15], selective nerve root blocks[16], lumbar transforaminal injections[17] and so on. However, due to occlusion of the lumbar spine, displaying the intervertebral foramen remains challenging. Recently, real-time US-MRI or US-CT fusion image virtual navigation has been demonstrated to be an effective and precise method for guiding PELD[18,19] or locating an intraspinal tumor[20]. However, the navigation process performed during these procedures is complicated and requires a special navigation system, such as electromagnetic tracking system, which is not easily available.

Few studies have focused on US-guided PELD. Wu *et al*[21] reported an initial study of US-assisted PELD and suggested that US-guided PELD can be successfully performed for patients with a BMI less than 24. In this study, we successfully performed US-guided PELD for disc herniation at two levels in a patient with a BMI of 24.6, which suggests that BMI is not always a problem for US guidance. The US guidance method used in our study is different from that used in the above research. They used the facet joint as target and we used the circular HZ above the transverse process, which is located below the facet joint, as the target. Furthermore, the needle was inserted from the 12 o'clock position to 3 o'clock position of the HZ in our study, and no longitudinal scanning was required in our method. The success of the study

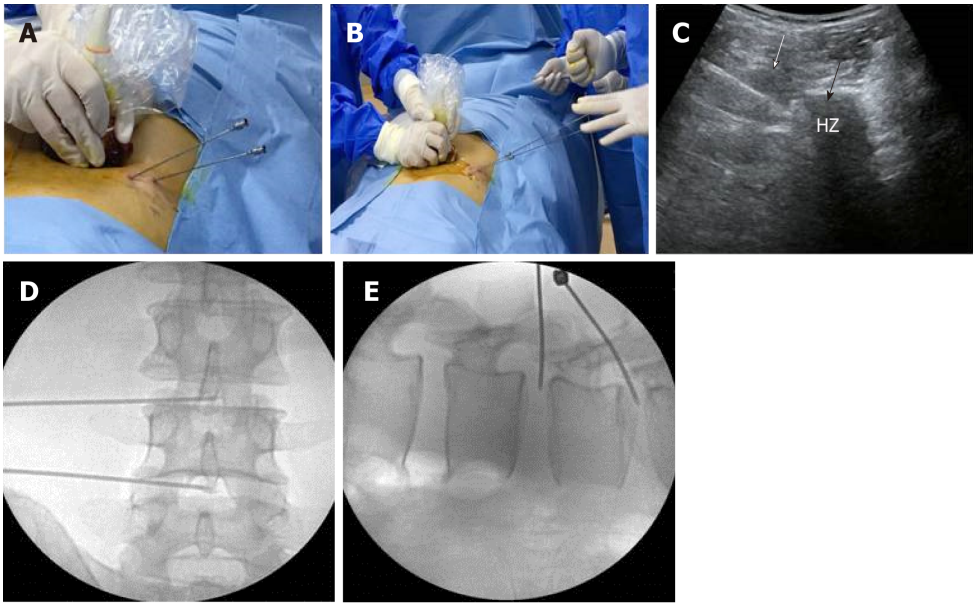

Figure 3 Puncture process of the two spinal needles. A: Ultrasound (US)-guided insertion of the two needles; B: Guidewires were then inserted through the two needles; C: US image of one needle (black arrow indicates the tip of the needle; white arrow indicates the track of the needle); D: Position of the needles in the anteroposterior X-ray image; E: Position of the needles in the lateral X-ray image.

proves that, although US cannot penetrate bone, soft tissue or bone markers on US can be used as guides to assist the puncture.

US guidance can not only reduce the radiation dose but also provide real-time dynamic guidance of the needle tip. It can reduce the risk for damage to abdominal and retroperitoneal organs, especially in high level disc herniation. The sheath position can also be monitored during cannulation, advising the surgeon when to be forceful and when to be careful.

Disc herniation of two levels requires double puncture time, longer surgical time, and higher radiation dose administered to the patient. However, with the guidance of US, punctures at two levels can be performed at the same time with only two shots of fluoroscopy (fluoroscopic time of 4.4 s and radiation dose of 3.98 mGy). The operation decompression time in our study lasted only 82 min, which is much more likely to be accepted by patients. The success of this case provides a potential for application of this technology. The inclusive and exclusive criteria are meaningful in the process. The inclusion criteria could be radicular leg pain caused by soft LDH with invalid conservative treatment. The exclusion criteria, except for the inherent contraindications of PELD, may include obese patients or patients with hyperechoic fascia muscularis, muscular atrophy, or calcification, since the high attenuation of US makes the anatomical landmarks surrounding the lumbar vertebrae visually unclear.

CONCLUSION

This study is a useful initial attempt and proves that US can be used in the guidance of the puncture and cannulation of PELD, and can largely reduce the radiation dose. The wide popularization of this technique still needs large samples and controlled study. However, with more orthopedists and US physicians mastering spine US and with the additional development of more practical tools, such as punctured guiding stents, this technology will become more mature and thus has great potential.

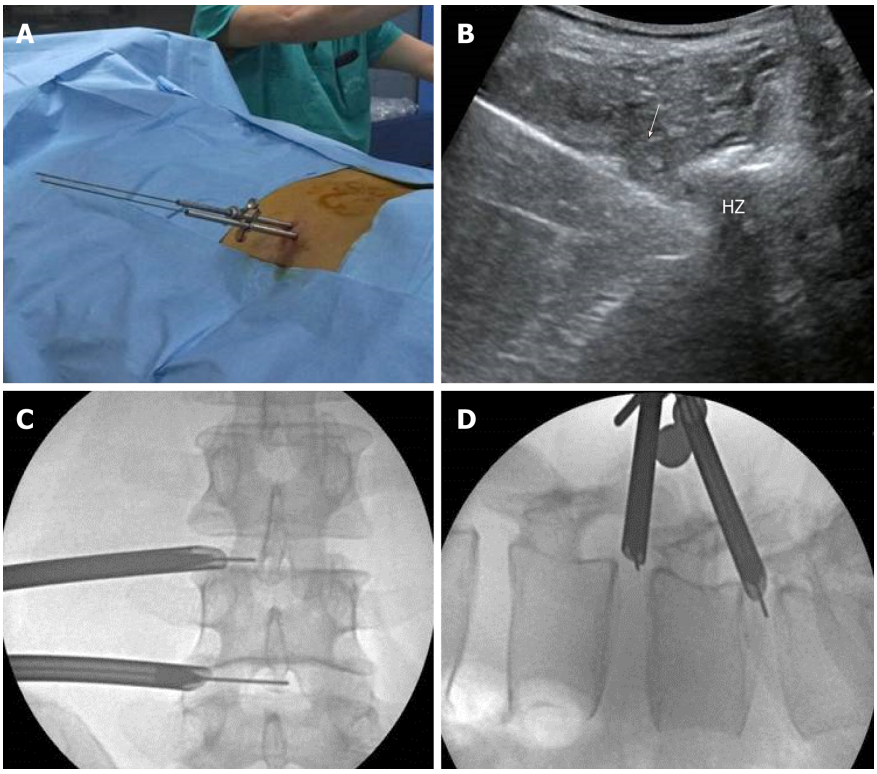

Figure 4 Cannulation process of the two endoscope outer sheaths. A: The endoscope outer sheaths were inserted through the guidance wire; B: Ultrasound (US) image of one sheath (white arrow indicates the track of the sheath; the tip of the sheath was hidden in the US shadow and could not be displayed); C: Position of the sheaths in the anteroposterior X-ray image; D: Position of the sheaths in the lateral X-ray image.

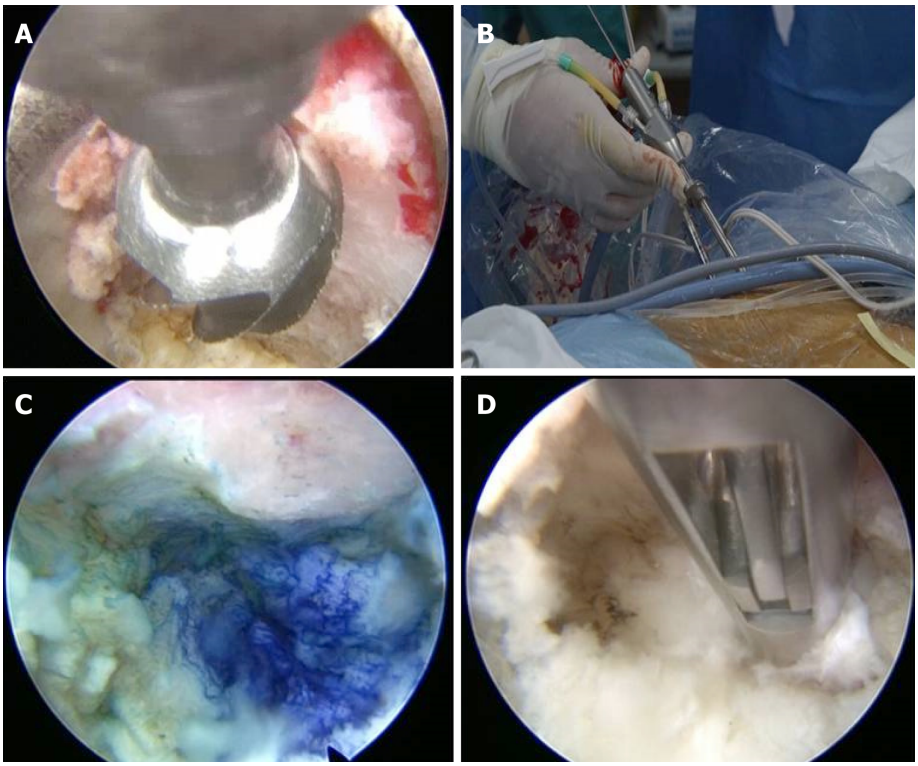

Figure 5 Percutaneous endoscopic lumbar discectomy for lumbar disc herniation at two levels. A: Partial hypertrophied facetectomy was performed using a 3.0-mm endoscopic lateral bur; B: Percutaneous endoscopic lumbar discectomy was performed for lumbar disc herniation at two levels at the same time; C: Direct visualization of the blue dye in the protruding intervertebral disc through the endoscope; D: The protruding intervertebral disc was removed to decompress the spinal nerve.

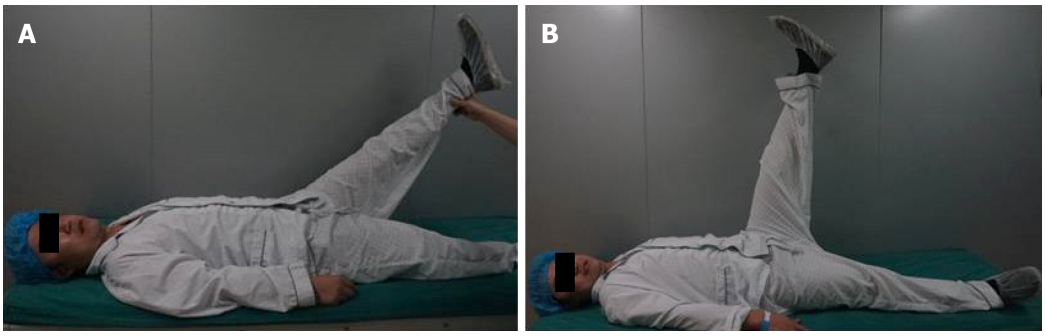

Figure 6 Straight leg elevations before and after percutaneous endoscopic lumbar discectomy. A: Straight leg elevation was 40 degrees before percutaneous endoscopic lumbar discectomy (PELD); B: Straight leg elevation increased to 90 degrees after PELD.

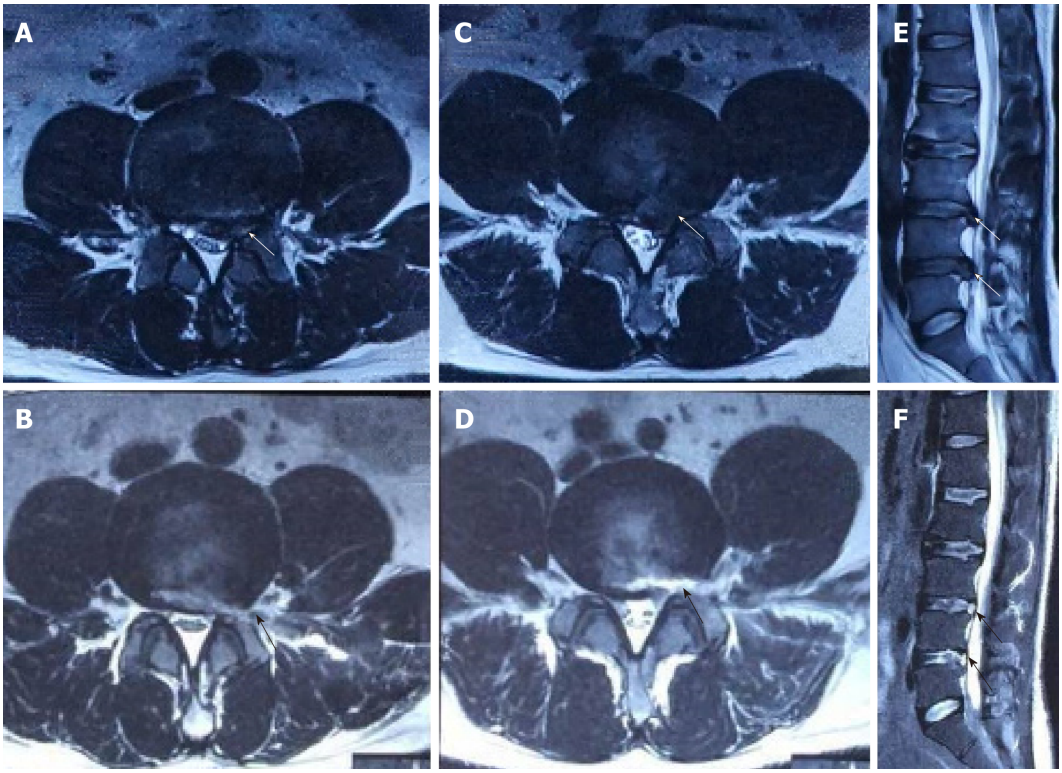

Figure 7 Lumbar spine magnetic resonance imaging before and after percutaneous endoscopic lumbar discectomy. A: Transverse section suggesting L3-4 disc herniation (white arrow, left margin type); B: Same section 1 day after percutaneous endoscopic lumbar discectomy (PELD) (black arrow indicates disappearance of the herniation); C: Transverse section suggesting L4-5 disc herniation (white arrow, left margin type); D: Same section 1 day after PELD (black arrow indicates disappearance of the herniation); E: Sagittal section suggesting L3-4 and L4-5 disc herniations (white arrows); F: Same section 1 d after PELD (black arrows indicate disappearance of the herniations).

REFERENCES

1 **Cong L**, Zhu Y, Tu G. A meta-analysis of endoscopic discectomy versus open discectomy for symptomatic lumbar disk herniation. *Eur Spine J* 2016; **25**: 134-143 [PMID: 25632840 DOI: 10.1007/s00586-015-3776-6]
2 **Choi KC**, Kim JS, Park CK. Percutaneous Endoscopic Lumbar Discectomy as an Alternative to Open Lumbar Microdiscectomy for Large Lumbar Disc Herniation. *Pain Physician* 2016; **19**: E291-E300 [PMID: 26815256]
3 **Eun SS**, Lee SH, Sabal LA. Long-term Follow-up Results of Percutaneous Endoscopic Lumbar Discectomy. *Pain Physician* 2016; **19**: E1161-E1166 [PMID: 27906946]
4 **Feng F**, Xu Q, Yan F, Xie Y, Deng Z, Hu C, Zhu X, Cai L. Comparison of 7 Surgical Interventions for Lumbar Disc Herniation: A Network Meta-analysis. *Pain Physician* 2017; **20**: E863-E871 [PMID: 28934804]
5 **Wen B**, Zhang X, Zhang L, Huang P, Zheng G. Percutaneous endoscopic transforaminal lumbar spinal canal decompression for lumbar spinal stenosis. *Medicine (Baltimore)* 2016; **95**: e5186 [PMID: 27977571 DOI: 10.1097/MD.0000000000005186]
6 **Fan G**, Gu X, Liu Y, Wu X, Zhang H, Gu G, Guan X, He S. Lower Learning Difficulty and Fluoroscopy

Reduction of Transforaminal Percutaneous Endoscopic Lumbar Discectomy with an Accurate Preoperative Location Method. *Pain Physician* 2016; **19**: E1123-E1134 [PMID: 27906942]
7 **Fan G**, Han R, Gu X, Zhang H, Guan X, Fan Y, Wang T, He S. Navigation improves the learning curve of transforamimal percutaneous endoscopic lumbar discectomy. *Int Orthop* 2017; **41**: 323-332 [PMID: 27591770 DOI: 10.1007/s00264-016-3281-5]
8 **Brenner DJ**, Doll R, Goodhead DT, Hall EJ, Land CE, Little JB, Lubin JH, Preston DL, Preston RJ, Puskin JS, Ron E, Sachs RK, Samet JM, Setlow RB, Zaider M. Cancer risks attributable to low doses of ionizing radiation: assessing what we really know. *Proc Natl Acad Sci USA* 2003; **100**: 13761-13766 [PMID: 14610281 DOI: 10.1073/pnas.2235592100]
9 **Desmond AN**, O'Regan K, Curran C, McWilliams S, Fitzgerald T, Maher MM, Shanahan F. Crohn's disease: factors associated with exposure to high levels of diagnostic radiation. *Gut* 2008; **57**: 1524-1529 [PMID: 18443021 DOI: 10.1136/gut.2008.151415]
10 **O'Connell OJ**, McWilliams S, McGarrigle A, O'Connor OJ, Shanahan F, Mullane D, Eustace J, Maher MM, Plant BJ. Radiologic imaging in cystic fibrosis: cumulative effective dose and changing trends over 2 decades. *Chest* 2012; **141**: 1575-1583 [PMID: 22207674 DOI: 10.1378/chest.11-1972]
11 **Coyle J**, Kinsella S, McCarthy S, MacWilliams S, McLaughlin P, Eustace J, Maher MM. Cumulative ionizing radiation exposure in patients with end stage kidney disease: a 6-year retrospective analysis. *Abdom Imaging* 2012; **37**: 632-638 [PMID: 21842156 DOI: 10.1007/s00261-011-9786-x]
12 **Naish C**, Mitchell R, Innes J, Halliwell M, McNally D. Ultrasound imaging of the intervertebral disc. *Spine (Phila Pa 1976)* 2003; **28**: 107-113 [PMID: 12544924 DOI: 10.1097/00007632-200301150-00003]
13 **Tervonen O**, Lähde S, Vanharanta H. Ultrasound diagnosis of lumbar disc degeneration. Comparison with computed tomography/discography. *Spine (Phila Pa 1976)* 1991; **16**: 951-954 [PMID: 1948381 DOI: 10.1097/00007632-199108000-00015]
14 **Engel JM**, Engel GM, Gunn DR. Ultrasound of the spine in focal stenosis and disc disease. *Spine (Phila Pa 1976)* 1985; **10**: 928-931 [PMID: 3914086 DOI: 10.1097/00007632-198512000-00011]
15 **Darrieutort-Laffite C**, Hamel O, Glémarec J, Maugars Y, Le Goff B. Ultrasonography of the lumbar spine: sonoanatomy and practical applications. *Joint Bone Spine* 2014; **81**: 130-136 [PMID: 24618457 DOI: 10.1016/j.jbspin.2013.10.009]
16 **Greher M**, Kirchmair L, Enna B, Kovacs P, Gustorff B, Kapral S, Moriggl B. Ultrasound-guided lumbar facet nerve block: accuracy of a new technique confirmed by computed tomography. *Anesthesiology* 2004; **101**: 1195-1200 [PMID: 15505456 DOI: 10.1097/00000542-200411000-00020]
17 **Gofeld M**, Bristow SJ, Chiu SC, McQueen CK, Bollag L. Ultrasound-guided lumbar transforaminal injections: feasibility and validation study. *Spine (Phila Pa 1976)* 2012; **37**: 808-812 [PMID: 21912311 DOI: 10.1097/BRS.0b013e3182340096]
18 **Liu YB**, Wang Y, Chen ZQ, Li J, Chen W, Wang CF, Fu Q. Volume Navigation with Fusion of Real-Time Ultrasound and CT Images to Guide Posterolateral Transforaminal Puncture in Percutaneous Endoscopic Lumbar Discectomy. *Pain Physician* 2018; **21**: E265-E278 [PMID: 29871381]
19 **Zhao Y**, Bo X, Wang C, Hu S, Zhang T, Lin P, He S, Gu G. Guided Punctures with Ultrasound Volume Navigation in Percutaneous Transforaminal Endoscopic Discectomy: A Technical Note. *World Neurosurg* 2018; **119**: 77-84 [PMID: 30071330 DOI: 10.1016/j.wneu.2018.07.185]
20 **Liu TJ**, Shen F, Zhang C, Huang PT, Zhu YJ. Real-time ultrasound-MRI fusion image virtual navigation for locating intraspinal tumour in a pregnant woman. *Eur Spine J* 2018; **27**: 436-439 [PMID: 29380148 DOI: 10.1007/s00586-017-5442-7]
21 **Wu R**, Liao X, Xia H. Radiation Exposure to the Surgeon During Ultrasound-Assisted Transforaminal Percutaneous Endoscopic Lumbar Discectomy: A Prospective Study. *World Neurosurg* 2017; **101**: 658-665.e1 [PMID: 28342919 DOI: 10.1016/j.wneu.2017.03.050]

World Journal of Clinical Cases

Submit a Manuscript: https://www.f6publishing.com

World J Clin Cases 2019 May 26; 7(10): 1169-1176

DOI: 10.12998/wjcc.v7.i10.1169

ISSN 2307-8960 (online)

CASE REPORT

Retroperitoneoscopic approach for partial nephrectomy in children with duplex kidney: A case report

Di-Xiang Chen, Zi-Hao Wang, Shan-Jie Wang, Yue-Yue Zhu, Nan Li, Xian-Qiang Wang

ORCID number: Di-Xiang Chen (0000-0003-1083-9902); Zi-Hao Wang (0000-0001-7241-6169); Shan-Jie Wang (0000-0002-5741-1762); Yue-Yue Zhu (0000-0002-1156-8510); Nan Li (0000-0001-7665-4527); Xian-Qiang Wang (0000-0002-8914-6545).

Author contributions: Chen DX and Wang ZH contribute equally to this article and should be considered as co-first authors; Chen DX and Wang XQ performed the operation; Chen DX, Wang ZH, and Wang SJ designed this case report; Wang ZH and Wang XQ wrote this paper; Zhu YY and Li N was responsible for sorting the data.

Informed consent statement: Informed consent was obtained from the patient.

Conflict-of-interest statement: The authors declare that they have no conflict of interest.

CARE Checklist (2016) statement: The authors have read the CARE Checklist (2016), and the manuscript was prepared and revised according to the CARE Checklist (2016).

Di-Xiang Chen, Xian-Qiang Wang, Department of Pediatrics, PLA General Hospital, Beijing 100853, China

Zi-Hao Wang, The Fourth Military Medical University, Xi'an 710032, Shannxi Province, China

Shan-Jie Wang, The Sixth People's Hospital of Jinan Affiliated to Jining Medical School, Jinan 250200, Shandong Province, China

Yue-Yue Zhu, Southern Medical University, Guangzhou 510515, Guangdong Province, China

Nan Li, Department of Ultrasound Diagnosis, PLA General Hospital, Beijing 100853, China

Corresponding author: Xian-Qiang Wang, MD, PhD, Attending Doctor, Department of Pediatric, PLA General Hospital, No. 28, Fuxing Road, Haidian District, Beijing 100853, China. wxq301@gmail.com
Telephone: +86-13522891848
Fax: +86-10-66938418

Abstract

BACKGROUND

Renal duplication is a common deformity of the urinary system, with an incidence of approximately 1/125 in children. Symptomatic patients with hydronephrosis, vesicoureteral reflux, or incontinence may require surgical interventions. Laparoscopy and retroperitoneoscopy are the two main accesses for partial nephrectomy.

CASE SUMMARY

A 9-year-old child was admitted to the hospital for hydronephrosis of the left kidney. Ultrasonography showed that the left kidney was larger, approximately 12.6 cm × 6.3 cm × 5.5 cm in size, with visible separation of the pelvis and an obviously separated lower portion. The upper segment of the left ureter was dilated (approximately 2.6 cm in width), and no significant dilation was observed in the middle and upper segments. The right kidney and ureter were normal. Primary diagnosis was left renal duplication malformation and hydronephrosis. Retroperitoneal laparoscopic nephrectomy and ureterectomy were performed. Intraoperative exploration revealed a dilated pelvis and thin renal parenchyma at the lower pole of the left kidney. The upper left kidney was smaller than normal, and the pelvis and ureter were larger than normal. The renal artery was blocked for 40 min. A hemolock was used to clamp down the kidney ureter, and a drainage tube was retained in the retroperitoneal cavity. The operation was uneventful, and the estimated amount of blood loss was 100 mL. Total abdominal

Manuscript source: Unsolicited manuscript

Received: January 4, 2019
Peer-review started: January 4, 2019
First decision: March 10, 2019
Revised: March 16, 2019
Accepted: March 26, 2019
Article in press: March 26, 2019
Published online: May 26, 2019

P-Reviewer: Facciorusso A, Musquer N
S-Editor: Wang JL
L-Editor: Wang TQ
E-Editor: Wu YXJ

drainage amount was 116 mL. The drainage tube was removed on postoperative day (POD) 3 and the patient was discharged on POD6. The pathological diagnosis confirmed the atrophy of the renal parenchyma, the dilation of the renal pelvis, hydronephrosis, and ureteral cystic dilation.

CONCLUSION
The retroperitoneoscopic approach for partial nephrectomy is feasible and effective in selective pediatric patients with a duplex kidney.

Key words: Retroperitoneoscopy; Duplex kidney; Nephrectomy; Pediatric; Case report

Core tip: Duplex kidney is a common congenital malformation of the urinary system in chil-dren, and most symptomatic patients should opt for surgical management. However, there is still some controversy on the applications of the translaparoscopic approach and retrolaparoscopic approach. We will discuss the advantages and disadvantages of both approaches in this case. These contents provide a basis for future research.

Citation: Chen DX, Wang ZH, Wang SJ, Zhu YY, Li N, Wang XQ. Retroperitoneoscopic approach for partial nephrectomy in children with duplex kidney: A case report. *World J Clin Cases* 2019; 7(10): 1169-1176
URL: https://www.wjgnet.com/2307-8960/full/v7/i10/1169.htm
DOI: https://dx.doi.org/10.12998/wjcc.v7.i10.1169

INTRODUCTION

Duplex kidney is a common congenital malformation of the urinary system in children, with an incidence of 1/125 individuals. More girls are afflicted with the disorder than boys, and the unilateral incidence of the disorder is higher than the bilateral incidence[1]. The main clinical manifestations are urinary tract infection, urinary incontinence, dysuria, and the presence of an abdominal mass. In addition to having well-developed kidneys that require no treatment, most symptomatic patients should opt for surgical management.

At present, laparoscopic nephrectomy is a mainstream choice in clinical practice. However, there is still some controversy on the applications of the translaparoscopic approach and retrolaparoscopic approach[2-4]. The laparoscopic approach can provide large operation space, and is more suitable for infants. However, complications such as urinary leakage, intestinal adhesion, and intestinal obstruction may occur after operation due to the dissection of abdominal organs and abdominal organs. The retroperitoneal laparoscopic approach is more direct, with less interference to other organs, postoperative urine leakage and bleeding or hematoma confined to the peritoneum, less stimulation, but has a steep learning curve[5].

Due to the lack of experience among surgeons in aspects of the retroperitoneal anatomy and the long operation time, the retroperitoneal laparoscopic technique has not been widely applied among pediatric surgeons[6]. Herein, we report our experience with a retroperitoneal laparoscopic surgery for duplex kidney.

CASE PRESENTATION

Chief complaints

A 9-year-old boy was admitted to the hospital with left-sided hydronephrosis for one week.

History of present illness

Due to abdominal pain, the patient underwent an ultrasonic examination in the outpatient department and was diagnosed as having "left hydronephrosis". It was suspected that the left side had the indication of a renal malformation. He was admitted to the hospital with "left hydronephrosis".

Physical examination

The patient exhibited abdominal flatness, a soft abdomen, normal bowel sounds, no varicose veins in the abdominal wall, no tenderness, no rebound pain, no abdominal masses, and slight percussion pain in the kidney.

Imaging examination

The following characteristics were observed *via* an ultrasound (abdominal) examination: The left kidney was enlarged (with a size of approximately 12.6 cm × 6.3 cm × 5.5 cm), the cortex was thin (with a thickness of approximately 1.0 cm), the pelvis was visibly separated, the lower part of the pelvis was obvious and separated within a range of approximately 7.8 cm × 5.9 cm × 5.4 cm, and the upper part of the pelvis was separated, both before and after treatment, with a diameter of approximately 2.2 cm. The size and morphology of the right kidney were normal, with a uniform cortical echo, a clear renal internal structure, no separation of the renal pelvis, and no clear occupying lesions. The upper segment of the left ureter was dilated (approximately 2.6 cm wide), and no significant dilation was observed in the middle and lower segments. No dilation was observed in the right ureter. Bladder filling was optimal, the wall was not thick, but smooth, and there was no abnormal echo inside of the kidney.

The following characteristics were observed *via* an intravenous pyelography (Figure 1): No positive stones were observed in the abnormalities of the ureters and the bladder on both sides. After the injection of the contrast agent, bilateral ureters and bilateral kidneys were developed. The left renal pelvis was dilated, and the calyx was blunt. The right renal pelvis was not enlarged, no filling defect was observed, and the calyx cup was sharp. The bilateral ureters showed no stenosis or dilations. The bladder was filled, but no defect was found.

The following characteristics were observed *via* a nuclear medicine examination (ECT): The excretion from the left kidney was not smooth, and the glomerular filtration rate (GFR) was slightly reduced. The right kidney function was generally normal. The following results were obtained: After the intravenous injection of a "pellet" tracer, a renal blood perfusion and the dynamic imaging of renal function were immediately performed. The renal blood perfusion imaging and curve exhibited normal renal perfusion. The renal function curve showed that the aggregation segment of the left kidney was available and that the peak time was delayed, thus showing a parabolic curve. The right kidney could be clustered and cleared. The GFR was as follows: 25.47 mL/min for the left kidney and 47.42 mL/min for the right kidney. Based on the kidney image, the left kidney had an irregular morphology, and the size and shape of the right renal shadow were acceptable.

A magnetic resonance examination (Figure 2) showed that the left renal pelvis and ureter were significantly dilated, the widest part of the ureter was approximately 29 mm, the left ureter was stenosed in the middle part, the right renal pelvis, calyces, and ureter were not abnormally stenosed or dilated, and no stones were observed.

Preoperative diagnosis and treatment plan

For the treatment of left renal duplication, kidney seeper, and left ureteral dilation, retroperitoneal laparoscopic nephrectomy and ureterectomy were performed under general anesthesia.

Operation procedure

Patients were placed into the right lateral position. After an incision of the upper lumbar triangle was performed in the abdominal cavity, an indicator finger and a balloon expansion were used to establish the pneumoperitoneum (Figure 3). The pressure was observed at 10 mmHg. A 10 mm trocar and laparoscopic lens were inserted, and two trocars (10 mm and 5 mm) were placed in the lower lumbar triangle and the twelve costal tips, respectively.

The left upper kidney was smaller than normal, and the pelvis and ureter were both larger than normal. The junction of the posterior renal fascia and the psoas major muscle was cut open with an ultrasound knife and extended to the upper pole of the kidney. No independent blood supply was found in the lower left kidney. The adhesion between the anterior fascia of the kidney and the posterior peritoneum was separated in the forward position. The peritoneum was broken, and a 5 mm trocar was placed under the xiphoid process, in order to allow for exhaust. The arteries and veins of the left kidney were exposed. The left upper kidney shared the main renal artery with the left lower kidney. There was no obvious boundary between the upper kidney and the lower kidney. The artery clamp was used to block the renal artery. The dilated renal pelvis was cut open, and the colorless clear liquid was absorbed. The duplex kidney was resected along the junction of the pyoid sac wall and the renal parenchyma with an ultrasonic knife. A 1-0 barbed wire was used to continuously

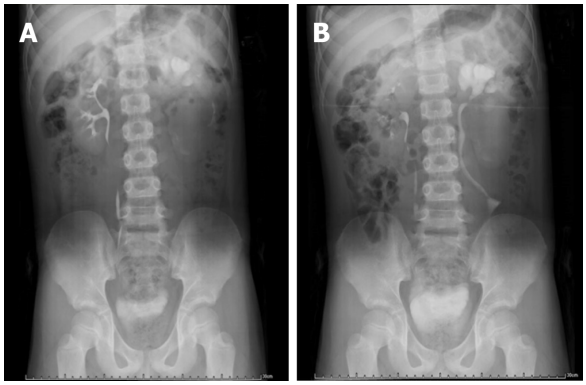

Figure 1 Intravenous pyelography. A: 10 min, B: 40 min.

suture the renal section, and the renal artery clamp was released. No obvious bleeding was observed. The renal artery was blocked for 40 minutes. The ureters of the left upper kidney and the left lower kidney converged below the level of the iliac crest. The ureter of the left lower kidney became significantly thinner at the junction, and a hemlock was used to clamp the lower kidney ureter. The lower left kidney and ureter were removed from the body with an 8 cm bag and were rinsed. No obvious bleeding was found during the reexamination period. The negative pressure drainage tube was retained in the retroperitoneal cavity and was drilled out of the body under the trocar in the lower lumbar triangle. The following sutures were utilized: A 3-0 absorbable line intermittent suture for the abdominal wall muscle, a 4-0 absorbable line intermittent suture for subcutaneous tissue, and a biological protein adhesive for the skin. A pull film was used to tighten the skin of all of the incisions, and a dressing was used to cover the incisions.

The patient was safely returned to the ward postoperation, with 100 mL of bleeding and no need for a blood transfusion. The left lower kidney and ureter were sent for pathological examinations.

Postoperative outcomes

The postoperative recovery consisted of diet, optimal consciousness levels, and good spirits. After a conventional anti-infection treatment, a total volume of 116 mL of the postoperative peritoneal drainage was drained (which was clear after bleeding), and the drainage tube was extracted on the third day after the surgery. On the sixth day after the surgery, the patient met the discharge indications and was discharged for treatment. The following pathological diagnoses were made: Lower left atrophy of the renal parenchyma, decrease of glomerular number with fibrosis, decrease of renal tubules in several regions, epithelial hyperplasia of the collecting tubes, and interstitial fibrous tissue hyperplasia with lymphocyte infiltration. The renal pelvis was dilated, the mucosa exhibited chronic inflammation, the epithelium underwent atrophy and became thinner, and the subepithelium underwent interstitial fibrous tissue hyperplasia, which conformed to the hydronephrosis change. There was also ureteral cystic dilation, with chronic inflammation of the mucosa.

FINAL DIAGNOSIS

The final diagnosis was left renal duplication, kidney seeper, and left ureteral dilation.

TREATMENT

For the treatment of left renal duplication, kidney seeper, and left ureteral dilation, retroperitoneal laparoscopic nephrectomy and ureterectomy were performed under general anesthesia.

OUTCOME AND FOLLOW-UP

The patient was discharged after recovery. No recurrence was found after two years of follow-up.

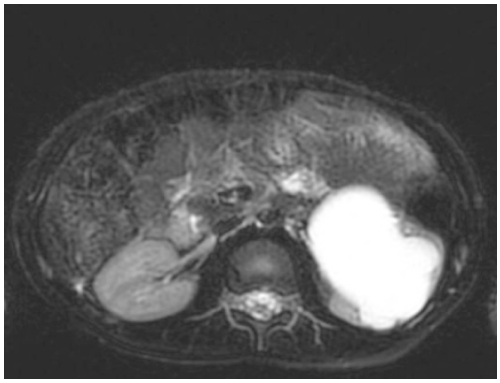

Figure 2 Magnetic resonance imaging of the patient (T2). The left renal pelvis and ureter were significantly dilated, the widest part of the ureter was approximately 29 mm, and the left ureter had stenosis in the middle part.

DISCUSSION

In clinical practice, duplicate kidney is closely related to the formation of ureteral malformations. Duplex kidney is usually divided into three types: Developmental type, hydronephrosis type, and dysplasia type. This patient was classified as having the hydronephrosis type; specifically, the patient had a left hydronephrosis combined with a ureteral cyst. Ureteral malformations can be divided into complete and incomplete types. This patient had a complete ureteral malformation with double ureters. B-ultrasound examination is the preferred method for preliminary screening and for follow-up review. The commonly used treatment method is laparoscopic heminephrectomy, which is divided into a peritoneal approach and retroperitoneal approach, both of which are relatively complex operations and are still not used to a high degree in pediatric urology[7,8].

In 1993, Jordan *et al*[9] first reported on the use of laparoscopic heminephrectomy, which caused great repercussions in this medical field. Afterwards, laparoscopic heminephrectomy gradually replaced the use of open surgery due to its unique advantages and was widely accepted for use by pediatric urologists. In 2000, with the development of endoscopic technology, Miyazato *et al*[10] reported on the first case of retroperitoneal laparoscopic heminephrectomy, which posed a challenge to the technology that was being used by pediatric urologists. Since then, the advantages and disadvantages of the two different surgical approaches have become a focus of debate.

The advantages of the laparoscopic approach mainly include comprehensive exposure to the anatomy of the kidney and its blood vessels, ability to easily suture the kidney *in vivo*, and ability to easily identify the nonfunctional kidney, which are crucial steps in this operation. Regardless of the age of the child, and as long as there is bowel preparation before the surgery, the entire kidney can then be assessed. Castellan *et al*[11] compared 48 cases of seminephrectomy through the abdominal cavity by the use of the retroperitoneal approach. They believed that the peritoneal approach provided better exposure space and recommended the use of the peritoneal approach for infants less than 1 year old[11]. Another advantage of the laparoscopic approach is that the entire ureter surrounding the bladder dome can be almost completely removed, which is a good choice for patients with ureteral dilation, reflux, and tortuosity, and is especially useful for patients with urinary tract infections. Esposito *et al*[3] analyzed 102 cases of partial nephrectomy and concluded that laparoscopic total ureterectomy was always recommended for patients with urinary tract infections.

However, there are some deficiencies associated with the translaparoscopic approach. Because it passes through the abdominal cavity, the intestinal tract needs to be intraoperatively dissected. Furthermore, the older the patient is, the more extensive the dissection will be. The aim is to obtain an optimal exposure of the kidney and the ureter. Subsequently, this increases the incidence of postoperative urine leakage in patients[3]; additionally, intestinal adhesion, intestinal obstruction, and other complications may occur. These conditions can affect postoperative healing and increase the average length of hospital stay.

In comparison, the advantages of retroperitoneoscopy mainly include the fact that it provides a more direct access to the kidney and avoids the risk of colon dissociation, damage to the hollow organs, and the potential risk of adhesion[12,13]. A retrospective comparative study, conducted by Rassweiler *et al*[14], concluded that the retro-

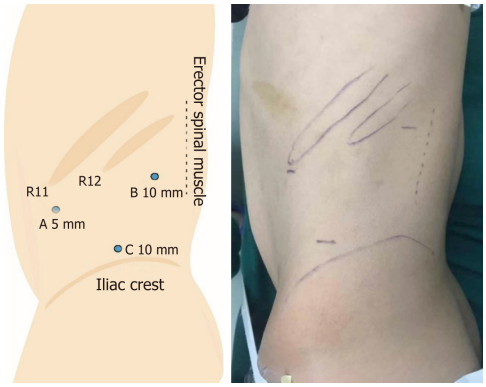

Figure 3 Trocar diagram. Point C is the endoscopic port.

peritoneal approach is less invasive to the body than the peritoneal approach. Singh *et al*[15] reported 42 cases of retroperitoneal laparoscopic heminephrectomy, and they believed that direct exposure through the use of retroperitoneal laparoscopy avoided intestinal complications and resulted in faster recovery rates. Another advantage of retroperitoneoscopy is that postoperative urine leakage and bleeding or hematomas are confined to the retroperitoneum. This reduces urine and blood irritation to the peritoneum and postoperative pain. Such limitations also facilitate drainage. In this case, we left a drainage tube in and pulled it out three days later.

CO_2 pneumoperitoneum is also a quiet critical factor during the operation. Schauer *et al*[16] believed that the amount of CO_2 absorption through the retroperitoneal route is less than that through the abdominal cavity. The absorbance of too much CO_2 will definitely increase the risk of hypercapnia, which will then lead to a series of complications. However, studies have shown that hemodynamic changes that are caused by retroperitoneal CO_2 pneumoperitoneum are statistically significant, compared with those that are caused by the peritoneum[17]. Therefore, this may be associated with reduced renal blood flow, which could then lead to functional renal ischemia. Wallis *et al*[13] believed that, due to the small retroperitoneal space, infants who are younger than 1 year old may be more affected by a pneumoperitoneum, and they recommended the use of an open heminephrectomy for infants under the age of 1 year.

Compared with laparoscopy, retroperitoneoscopy requires higher technical requirements, which involves a narrow space of operation of the surgeon[18-20], as well as the reverse anatomy of the kidney and umbilical regions. Additionally, the younger the child is, the narrower the peritoneal space becomes. In this case, the retroperitoneal approach exhibits its advantage, and our traditional retroperitoneal approach is used as the lateral approach in the lateral supine position. Borzi[19] and Mushtaq *et al*[21] described the method of the posterior approach in the prone position. They believed that, although the posterior approach required the continuous traction of the kidney, it was easier to enter the renal blood vessels in a completely prone position, and the effects of peritoneal tear and pneumoperitoneum were avoided.

Retroperitoneal laparoscopy may not be able to maximally remove dilated ureters, thus resulting in an increased incidence of postoperative symptomatic ureteral residues[3,19]. The ureter near the bladder dome can be completely removed by the use of the laparoscopic approach, but Borzi[19] believes that, when a ureterectomy is needed, the lateral approach can be utilized in older children, which can create a larger working space and a wider field of vision in ureterectomy.

The incidence rates of complications and conversion to open surgery in the retroperitoneoscopic approach are higher than those through the laparoscopic approach, which has been reported more in domestic and foreign studies concerning the use of retroperitoneal laparoscopic heminephrectomy in children[3,11,13]. In 2015, Esposito *et al*[20] reported that the high technical requirements and small operating range of retroperitoneoscopy led to higher complication and conversion rates, and their recent studies have shown that these rates are decreasing.

Leclair *et al*[8] found that the probability of switching to open surgery was related to surgical experience, and these findings reflected that retroperitoneal laparoscopic technology was not fully popularized in the field of pediatric urology, and these pediatric urologists need this experience.

In recent years, with the development of surgical techniques and surgical instruments in the medical industry, robotic[22] and tranumbilical single-hole[23] heminephrectomy have emerged, which have caused great repercussions in the

industry. But research into these new technologies is scarce, and the increased financial burden on patients requires further investigation.

CONCLUSION

Laparoscopic and retroperitoneal heminephrectomies are the standard procedures in most pediatric urological centers. The retroperitoneoscopic approach is more consistent with the principle of minimally invasive surgery than the laparoscopic approach, even with a steep learning curve and restricted space. It may be a feasible surgical approach for selective pediatric patients.

REFERENCES

1 **Kazemi-Rashed F**, Simforoosh N. Gil-Vernet antireflux surgery in treatment of lower pole reflux. *Urol J* 2005; **2**: 20-22 [PMID: 17629890]
2 **Seibold J**, Schilling D, Nagele U, Anastasiadis AG, Sievert KD, Stenzl A, Corvin S. Laparoscopic heminephroureterectomy for duplex kidney anomalies in the pediatric population. *J Pediatr Urol* 2008; **4**: 345-347 [PMID: 18790417 DOI: 10.1016/j.jpurol.2008.03.002]
3 **Esposito C**, Escolino M, Miyano G, Caione P, Chiarenza F, Riccipetitoni G, Yamataka A, Savanelli A, Settimi A, Varlet F, Patkowski D, Cerulo M, Castagnetti M, Till H, Marotta R, La Manna A, Valla JS. A comparison between laparoscopic and retroperitoneoscopic approach for partial nephrectomy in children with duplex kidney: a multicentric survey. *World J Urol* 2016; **34**: 939-948 [PMID: 26577623 DOI: 10.1007/s00345-015-1728-8]
4 **You D**, Bang JK, Shim M, Ryu DS, Kim KS. Analysis of the late outcome of laparoscopic heminephrectomy in children with duplex kidneys. *BJU Int* 2010; **106**: 250-254 [PMID: 19888983 DOI: 10.1111/j.1464-410X.2009.09038.x]
5 **Gundeti MS**, Patel Y, Duffy PG, Cuckow PM, Wilcox DT, Mushtaq I. An initial experience of 100 paediatric laparoscopic nephrectomies with transperitoneal or posterior prone retroperitoneoscopic approach. *Pediatr Surg Int* 2007; **23**: 795-799 [PMID: 17571271 DOI: 10.1007/s00383-007-1941-7]
6 **Esposito C**, Escolino M, Castagnetti M, Savanelli A, La Manna A, Farina A, Turrà F, Roberti A, Settimi A, Varlet F, Till H, Valla JS. Retroperitoneal and laparoscopic heminephrectomy in duplex kidney in infants and children. *Transl Pediatr* 2016; **5**: 245-250 [PMID: 27867847 DOI: 10.21037/tp.2016.09.12]
7 **Miranda ML**, Oliveira-Filho AG, Carvalho PT, Ungersbock E, Olimpio H, Bustorff-Silva JM. Laparoscopic upper-pole nephroureterectomy in infants. *Int Braz J Urol* 2007; **33**: 87-91; discussion 91-3 [PMID: 17335605 DOI: 10.1590/S1677-55382007000100015]
8 **Leclair MD**, Vidal I, Suply E, Podevin G, Héloury Y. Retroperitoneal laparoscopic heminephrectomy in duplex kidney in infants and children: a 15-year experience. *Eur Urol* 2009; **56**: 385-389 [PMID: 18649989 DOI: 10.1016/j.eururo.2008.07.015]
9 **Jordan GH**, Winslow BH. Laparoendoscopic upper pole partial nephrectomy with ureterectomy. *J Urol* 1993; **150**: 940-943 [PMID: 8345614 DOI: 10.1016/S0022-5347(17)35656-2]
10 **Miyazato M**, Hatano T, Miyazato T, Kagawa H, Yonou H, Ogawa Y. Retroperitoneoscopic heminephrectomy of the right upper collecting system emptying into an ectopic ureterocele in a 5-year-old girl: a case report. *Hinyokika Kiyo* 2000; **46**: 413-416 [PMID: 10934612]
11 **Castellan M**, Gosalbez R, Carmack AJ, Prieto JC, Perez-Brayfield M, Labbie A. Transperitoneal and retroperitoneal laparoscopic heminephrectomy--what approach for which patient? *J Urol* 2006; **176**: 2636-9; discussion 2639 [PMID: 17085179 DOI: 10.1016/j.juro.2006.08.053]
12 **Lee RS**, Retik AB, Borer JG, Diamond DA, Peters CA. Pediatric retroperitoneal laparoscopic partial nephrectomy: comparison with an age matched cohort of open surgery. *J Urol* 2005; **174**: 708-11; discussion 712 [PMID: 16006955 DOI: 10.1097/01.ju.0000164748.00339.4c]
13 **Wallis MC**, Khoury AE, Lorenzo AJ, Pippi-Salle JL, Bägli DJ, Farhat WA. Outcome analysis of retroperitoneal laparoscopic heminephrectomy in children. *J Urol* 2006; **175**: 2277-80; discussion 2280-2 [PMID: 16697855 DOI: 10.1016/S0022-5347(06)00338-7]
14 **Rassweiler J**, Frede T, Henkel TO, Stock C, Alken P. Nephrectomy: A compara-tive study between the transperitoneal and retroperitoneal laparoscopic versus the open approach. *Eur Urol* 1998; **33**: 489-496 [PMID: 9643669 DOI: 10.1159/000019640]
15 **Singh RR**, Wagener S, Chandran H. Laparoscopic management and outcomes in non-functioning moieties of duplex kidneys in children. *J Pediatr Urol* 2010; **6**: 66-69 [PMID: 19428304 DOI: 10.1016/j.jpurol.2009.04.005]
16 **Schauer PR**, Luna J, Ghiatas AA, Glen ME, Warren JM, Sirinek KR. Pulmonary function after laparoscopic cholecystectomy. *Surgery* 1993; **114**: 389-97; discussion 397-9 [PMID: 8342140]
17 **Halachmi S**, El-Ghoneimi A, Bissonnette B, Zaarour C, Bagli DJ, McLorie GA, Khoury AE, Farhat W. Hemodynamic and respiratory effect of pediatric urological laparoscopic surgery: a retrospective study. *J Urol* 2003; **170**: 1651-4; discussion 1654 [PMID: 14501683 DOI: 10.1097/01.ju.0000084146.25552.9c]
18 **Valla JS**. Retroperitoneoscopic surgery in children. *Semin Pediatr Surg* 2007; **16**: 270-277 [PMID: 17933670 DOI: 10.1053/j.sempedsurg.2007.06.010]
19 **Borzi PA**. A comparison of the lateral and posterior retroperitoneoscopic approach for complete and partial nephroureterectomy in children. *BJU Int* 2001; **87**: 517-520 [PMID: 11298047 DOI: 10.1046/j.1464-410X.2001.00130.x]
20 **Esposito C**, Miyano G, Caione P, Escolino M, Chiarenza F, Riccipetitoni G, Yamataka A, Cerulo M, Savanelli A, Settimi A, Valla JS. Retroperitoneoscopic Heminephrectomy in Duplex Kidney in Infants and Children: Results of a Multicentric Survey. *J Laparoendosc Adv Surg Tech A* 2015; **25**: 864-869 [PMID: 26390256 DOI: 10.1089/lap.2014.0654]
21 **Mushtaq I**, Haleblian G. Laparoscopic heminephrectomy in infants and children: first 54 cases. *J Pediatr Urol* 2007; **3**: 100-103 [PMID: 18947711 DOI: 10.1016/j.jpurol.2006.05.011]
22 **Ballouhey Q**, Binet A, Clermidi P, Braik K, Villemagne T, Cros J, Lardy H, Fourcade L. Partial

nephrectomy for small children: Robot-assisted versus open surgery. *Int J Urol* 2017; **24**: 855-860 [PMID: 29027269 DOI: 10.1111/iju.13466]

23 **Urbanowicz W**, Sulisławski J, Wolnicki M. Pediatric single port transumbilical nephrectomy and nephroureterectomy. *Cent European J Urol* 2011; **64**: 240-242 [PMID: 24578903 DOI: 10.5173/ceju.2011.04.art12]

World Journal of Clinical Cases

Submit a Manuscript: https://www.f6publishing.com

World J Clin Cases 2019 May 26; 7(10): 1177-1183

DOI: 10.12998/wjcc.v7.i10.1177

ISSN 2307-8960 (online)

CASE REPORT

Small cell lung cancer with panhypopituitarism due to ectopic adrenocorticotropic hormone syndrome: A case report

Ting Jin, Fang Wu, Shui-Ya Sun, Fen-Ping Zheng, Jia-Qiang Zhou, Yi-Ping Zhu, Zhou Wang

ORCID number: Ting Jin (0000-0002-8688-0445); Fang Wu (0000-0002-0948-3884); Shui-Ya Sun (0000-0002-3052-4935); Fen-Ping Zheng (0000-0002-1091-2367); Jia-Qiang Zhou (0000-0001-8372-0940); Yi-Ping Zhu (0000-0001-7986-3906); Zhou Wang (0000-0002-9412-0876).

Author contributions: All the authors materially participated in this work and have read and approved the final manuscript; Jin T is the first authors for this study; Wang Z is the corresponding author supervising this work; Jin T and Wu F managed the case and drafted the manuscript; Jin T, Wu F and Sun SY performed analysis on all data interpretation from literature review; Zheng FP, Zhou JQ, Zhu YP and Wang Z reviewed the manuscript; we acknowledge that all authors participated sufficiently in the work and take public responsibility for its content.

Supported by the National Science Foundation for Youth, No. 30800533; and the Public Welfare Project of Science and Technology Department of Zhejiang Province, China, No. 2017C33056.

Informed consent statement: Written consent was obtained from the patient. The patient consented to the publication of medical data (including figures from diagnostic imaging results and from histological examination results).

Conflict-of-interest statement: The authors declare that there is no conflict of interest that could be perceived as prejudicing the impartiality of the research reported.

Ting Jin, Fang Wu, Shui-Ya Sun, Fen-Ping Zheng, Jia-Qiang Zhou, Zhou Wang, Department of Endocrinology, Zhejiang University School of Medicine Sir Run Run Shaw Hospital, Hangzhou 310016, Zhejiang Province, China

Yi-Ping Zhu, Department of General Surgery, Zhejiang University School of Medicine Sir Run Run Shaw Hospital, Hangzhou 310016, Zhejiang Province, China

Corresponding author: Zhou Wang, MD, Professor, Department of Endocrinology, Zhejiang University School of Medicine Sir Run Run Shaw Hospital, 3 East Qing Chun Road, Hangzhou 310016, Zhejiang Province, China. 3405008@zju.edu.cn
Telephone: +86-571-86006176
Fax: +86-571-86006176

Abstract

BACKGROUND

Small cell lung cancer (SCLC) accounts for 15% of lung cancers, and it commonly expresses peptide and protein factors that are active as hormones. These secreting factors manifest as paraneoplastic disorders, such as ectopic adrenocorticotropic hormone (ACTH) syndrome (EAS). The clinical features are abnormalities in carbohydrate metabolism, hypokalemia, peripheral edema, proximal myopathy, hypertension, hyperpigmentation, and severe systemic infection. However, it is uncommon that EAS has an influence on hypothalamus-pituitary function.

CASE SUMMARY

A 62-year-old man presented with complaints of haemoptysis, polyuria, polydipsia, increased appetite, weight loss, and pigmentation. Following a series of laboratory and imaging examinations, he was diagnosed with SCLC, EAS, hypogonadism, hypothyroidism, and central diabetes insipidus. After three rounds of chemotherapy, levels of ACTH, cortisol, thyroid hormone, gonadal hormone, and urine volume had returned to normal levels. In addition, the pulmonary tumor was reduced in size.

CONCLUSION

We report a rare case of SCLC complicated with panhypopituitarism due to EAS. We hypothesize that EAS induced high levels of serum glucocorticoid and negative feedback for the synthesis and secretion of antidiuretic hormone from the paraventricular nucleus, and trophic hormones from the anterior pituitary. Therefore, patients who present with symptoms of hypopituitarism, or even panhypopituitarism, with SCLC should be evaluated for EAS.

CARE Checklist (2016) statement: This report follows the guidelines of the CARE Checklist (2016).

Manuscript source: Unsolicited manuscript

Received: December 29, 2018
Peer-review started: December 29, 2019
First decision: March 10, 2019
Revised: March 29, 2019
Accepted: April 9, 2019
Article in press: April 9, 2019
Published online: May 26, 2019

P-Reviewer: Neninger E, Su CC
S-Editor: Ji FF
L-Editor: A
E-Editor: Wu YXJ

Key words: Small cell lung cancer; Ectopic adrenocorticotropic hormone syndrome; Panhypopituitarism; Case report

Core tip: Ectopic adrenocorticotropic hormone syndrome (EAS) is the common paraneoplastic disorder in patients with small cell lung cancer (SCLC). However, it is uncommon that EAS has an influence on hypothalamus-pituitary function. Here, we report a rare case of SCLC complicated with panhypopituitarism due to EAS. We hypothesize that EAS induced high levels of serum glucocorticoid and negative feedback for the synthesis and secretion of antidiuretic hormone from the paraventricular nucleus, and trophic hormones from the anterior pituitary.

Citation: Jin T, Wu F, Sun SY, Zheng FP, Zhou JQ, Zhu YP, Wang Z. Small cell lung cancer with panhypopituitarism due to ectopic adrenocorticotropic hormone syndrome: A case report. *World J Clin Cases* 2019; 7(10): 1177-1183
URL: https://www.wjgnet.com/2307-8960/full/v7/i10/1177.htm
DOI: https://dx.doi.org/10.12998/wjcc.v7.i10.1177

INTRODUCTION

Small cell lung cancer (SCLC), which derived from neuroendocrine tissue, can appear the paraneoplastic disorders, such as ectopic adrenocorticotropic hormone (ACTH) syndrome (EAS). With regards to the clinical features of EAS, the degree of glucocorticoid level seems to be the major determinant. We report a case of SCLC with panhypopituitarism due to EAS presenting with hypogonadotropic, hypogonadism, secondary hypothyroidism, and central diabetes insipidus.

CASE PRESENTATION

Medical history

A 62-year-old male patient admitted to endocrinology clinic with polyuria, polydipsia, increased appetite, weight loss, pigmentation, haemoptysis, and fatigue that developed over two months. This was his first coming to the hospital.

History of past illness

The patient had underwent phacoemulsification ten years ago.

Personal and family history

The patient reported a history of smoking (40 packs/year), and denied drug use. His father died of the unknown cause and his mother died of a heart attack. His brother had diabetes mellitus.

Physical examination

The blood pressure was 151/99 mmHg (1 mmHg = 0.133 kPa), and body mass index was 21.09 kg/m^2. Pigmentation was observed on his face, his lip and buccal mucosa. Respiratory sounds in the bilateral lungs were rough, although no rales were heard.

Laboratory and imaging examination

Laboratory data also revealed an increase in levels of carcinoembryonic antigen (12.37 ng/mL), fasting plasma glucose (FPG) (12.76 mmol/L), HbA1c (8.9%), and urine sugar (3+). An oral glucose tolerance test indicated diabetes mellitus. Levels of blood ACTH, blood cortisol, and 24 h urine cortisol were elevated, and cortisol secretion was found to be disordered (Table 1). Low-dose and high-dose dexamethasone suppression tests both were not suppressed (8 am cortisol before test was 31.17 μg/dL, after low-dose dexamethasone suppression test was 37.04 μg/dL, after high-dose dexamethasone suppression test was 53.5 μg/dL). Levels of testosterone, thyroid stimulating hormone (TSH), total thyroxine (TT_4), total tri-iodothyronine (TT_3), and free tri-iodothyronine (FT_3) were all reduced, although levels of blood luteinizing hormone, follicle-stimulating hormone, prolactin, growth hormone (GH), free

thyroxine (FT_4) were all normal (Table 1). The patient's 24 h urine potassium level was 105.5 mmol, while the synchronous serum potassium level was 2.96 mmol/L. Water deprivation and vasopressin tests indicate partial central diabetes insipidus (Table 2). A chest computed tomography (CT) scan showed a hilar mass and chronic obstructive inflammation in the left lower lung (Figure 1A and B). A fiber optic bronchoscopy revealed a neoplasm present on the lower segment of the left main bronchus. A brush cell pathological examination showed a very small amount of heterocyst, and a histopathological examination detected expression of Leukocyte differentiation antigen (CD56), synaptophysin (Syn), chromogranin A (CgA), and cytokeratin (CK). Assays of NSE and ACTH were found to be positive. Thus, SCLC of the left lower bronchus was diagnosed (Figure 2). Magnetic resonance imaging (MRI) of the pituitary showed normal and MRI of the adrenal glands revealed bilateral adrenal hyperplasia (Figure 3). An emission computed tomography of the patient's bones revealed radioactivity concentrated in the sixth and seventh right anterior ribs, and a punctiform concentration of radioactivity was observed on the right oxter. In combination, the results of these examinations suggest that the neoplasm staging is IIIA ($T_3N_1M_0$).

FINAL DIAGNOSIS

According to the above results, SCLC ($T_3N_1M_0$), EAS, hypothyroidism, hypogonadism, diabetes insipidus, and dubious special type diabetes mellitus were diagnosed.

TREATMENT

An EP regimen of chemotherapy, including etoposide (170 mg administration d 1-3) and cis-platinum (100 mg administration d 1) were administered once every 21 d, with four rounds completed to date. In addition, insulin aspart and glargine were used to control the patient's blood glucose level. However, no medicine was administered to treat EAS, hypothyroidism, hypogonadism and diabetes insipidus (Table 1).

OUTCOME AND FOLLOW-UP

After the second round of chemotherapy, the patient's tumor markers, blood ACTH, blood cortisol, 24 h urine cortisol, gonadal hormone, gonadotrophins, TH, TSH, 24 h urine volume, and urine specific gravity returned to normal levels. In addition, the insulin dose administered was gradually decreased. Currently, the patient receives Glucobay (50 mg tid) only, and his FPG and postprandial plasma glucose are both well controlled (Table 1). A chest CT scan after the third round of chemotherapy also indicated that the volume of the hilar mass was reduced (Figure 1C and D). However, the follow-up survey of the patient was terminated because of the contact information change of the patient.

DISCUSSION

EAS is typically more common in males than females (3:1), and often occurs between the ages of 40 and 60 years[1]. Previously, SCLC has accounted for most cases of EAS[2]. However, in recent surveys, cases of EAS have been found to involve bronchial carcinoid tumours (> 25%), SCLC (approximately 20%), adenocarcinomas (about 20%), tumors of the thymus (11%), and pancreatic tumors (8%). In addition, medullary thyroid carcinoma, mediastinal tumors, gastrointestinal tumors, and genital tract tumors have been found to cause EAS[3]. Patients with EAS may develop hypokalemia accompanied by alkalosis, myasthenia, edema, pigmentation, crinosity, hypertention, and hyperglycemia. Moreover, Isidori *et al*[4] reported that EAS patients with SCLC more commonly presented with skin pigmentation, while symptoms of Cushing's syndrome were absent. These characteristics may be due to the rapidity of tumor development and the severity of hypercortisolaemia induced by SCLC[4].

In the present case, a 62-year-old male patient was diagnosed with SCLC, EAS, hypogonadism, hypothyroidism, and central diabetes insipidus. It is unusual that EAS would have an influence on hypothalamus-pituitary function and affect functions of the thyroid, gonad, or other target glands. In recent years, however,

Table 1 Hormone levels and biochemical indexes detected before and after chemotherapy

Biochemical assay	Normal range	Prior to chemotherapy	After 1st round	After 2nd round	After 3rd round
8 am ACTH	10–80 ng/L	210	127	74	45
4 pm ACTH	5–40 ng/L	192	100	43	21
8 am cortisol	8.7–22.4 μg/dL	31.17	16.79	8.8	8.64
4 pm cortisol	0–10 μg/dL	35.18	11.26	2.36	2.47
0 am cortisol	0–5 μg/dL	31.27	14.47	1.75	3.64
24 h urine cortisol		> 1932.8	341.6	154.4	120.5
FPG (mmol/L)		5.6	4	5.8	5.4
2 h PPG (mmol/L)		13	7.9	6.9	6.8
Testosterone	1.75–7.81 μg/L	0.98	0.94	3.57	4.01
FSH	1.27–19.26 IU/L	5.58	5.09	12.79	16.68
LH	1.24–8.62 IU/L	4.18	2.02	6.08	5.42
TSH	0.35–4.94 mIU/L	0.07	1.36	1.46	0.94
TT_4	4.87–11.72 μg/dL	4.19	4.41	7.83	6.15
TT_3	0.58–1.59 ng/mL	0.43	0.56	1.31	1.19
FT_4	0.7–1.48 ng/dL	0.94	0.83	1.17	0.84
FT_3	1.71–3.71 pg/mL	1.4	1.63	3.7	2.82
24 h urine volume (mL/d)		3200	2800	2400	1170
Urine specific gravity	1.015–1.025	1.010	1.014	1.016	1.020
NSE	0–15.2 ng/mL	18.27	9.59	10.39	-
CEA	0–5 ng/mL	7.35	2.91	2.69	-

ACTH: Adrenocorticotropic hormone; FPG: Fasting plasma glucose; PPG: Postprandial plasma glucose; FSH: Follicle-stimulating hormone; LH: Luteinizing hormone; TSH: Thyroid stimulating hormone; TT_4: Total thyroxine; TT_3: Total tri-iodothyronine; FT_3: Free tri-iodothyronine; FT_4: Free thyroxine; NSE: Neuron-specific enolase; CEA: Carcinoembryonic antigen.

several cases of SCLC complicated with EAS, hypothyroidism, and hypogonadism have been reported worldwide[5]. Previous studies have demonstrated that serum TSH levels often decrease as a result of glucocorticoid effects at both the hypothalamic and pituitary levels[6], while serum T_3 levels can decrease due to an inhibition of peripheral conversion of T_4 by glucocorticosteroids[7]. Hypogonadotropic hypogonadism have also been reported, which are hypothesized to be the result of glucocorticoid suppression at the hypothalamo-pituitary level[8]. Since the patient's pituitary-gonad and pituitary-thyroid axes were both suppressed by hypercortisolism, these results suggest that the level of GH might also be suppressed. In this study, the patient's level of GH was within the lower limit of the normal range. However, the patient refused an insulin tolerance test, which is considered the gold standard for diagnosing GH deficiency.

In addition, the patient also developed apparent polyuria and polydipsia. A urine test revealed a lower specific gravity, water deprivation and vasopressin tests indicate partial central diabetes insipidus. Previously, cases of EAS complicated with central diabetes insipidus have been reported, most of which involved posterior pituitary metastasis[9]. Since the patient in the present case had a urine volume of 3-4 L/d, water deprivation and vasopressin tests (Table 2) showed incomplete diabetes insipidus, and a pituitary MRI revealed normal (Figure 3A and B), the possibility of early pituitary metastasis could not be completely excluded. Moreover, there may be other mechanism responsible for the development of diabetes insipidus. Glucocorticoid has also been associated with mediating a negative feedback loop that affects secretion of corticotropin-releasing hormone and antidiuretic hormone (ADH) from the paraventricular nucleus[10]. Therefore, high serum levels of glucocorticoid associated with ectopic ACTH syndrome could result in central diabetes insipidus.

According to the pathology and staging of the tumor determined, EP chemotherapy was administered. Following treatment, the hilar mass was reduced in size and levels of tumor markers returned to a normal range. Furthermore, the blood ACTH, blood cortisol, 24 h urine cortisol, blood pressure, gonadal hormone, and TH all gradually returned to normal ranges without any treatment. Blood glucose levels were also well-controlled and insulin dosages were decreased day by day. The patient's 24 h urine volume was reduced, and the urine specific gravity increased too. Based on these outcomes, the diagnosis that hypogonadism, hypothyroidism, and diabetes insipidus experienced by the patient were related to EAS was confirmed.

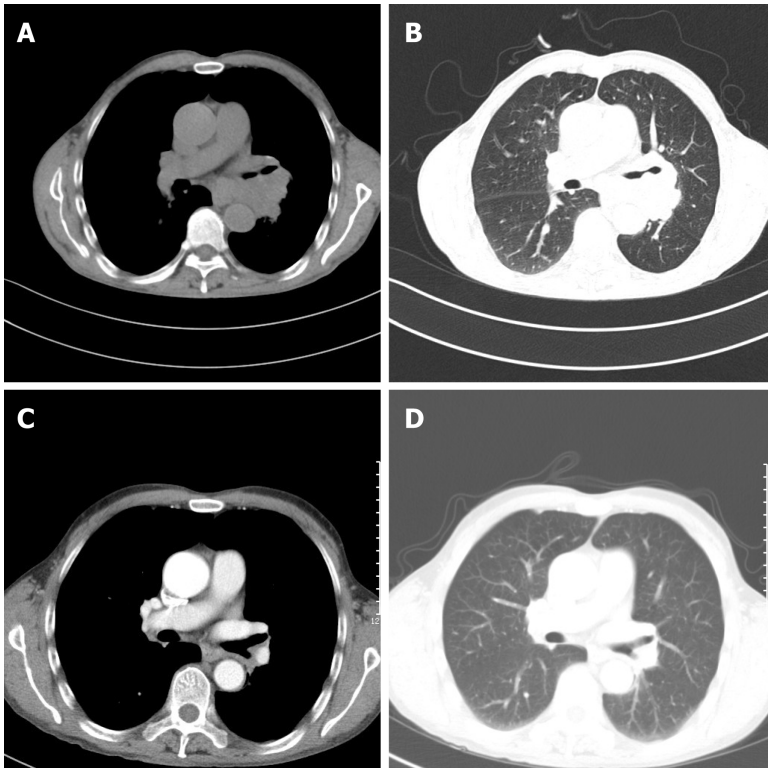

Figure 1 Computed tomography scan of the lung. A, B: Chest computed tomography (CT) images obtained before chemotherapy indicated a central lung cancer was present. A lobulated, low density hilar mass (indicated with arrows) was found to be pressing and narrowing the left main bronchus. No lymph node enlargement was seen in the mediastinum; C, D: Chest CT images obtained after three rounds of chemotherapy. The left hilar mass (indicated with arrows) exhibited a marked reduction in size.

CONCLUSION

This case of SCLC complicated with EAS, hypogonadotropic hypogonadism, secondary hypothyroidism, and central diabetes insipidus is unique, and to our knowledge, is the first of its type to be reported. EP chemotherapy was found to treat the SCLC, and also served to correct the clinical disorders caused by EAS. We hypothesize that negative feedback by high levels of serum glucocorticoid affected the synthesis and secretion of ADH from the paraventricular nucleus and trophic hormones from the anterior pituitary to contribute to the patient's condition. It is also possible that inadequate secretion of ADH due to tumor metastasis to the posterior pituitary may have been involved. Further studies will be needed to distinguish these possibilities.

Table 2 Water deprivation and vasopressin test data

Time	Urine volume (mL)	Urine specific gravity	Plasma osmotic pressure (osmo/kg)	Weight (kg)	Blood pressure (mmHg)	Heart rate (bpm)	Notes
1st day 22:00	250	1.010	298	51.0	136/75	73	Start water deprivation
2nd day 11:50	100	1.012	305	48.5	131/77	81	Platform stage pituitrin administration
2nd day 12:50	100	1.018	-	49.0	103/74	75	-
2nd day 13:50	50	1.018	301	49.0	121/76	76	Off-test

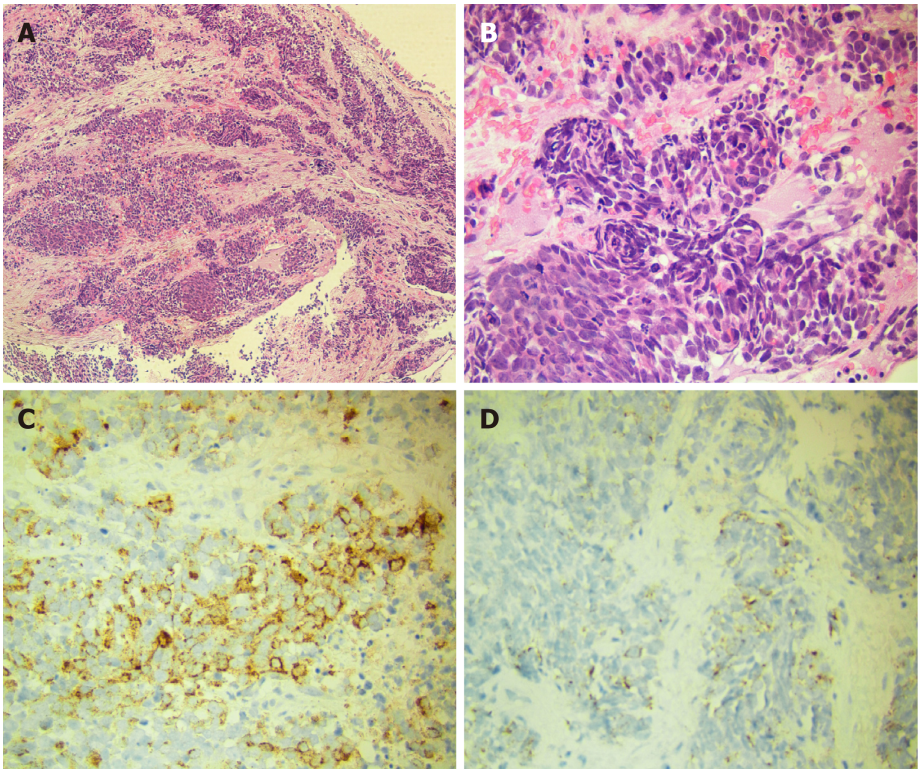

Figure 2 Immunohistochemical stainings of the hilar mass tissue biopsy sample. A, B: HE staining detected small cells with hyperchromatic nuclei and minimal cytoplasm. Both spindly and lymphocytoid cancer cells were observed. Magnification, 100× and 400×, respectively; C, D: Immunohistochemical staining was also performed and focal positive staining for chromogranin A (C) and adrenocorticotropic hormone (D) were detected.

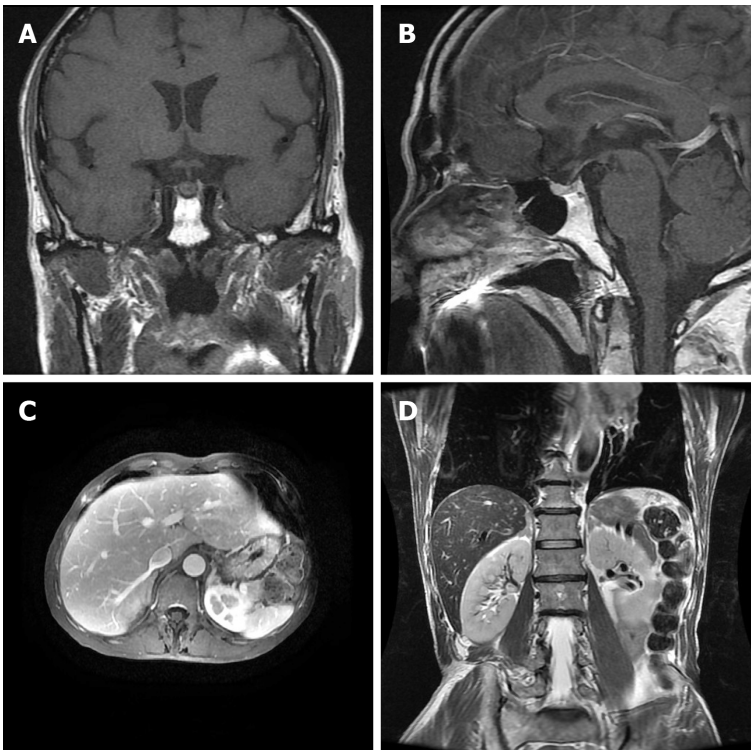

Figure 3 Magnetic resonance images of the head and the epigastrium. A, B: Magnetic resonance imaging (MRI) of the pituitary. No obvious abnormalities were observed. Arrows are labeling the pituitary in both views; C, D: MRI of the epigastrium with bilateral adrenal thickening detected. Arrows are labeling the epigastrium in both views.

ACKNOWLEDGEMENTS

We wish to thank Dr. Beibei Zhang, who ever was one of our colleagues, for kindly helping in the writing in this manuscript. And we wish to thank Hong Li, now the department director, for support in the clinical management.

REFERENCES

1 **Yang YN**. *Disease of endocrinology system: heterologous endocrine syndrome: ectopic ACTH syndrome*. In: Haozhu Chen (ed). Practice of Internal Medicine (12th). People's Medical Publishing House, Beijing 2005; 1300-1301 (In Chinese)
2 **Beuschlein F**, Hammer GD. Ectopic pro-opiomelanocortin syndrome. *Endocrinol Metab Clin North Am* 2002; **31**: 191-234 [PMID: 12055989 DOI: 10.1016/S0889-8529(01)00025-1]
3 **Isidori AM**, Lenzi A. Ectopic ACTH syndrome. *Arq Bras Endocrinol Metabol* 2007; **51**: 1217-1225 [PMID: 18209859 DOI: 10.1159/000094323]
4 **Isidori AM**, Kaltsas GA, Pozza C, Frajese V, Newell-Price J, Reznek RH, Jenkins PJ, Monson JP, Grossman AB, Besser GM. The ectopic adrenocorticotropin syndrome: clinical features, diagnosis, management, and long-term follow-up. *J Clin Endocrinol Metab* 2006; **91**: 371-377 [PMID: 16303835 DOI: 10.1210/jc.2005-1542]
5 **Lin CJ**, Perng WC, Chen CW, Lin CK, Su WL, Chian CF. Small cell lung cancer presenting as ectopic ACTH syndrome with hypothyroidism and hypogonadism. *Onkologie* 2009; **32**: 427-430 [PMID: 19556823 DOI: 10.1159/000219433]
6 **Kakucska I**, Qi Y, Lechan RM. Changes in adrenal status affect hypothalamic thyrotropin-releasing hormone gene expression in parallel with corticotropin-releasing hormone. *Endocrinology* 1995; **136**: 2795-2802 [PMID: 7789304 DOI: 10.1210/endo.136.7.7789304]
7 **Duick DS**, Warren DW, Nicoloff JT, Otis CL, Croxson MS. Effect of single dose dexamethasone on the concentration of serum triiodothyronine in man. *J Clin Endocrinol Metab* 1974; **39**: 1151-1154 [PMID: 4430708 DOI: 10.1210/jcem-39-6-1151]
8 **Marazuela M**, Cuerda C, Lucas T, Vicente A, Blanco C, Estrada J. Anterior pituitary function after adrenalectomy in patients with Cushing's syndrome. *Postgrad Med J* 1993; **69**: 547-551 [PMID: 8415342 DOI: 10.1136/pgmj.69.813.547]
9 **Tanaka H**, Kobayashi A, Bando M, Hosono T, Tsujita A, Yamasawa H, Ohno S, Hironaka M, Sugiyama Y. [Case of small cell lung cancer complicated with diabetes insipidus and Cushing syndrome due to ectopic adrenocorticotropic hormone secretion]. *Nihon Kokyuki Gakkai Zasshi* 2007; **45**: 793-798 [PMID: 18018629]
10 **Huang CH**, Chou KJ, Lee PT, Chen CL, Chung HM, Fang HC. A case of lymphocytic hypophysitis with masked diabetes insipidus unveiled by glucocorticoid replacement. *Am J Kidney Dis* 2005; **45**: 197-200 [PMID: 15696461 DOI: 10.1053/j.ajkd.2004.09.033]

World Journal of Clinical Cases

Submit a Manuscript: https://www.f6publishing.com

World J Clin Cases 2019 May 26; 7(10): 1184-1190

DOI: 10.12998/wjcc.v7.i10.1184

ISSN 2307-8960 (online)

CASE REPORT

Therapeutic plasma exchange and a double plasma molecular absorption system in the treatment of thyroid storm with severe liver injury: A case report

You-Wen Tan, Li Sun, Kai Zhang, Li Zhu

ORCID number: You-Wen Tan (0000-0002-5464-1407); Li Sun (0000-0002-7989-6190); Kai Zhang (0000-0003-4296-4687); Li zhu (0000-0002-9009- 9109).

Author contributions: Tan YW and Sun L contributed equally to this work; Tan YW and Sun L designed the research; Zhang K and Sun L collected and analyzed the data, and drafted the manuscript; Zhu L performed therapeutic plasma exchange and double plasma molecular absorption system; Tan YW wrote and revised the manuscript; all authors have read and approved the final version to be published.

Informed consent statement: Informed consent was obtained from the patient.

Conflict-of-interest statement: All authors have no conflict of interest related to the manuscript.

CARE Checklist (2016) statement: We are committed to writing in CARE Checklist (2016) format.

You-Wen Tan, Li Sun, Kai Zhang, Li Zhu, Department of Hepatology, the Third Hospital of Zhenjiang Affiliated Jiangsu University, Zhenjiang 212003, Jiangsu Province, China

Corresponding author: You-Wen Tan, MD, PhD, Chief Doctor, Department of Hepatosis, the Third Hospital of Zhenjiang Affiliated Jiangsu University, No. 300, Daijiamen, Runzhou Distinct, Zhenjiang 212003, Jiangsu Province, China. tyw915@sina.com
Telephone: +86-511-88970796
Fax: +86-511-88970796

Abstract

BACKGROUND

Thyroid storm is resistant to conventional treatments including antithyroid drugs and ^{131}I therapeutic means. Plasma exchange (PE) and double plasma molecular absorption system (DPMAS) can be used as an effective treatment for thyroid storm with severe liver injury.

CASE SUMMARY

A 52-year-old woman presented with a 10-day history of nausea and vomiting accompanied by yellowing of the skin and mucosa. Further, her free T3 (FT3) and FT4 levels were significantly elevated, whereas her thyrotropin level was reduced. After admission, her condition continued to deteriorate, and she presented with continued high fever, vomiting, palpitation, and shortness of breath. After being diagnosed with thyroid storm, the patient was immediately treated with PE combined with DPMAS. Her symptoms improved immediately. After three PE + DPMAS treatments, and she was discharged from the hospital. She was treated with methylprednisolone and methylthimidazole. After six months, the patient spontaneously discontinued methylthimidazole treatment. Her previous clinical manifestations and liver dysfunction reoccurred. The patient was treated with PE + DPMAS two times, and her condition rapidly improved. Liver histopathology indicated immunological liver injury.

CONCLUSION

Our experience suggests that PE combined with DPMAS can effectively relieve the development of thyroid storm.

Key words: Plasma exchange; Thyroid storm; Immunological liver injury; Case report

Manuscript source: Unsolicited manuscript

Received: January 13, 2019
Peer-review started: January 13, 2019
First decision: January 26, 2019
Revised: January 29, 2019
Accepted: March 8, 2019
Article in press: March 9, 2019
Published online: May 26, 2019

P-Reviewer: Gabriel S, Loustaud-Ratti V, Milovanovic T
S-Editor: Ji FF
L-Editor: A
E-Editor: Wu YXJ

Core tip: Plasma exchange (PE) and double plasma molecular absorption system (DPMAS) can be used as an effective treatment for thyroid storm with severe liver injury. A 52-year-old woman presented with a 10-d history of nausea and vomiting accompanied by yellowing of the skin and mucosa. After being diagnosed with thyroid storm accompanied by severe liver injury, the patient was immediately treated with PE combined with DPMAS for three times and discharged from the hospital. After six months, her previous clinical manifestations and liver dysfunction reoccurred and treated with PE + DPMAS again, her condition rapidly improved and liver histopathology indicated immunological liver injury.

Citation: Tan YW, Sun L, Zhang K, Zhu L. Therapeutic plasma exchange and a double plasma molecular absorption system in the treatment of thyroid storm with severe liver injury: A case report. *World J Clin Cases* 2019; 7(10): 1184-1190
URL: https://www.wjgnet.com/2307-8960/full/v7/i10/1184.htm
DOI: https://dx.doi.org/10.12998/wjcc.v7.i10.1184

INTRODUCTION

Thyroid storm is a syndrome of acute hyperthyroidism exacerbation[1] that can lead to high fever, heart failure, shock, coma, and other life-threatening manifestations. Thyroid storm accounts for about 1%-2% of hyperthyroidism patients, the incidence is about 0.002%, and the mortality rate after acute onset is high, above 20%[2]. Thyroid storm is resistant to conventional treatments including antithyroid drugs and ^{131}I therapeutic means. Drug therapy increases the risk of progressing to liver failure in hyperthyroidism storm patients with severe liver injury[3]. Plasma exchange (PE) is a method to purify blood by replacing abnormal components of plasma with fresh normal human plasma or plasma substitutes[4]. The whole plasma containing pathogenic factors (drugs, poisons and toxins) that cannot be controlled or expelled by drugs are discarded by blood purification technology in vitro and then resume load fresh plasma. As the most commonly used treatment in artificial liver support system, PE has been widely used in the treatment of liver failure in China and is considered to have a good therapeutic effect[5]. Severe liver injury in thyroid storm is rare[3,6]. We report a case of hyperthyroidism with thyroid storm accompanied by severe liver damage that was successfully treated with PE and double plasma molecular absorption system (DPMAS).

CASE PRESENTATION

Chief complaint

A 52-year-old woman presented with a 10-d history of nausea and vomiting accompanied by yellowing of the skin and mucosa and reoccurred after six months.

History of present illness

On the evening of admission, April 4, 2018, the patient began to vomit her stomach content frequently. The patient's condition gradually worsened, and irritability and heart rate gradually increased. The patient had no history of hyperthyroidism, but often had palpitation, sweating, agitation, and other symptoms.

History of past illness

No viral hepatitis (A–E) history, no nonalcoholic fatty liver disease history and no cholestatic liver diseases include primary biliary cirrhosis, primary sclerosing cholangitis, and secondary sclerosing cholangitis.

Personal and family history

No alcohol abuse and no other drug and herbal used. No additional family history.

Physical examination upon admission

Her highest heart rate was 180 beats per minute, body temperature 39.8 °C, highest breathing rate was 25 breaths per minute, blood pressure 147/86 mmHg. PE + DPMAS were conducted once every other day, and three times in all. The patient's symptoms improved obviously and rapidly. Nausea and vomiting stopped, and body

temperature, heart rate, and respiration gradually returned to normal the next day.

Laboratory examinations

On April 4, 2018, her liver function test showed significantly increased transaminase and bilirubin levels [aspartate aminotransferase (AST) 1364 U/L, alanine aminotransferase (ALT) 521 U/L, alkaline phosphatase 153 U/L, glutamete transpeptidase 68 U/L, total bilirubin (TBIL) 223.3 μmol/L, direct bilirubin 164.4 μmol/L)]. Her prothrombin time (PT) was 16 s, PT activity was 67%, and international ratio was 1.54. Her thyrotropin (TSH) level was decreased, and free T3 (FT3) and her free T4 (FT4) levels were significantly increased (TSH < 0.005 mIU/L, FT3 28.6 pmol/L, FT4 81.273 pmol/L). The antinuclear antibody (ANA) test was positive (1:320), and the anti-smooth muscle antibody, anti-liver/kidney microsome antibody type 1, anti-nuclear glycoprotein antibody, anti-soluble acid nucleoprotein antibody, soluble acidic nucleoprotein antibody, anti-hepatocyte cytoplasmic antigen type 1 antibody, anti-soluble liver antigen/hepatopancreatic antigen antibody, and other tests were negative. The immunoglobulin G (IgG) level was 19.1 g/L (< 17.1 g/L). Liver function returned to normal (TBIL 15.2 μmol/L, ALT 26 U/L, AST 31 U/L), and the hyperthyroidism index was restored (FT3 6.1 pmol/L, FT4 20.4 pmol/L, TSH 0.007 μU/mL) at first discharge. Liver and thyroid function were normal during follow-ups on June 16 and August 28, 2018. By November, methylthimidazole administration was discontinued by the patient without a doctor's advice. About 40 d later, symptoms including fatigue, loss of appetite, and urinary yellowing reoccurred. Liver function (TBIL 115.6 μmol/L, ALT 473 U/L, AST 664 U/L) and thyroid index (TSH < 0.005 mIU/L, FT3 13.6 pmol/L) abnormalities were checked for, and the patient was re-admitted. Changes in liver function and thyroid index are shown in Table 1. Epstein-Barr virus, and cytomegalovirus infections were ruled out. No pathogenic bacteria were found in blood culture

Imaging examinations and liver histopathology

Thyroid B-ultrasonography showed diffuse thyroid lesions and abdominal B-ultrasonography showed no hepatic space-occupying lesions, echoes dense and uniform in the liver, and no abnormalities in other organs. Liver biopsy was performed one week later at second hospitalization, and showed the pathological features of AIH including moderate interfacial inflammation, lymphocyte-plasma cell infiltration, rosette-like hepatocyte infiltration, and hepatocyte lymphocyte penetration (Figure 1).

FINAL DIAGNOSIS

Thyroid storm with severe liver injury.

TREATMENT

Forty milligram methylprednisolone, 50 mg methimazole, and 20 mg propranolol were given orally each day, and the patient was treated immediately with PE + DPMAS. The velocity of PE was 25-30 mL/min, PE volume was 1500 mL, and DPMAS was performed after PE. DPMAS consists of blood and plasma circuits and is shown in Figure 2. First, whole blood was collected from the femoral vein and pumped into the plasma separator. Plasma was then adsorbed by a bilirubin adsorber (BS330, Zhuhai Health Sails Biotechnology Co., LTD) and a macroporous neutral resin (HA330, Zhuhai Health Sails Biotechnology Co., LTD) in turn. Later, plasma was merged with the separated blood cells and reintroduced into the body (Figure 1). PE + DPMAS were conducted once every other day, and three times in all performed at first addmited. After 22 d, it was suggested that the patient continue with 8 mg/d methylprednisolone, 10 mg/d methylthimidazole, and 10 mg/d propranolol and attend regular follow-up appointments. However, methylthimidazole administration was discontinued by the patient without a doctor's advice. About 40 d later, the patient was re-admitted presented similar symptoms and liver function and thyroid index abnormalities. Methylprednisolone (32 mg) and PE + DPMAS were administered for twice.

OUTCOME AND FOLLOW-UP

Liver function and hyperthyroidism index returned to normal and the patient was

Table 1 The clinical features of pre- and post-operative of plasma exchange and double plasma molecular absorption system

PE + DPMAS		T (36.2-37.2 °C)	P (60-100 beats/min)	TBIL (1.71-17.1 μmol/L)	DBIL (0-6.8 μmol/L)	ALT (10-40 U/L)	AST (10-40 U/L)	ALP (40-120 U/L)	GGT (10-40U/L)	FT3 (3.1-6.8 pmol/L)	FT4 (9.2-22.8 pmol/L)	TSH (0.27-4.2 μU/mL)	TG (5-40 μg/L)
First attack													
1st	Preoperative	39.8	180	223.3	164.4	521	1364	153	68	28.6	81.3	< 0.005	364.6
	Postoperative	37.5	86	102.4	64.3	253	643	124	47	15.3	36.8	0.008	204.4
2nd	Preoperative	38.4	102	116.4	74.3	226	1054	115	42	17.4	46.6	< 0.005	286.4
	Postoperative	36.7	76	63.4	37.5	123	436	57	37	10.4	25.4	0.006	126.5
3rd	Preoperative	37.2	74	79.4	42.8	78	332	64	41	16.4	34.2	< 0.005	171.7
	Postoperative	37.1	73	53.7	26.7	64	117	47	37	8.4	21.6	0.006	97.5
Second attack													
1st	Preoperative	39.1	142	115.6	64.2	473	664	116	57	13.4	49.3	< 0.005	263.5
	Postoperative	38.3	112	63.2	32.4	216	312	78	42	6.3	25.8	0.007	167.4
2nd	Preoperative	36.8	85	46.4	31.8	163	226	83	41	8.4.	33.5	< 0.005	183.4
	Postoperative	36.6	76	32.7	16.4	64	75	54	36	4.4	16.4	0.008	74.3

T: Temperature; P: Pulse; TG: Thyroglobulin; TSH: Thyroid stimulating hormone; FT3: Free triiodothyronine; FT4: Free thyroxine; DBIL: Direct bilirubin; TBIL: Total bilirubin; AST: Aspartate aminotransferase; ALT: Alanine aminotransferase; ALP: Alkaline phosphatase; GGT: Glutamete transpeptidase.

discharged two weeks later. Long-term oral administration of 10 mg methylprednisolone and 10 mg methylthimidazole was prescribed. The discharging doctor suggested long-term treatment with 8 mg oral methylprednisolone and 10 mg oral methylthimidazole and regular follow-up appointments.

DISCUSSION

The etiology of hyperthyroidism-induced liver injury includes Graves' disease hyperthyroidism, antithyroid drugs, and basic liver diseases[7]. Its pathogenesis may be related to the following factors[8]: (1) The direct toxic effect of thyroid hormone on the liver; (2) Hyperthyroidism making the liver relatively hypoxic, causing free radical production and hepatocyte damage; (3) Hyperthyroidism leading to Kupffer cell proliferation and serum AST elevation; (4) Thyroid hormone affecting intrahepatic enzyme activity to alter bilirubin metabolism and binding; and (5) Immune damage. According to clinical manifestation and laboratory examination, hyperthyroidism-induced liver injury can be divided into hepatocyte, cholestasis, and mixed types.

Thyroid storm is a pathological condition characterized by high elevated thyroid hormone levels leading to multiple organ failure[9]. Thyroid storms often occur in untreated or inadequately treated patients with hyperthyroidism and are often triggered by infection, high fever, and so on. Common manifestations include severe heart, lung, liver, and gastrointestinal damage and neurological dysfunction. Thyroid storm has a very high mortality rate of 10%-30%[10]. Traditional thyroid storm therapies include beta blockers, antithyroid drugs, iodine, and glucocorticoids.

AIH is a hepatic parenchymal inflammation mediated by an autoimmune response to hepatocytes. It is characterized by positive serum autoantibodies, hyperimmunoglobulinemia, and/or γ-globulinemia and histologically demonstrates interface hepatitis. AIH is often associated with other organ or systemic autoimmune diseases such as Hashimoto's disease. Thyroiditis (10%-23%), diabetes mellitus (7%-9%), inflammatory bowel disease (2%-8%), rheumatoid arthritis (2%-5%), Sjogren's syndrome (1%-4%), psoriasis (3%), and systemic lupus erythematosus (1%-2%) are

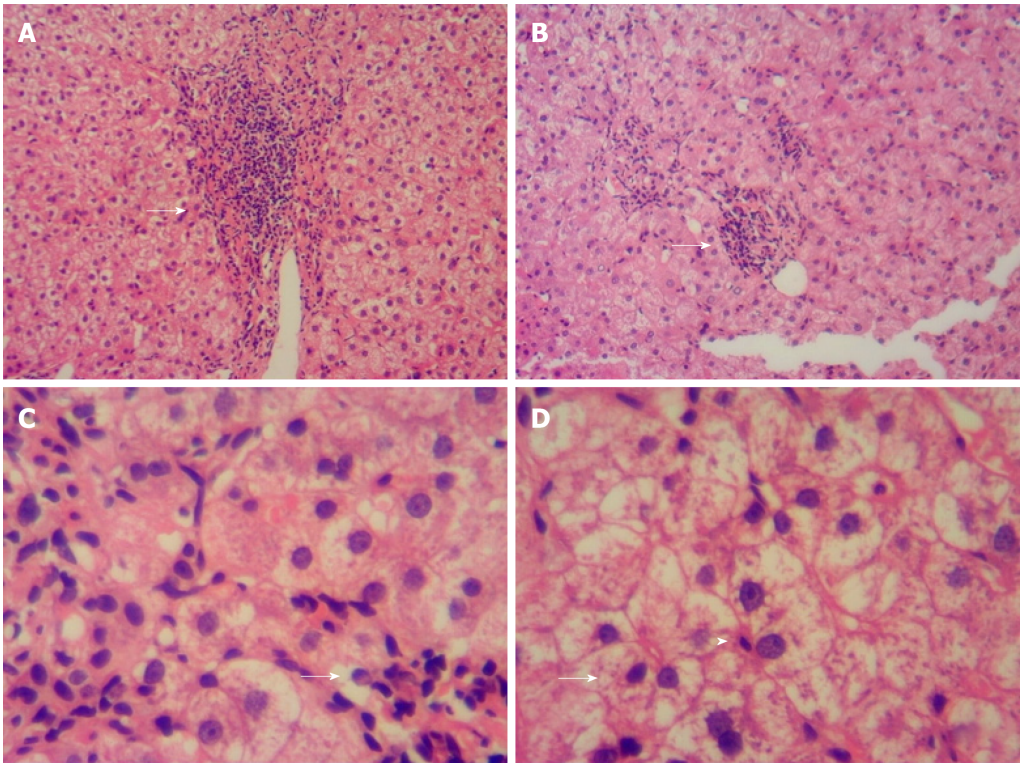

Figure 1 Liver histology (hematoxylin and eosin staining). A: Mild interfacial inflammation and in portal area; B: Focal necrosis (arrows, 10 × 20); C: lymphatic-plasma cell infiltration and plasma cell infiltration (arrows, 10 × 20); and D: Rosetting of hepatocytes (arrows) and lymphocyte penetration (arrowheads, 10 × 40).

common associations[11]. On the other hand, one mechanism of hyperthyroidism-induced liver injury is an immune-mediated liver disorder[12].

Is AIH complicated by thyroid storm or liver immune injury caused by hyperthyroidism? According to the simplified criteria for the diagnosis of AIH by the International Autoimmune Hepatitis Group[13], AIH can be diagnosed by a score of 7 points (ANA 1:320, +2; IgG > 1.1 ULN, +2; pathological characteristics of liver, +1; excluding viral hepatitis, +2). In our patient, however, immune liver injury was more likely to be caused by hyperthyroidism storm rather than AIH complicated by thyroid storm. Although the patient had severe liver dysfunction, pathological characteristics, namely, inflammation and necrosis, were not serious, and pathological features and clinical and biochemical manifestations are separated. Furthermore, the second relapse was caused by anti-hyperthyroidism drug discontinuation and not corticosteroid discontinuation.

PE, which is called an intermediate artificial liver, can not only remove toxins, but also supplement coagulation factors, albumin, complements, and other beneficial substances lacking in liver failure. It has become the most important artificial liver treatment mode in the past decade, and is widely used. Since the 1970s, there have been many reports on the treatment of hyperthyroidism storm[14-19]. PE can quickly remove antibodies, thyroid hormones, and a large number of inflammatory factors from the blood and achieves good clinical results.

However, for a hyperbilirubinemia caused by liver failure, it may take more than 5 L plasma to replace 50% of the serum hyperbilirubin levels. Similarly, for a thyroid strom, it may take 30-50 L plasma to dilute FT3 to normal levels. It is obviously difficult to achieve adequate blood purification by PE alone. In recent years, decreased plasma collection has greatly limited the clinical application of PE. Blood adsorption technology is a blood purification method that uses different adsorbents to non-selectively absorb and remove endogenous or exogenous poisons in the blood. DPMAS is a combination of BS330 bilirubin adsorption and HA330-II hemoperfusion. The resin in a BS330 bilirubin adsorber is specific for bilirubin. It adsorbs bilirubin and bile acid by electrostatic force and lipophilic binding properties. Resin in a HA330-II hemoperfusion device is a relatively broad-spectrum adsorbent with a macroporous structure and large surface area. It can adsorb macromolecular toxins (such as inflammatory mediators IL-6 and IL-10) by Van der Waals force and a skeleton molecular sieve[20]. The combination of the two adsorbents can quickly remove harmful substances such as bilirubin, antibodies, thyroid hormones, and inflammatory mediators, alleviate inflammation, and improve the immune response.

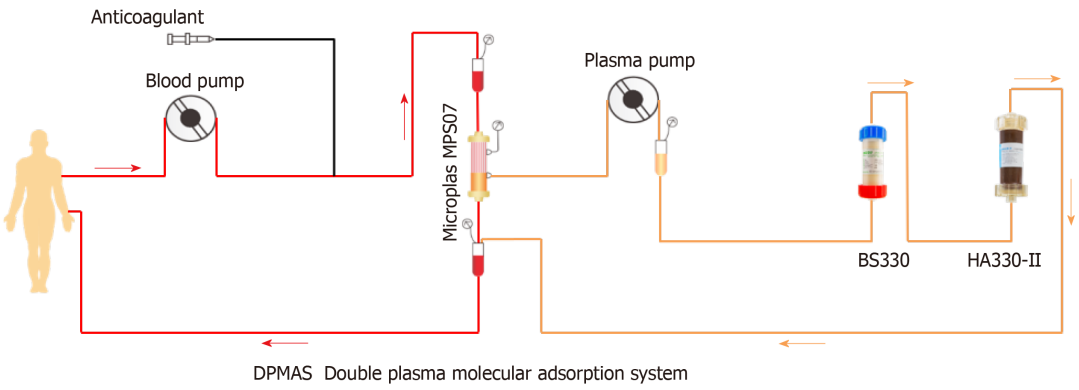

Figure 2 Double plasma molecular absorption system flowchart.

A DPMAS system can purify and absorb more than 6000 mL of plasma at a time, which can compensate for the decrease in clearance efficiency caused by insufficient PE.

CONCLUSION

We report a case of severe liver injury in a patient with severe hyperthyroidism and thyroid storm. The liver histopathology suggests that the immunological liver injury was caused by hyperthyroidism. This patient was treated with PE combined with DPMAS and achieved a good curative effect. This novel therapeutic combination may be worth popularizing.

REFERENCES

1 **Galindo RJ**, Hurtado CR, Pasquel FJ, García Tome R, Peng L, Umpierrez GE. National Trends in Incidence, Mortality, and Clinical Outcomes of Patients Hospitalized for Thyrotoxicosis With and Without Thyroid Storm in the United States, 2004-2013. *Thyroid* 2019; **29**: 36-43 [PMID: 30382003 DOI: 10.1089/thy.2018.0275]
2 **Thumma S**, Manchala V, Mattana J. Radiocontrast-Induced Thyroid Storm. *Am J Ther* 2018 [PMID: 30299273 DOI: 10.1097/MJT.0000000000000844]
3 **Choudhary AM**, Roberts I. Thyroid storm presenting with liver failure. *J Clin Gastroenterol* 1999; **29**: 318-321 [PMID: 10599633 DOI: 10.1097/00004836-199912000-00004]
4 **Riveiro-Barciela M**, Muñoz-Couselo E, Fernandez-Sojo J, Diaz-Mejia N, Parra-López R, Buti M. Acute liver failure due to immune-mediated hepatitis successfully managed with plasma exchange: New settings call for new treatment strategies? *J Hepatol* 2018; **pii**: S0168-8278(18)32504-2 [PMID: 30503040 DOI: 10.1016/j.jhep.2018.10.020]
5 **Chen JJ**, Huang JR, Yang Q, Xu XW, Liu XL, Hao SR, Wang HF, Han T, Zhang J, Gan JH, Gao ZL, Wang YM, Lin SM, Xie Q, Pan C, Li LJ. Plasma exchange-centered artificial liver support system in hepatitis B virus-related acute-on-chronic liver failure: a nationwide prospective multicenter study in China. *Hepatobiliary Pancreat Dis Int* 2016; **15**: 275-281 [PMID: 27298103]
6 **Oguntolu V**. Severe thyrotoxicosis (thyroid storm) with liver failure. *Acute Med* 2007; **6**: 30-32 [PMID: 21611612]
7 **Khemichian S**, Fong TL. Hepatic dysfunction in hyperthyroidism. *Gastroenterol Hepatol (NY)* 2011; **7**: 337-339 [PMID: 21857837 DOI: 10.1038/bdj.2007.482]
8 **Bhuyan AK**, Sarma D, Kaimal Saikia U, Choudhury BK. Grave's Disease with Severe Hepatic Dysfunction: A Diagnostic and Therapeutic Challenge. *Case Rep Med* 2014; **2014**: 790458 [PMID: 25317178 DOI: 10.1155/2014/790458]
9 **Soleimanpour SA**. Fulminant liver failure associated with delayed identification of thyroid storm due to heterophile antibodies. *Clin Diabetes Endocrinol* 2015; **1**: pii: 12 [PMID: 26491542 DOI: 10.1186/s40842-015-0012-6]
10 **Kanbay M**, Sengul A, Güvener N. Trauma induced thyroid storm complicated by multiple organ failure. *Chin Med J (Engl)* 2005; **118**: 963-965 [PMID: 15978201 DOI: 10.1503/cmaj.1041179]
11 **Liberal R**, Grant CR, Mieli-Vergani G, Vergani D. Autoimmune hepatitis: a comprehensive review. *J Autoimmun* 2013; **41**: 126-139 [PMID: 23218932 DOI: 10.1016/j.jaut.2012.11.002]
12 **Yamada M**, Shibata H, Masugi Y, Ishi T, Kameyama K, Ebinuma H, Hasegawa T. Histological Changes in Autoimmune Hepatitis with Graves' Disease: A Child Case Report. *Intern Med* 2017; **56**: 2139-2143 [PMID: 28781316 DOI: 10.2169/internalmedicine.8417-16]
13 **Hennes EM**, Zeniya M, Czaja AJ, Parés A, Dalekos GN, Krawitt EL, Bittencourt PL, Porta G, Boberg KM, Hofer H, Bianchi FB, Shibata M, Schramm C, Eisenmann de Torres B, Galle PR, McFarlane I, Dienes HP, Lohse AW; International Autoimmune Hepatitis Group. Simplified criteria for the diagnosis of autoimmune hepatitis. *Hepatology* 2008; **48**: 169-176 [PMID: 18537184 DOI: 10.1002/hep.22322]
14 **Schlienger JL**, Faradji A, Demangeat C, Sapin R, Chabrier G, Simon C, Imler M. [Quantitative evaluation of hormonal extraction performed by continuous plasma exchange in euthyroid patients. Application to the treatment of severe hyperthyroidism]. *Presse Med* 1983; **12**: 499-502 [PMID: 6219358 DOI:

10.1007/s11837-003-0157-0]
15 **Schlienger JL**, Faradji A, Sapin R, Blickle JF, Chabrier G, Simon C, Imler M. [Treatment of severe hyperthyroidism by plasma exchange. Clinical and biological efficacy. 8 cases]. *Presse Med* 1985; **14**: 1271-1274 [PMID: 3160032]
16 **Pinsard D**, Chadenas D, Pierre D, Walle T, Aumaitre J. [Plasma exchange and hyperthyroidism. Current indications]. *Ann Endocrinol (Paris)* 1985; **46**: 89-98 [PMID: 3898988]
17 **Miljić D**, Stojanović M, Ješić R, Bogadnović G, Popović V. Role of plasma exchange in autoimmune hyperthyroidism complicated by severe tiamazol-induced cholestatic jaundice. *Transfus Apher Sci* 2013; **49**: 354-356 [PMID: 23756266 DOI: 10.1016/j.transci.2013.05.007]
18 **Keklik M**, Kaynar L, Yilmaz M, Sivgin S, Solmaz M, Pala C, Aribas S, Akyol G, Unluhizarci K, Cetin M, Eser B, Unal A. The results of therapeutic plasma exchange in patients with severe hyperthyroidism: a retrospective multicenter study. *Transfus Apher Sci* 2013; **48**: 327-330 [PMID: 23611685 DOI: 10.1016/j.transci.2013.04.010]
19 **Garla V**, Kovvuru K, Ahuja S, Palabindala V, Malhotra B, Abdul Salim S. Severe Hyperthyroidism Complicated by Agranulocytosis Treated with Therapeutic Plasma Exchange: Case Report and Review of the Literature. *Case Rep Endocrinol* 2018; **2018**: 4135940 [PMID: 29552362 DOI: 10.1155/2018/4135940]
20 **Wan YM**, Li YH, Xu ZY, Yang J, Yang LH, Xu Y, Yang JH. Therapeutic plasma exchange versus double plasma molecular absorption system in hepatitis B virus-infected acute-on-chronic liver failure treated by entercavir: A prospective study. *J Clin Apher* 2017; **32**: 453-461 [PMID: 28304106 DOI: 10.1002/jca.21535]

World Journal of Clinical Cases

Submit a Manuscript: https://www.f6publishing.com

World J Clin Cases 2019 May 26; 7(10): 1191-1199

DOI: 10.12998/wjcc.v7.i10.1191

ISSN 2307-8960 (online)

CASE REPORT

Multiple rare causes of post-traumatic elbow stiffness in an adolescent patient: A case report and review of literature

Bai-Qi Pan, Jun Huang, Jiang-Dong Ni, Ming-Ming Yan, Qin Xia

ORCID number: Bai-Qi Pan (0000-0002-3127-240X); Jun Huang (0000-0001-8714-483X); Jiang-Dong Ni (0000-0003-2725-5479); Ming-Ming Yan (0000-0001-5285-7346); Qin Xia (0000-0002-5578-9438).

Author contributions: Pan BQ performed the research and follow-up, and wrote the paper; Huang J designed the research and wrote the paper; Ni JD, Yan MM and Xia Q contributed some advice to this work.

Informed consent statement: Informed consent to publish was obtained from the patient.

Conflict-of-interest statement: All authors declare no conflict of interest for this article.

CARE Checklist (2016) statement: The authors have read the CARE Checklist (2016), and the manuscript was prepared and revised according to the CARE Checklist (2016).

Bai-Qi Pan, Jun Huang, Jiang-Dong Ni, Ming-Ming Yan, Qin Xia, Department of Orthopedics, The Second Xiangya Hospital, Central South University, Changsha 410011, Hunan Province, China

Corresponding author: Jun Huang, MD, PhD, Doctor, Department of Orthopedics, The Second Xiangya Hospital, Central South University, No. 139, Middle of Renmin Road, Changsha 410011, Hunan Province, China. 505447@csu.edu.cn
Telephone: +86-134-67699531
Fax: +86-731-85295126

Abstract

BACKGROUND

Joint stiffness after elbow surgery is not a rare complication, and is always accompanied by deformity. The causes of joint stiffness are multiple in different patients, and divided into intrinsic and extrinsic causes. Herein, we report an unusual case of posttraumatic elbow stiffness due to multiple and rare causes.

CASE SUMMARY

A 19-year-old male was hospitalized with the loss of motion of the left elbow for over ten years. Left limb computed tomography revealed left elbow stiffness with bony block and connection. The patient underwent surgery, and the etiology of joint stiffness was found to be a rare combination of common and uncommon causes. During an 18-mo follow-up period, the patient's left elbow had normal motion and he was symptom-free.

CONCLUSION

However, this case combined with multiple and rare causes highlights that the patient with scar physique is likely to be accompanied with more severe soft tissue, nerve contracture, and heterotypic ossification, even during recurrence.

Key words: Post-traumatic; Elbow stiffness; Open surgery; Contracture; Ulnar neuritis; Radial nerve; Scar; Case report

Core tip: Elbow stiffness is a well-known complication after elbow fractures/surgeries. Common causes of elbow stiffness include intra-articular adhesions, soft tissue contracture and heterotypic ossification (HO), *etc*. We report a case of post-traumatic elbow stiffness due to multiple and rare causes, including a bony connection, scar keloid

Manuscript source: Unsolicited manuscript

Received: December 26, 2018
Peer-review started: December 27, 2018
First decision: March 10, 2019
Revised: March 26, 2019
Accepted: April 19, 2019
Article in press: April 19, 2019
Published online: May 26, 2019

P-Reviewer: Ueda B
S-Editor: Dou Y
L-Editor: Filipodia
E-Editor: Wu YXJ

and abnormal radial nerve. There have been no reports regarding such factors, which made the treatment of this patient more complicated. The patient was treated successfully with surgery and had a satisfactory recovery. However, this reminds us that the patient with scar physique is more likely to be accompanied with severe soft tissue or nerve contracture, or HO, even during recurrence.

Citation: Pan BQ, Huang J, Ni JD, Yan MM, Xia Q. Multiple rare causes of post-traumatic elbow stiffness in an adolescent patient: A case report and review of literature. *World J Clin Cases* 2019; 7(10): 1191-1199
URL: https://www.wjgnet.com/2307-8960/full/v7/i10/1191.htm
DOI: https://dx.doi.org/10.12998/wjcc.v7.i10.1191

INTRODUCTION

Elbow stiffness is a common complication of elbow trauma, and it has been hypothesized that a 50% reduction in elbow range of motion (ROM) can reduce upper extremity function by as much as 80%. The most common cause of elbow stiffness is soft tissue contracture after initial injury[1,2]. The causes of elbow stiffness in the present case were rare, which included a keloid scar, high tension of the radial nerve, a bony connection and block. There are several treatment options for elbow stiffness including surgical and non-surgical. Treatment selection should be based on history, stiffness severity, complications and progression. In this report, we present a case of post-traumatic elbow stiffness in a teenager with multiple problems for over ten years, which was successfully treated by open surgery.

CASE PRESENTATION

Chief complaints

Left elbow joint extended /flexion disorder for ten years

History of present illness

Loss of motion in the left elbow was the only symptom in this adolescent patient. The patient complained of a left elbow joint with extended/flexion disorder for ten years, which was gradually found, since his left supracondylar humerus fracture was treated by open reduction and Kirschner wire internal fixation when he was nine years old (Figure 1, 2). For further diagnosis and treatment, this teenager came to our hospital clinic. With the diagnosis "left elbow joint stiffness", he was charged in our department.

History of past illness

This 19-year-old right-hand-dominant male patient fell directly on his left elbow while climbing a tree approximately ten years previously. He visited the emergency department for immediate elbow pain and swelling. Radiography showed a left supracondylar humerus fracture (Figure 1). Emergent open reduction and Kirschner wire fixation were performed (Figure 2), and plaster external fixation was applied postoperatively. The splint and Kirschner wires were removed 1 mo later (Figure 3). After surgery, the patient had severe and persistent motion restriction of the left elbow for more than ten years, without receiving any rehabilitation or further treatment due to economic reasons and a misunderstanding of the disease.

Personal and family history

There is no related family history of this patient.

Physical examination upon admission

Upon physical examination, the arc of motion of the left elbow was 35° (flexion in 105-70°) (Figure 4A, B), loss of pronation/supination was 5° and 5°, respectively.

Laboratory examinations

All the laboratory examinations are normal, including routine blood tests, routine urine tests and urinary sediment examination, routine fecal tests and occult blood tests, blood biochemistry, immune indexes, and infection indexes.

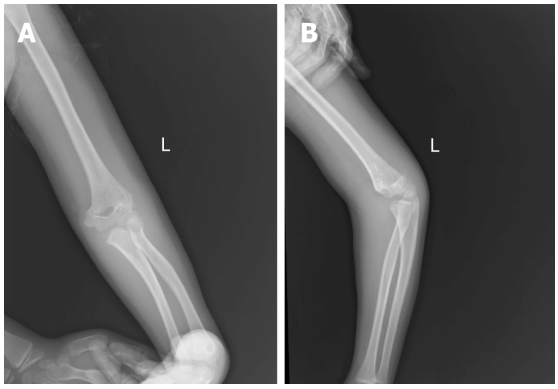

Figure 1 Radiography at the time of injury. A: Frontal x-ray of the left elbow; B: Lateral x-ray of the left elbow.

Imaging examinations

Radiography with oblique views (Figure 5A, B), computed tomography (CT) scan (Figure 5C, D) and 3-dimensional CT reconstructions were performed to evaluate the left elbow stiffness.

FINAL DIAGNOSIS

(1) Left elbow joint stiffness; (2) Scar physique.

TREATMENT

Considering the deformity caused by elbow stiffness, surgery was performed under general anesthesia. The patient was placed in the supine position with his free left arm on his chest, and a sterile tourniquet was applied. A 15 cm previous incision was present laterally, which was severely scarred around the elbow joint, measuring 4 cm × 2 cm in the widest area (Figure 6D). Following removal of all scar tissue, we decided to use the original surgical incision. We incised the deep fascia along the medial border of the brachioradialis and identified the radial nerve covered by a thin layer of fat between the brachialis and the brachioradialis, uncovering the origins of the extensor carpi radialis longus and brachioradialis along the humeral lateral ridge. When two humeral muscular origins were partially released, the anterior part of the lateral capsule was exposed and resected to reach the coronoid, and a 3 cm × 1 cm × 0.5 cm bony block in the coronoid fossa was subsequently removed (Figure 6B). As flexion of the elbow was still limited, we released the triceps from the posterior humerus to examine the posterior joint capsule. The contracted joint capsule and other fibrous tissue, including callus and scarring in the olecranon fossa, were completely removed. We performed neurolysis of the radial nerve contracture, and released the remaining soft tissue contracture and all bony blocker and muscular reconstruction. The ulnar nerve was detected and the bony connection between olecranon and dorsal humerus was removed *via* the medial incision, to then rule out ulnar nerve compression (Figure 6A). As no ulnar nerve compression was detected, anterior subcutaneous transposition of the nerve was not performed. However, after these procedures, excessive tension of the contractural radial nerve was still present when the arc flexed to 30° (Figure 6C). Following surgery, the motion arc of the elbow in flexion was 30-145° under manipulation (Figure 4C, D). The incision was closed with full hemostasis and placement of a wound drainage tube. A splint was placed on the left arm.

OUTCOME AND FOLLOW-UP

Celecoxib was prescribed for analgesia, and rehabilitation started from the first postoperative day (Figure 7). One month after surgery, the ROM in the left elbow was completely normal and the patient was pain-free, without evidence of neurological dysfunction. Histopathologic analysis of the scar demonstrated fibrous tissue with tumor-like hyperplasia and hyalinization, and evidence of malignancy was not observed (Figure 6E). Following an 18-mo follow-up, recovery was uneventful and

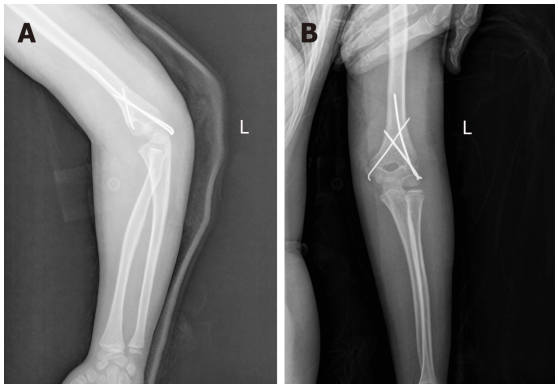

Figure 2 Radiography after the first operation. A: Lateral s-ray of the left elbow; B: TFrontal x-ray of the left elbow.

satisfactory.

DISCUSSION

Elbow stiffness is a common complication of intra-articular fracture, is a frequent disabling condition that interferes with daily activities, and typically occurs in young individuals[3,4]. The general definition of elbow stiffness is: a flexion-extension arc of < 100° and/or flexion contracture > 30°. Therefore, if the ROM is less than 30-130°, this would be an indication for surgical treatment by some authors[2,5,6].

Many causes of elbow contracture have been described, including intrinsic and extrinsic causes - soft tissue contracture, heterotypic ossification (HO), and mal-union or nonunion of a fracture, *etc*. Other conditions also play a role in the occurrence of elbow stiffness, such as long-term articular immobilization and non-rehabilitation[2]. However, our case was rare because of its complicated and special causes, including a keloid scar, high tension of the radial nerve, as well as the bony connection and block (Table 1)[1], in which we find a relationship between the elbow stiffness and scar physique.

There are several treatment options for elbow stiffness, such as open surgery, splint, and arthroscopy. Chronic stiffness is usually managed by arthroscopic or surgical release, with good results (the recovery of ROM can be at least 100°)[1,7,8]. It has also been reported that recovery of elbow stiffness in adolescents was satisfactory after surgical release. The exact intra-operative adjustment of the elbow ROM depends on the specific condition of the patient. The goal of progressive ROM is to increase this motion by lengthening and isolating tissue, not by tearing tissue. Kruse *et al*[9] reported a technique that maximized elbow ROM by combining lateral and minimal posterior triceps-splinting open elbow contracture release, and the use of a splint with the elbow at 20° of flexion and the forearm neutral at the end of the procedure, which is a safe and effective alternative[10]. However, in the present case, after removing soft tissue contracture and performing complete neurolysis of the left radial nerve surrounding the incision, we found excessive tension of the radial nerve at an elbow flexion of 30° intraoperatively (Figure 6C). No contracture or lesion/deficits were observed in the median nerve and ulnar nerve. Excessive tension of the radial nerve directly affects the surgical outcome of such patients, as this is the limiting factor in the recovery of ROM. The different conditions of these three nerves in the elbow could not be fully explained.

Many studies have correlated outcome with management of the ulnar nerve, but very few studies have reported management of the radial nerve, especially with abnormal tension[1-6,8-38] (Table 1). There are also few data in the literature on the radial nerve with excessive traction, as these patients had no neural symptoms. Cantin *et al*[11] reported their observations in a child with congenital and isolated elbow contracture in flexion who was 16 mo old. They mentioned excessive traction in elbow extension on the neurovascular structures (radial nerve and vascular humeral bundle, particularly the radial nerve), which is the limiting factor in the surgical procedure[11]. However, our patient was a teenager with chronic posttraumatic elbow stiffness. According to the structural and biochemical evaluation of the elbow capsule following trauma, disorganization of collagen fiber arrangements, altered cytokine and enzyme levels, and an elevated number of myofibroblasts may also lead to a contracture with high tension of the radial nerve after open surgery for supracondylar humerus fracture *via* a lateral incision[12-15]. Following this procedure, our patient lived

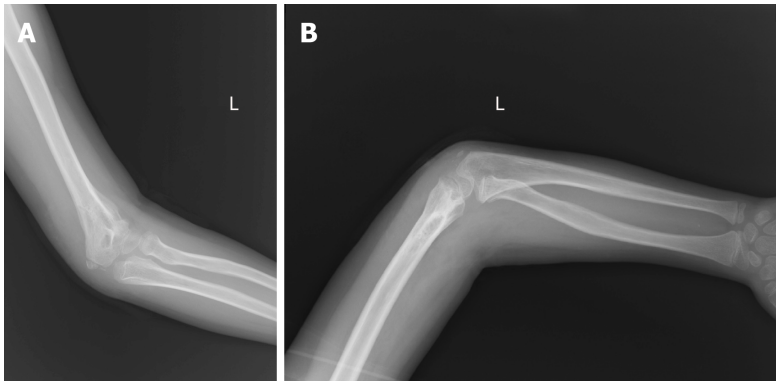

Figure 3 Radiography after removal of the Kirschner wire fixation. A: Frontal x-ray of the left elbow; B: Lateral x-ray of the left elbow.

with loss of motion of the left elbow for approximately ten years (the ROM was 70-105° from nine to 19 years of age), and the limitation of ability to distend further exacerbated the problem. Nerves may be relocated away from the influence of a possible irritating callus[16]. A special point of this patient is that the elbow stiffness lasted throughout puberty with scar physique. Thus, under such circumstances, pathological tissue changes during growth and development may lead to growth disturbance (anatomy route or length) and contracture formation in the radial nerve in his adolescent age. The contracture of a nerve and surrounding soft tissue (such as membrane) resulting in over-high tension of the radial nerve leads to limited ROM (Figure 6C). To some extent, we also consider that there may be some relationships between the contracture of nerve with the scar physique (the genetically driven fibrotic scar formation). Thus, the patient with the history of keloid scar formation may be more likely to be accompanied with more severe soft tissue and nerve contracture, causing the elbow stiffness.

Safety of the radial nerve should not be neglected when pursuing the desired recovery of ROM during treatment. When the etiology of elbow stiffness is known, in order to increase the left elbow ROM, excessive traction must be reduced. Intraoperatively, the contracture of tissues should be removed as much as possible, and complete neurolysis, athrolysis and the reconstruction of muscular stop points should be performed to reduce over-high tension[17]. Postoperatively, the remaining over-high tension of the radial nerve can be reduced by appropriate rehabilitation. Following successful surgery, an improvement in the ROM in this patient's left elbow was achieved from 70-105° to 30-145°. We placed a splint on the elbow to obtain flexion of 30° (decided based on individual situation) to protect against over-distension, which ensured that the nerves or vessels were in the safe position of normal tension to avoid injury. Rehabilitation started immediately, allowing gentle elbow ROM in the flexion extension plane without varus or valgus force[18]. Passive motion, physical therapy, splinting and anti-scaring play important roles in the postoperative protocol in such special patients[11]. The elbow ROM gradually improved in our patient with decreased motion tension.

It is inconclusive whether ulnar nerve transposition or decompression is required in such patients. Many studies have shown that it is necessary to perform transposition of the ulnar nerve intraoperatively to avoid delayed-onset ulnar neuritis and other complications[19,20]. Similarly, some studies showed that the ulnar nerve should be mobilized and retracted anteriorly[10]. However, although subcutaneous ulnar nerve transposition is performed during open arthrolysis for posttraumatic elbow stiffness, ulnar neuritis is still an important complication[21]. Ulnar neuritis is associated with deformity or abnormality of the elbow joint. The symptoms become more and more severe if there is a progressive lesion of the ulnar nerve[22]. In addition, it has been shown that transposition had a higher rate of wound complications than decompression, and it had equal preventive effects[20]. Compared with decompression, transposition may be more likely to cause iatrogenic injury resulting in entrapment, neural slippage and other complications[23]. Our patient's fracture healed well without preoperative nerve symptoms, and no lesions or adhesions were found following prophylactic ulnar nerve neurolysis[18] (Figure 6A). Also, the Grade B recommendations for care from the article of Attum *et al*[1] is that the occurrence of nerve palsy is rare. Therefore, in our opinion, in such cases there is no need for ulnar nerve transposition.

The scar contracture was on the elbow joint skin before the third surgery, which

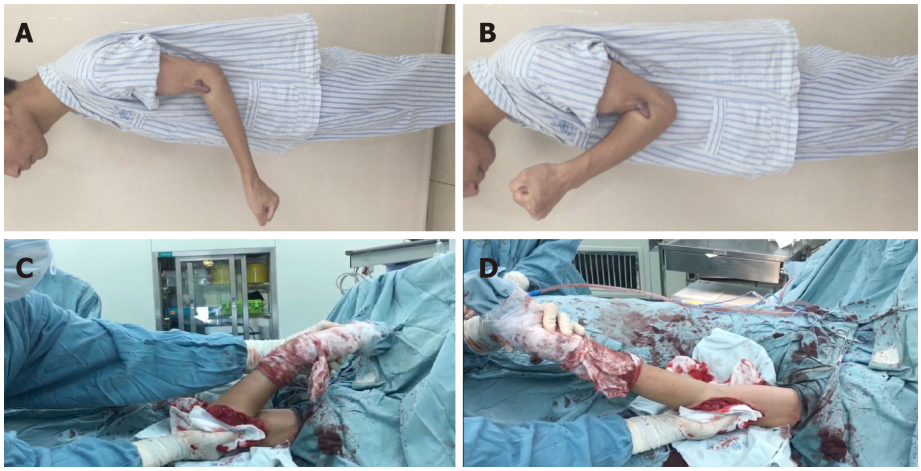

Figure 4 Pre-operative and postoperative flexion/extension range of motion of the left elbow. A: The best position of extension pre-operatively; B: The best position of flexion pre-operatively; C: The best position of flexion postoperatively; D: The best position of extension postoperatively.

severely restricted elbow function, making it difficult to perform preoperative rehabilitation to release soft tissue contracture. The scar formed approximately 2 wk after the first operation, but the reason it extended across the joint may be associated with the following: (1) The patient was fixed in the flexion position postoperatively for too long; (2) No rehabilitation was carried out; (3) The scar physique (genetically driven fibrotic scar formation)[1,24]; and (4) After the first surgery, failed pain control resulted in limited left arm motion. So, in our department, the patient was asked to take part in rehabilitation exercises as soon as possible, and anti-scarring drugs were administered to prevent the same situation from recurring. Thus, aggressive treatment and timely rehabilitation are essential in patients with scar tissue.

In this patient, the incision using the lateral approach was insufficient. The medial bony block and bony connection should be removed to achieve successful arthrolysis *via* a medial incision, which is used to probe and decompress the ulnar nerve, remove heterotopic ossification, and release the medial collateral ligament or contracted joint capsule[12]. Therefore, we recommend the medial and lateral approaches to optimize treatment outcome in patients with elbow stiffness caused by different factors[17,25].

This adolescent patient is noteworthy, due to the fact that elbow stiffness was not only caused by the intra-articular adhesions, soft tissue contracture and HO, but also by the changes in the contractural radial nerve with excessive tension, keloid scarring of the skin across the joint limiting elbow motion, and the bony block and connection, making treatment challenging. Reducing excessive tension of the radial nerve with complete neurolysis, protecting the nerves or vessels from rupture with maintenance of elbow ROM at 30° to 145° in flexion temporarily after operation, and a regular rehabilitation plan to achieve normal tension of the nerves resulting in safe and optimal elbow ROM proved to be effective in this patient.

Following successful surgery, early rigorous rehabilitation of the left elbow achieved normal activity, and after 18 mo of follow-up, recovery was uneventful and satisfactory (flexion/extension: 135-0-0 degrees for the left elbow). To our knowledge, there are no other detailed reports on such complicated causes in an adolescent patient, and further studies are needed.

CONCLUSION

Upon encountering joint trauma, the patient with a history of keloid scar formation is prone to be accompanied with more severe soft tissue, nerve contracture and even HO, as well as recurrence of joint stiffness. Although the contracture could be reversible, such elbow stiffness in a teenage patient, with rare multiple etiologies, and radial nerve contracture with over-high tension for over ten years, is a rare condition with a possible dire outcome if not managed appropriately. Clinicians should be aware of the pertinent etiology in order to determine the correct treatment option to avoid complications.

Table 1 Causes of elbow stiffness reported in the included studies

Authors	No. of patients	Causes						
		Soft tissue contracture	Bony blocker	Malunion of fracture	HO(Hetero-topic ossification)	Keloid scar	Bony connection	Nerve contracture
Koh *et al*[24]	77	Yes	Yes	Yes	Yes	No	No	No
Ring *et al*[26]	46	Yes	Yes	Yes	Yes	No	No	No
Morrey *et al*[27]	38	Yes	Yes	Yes	Yes	No	No	No
Birjandi Nejad *et al*[28]	14	Yes	Yes	Yes	Yes	No	No	No
Rhee *et al*[29]	18	Yes	Yes	Yes	Yes	No	No	No
Sharma and Rymaswski[30]	25	Yes	Yes	Yes	Yes	No	No	No
Tan *et al*[31]	52	Yes	Yes	Yes	Yes	No	No	No
Aldridge *et al*[32]	106	Yes	Yes	Yes	Yes	No	No	No
Cikes *et al*[33]	18	Yes	Yes	Yes	Yes	No	No	No
Marti *et al*[34]	46	Yes	Yes	Yes	Yes	No	No	No
Gundlach and Eygendaal[35]	21	Yes	Yes	Yes	Yes	No	No	No
Mansat and Morrey[25]	38	Yes	Yes	Yes	Yes	No	No	No
Kulkarni *et al*[36]	26	Yes	Yes	Yes	Yes	No	No	No
Heirweg and De Smet[37]	16	Yes	Yes	Yes	Yes	No	No	No
Park *et al*[38]	27	Yes	Yes	Yes	Yes	No	No	No
Cantin *et al*[11]	1	Yes	No	No	No	No	No	Yes

Figure 5 Pre-operative radiograph and representative axillary computed tomography image. A: Frontal x-ray of the left elbow, with the arrow pointing to the bone connection; B: Lateral x-ray of the left elbow; C: CT scan of the cross section; D: CT coronal scan, with the arrow pointing to the bony block of the humerus coronoid fossa. CT: Computed tomography.

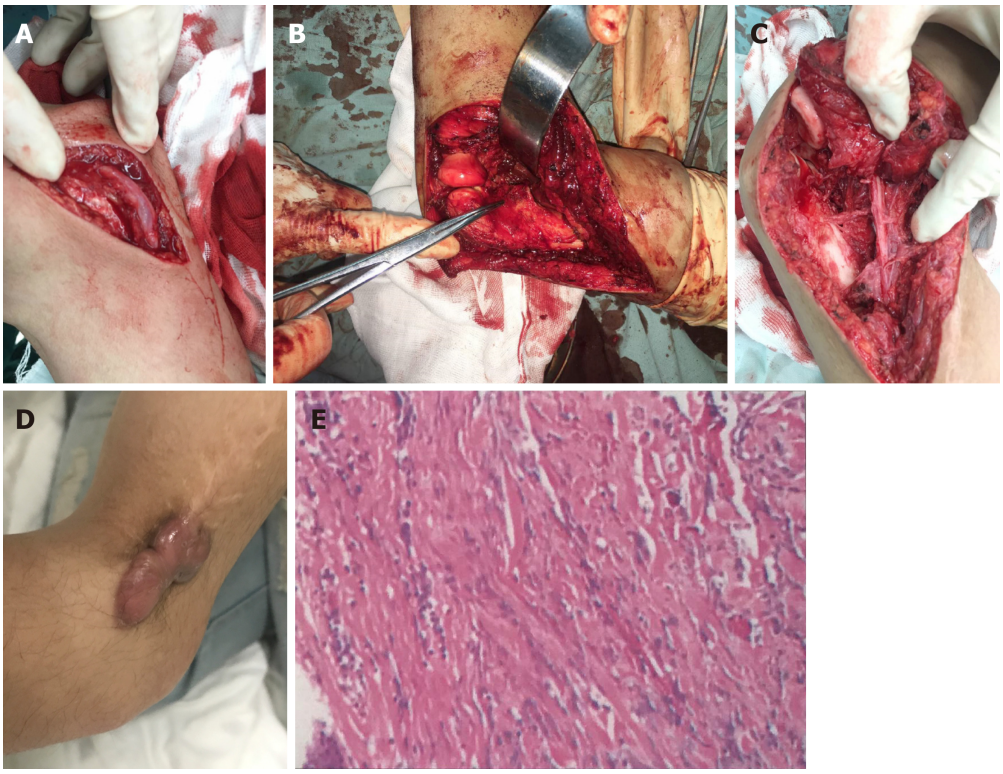

Figure 6 Detailed images of our surgery. A: Intact ulnar nerve; B: Bony block of the humerus coronoid fossa; C: Radial nerve contracture; D: Scar of skin; E: Pathological section of the scar.

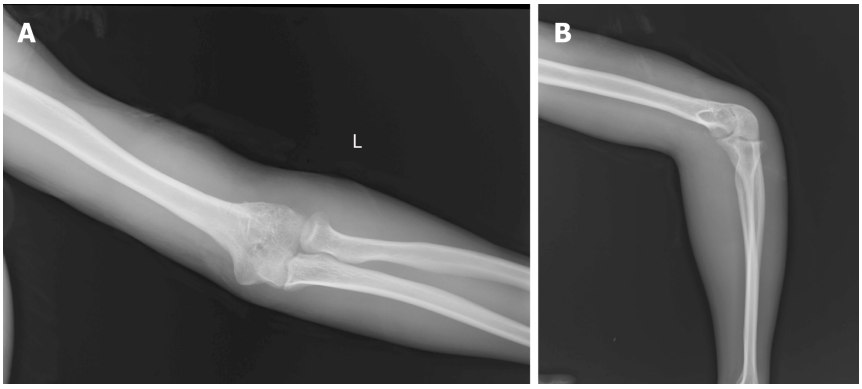

Figure 7 Radiography after the third operation. A: Frontal x-ray of the left elbow; B: Lateral x-ray of the left elbow.

REFERENCES

1 **Attum B**, Obremskey W. Posttraumatic Elbow Stiffness: A Critical Analysis Review. *JBJS Rev* 2016; 4 [PMID: 27760073 DOI: 10.2106/JBJS.RVW.15.00084]

2 **Lindenhovius AL**, Jupiter JB. The posttraumatic stiff elbow: a review of the literature. *J Hand Surg Am* 2007; **32**: 1605-1623 [PMID: 18070653 DOI: 10.1016/j.jhsa.2007.09.015]

3 **Edelson G**, Ganayem M, Obid E. A novel surgical approach to post-traumatic elbow stiffness: case report and operative technique. *J Shoulder Elbow Surg* 2006; **15**: e37-e40 [PMID: 17126235 DOI: 10.1016/j.jse.2005.10.017]

4 **Zheng W**, Song J, Sun Z, Liu J, Chen S, Fan C. Effect of disease duration on functional outcomes and complications after arthrolysis in patients with elbow stiffness. *J Shoulder Elbow Surg* 2018; **27**: 381-386 [PMID: 29310915 DOI: 10.1016/j.jse.2017.11.012]

5 **Cefo I**, Eygendaal D. Arthroscopic arthrolysis for posttraumatic elbow stiffness. *J Shoulder Elbow Surg* 2011; **20**: 434-439 [PMID: 21397792 DOI: 10.1016/j.jse.2010.11.018]

6 **Kodde IF**, van Rijn J, van den Bekerom MP, Eygendaal D. Surgical treatment of post-traumatic elbow stiffness: a systematic review. *J Shoulder Elbow Surg* 2013; **22**: 574-580 [PMID: 23375881 DOI: 10.1016/j.jse.2012.11.010]

7 **Darlis NA**, Kaufmann RW, Sotereanos DG. Open surgical treatment of post-traumatic elbow contractures in adolescent patients. *J Shoulder Elbow Surg* 2006; **15**: 709-715 [PMID: 17126243 DOI: 10.1016/j.jse.2006.01.006]

8 **Mansat P**, Morrey BF. Semiconstrained total elbow arthroplasty for ankylosed and stiff elbows. *J Bone Joint Surg Am* 2000; **82**: 1260-1268 [PMID: 11005517 DOI: 10.2106/00004623-200009000-00006]
9 **Kruse KK**, Papatheodorou LK, Weiser RW, Sotereanos DG. Release of the stiff elbow with mini-open technique. *J Shoulder Elbow Surg* 2016; **25**: 355-361 [PMID: 26927431 DOI: 10.1016/j.jse.2015.10.025]
10 **Strauss NL**, Lattanza L. Open surgical treatment of posttraumatic elbow contractures in children. *Tech Hand Up Extrem Surg* 2010; **14**: 108-113 [PMID: 20526165 DOI: 10.1097/BTH.0b013e3181e2d3bb]
11 **Cantin O**, Mezzadri G, Gazarian A, Abelin-Genevois K, Kohler R, Bérard J, Chotel F. Early surgical anterior release for congenital and isolated elbow contracture in flexion: a case report of a 16-month-old child. *Orthop Traumatol Surg Res* 2012; **98**: 465-469 [PMID: 22583894 DOI: 10.1016/j.otsr.2012.02.002]
12 **Mellema JJ**, Lindenhovius AL, Jupiter JB. The posttraumatic stiff elbow: an update. *Curr Rev Musculoskelet Med* 2016; **9**: 190-198 [PMID: 26984466 DOI: 10.1007/s12178-016-9336-9]
13 **Cohen MS**, Schimmel DR, Masuda K, Hastings H 2nd, Muehleman C. Structural and biochemical evaluation of the elbow capsule after trauma. *J Shoulder Elbow Surg* 2007; **16**: 484-490 [PMID: 17368926 DOI: 10.1016/j.jse.2006.06.018]
14 **Hildebrand KA**, Zhang M, Hart DA. High rate of joint capsule matrix turnover in chronic human elbow contractures. *Clin Orthop Relat Res* 2005; **439**: 228-234 [PMID: 16205164 DOI: 10.1097/01.blo.0000177718.78028.5c]
15 **Hildebrand KA**, Zhang M, van Snellenberg W, King GJ, Hart DA. Myofibroblast numbers are elevated in human elbow capsules after trauma. *Clin Orthop Relat Res* 2004; 189-197 [PMID: 15021153]
16 **Adams JE**, Steinmann SP. Nerve injuries about the elbow. *J Hand Surg Am* 2006; **31**: 303-313 [PMID: 16473695 DOI: 10.1016/j.jhsa.2005.12.006]
17 **Dávila SA**, Johnston-Jones K. Managing the stiff elbow: operative, nonoperative, and postoperative techniques. *J Hand Ther* 2006; **19**: 268-281 [PMID: 16713873 DOI: 10.1197/j.jht.2006.02.017]
18 **Haglin JM**, Kugelman DN, Christiano A, Konda SR, Paksima N, Egol KA. Open surgical elbow contracture release after trauma: results and recommendations. *J Shoulder Elbow Surg* 2018; **27**: 418-426 [PMID: 29290605 DOI: 10.1016/j.jse.2017.10.023]
19 **Shuai C**, Hede Y, Shen L, Yuanming O, Hongjiang R, Cunyi F. Is routine ulnar nerve transposition necessary in open release of stiff elbows? Our experience and a literature review. *Int Orthop* 2014; **38**: 2289-2294 [PMID: 25082178 DOI: 10.1007/s00264-014-2465-0]
20 **Blonna D**, O'Driscoll SW. Delayed-onset ulnar neuritis after release of elbow contracture: preventive strategies derived from a study of 563 cases. *Arthroscopy* 2014; **30**: 947-956 [PMID: 24974167 DOI: 10.1016/j.arthro.2014.03.022]
21 **Cai J**, Zhou Y, Chen S, Sun Y, Yuanming O, Ruan H, Fan C. Ulnar neuritis after open elbow arthrolysis combined with ulnar nerve subcutaneous transposition for post-traumatic elbow stiffness: outcome and risk factors. *J Shoulder Elbow Surg* 2016; **25**: 1027-1033 [PMID: 27039670 DOI: 10.1016/j.jse.2016.01.013]
22 **OSBORNE G**. Ulnar neuritis. *Postgrad Med J* 1959; **35**: 392-396 [PMID: 14429192 DOI: 10.1136/pgmj.35.405.392]
23 **Zhong W**, Zhang W, Zheng X, Li S, Shi J. Comparative study of different surgical transposition methods for ulnar nerve entrapment at the elbow. *J Int Med Res* 2011; **39**: 1766-1772 [PMID: 22117977 DOI: 10.1177/147323001103900519]
24 **Koh KH**, Lim TK, Lee HI, Park MJ. Surgical treatment of elbow stiffness caused by post-traumatic heterotopic ossification. *J Shoulder Elbow Surg* 2013; **22**: 1128-1134 [PMID: 23796381 DOI: 10.1016/j.jse.2013.04.019]
25 **Mansat P**, Morrey BF. The column procedure: a limited lateral approach for extrinsic contracture of the elbow. *J Bone Joint Surg Am* 1998; **80**: 1603-1615 [PMID: 9840628 DOI: 10.2106/00004623-199811000-00006]
26 **Ring D**, Adey L, Zurakowski D, Jupiter JB. Elbow capsulectomy for posttraumatic elbow stiffness. *J Hand Surg Am* 2006; **31**: 1264-1271 [PMID: 17027785 DOI: 10.1016/j.jhsa.2006.06.009]
27 **Morrey BF**. Surgical treatment of extraarticular elbow contracture. *Clin Orthop Relat Res* 2000; 57-64 [PMID: 10660702 DOI: 10.1097/00003086-200001000-00007]
28 **Birjandi Nejad A**, Ebrahimzadeh MH, Moradi A. Clinical outcomes after posterior open elbow arthrolysis for posttraumatic elbow stiffness. *Arch Trauma Res* 2014; **3**: e21742 [PMID: 25599069 DOI: 10.5812/atr.21742]
29 **Rhee YG**, Cho NS, Lim CT, Yi JW. Debridement arthroplasty for post-traumatic stiff elbow: intraoperative factors affecting the clinical results of surgical treatment. *Clin Orthop Surg* 2009; **1**: 27-33 [PMID: 19884994 DOI: 10.4055/cios.2009.1.1.27]
30 **Sharma S**, Rymaszewski LA. Open arthrolysis for post-traumatic stiffness of the elbow: results are durable over the medium term. *J Bone Joint Surg Br* 2007; **89**: 778-781 [PMID: 17613503 DOI: 10.1302/0301-620X.89B6.18772]
31 **Tan V**, Daluiski A, Simic P, Hotchkiss RN. Outcome of open release for post-traumatic elbow stiffness. *J Trauma* 2006; **61**: 673-678 [PMID: 16967006 DOI: 10.1097/01.ta.0000196000.96056.51]
32 **Aldridge JM**, Atkins TA, Gunneson EE, Urbaniak JR. Anterior release of the elbow for extension loss. *J Bone Joint Surg Am* 2004; **86-A**: 1955-1960 [PMID: 15342758 DOI: 10.2106/00004623-200409000-00014]
33 **Cikes A**, Jolles BM, Farron A. Open elbow arthrolysis for posttraumatic elbow stiffness. *J Orthop Trauma* 2006; **20**: 405-409 [PMID: 16825966 DOI: 10.1097/00005131-200607000-00007]
34 **Marti RK**, Kerkhoffs GM, Maas M, Blankevoort L. Progressive surgical release of a posttraumatic stiff elbow. Technique and outcome after 2-18 years in 46 patients. *Acta Orthop Scand* 2002; **73**: 144-150 [PMID: 12079010 DOI: 10.1080/000164702753671713]
35 **Gundlach U**, Eygendaal D. Surgical treatment of posttraumatic stiffness of the elbow: 2-year outcome in 21 patients after a column procedure. *Acta Orthop* 2008; **79**: 74-77 [PMID: 18283576 DOI: 10.1080/17453670710014798]
36 **Kulkarni GS**, Kulkarni VS, Shyam AK, Kulkarni RM, Kulkarni MG, Nayak P. Management of severe extra-articular contracture of the elbow by open arthrolysis and a monolateral hinged external fixator. *J Bone Joint Surg Br* 2010; **92**: 92-97 [PMID: 20044685 DOI: 10.1302/0301-620X.92B1.22241]
37 **Heirweg S**, De Smet L. Operative treatment of elbow stiffness: evaluation and outcome. *Acta Orthop Belg* 2003; **69**: 18-22 [PMID: 12666286]
38 **Park MJ**, Kim HG, Lee JY. Surgical treatment of post-traumatic stiffness of the elbow. *J Bone Joint Surg Br* 2004; **86**: 1158-1162 [PMID: 15568530 DOI: 10.1302/0301-620X.86B8.14962]

World Journal of Clinical Cases

Submit a Manuscript: https://www.f6publishing.com

World J Clin Cases 2019 May 26; 7(10): 1200-1205

DOI: 10.12998/wjcc.v7.i10.1200

ISSN 2307-8960 (online)

CASE REPORT

Liquorice-induced severe hypokalemic rhabdomyolysis with Gitelman syndrome and diabetes: A case report

Lu-Yang Yang, Jin-Hua Yin, Jing Yang, Yi Ren, Chen-Yu Xiang, Chun-Yan Wang

ORCID number: Lu-Yang Yang (0000-0002-1637-4002); Jin-Hua Yin (0000-0002-5495-995X); Jing Yang (0000-0001-8855-6254); Yi Ren (0000-0002-1163-3642); Chen-Yu Xiang (0000-0002-4555-3501); Chun-Yan Wang (0000-0003-2101-7461).

Author contributions: All authors contributed to this paper.

Supported by the Fund Program for Scientific Activities of Selected Returned Overseas Professionals in Shanxi Province, No. 2017-397.

Informed consent statement: The patient provided written informed consent to the publication of this case report.

Conflict-of-interest statement: The authors declare that they have no conflicts of interest.

CARE Checklist (2016) statement: The authors have read the CARE Checklist (2016), and the manuscript was prepared and revised according to the CARE Checklist (2016).

Lu-Yang Yang, Jing Yang, Chen-Yu Xiang, Chun-Yan Wang, Department of Endocrinology, First Hospital of Shanxi Medical University, Taiyuan 030001, Shanxi Province, China

Jin-Hua Yin, Yi Ren, Department of Endocrinology, First Hospital of Shanxi Medical University, Shanxi Medical University, Taiyuan 030001, Shanxi Province, China

Corresponding author: Jin-Hua Yin, MD, Assistant Professor, Department of Endocrinology, First Hospital of Shanxi Medical University, Shanxi Medical University, No. 85, South Jiefang Road, Taiyuan 030001, Shanxi Province, China. yinjjhh@163.com
Telephone: +86-351-4639756
Fax: +86-351-4639758

Abstract

BACKGROUND

Licorice-induced severe hypokalemic rhabdomyolysis is clinically rare. Gitelman syndrome (GS) is the most common inherited renal tubular disease, while diabetes is one of the most prevalent diseases in the world. Recently, some studies have found that GS patients had higher diabetic morbidity. However, the coexistence of these three diseases has yet to be reported.

CASE SUMMARY

We report the case of a 62-year-old Chinese man who was admitted with weakness in the extremities, muscle pain, and dark-colored urine. He had consumed liquorice water daily for seven days prior to admission. The laboratory tests revealed a serum potassium level of 1.84 mmol/L, magnesium 0.68 mmol/L, creatinine phosphokinase (CK) 10117 IU/L, and marked hemoglobinuria. Fractional chloride excretion and fractional magnesium excretion were increased. Plasma renin activity and aldosterone concentration were within the normal ranges. Sequence analysis of the *SLC12A3* gene revealed that he had compound heterozygous mutations. The diagnosis of liquorice-induced severe hypokalemic rhabdomyolysis with GS and diabetes was thus genetically confirmed. Serum potassium and CK quickly improved with potassium replacement therapy, hydration, and discontinuation of liquorice ingestion. Upon follow-up at 3 mo, the levels of CK, myoglobin, and potassium remained normal, and magnesium was above 0.6 mmol/L.

CONCLUSION

This case emphasizes that liquorice consumption and GS should be considered causes of hypokalemia and that the diabetic status of GS patients should be noted in the clinic.

Manuscript source: Unsolicited manuscript

Received: January 30, 2019
Peer-review started: January 31, 2019
First decision: April 18, 2019
Revised: April 25, 2019
Accepted: May 2, 2019
Article in press: May 2, 2019
Published online: May 26, 2019

P-Reviewer: Chen GX, Dabla PK
S-Editor: Ji FF
L-Editor: Wang TQ
E-Editor: Wu YXJ

Key words: Hypokalemia; Rhabdomyolysis; Liquorice; Gitelman syndrome; Diabetes; Case report

Core tip: This is the first reported case of liquorice-induced severe hypokalemic rhabdomyolysis with Gitelman syndrome and diabetes.

Citation: Yang LY, Yin JH, Yang J, Ren Y, Xiang CY, Wang CY. Liquorice-induced severe hypokalemic rhabdomyolysis with Gitelman syndrome and diabetes: A case report. *World J Clin Cases* 2019; 7(10): 1200-1205
URL: https://www.wjgnet.com/2307-8960/full/v7/i10/1200.htm
DOI: https://dx.doi.org/10.12998/wjcc.v7.i10.1200

INTRODUCTION

Rhabdomyolysis is a relatively rare but potentially lethal condition. Hypokalemia is a common electrolyte disorder and an established cause of rhabdomyolysis[1]. Frequent causes of hypokalemia are intestinal and urinary potassium loss through diarrhea or the use of diuretics. Liquorice-induced pseudo-hyperaldosteronism and Gitelman syndrome (GS) are well known but rare causes of hypokalemia. GS is an autosomal recessive disorder, which was first described by Gitelman, Graham, and Welt[2] in 1966. Symptoms of liquorice-induced hypokalemia and GS are usually mild. However, GS combined with liquorice-induced pseudo-hyperaldosteronism may cause weakness followed by paralysis, and even rhabdomyolysis or ventricular fibrillation, which can be deadly if left untreated. Furthermore, hypokalemia and hypomagnesemia in GS patients may cause abnormal glucose metabolism[3]. Here, we report the first case of liquorice-induced severe hypokalemic rhabdomyolysis with GS and diabetes.

CASE PRESENTATION

Chief complaints

A 62-year-old Chinese man complained of intermittent weakness in the extremities (particularly the calves), muscle pain, and walking difficulty.

History of present illness

The patient's weakness in the extremities started 30 years ago, but spontaneously recovered in one week after each instance. Twenty years ago, he was admitted to the hospital because of difficulty walking upstairs and a diagnosis of hypokalemia was made. The patient's symptoms quickly improved with potassium replacement therapy. Despite any medicine treatment, his serum potassium levels ranged from 2.8 to 3.1 mmol/L in the past 10 years. The patient presented with muscle pain and walking difficulty 15 d ago. He took potassium chloride sustained-release tablets 1.5 g per day for 5 d. Furthermore, he described dark-colored urine for 3 days. Thus, the patient was sent to the hospital for further evaluation. There was no history of diarrhea or vomiting, signs of infection or alcohol intoxication. He denied ever taking any statins. Upon further questioning, a detailed history revealed that he had consumed liquorice water daily for 7 days preceding admission.

History of past illness

The past medical history revealed only type 2 diabetes mellitus since the age of 52. For that reason, he was treated with 10 mg of dapagliflozin and 25 mg of alogliptin daily.

Personal and family history

The patient denied tobacco, alcohol, and illicit drug use. His family history was unremarkable, and there were no similar cases in his family.

Physical examination upon admission

On admission, the patient's body weight was 60.0 kg, and his height was 168.2 cm. His blood pressure was 128/92 mmHg and his pulse rate was 86 beats/min. There

was generalized paralysis in all four limbs (power grade 3/5). There was no sensory deficit. The examination of the thyroid and other systems was unremarkable.

Laboratory examinations

Table 1 shows laboratory data of the patient. Serum potassium level was 1.84 mmol/L. Serum magnesium was 0.68 mmol/L. Creatinine phosphokinase (CK) was 10117 IU/L, and he had marked hemoglobinuria. Fractional chloride excretion and fractional magnesium excretion were calculated as 1.9% and 4.4%, respectively. Urinary calcium/creatinine ratio was calculated as 0.24. Plasma renin activity and aldosterone concentration were within the normal ranges. Serum alkaline phosphatase and parathormone levels were normal. According to the laboratory tests, the level of CK at presentation was 30 times more than the upper limit of the normal range. Furthermore, the level of serum myoglobin (MYO) was significantly increased. Consequently, rhabdomyolysis was diagnosed.

Rhabdomyolysis can have various causes, such as metabolic disease, direct trauma to muscle, muscle necrosis due to ischemia, muscle inflammation, or exposure to drugs and toxins[2]. Recent studies suggest that liquorice can induce hypokalemia and muscle weakness and can even lead to life-threatening rhabdomyolysis[4]. However, considering the medical history, the patient had a history of hypokalemia for 30 years. Moreover, considering the results of the laboratory tests including hypomagnesemia, normal plasma renin activity, and aldosterone concentration, the etiology of pre-existing hypokalemia should be considered. With informed consent, we investigated the *SLC12A3* gene of the patient. Sequence analysis of the *SLC12A3* gene of the patient revealed that he had compound heterozygous mutations. One missense mutation was a heterozygous G to A base pair substitution at position 1567 in exon 12, which caused an Ala to Thr substitution at position 523. A second missense mutation, a heterozygous G to A base pair substitution at position 2542 in exon 21, causing an Asp to Asn substitution at position 848, was also present (Figure 1).

Imaging examinations

The 12-lead electrocardiogram (ECG) demonstrated a sinus rhythm with inverted T-waves on leads V1-V6 and ST-depression on leads V4-V6, but no prolongation of the QTc interval and U waves. Abdominal sonography did not reveal renal stones or nephrocalcinosis. Peripheral neuropathy in both lower limbs was found by examining the electromyogram. Muscle biopsy was rejected by the patient.

FINAL DIAGNOSIS

Liquorice-induced severe hypokalemic rhabdomyolysis with GS syndrome and diabetes.

TREATMENT

The patient's signs and symptoms improved with potassium replacement therapy (10 g of potassium chloride injection daily), hydration, and discontinuation of liquorice ingestion. His serum potassium was increased to normal within 5 days. Correspondingly, CK decreased to normal within 8 days. Moreover, the ECG returned to normal on the third hospital day. Five weeks later, the patient was started on antisterone (20 mg, po, bid) and potassium magnesium aspartate tablets (2 tablets, po, tid), following the *SLC12A3* gene results.

OUTCOME AND FOLLOW-UP

Upon follow-up at 3 mo, the levels of CK, MYO, and potassium remained normal and magnesium was above 0.6 mmol/L.

DISCUSSION

Liquorice is the root of *Glycyrrhiza glabra* and is mostly recognized as a flavoring agent. It has also been used in herbal medicine and even in anti-inflammatory, antiviral, antimicrobial, antioxidative, hepatoprotective, and cardioprotective properties[5]. Glycyrrhizic acid or its hydrolytic product, glycyrrhetinic acid, is found in liquorice extracts and has a well-known mineralcorticoid activity, inhibiting 11

Table 1 Laboratory investigations of the patient

Parameter	Test value before treatments	Test value after treatments	Reference range
Potassium (mmol/L)	1.84[1]	4.05	3.5-5.5
Sodium (mmol/L)	144	138	137-147
Chlorine (mmol/L)	98[1]	99	99-110
Calcium (mmol/L)	2.31	2.14	2.11-2.52
Magnesium (mmol/L)	0.68[1]	0.78	0.75-1.02
CK (U/L)	10117[1]	275	50-310
Myoglobin(μg/L)	>4150[1]	98.4	17.4-105.7
HbA1c (%)	7.03%[1]	-	4.8-5.9 %
8 am cortisol (nmol/L)	423.5	-	171-536
4 pm cortisol (nmol/L)	183.7	-	64-327
0 am cortisol (nmol/L)	279.1	-	-
ACTH (pmol/L)	4.76	-	1.6-13.9
pH	7.47[1]	7.40	7.35-7.45
HCO_3^- (mmol/L)	32[1]	24	21-26
BE (mmol/L)	7.1[1]	2.4	-3-3
Urinary pH	8.0[1]	6.0	5-6
Urinary sodium (mmol/24 h)	240[1]	-	40-220
Urinary potassium (mmol/24 h)	109[1]	-	25-125
Urinary chloride (mmol/24 h)	260[1]	-	110-250
Urinary calcium (mmol/24 h)	2.0[1]	-	2.5-7.5
Urinary magnesium (mmol/24 h)	4	-	3.0-4.5
Urinary free cortisol (mmol/24 h)	379.68[1]	-	100-379
FE_{Cl}	1.9%[1]	-	-
FE_{Mg}	4.4%[1]	-	-
Urinary calcium/creatinine	0.24	-	-

[1]Abnormal values. FECl: Fractional chloride excretion; FEMg: Fractional magnesium excretion; ACTH: Adrenocorticotropic hormone; CK: Creatinine phosphokinase; HbA1c: Haemoglobin A1c.

beta-hydroxysteroid dehydrogenase type 2, the enzyme that converts cortisol to cortisone[4]. Glycyrrhizic acid can also directly bind to the mineralocorticoid receptor or suppress 5-β-reductase activity and can therefore slow down the hepatic metabolism of aldosterone, resulting in pseudo-hyperaldosteronism and suppression of plasma renin activity, which manifests as hypokalemia, hypertension, and metabolic alkalosis[6]. The onset and severity of the symptoms depend on the dose and duration of liquorice intake, as well as individual susceptibility[7]. GS is characterized by hypokalemia, hypomagnesemia, metabolic alkalosis, and hypocalciuria, with secondary renin-angiotensin-aldosterone system (RAAS) activation and normal blood pressure[8]. With an incidence of 1 in 40000, GS is one of the prevalent autosomal recessive diseases[9]. The *SLC12A3* gene is located on chromosome 16 and comprises 26 exons. Liu *et al*[10] analyzed the characteristics of the genotype and phenotype in 67 patients with GS. They found that compound heterozygous mutations were detected in 42 (62.7%) patients, 10 (14.9%) patients carried homozygous mutations, and 11 patients had only one heterozygous mutation. Of note, there were four patients who had three different mutations, while three unrelated (5.7%) families were found to have triple *SLC12A3* mutant alleles[10]. Mutations in the *SLC12A3* gene encoding the thiazide sensitive Na^+Cl^- cotransporter (NCCT) on the apical membrane of distal convoluted tubule cells are usually responsible for GS. Until now, more than 180 mutations in the *SLC12A3* gene have been identified in patients with GS[11]. Impaired NCCT function leads to decreased Na^+ and Cl^- reabsorption in the distal convoluted tubule. Secondary hyperaldosteronism results in renal potassium wasting[12]. Both mutations in this case have been previously reported[13,14]. Unfortunately, the patient's father was not currently alive. Only his asymptomatic mother was alive; thus, his carrier status could not be ascertained. There were no other family members who underwent genetic testing. This is a deficiency of our case.

Based on the above metabolic pathways, the hypokalemia, rhabdomyolysis, increased cortisol, and normal RAAS level in our case can be explained. In the past 5

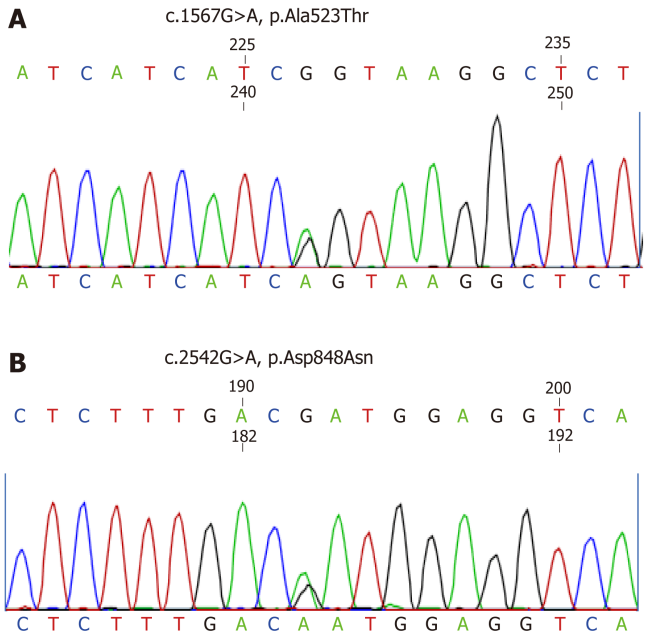

Figure 1 Partial electropherograms from exon 10 and exon 21 of the *SLC12A3* gene showing two heterozygous missense mutations in the patient. A and B: One is from G to A at nucleotide position 1567 [NM_000339, c.1567G>A; p.Ala523Thr] (A), and the other is from G to A at nucleotide position 2542 [NM_000339, c.2542G>A; p.Asp523Asn] (B).

years, abnormal glucose metabolism and insulin secretion have been reported in GS patients[11]. Liu's study indicated that compared with normal Chinese adults, GS patients had a higher diabetic morbidity[10]. Hypokalemia and hypomagnesemia were thought to be the main reasons for diabetes in GS patients. However, the exact mechanism has not been well understood until recently. The pancreatic release of insulin is controlled by ATP-sensitive potassium channels and L-type calcium channels on the β cell surface. Hypokalemia may prevent the closure of these channels and consequently prevent glucose-stimulated insulin secretion[4]. It is thought that chronic hypomagnesemia may induce altered cellular glucose transport, reduce pancreatic insulin secretion, increase defective post receptor insulin signaling, and alter insulin-insulin receptor interactions[15]. Furthermore, secondary RAAS activation may lead to insulin resistance[16]. However, a study[3] in 2017 showed that glucose metabolism and insulin secretion were impaired in GS patients, but insulin sensitivity was comparable between GS patients and patients with type 2 diabetes mellitus. Therefore, further studies are required to address this question.

CONCLUSION

In conclusion, hypokalemic rhabdomyolysis is often under-recognized and can be associated with life-threatening sequelae. Vigilance and prompt treatment are crucial to improve clinical outcomes. From this case, we would like to stress the importance for physicians to keep liquorice consumption and GS in mind as a cause for hypokalemia. We suggest that genetic analysis is advisable to determine whether the suspicion of GS is warranted. At the same time, the diabetic status of GS patients should be considered.

REFERENCES

1 **Pecnik P**, Müller P, Vrabel S, Windpessl M. Two cases of hypokalaemic rhabdomyolysis: same but different. *BMJ Case Rep* 2018; **2018**: pii: bcr-2017-223609 [PMID: 29572370 DOI: 10.1136/bcr-2017-223609]
2 **Kumagai H**, Matsumoto S, Nozu K. Hypokalemic rhabdomyolysis in a child with Gitelman's syndrome. *Pediatr Nephrol* 2010; **25**: 953-955 [PMID: 20072789 DOI: 10.1007/s00467-009-1412-6]
3 **Yuan T**, Jiang L, Chen C, Peng X, Nie M, Li X, Xing X, Li X, Chen L. Glucose tolerance and insulin responsiveness in Gitelman syndrome patients. *Endocr Connect* 2017; **6**: 243-252 [PMID: 28432081 DOI: 10.1530/EC-17-0014]
4 **He R**, Guo WJ, She F, Miao GB, Liu F, Xue YJ, Liu YW, Wang HT, Zhang P. A rare case of

hypokalemia-induced rhabdomyolysis. *J Geriatr Cardiol* 2018; **15**: 321-324 [PMID: 29915623 DOI: 10.11909/j.issn.1671-5411.2018.04.005]
5 **de Putter R**, Donck J. Low-dose liquorice ingestion resulting in severe hypokalaemic paraparesis, rhabdomyolysis and nephrogenic diabetes insipidus. *Clin Kidney J* 2014; **7**: 73-75 [PMID: 25859357 DOI: 10.1093/ckj/sft159]
6 **Omar HR**, Komarova I, El-Ghonemi M, Fathy A, Rashad R, Abdelmalak HD, Yerramadha MR, Ali Y, Helal E, Camporesi EM. Licorice abuse: time to send a warning message. *Ther Adv Endocrinol Metab* 2012; **3**: 125-138 [PMID: 23185686 DOI: 10.1177/2042018812454322]
7 **van den Bosch AE**, van der Klooster JM, Zuidgeest DM, Ouwendijk RJ, Dees A. Severe hypokalaemic paralysis and rhabdomyolysis due to ingestion of liquorice. *Neth J Med* 2005; **63**: 146-148 [PMID: 15869043 DOI: 10.1089/jwh.2005.14.263]
8 **Biagioni M**, Marigliano M, Iannilli A, Cester A, Gatti S, D'Alba I, Tedeschi S, Syren ML, Cherubini V. Diabetic ketoacidosis complicated with previously unknown Gitelman syndrome in a Tunisian child. *Diabetes Care* 2011; **34**: e107 [PMID: 21617100 DOI: 10.2337/dc11-0127]
9 **Khan J**. Poster 105 Chronic Leg Weakness Complicated by Rhabdomyolysis as a Result of Gitelman Syndrome: A Case Report. *PM R* 2016; **8**: S196 [PMID: 27672873 DOI: 10.1016/j.pmrj.2016.07.148]
10 **Liu T**, Wang C, Lu J, Zhao X, Lang Y, Shao L. Genotype/Phenotype Analysis in 67 Chinese Patients with Gitelman's Syndrome. *Am J Nephrol* 2016; **44**: 159-168 [PMID: 27529443 DOI: 10.1159/000448694]
11 **Ren H**, Qin L, Wang W, Ma J, Zhang W, Shen PY, Shi H, Li X, Chen N. Abnormal glucose metabolism and insulin sensitivity in Chinese patients with Gitelman syndrome. *Am J Nephrol* 2013; **37**: 152-157 [PMID: 23392128 DOI: 10.1159/000346708]
12 **Akinci B**, Celik A, Saygili F, Yesil S. A case of Gitelman's syndrome presenting with extreme hypokalaemia and paralysis. *Exp Clin Endocrinol Diabetes* 2009; **117**: 69-71 [PMID: 18523931 DOI: 10.1055/s-2008-1078705]
13 **Jang HR**, Lee JW, Oh YK, Na KY, Joo KW, Jeon US, Cheong HI, Kim J, Han JS. From bench to bedside: diagnosis of Gitelman's syndrome -- defect of sodium-chloride cotransporter in renal tissue. *Kidney Int* 2006; **70**: 813-817 [PMID: 16837915 DOI: 10.1038/sj.ki.5001694]
14 **Riveira-Munoz E**, Chang Q, Godefroid N, Hoenderop JG, Bindels RJ, Dahan K, Devuyst O; Belgian Network for Study of Gitelman Syndrome. Transcriptional and functional analyses of SLC12A3 mutations: new clues for the pathogenesis of Gitelman syndrome. *J Am Soc Nephrol* 2007; **18**: 1271-1283 [PMID: 17329572 DOI: 10.1681/ASN.2006101095]
15 **Subasinghe CJ**, Sirisena ND, Herath C, Berge KE, Leren TP, Bulugahapitiya U, Dissanayake VHW. Novel mutation in the SLC12A3 gene in a Sri Lankan family with Gitelman syndrome & coexistent diabetes: a case report. *BMC Nephrol* 2017; **18**: 140 [PMID: 28446151 DOI: 10.1186/s12882-017-0563-0]
16 **Rahimi Z**, Moradi M, Nasri H. A systematic review of the role of renin angiotensin aldosterone system genes in diabetes mellitus, diabetic retinopathy and diabetic neuropathy. *J Res Med Sci* 2014; **19**: 1090-1098 [PMID: 25657757]

World Journal of Clinical Cases

Submit a Manuscript: https://www.f6publishing.com

World J Clin Cases 2019 May 26; 7(10): 1206-1212

DOI: 10.12998/wjcc.v7.i10.1206

ISSN 2307-8960 (online)

CASE REPORT

Hepatitis B virus-related liver cirrhosis complicated with dermatomyositis: A case report

Juan Zhang, Xiao-Yu Wen, Run-Ping Gao

ORCID number: Juan Zhang (0000-0001-8866-8926); Xiao-Yu Wen (0000-0002-9037-8693); Run-Ping Gao (0000-0003-0110-6977).

Author contributions: Wen XY and Gao RP designed the study and took care of the patient. Zhang J collected the clinical data and wrote the manuscript. Wen XY and Gao RP revised the manuscript. Wen XY and Gao RP are co-corresponding authors.

Supported by Natural Science Foundation of Jilin Science and Technology Department, No. 20190201065JC.

Informed consent statement: The patient and his family members provided written informed consent.

Conflict-of-interest statement: The authors have no conflicts of interest to declare.

CARE Checklist (2016) statement: The authors have read the CARE Checklist (2016) and prepared the manuscript accordingly.

Juan Zhang, Xiao-Yu Wen, Run-Ping Gao, Department of Hepatic-Biliary-Pancreatic Medicine, the First Hospital of Jilin University, Changchun 130021, Jilin Province, China

Corresponding author: Run-Ping Gao, MD, PhD, Professor, Department of Hepatic-Biliary-Pancreatic Medicine, The First Hospital of Jilin University, No. 71 Xinmin Avenue, Changchun 130021, Jilin Province, China. gaorp@jlu.edu.cn
Telephone: +86-431-88785110
Fax: +86-431-65612468

Abstract

BACKGROUND

Twenty percent of patients infected with hepatitis B virus (HBV) develop extrahepatic manifestations with HBV detected in the lymph nodes, spleen, bone marrow, kidneys, and skin. HBV infection has been associated with some autoimmune disorders. Dermatomyositis (DM) is an idiopathic inflammatory myopathy, which involves a viral infection, and DM has been identified in patients infected with HBV, but there is no direct histological evidence for an association between HBV and DM.

CASE SUMMARY

We describe a familial HBV-infected patient admitted with liver function abnormality, rashes, a movement disorder, and an elevated level of creatine kinase (CK). A computed tomography scan of the lung showed pulmonary fibrosis, and a liver biopsy identified nodular cirrhosis. An electromyogram revealed myogenic damage, and a muscle biopsy showed nuclear migration in local sarcolemma and infiltration of chronic inflammatory cells. Immunohistochemical staining showed negative results for HBsAg and HBcAg. Fluorescence in situ hybridization showed a negative result for HBV DNA. The patient was diagnosed with HBV-related liver cirrhosis complicated with DM and was treated with methylprednisolone, mycophenolate mofetil, and lamivudine. Eight months later, the patient was readmitted for anorexia and fatigue. The blood examination showed elevated levels of aminotransferases and HBV DNA, however, the CK level was within the normal range. The patient developed a virological breakthrough and lamivudine was replaced with tenofovir.

CONCLUSION

DM in chronic HBV-infected patients does not always associate with HBV. Antiviral and immunosuppressive drugs should be taken into consideration.

Manuscript source: Unsolicited manuscript

Received: January 16, 2019
Peer-review started: January 17, 2019
First decision: March 10, 2019
Revised: March 25, 2019
Accepted: April 9, 2019
Article in press: April 9, 2019
Published online: May 26, 2019

P-Reviewer: Asaad AM, Abushady EA
S-Editor: Dou Y
L-Editor: A
E-Editor: Wu YXJ

Key words: Chronic hepatitis B; Dermatomyositis; Extrahepatic manifestations; Case report

Core tip: We report a patient diagnosed with hepatitis B virus (HBV)-related liver cirrhosis complicated with dermatomyositis (DM). However, HBV was not detected in his muscle sample, thus we concluded that his DM did not associate with his HBV infection. Diagnosis of DM on the basis of HBV infection is relatively uncommon. Diagnosis and treatment are difficult due to the complex relationship between these diseases and their conflicting treatment strategies. By providing our experience in diagnosing and treating DM with HBV, we hope to assist with similar cases and to stimulate further research on the relationship between DM and HBV.

Citation: Zhang J, Wen XY, Gao RP. Hepatitis B virus-related liver cirrhosis complicated with dermatomyositis: A case report. *World J Clin Cases* 2019; 7(10): 1206-1212
URL: https://www.wjgnet.com/2307-8960/full/v7/i10/1206.htm
DOI: https://dx.doi.org/10.12998/wjcc.v7.i10.1206

INTRODUCTION

Dermatomyositis (DM) is an idiopathic inflammatory myopathy with typical rashes yet little is known about the etiology of DM. DM is accepted widely as an autoimmune disease induced by infectious and noninfectious environmental factors in genetically susceptible individuals[1-4]. Hepatitis B virus (HBV) infection is a global public health problem with up to two billion people with pre-existing and current HBV infections[5], HBV was detected in the lymph nodes, spleen, bone marrow, kidneys, and skin[6] and 20% of patients infected with HBV develop extrahepatic manifestations, such as polyarteritis nodosa, polymyositis, Sjogren's syndrome, and glomerulonephritis[7,8]. One DM case as the consequence of HBV infection has been reported[9], but DM does not always associate with hepatitis. Here, we report a case of HBV-related liver cirrhosis complicated with DM.

CASE PRESENTATION

Chief complaints

A 46-year-old man presented with rashes and a movement disorder.

History of present illness

The patient has been HBsAg-positive for 15 years and has had moderate fatigue and elevated aminotransferases for four years, he was not treated. Facial and peripheral rashes were present for four months with no definitive cause. The patient suffered from simultaneous muscle soreness for half a month, which did not draw his attention until he could not move his extremities.

History of past illness

The patient reported no known systemic illness.

Personal and family history

The patient's mother, brother, and grandfather had chronic HBV infections.

Physical examination upon admission

On physical examination, the patient's pharynx was congested. Purple-red edematous maculae were on the patient's forehead and the malar areas around on his orbits. The peripheral skin was also involved sporadically, and telangiectasia was observed on the anterior chest wall. The abdominal examination was normal. A neurologic examination indicated muscle strength of 3/5 and limb muscle pain was positive.

Laboratory examinations

The blood examination showed increased levels of creatine kinase (CK, 11889 U/L),

C-reactive protein (32.4 mg/L), aspartate aminotransferase (AST, 280 U/L), and alanine aminotransferase (ALT, 242 U/L). The tests for HBsAg, HBeAb, and HBcAb were positive, and the tests for anti-HIV, anti-HCV, anti-EBV IgM, anti-cytomegalovirus IgM and HCV RNA were negative. HBV DNA was undetectable (< 50 IU/mL). Alpha fetoprotein (AFP) and Carbohydrate antigen 19-9 (CA19-9) were within normal range. Tests for the autoantibodies anti-PM-Scl and anti-Jo-1 were negative, and the test for anti-Ro-52 was positive. With regards to antinuclear antibodies, the membranous pattern was 1:1000 and the particle type cytoplasm was 1:100. The test for anti-M2 was negative. The indocyanine green retention rate at 15 min was 11.7% and a FibroScan revealed a stiffness value of 21.3 kPa. A liver biopsy showed nodular cirrhosis with extensive lymphocytes and few plasmocytes infiltrating the fibrous septa (Figure 1A).

Imaging examinations

Magnetic resonance imaging (MRI) of the abdomen revealed hepatic cirrhosis and mild splenomegaly. A computed tomography (CT) scan of the lung showed streaky opacities in the right middle lobe, right lower lobe, and ligula.

FINAL DIAGNOSIS

The patient was diagnosed with hepatitis B cirrhosis, liver function compensation, and preliminary pneumonia or pulmonary fibrosis. Upon admission, the patient accepted antibiotic (ceftezole), hepatoprotective, and supportive treatment. Nine days after admission, the patient developed dysphagia, dyspnea, and incontinence, and an electromyogram (EMG) revealed myogenic damage. A muscle biopsy showed nuclear migration in local sarcolemma and infiltration of chronic inflammatory cells (Figure 1B). Immunohistochemical staining showed negative results for HBsAg and HBcAg. Fluorescence in situ hybridization showed a negative result for HBV DNA. The streaky opacities in the lungs were more severe. The patient was finally diagnosed with HBV-related liver cirrhosis complicated with DM and pulmonary fibrosis.

TREATMENT

The patient was treated with 80 mg/d of methylprednisolone instead of antibiotics. Lamivudine was given at a dose of 100 mg/d to prevent virus replication. Additional treatments were supportive and symptomatic. After seven days of steroid treatment, the dysphagia, dyspnea, and incontinence improved and the CK level was 4791 U/L. After seventeen days of steroid treatment, the CK level was 5710 U/L leading to administration of 750 mg of mycophenolate mofetil twice a day. After a week, the patient's eating and sleeping improved, micturition and defecation were normal, and the patient's facial and peripheral rashes faded. The patient's AST level was 166 U/L, ALT level was 290 U/L, and CK level was 4581 U/L. The streaky opacities did not change. The patient was prescribed 40 mg of methylprednisolone, 1500 mg of mycophenolate mofetil, and 100 mg of lamivudine per day for another three months after discharge.

OUTCOME AND FOLLOW-UP

Upon discharge, the patient did not feel uncomfortable. The patient's amino-transferase and CK levels were in the normal range during the three months after discharge, and there were no more streaky opacities in the lungs. The mycophenolate mofetil treatment was stopped after another six months, but one week after stopping this immunosuppressive drug, the patient was readmitted for anorexia and fatigue. The blood examination showed increased levels of HBV DNA (5.05×10^5 IU/L) and AST (840 U/L), but the CK level was normal (53 U/L) (Figure 2A, B). The frequency of the L180M mutation in HBV is 51.8%, and the frequency of the M204V mutation in HBV is 78.2%. In this patient, HBV reactivation followed lamivudine drug resistance that arose due to long-term lamivudine treatment along with long-term immunosuppressive therapy. To reduce HBV replication, the patient was given 300 mg of tenofovir per day. One month later, the patient's aminotransferase levels returned to normal and his HBV DNA levels fell to a level below detection (Figure 2B). The patient was prescribed tenofovir as a long-term antiviral therapy, his aminotransferase and CK levels remained normal at the subsequent five-year follow-up (Figure 2A, B), and he was able to perform moderate-intensity physical activities.

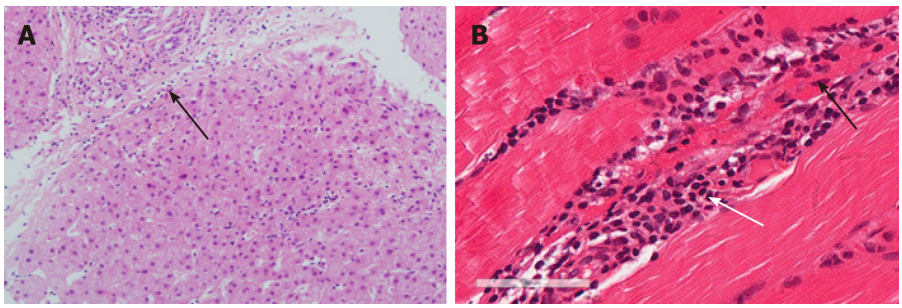

Figure 1 Histopathologic manifestations. A: A hematoxylin-eosin stained liver biopsy (200× magnification) showed nodular cirrhosis with extensive lymphocytes and few plasmocytes infiltrating fibrous septa (black arrow); B: A hematoxylin-eosin stained muscle biopsy (400× magnification) showed nuclear migration in local sarcolemma (black arrow) and infiltration of chronic inflammatory cells (white arrow).

DISCUSSION

The presentations of DM are proximal weakness, elevated CK, myopathic EMG, inflammatory pathology, and typical rashes. The characteristic rashes include periorbital violaceous erythema, Gottron's sign, periungual telangiectasia, mechanic's hands, and other mucocutaneous lesions. In addition, DM can affect the lung (interstitial pneumonia, pulmonary fibrosis, and pleurisy) and the alimentary tract (the pharynx and the striated muscle at the lower end of the esophagus)[10]. The patient in this study fully met the diagnostic criteria for DM[1]. The patient's lung and pharyngeal muscle were affected.

The etiology and pathogenesis of DM are uncertain, and DM is generally recognized as an autoimmune disorder induced by environmental factors in genetically susceptible individuals[1]. Tests for autoantibodies in DM patients are usually partial positive. Tests for anti-aminoacyl-tRNA synthetases, such as anti-Jo1, and anti-Mi autoantibodies, which associate with the hepatitis C virus (HCV), may be positive in DM patients. HCV may cross-react with the host to produce specific autoantibodies that result in DM[11]. However, we can exclude the possibility of HCV-related DM in this patient based on the lack of anti-HCV and HCV RNA in his serum.

Distinct from the mechanism of HCV-related DM, approximately 20% of HBV-infected patients develop extrahepatic disorders, including glomerulonephritis, polyarteritis nodosa, arthritis, and polymyositis through HBV-related immune complex circulation and deposition. In 2005, Mason A reported a case of HBV-related polymyositis in which HBV immune complex deposition and HBV DNA replication were detected in the interstitial vascular endothelium of diseased muscle tissues[8]. We summarized ten hepatitis virus infection and DM cases since 2000 (Table 1, Table 2), and found that HBV production was absent in the skeletal muscle samples of these patients. Most of these patients were diagnosed with DM associated with hepatocellular carcinoma (HCC). In these patients with HCC, paraneoplastic syndrome, a compromised immune system, common carcinogenic environmental factors, and cross-reactive immune reactions against the tumor may have played a role in disease development. Cross-reactions with cutaneous and muscular antigens may have led to the autoimmune syndrome[12-14]. DM improved after cancer resection but recurred upon relapse of the cancer demonstrating that paraneoplastic syndrome plays an important role in HCC-related DM[14]. However, the effect of HBV infection on HCC-related DM has not yet been proven. Recently, Han *et al*[9] reported a case of DM associated with HCC in which steroid treatment had limited effect, but antiviral therapy improved muscle strength, thus Han hypothesized that DM developed as a consequence of HBV infection. Muscle biopsy evidence remains to be obtained to confirm the association between HBV and DM.

Upon initial admission, our patient presented AFP within normal range in serum and MRI without mass lesion in liver, we excluded the possibility of HCC-associated DM in this study. The level of HBV DNA in our patient was below detection, and HBsAg, HBcAg, and HBV DNA were not found in diseased muscle tissues suggesting no HBV immune complex deposition or HBV DNA replication. The patient's tests for anti-Ro-52 and anti-antinuclear antibodies were positive. The patient responded well to treatment with methylprednisolone and mycophenolate mofetil. Nevertheless, the immunosuppressive therapy reactivated the HBV and HBV-related liver cirrhosis symptoms recurred, but the DM symptoms did not recur. The patient did not meet the diagnosis criteria for HBV-related DM as described above. In this case, the DM occurred independently of the HBV infection.

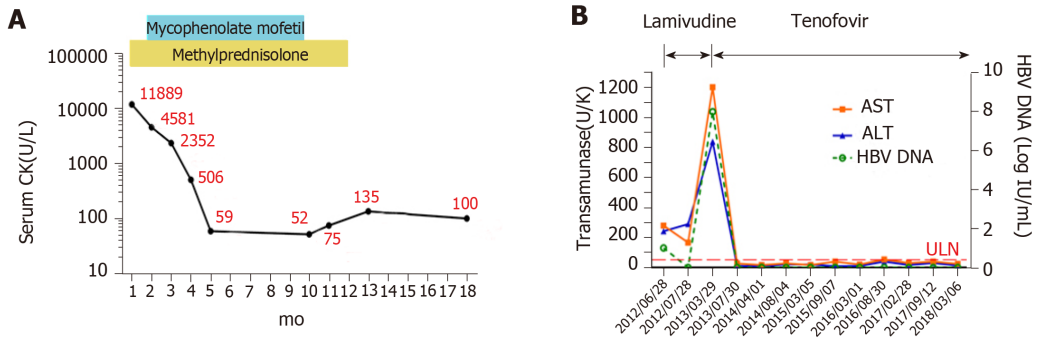

Figure 2 Laboratory examination results during patient follow-up. A: Serum creatine kinase levels during the 18-mo follow-up. After the patient's symptoms improved and he underwent biochemical remission, the methylprednisolone treatment was tapered at a rate of 10% per week until the dose reached 4 mg per day. The patient was on the 4 mg per day dose until one year. The mycophenolate mofetil dose remained at 750 mg twice a day for nine months; B: Changes in transaminase (Alanine transaminase; aspartate transminase) and hepatis B virus desoxyribonucleic acid levels during antiviral therapy. ULN: Upper limit of normal for transaminases; ALT: Alanine transaminase; AST: Aspartate Transminase; CK: Creatine kinase; HBV DNA: Hepatis B virus desoxyribonucleic acid.

Although patients have been reported that their symptoms improved after tumor controlling, antiviral, and immunosuppressive therapies, long-term follow-up information is lacking. In this case, lamivudine was not able to prevent HBV reactivation caused by immunosuppressive agents, which contributed to lamivudine resistance and recurrence of HBV-related liver cirrhosis. The patient was stabilized after changing the treatment from lamivudine to tenofovir. Lamivudine is the first nucleoside analogue used to treat chronic hepatitis B virus infections and it is widely used because of its low price and minimal side effects, but high rates of resistance with long-term lamivudine monotherapy have been observed. The incidence of HBV resistance to lamivudine in nucleoside-naive patients with chronic hepatitis B is 24% after one year of treatment and 70% after five years of treatment[15]. Thirty-three percent of patients who were treated with lamivudine for five years and who had a virological response showed virological breakthrough after 15 mo of treatment with a median dose. Lamivudine resistant mutations occurred in 97.4% of the breakthrough patients[16]. According to recent expert recommendations for antiviral therapy based on the risk of HBV recurrence, in this HBV-related cirrhosis patient, an HBsAg-positive result, and methylprednisolone combined with mycophenolate mofetil treatment are both high-risk factors that contribute to HBV recurrence. Thus, efficacious treatment with an antiviral with a low resistance rate, such as tenofovir or entecavir, should be considered[17].

CONCLUSION

Not all DM cases based on chronic HBV infections are associated with HBV. Therefore, when HBV coexists with DM, it is necessary to define HBV-related DM, strictly evaluate the risk factors for HBV recurrence, and use antiviral drugs and immunosuppressive agents reasonably to control DM and HBV.

Table 1 A case review of dermatomyositis complicated with hepatitis virus infection since 2000

Ref.	Published yr	Age / Sex	Virus infection	Associated disorders	Autoantibody profile	Treatment	Outcome
Nakamura *et al*[18]	2000	60/F	HCV	Left ventricular dysfunction	ANA(+), Anti-Jo-1(-)	Interferon-α, Steroid	ND
Germany *et al*[19]	2002	40/F	HCV	Collagenous colitis	ANA(+), RF(-).	Azathioprine	Improved
Altman *et al*[20]	2008	6/F	HBV vaccine	-	ND	ND	ND
Our case		46/M	HBV	Pulmonary fibrosis	ANA(+), Anti-Jo-1(-), Anti-Mi2(-)	Steroid, Mycophenolate mofetil, Tenofovir	Stable

ND: Not described; F: Female; M: Male; ANA: Antinuclear antibody; RF: Rheumatoid factor; HBV: Hepatitis B virus; HCV: Hepatitis C virus.

Table 2 A case reviews of dermatomyositis associated with hepatocellular carcinoma since 2000

Ref.	Published yr	Age / Sex	Virus infection	Associated disorders	Autoantibody profile	Treatment	Outcome
Cheng *et al*[21]	2002	50/F	HBV	Erythrocytosis	ND	Steroid, TACE, Hepatectomy	Died
Inuzuka *et al*[22]	2001	51/M	HCV	Acquired ichthyosis	ANA(+), Anti-Jo-1(-)	Steroid	Died
Kee *et al*[11]	2004	71/M	HCV	-	ANA(+), Anti-Jo-1(-)	Steroid	ND
Toshikuni *et al*[23]	2006	79/F	HCV	-	ANA(+), RF(-), Anti-Jo-1 (-)	Steroid, TACE	Died
Kee *et al*[13]	2009	58/M	HBV	-	ANA(+), RF(-), Anti-Jo-1 (-)	Steroid, IVIG, TACE	Died
Yang *et al*[14]	2014	55/M	HBV	-	ANA(+), Anti-Jo-1(-)	Lamivudine, Steroid	Died
Han *et al*[9]	2018	62/M	HBV	-	ANA(+), Anti-Jo-1(-), Anti-Mi2(-)	Steroid, Entecavir, Radio-frequency ablation	Died

ND: Not described; F: Female; M: Male; ANA: Antinuclear antibody; RF: Rheumatoid factor; TACE: Transarterial chemoembolization; IVIG: Intravenous immunoglobulin; HBV: Hepatitis B virus; HCV: Hepatitis C virus.

REFERENCES

1 **Sasaki H**, Kohsaka H. Current diagnosis and treatment of polymyositis and dermatomyositis. *Mod Rheumatol* 2018; **28**: 913-921 [PMID: 29669460 DOI: 10.1080/14397595.2018.1467257]
2 **Pandya JM**, Loell I, Hossain MS, Zong M, Alexanderson H, Raghavan S, Lundberg IE, Malmström V. Effects of conventional immunosuppressive treatment on CD244+ (CD28null) and FOXP3+ T cells in the inflamed muscle of patients with polymyositis and dermatomyositis. *Arthritis Res Ther* 2016; **18**: 80 [PMID: 27039301 DOI: 10.1186/s13075-016-0974-5]
3 **Rajadhyaksha A**, Baheti TG, Mehra S, Sonawale AS, Jain N. Dermatomyositis: a rare presentation of HIV seroconversion illness. *J Clin Rheumatol* 2012; **18**: 298-300 [PMID: 22955479 DOI: 10.1097/RHU.0b013e318268566c]
4 **Yamamoto SP**, Kaida A, Naito T, Hosaka T, Miyazato Y, Sumimoto S, Kohdera U, Ono A, Kubo H, Iritani N. Human parechovirus infections and child myositis cases associated with genotype 3 in Osaka City, Japan, 2014. *J Med Microbiol* 2015; **64**: 1415-1424 [PMID: 26358716 DOI: 10.1099/jmm.0.000167]
5 **Schweitzer A**, Horn J, Mikolajczyk RT, Krause G, Ott JJ. Estimations of worldwide prevalence of chronic hepatitis B virus infection: a systematic review of data published between 1965 and 2013. *Lancet* 2015; **386**: 1546-1555 [PMID: 26231459 DOI: 10.1016/S0140-6736(15)61412-X]
6 **Mason A**, Wick M, White H, Perrillo R. Hepatitis B virus replication in diverse cell types during chronic hepatitis B virus infection. *Hepatology* 1993; **18**: 781-789 [PMID: 8406351 DOI: 10.1002/hep.1840180406]
7 **Cacoub P**, Terrier B. Hepatitis B-related autoimmune manifestations. *Rheum Dis Clin North Am* 2009; **35**: 125-137 [PMID: 19481001 DOI: 10.1016/j.rdc.2009.03.006]
8 **Mason A**, Theal J, Bain V, Adams E, Perrillo R. Hepatitis B virus replication in damaged endothelial tissues of patients with extrahepatic disease. *Am J Gastroenterol* 2005; **100**: 972-976 [PMID: 15784044 DOI: 10.1111/j.1572-0241.2005.41308.x]
9 **Han J**, Wang S, Kwong TNY, Liu J. Dermatomyositis as an extrahepatic manifestation of hepatitis B virus-related hepatocellular carcinoma: A case report and literature review. *Medicine (Baltimore)* 2018; **97**:

e11586 [PMID: 30113453 DOI: 10.1097/MD.0000000000011586]
10 **Shu XM**, Ma L, Lu X, Xie Y, Wang GC. [Myositis disease activity tool in Chinese patients with polymyositis/dermatomyositis]. *Zhonghua Yi Xue Za Zhi* 2011; **91**: 1328-1330 [PMID: 21756759]
11 **Kee KM**, Wang JH, Lee CM, Changchien CS, Eng HL. Chronic hepatitis C virus infection associated with dermatomyositis and hepatocellular carcinoma. *Chang Gung Med J* 2004; **27**: 834-839 [PMID: 15796260]
12 **András C**, Ponyi A, Constantin T, Csiki Z, Szekanecz E, Szodoray P, Dankó K. Dermatomyositis and polymyositis associated with malignancy: a 21-year retrospective study. *J Rheumatol* 2008; **35**: 438-444 [PMID: 18203322]
13 **Kee SJ**, Kim TJ, Lee SJ, Cho YN, Park SC, Kim JS, Kim JC, Kang HS, Lee SS, Park YW. Dermatomyositis associated with hepatitis B virus-related hepatocellular carcinoma. *Rheumatol Int* 2009; **29**: 595-599 [PMID: 18802699 DOI: 10.1007/s00296-008-0718-1]
14 **Yang SY**, Cha BK, Kim G, Lee HW, Kim JG, Chang SK, Kim HJ. Dermatomyositis associated with hepatitis B virus-related hepatocellular carcinoma. *Korean J Intern Med* 2014; **29**: 231-235 [PMID: 24648807 DOI: 10.3904/kjim.2014.29.2.231]
15 **European Association For The Study Of The Liver**. EASL clinical practice guidelines: Management of chronic hepatitis B virus infection. *J Hepatol* 2012; **57**: 167-185 [PMID: 22436845 DOI: 10.1016/j.jhep.2012.02.010]
16 **Fasano M**, Lampertico P, Marzano A, Di Marco V, Niro GA, Brancaccio G, Marengo A, Scotto G, Brunetto MR, Gaeta GB, Rizzetto M, Angarano G, Santantonio T. HBV DNA suppression and HBsAg clearance in HBeAg negative chronic hepatitis B patients on lamivudine therapy for over 5 years. *J Hepatol* 2012; **56**: 1254-1258 [PMID: 22343167 DOI: 10.1016/j.jhep.2012.01.022]
17 **Aygen B**, Demir AM, Gümüş M, Karabay O, Kaymakoğlu S, Köksal AŞ, Köksal İ, Örmeci N, Tabak F. Immunosuppressive therapy and the risk of hepatitis B reactivation: Consensus report. *Turk J Gastroenterol* 2018; **29**: 259-269 [PMID: 29755010 DOI: 10.5152/tjg.2018.18263]
18 **Nakamura K**, Matsumori A, Kusano KF, Banba K, Taniyama M, Nakamura Y, Morita H, Matsubara H, Yamanari H, Ohe T. Hepatitis C virus infection in a patient with dermatomyositis and left ventricular dysfunction. *Jpn Circ J* 2000; **64**: 617-618 [PMID: 10952160 DOI: 10.1253/jcj.64.617]
19 **Germany RE**, Cohen SM. Hepatitis C, collagenous colitis, and dermatomyositis occurring in the same patient. *Am J Gastroenterol* 2002; **97**: 1848-1849 [PMID: 12135055 DOI: 10.1111/j.1572-0241.2002.05868.x]
20 **Altman A**, Szyper-Kravitz M, Shoenfeld Y. HBV vaccine and dermatomyositis: is there an association? *Rheumatol Int* 2008; **28**: 609-612 [PMID: 18034245 DOI: 10.1007/s00296-007-0485-4]
21 **Cheng TI**, Tsou MH, Yang PS, Sung SM, Chuang VP, Sung JL. Dermatomyositis and erythrocytosis associated with hepatocellular carcinoma. *J Gastroenterol Hepatol* 2002; **17**: 1239-1240 [PMID: 12453288 DOI: 10.1046/j.1440-1746.2002.t01-1-02851.x]
22 **Inuzuka M**, Tomita K, Tokura Y, Takigawa M. Acquired ichthyosis associated with dermatomyositis in a patient with hepatocellular carcinoma. *Br J Dermatol* 2001; **144**: 416-417 [PMID: 11251586 DOI: 10.1046/j.1365-2133.2001.04040.x]
23 **Toshikuni N**, Torigoe R, Mitsunaga M, Omoto A, Nakashima K. Dermatomyositis associated with hepatocellular carcinoma in an elderly female patient with hepatitis C virus-related liver cirrhosis. *World J Gastroenterol* 2006; **12**: 1641-1644 [PMID: 16570363 DOI: 10.3748/wjg.v12.i10.1641]

World Journal of Clinical Cases

Submit a Manuscript: https://www.f6publishing.com

World J Clin Cases 2019 May 26; 7(10): 1213-1220

DOI: 10.12998/wjcc.v7.i10.1213

ISSN 2307-8960 (online)

CASE REPORT

Small cell lung cancer starting with diabetes mellitus: Two case reports and literature review

Tong Zhou, Yao Wang, Xue Zhao, Yang Liu, Ying-Xuan Wang, Xiao-Kun Gang, Gui-Xia Wang

ORCID number: Tong Zhou (0000-0002-3158-1616); Yao Wang (0000-0002-3688-6099); Xue Zhao (0000-0001-8985-1861); Yang Liu (0000-0002-3852-6468); Ying-Xuan Wang (0000-0003-1830-7134); Xiao-Kun Gang (0000-0003-0855-6954); Gui-Xia Wang (0000-0001-8107-616X).

Author contributions: Zhou T, Wang GX and Gang XK conceived the study; Wang Y, Liu Y and Wang YX collected the human documents; Zhou T, Gang XK and Zhao X wrote the paper.

Supported by Development and Reform Commission Jilin Province, NO. 2017C019; and Science and Technology Agency of Jilin Province, No. 20170623092TC-01 and No. 20180623083TC-01.

Informed consent statement: Informed consent was obtained from patients regarding the use of specimens for case report.

Conflict-of-interest statement: The authors declare that they have no conflict of interest.

CARE Checklist (2016) statement: The guidelines of the CARE Checklist (2016) have been adopted.

Tong Zhou, Xue Zhao, Ying-Xuan Wang, Xiao-Kun Gang, Gui-Xia Wang, Department of Endocrinology and Metabolism, The First Hospital of Jilin University, Jilin University, Changchun 130021, Jilin Province, China

Yao Wang, Department of Orthopedics, The Second Hospital of Jilin University, Jilin University, Changchun 130041, Jilin Province, China

Yang Liu, Department One of The Health Careful VIP, Jilin Provincial People's Hospital, Changchun 130000, Jilin Province, China

Corresponding author: Gui-Xia Wang, MD, PhD, Professor, Department of Endocrinology and Metabolism, The First Hospital of Jilin University, Jilin University, 71 Xinmin Street, Changchun 130021, Jilin Province, China. gwang168@jlu.edu.cn
Telephone: +86-431-88782557
Fax: +86-431-88782557

Abstract

BACKGROUND

Small-cell lung cancer (SCLC) is a type of fatal tumor that is increasing in prevalence. While these are unpleasant facts to consider, it is vitally important to be informed, and it is important to catch the disease early. Typically, lung cancer does not show severe clinical symptoms in the early stage. Once lung cancer has progressed, patients might present with classical symptoms of respiratory system dysfunction. Thus, the prognosis of SCLC is closely related to the early diagnosis of the disease. Ectopic adrenocorticotropic hormone (ACTH) syndrome (EAS) is related to cancer occurrence, especially for SCLC with the presence of Cushing's syndrome, which is dependent on markedly elevated ACTH and cortisol levels.

CASE SUMMARY

In the current report, we describe two middle-age patients who were originally diagnosed with diabetes mellitus with no classical symptoms of lung cancer. The patients were eventually diagnosed with SCLC, which was confirmed by bronchoscopic biopsy and histopathology. SCLC-associated diabetes was related to EAS, which was an endogenous ACTH-dependent form of Cushing's syndrome with elevated ACTH and cortisol levels. Multiple organ metastases were found in Patient 1, while Patient 2 retained good health at 2 years follow-up. EAS symptoms including thyroid dysfunction, hypercortisolism and glucose intolerance were all resolved after anticancer treatment.

CONCLUSION

In conclusion, SCLC might start with diabetes mellitus and increased cortisol and

Manuscript source: Unsolicited manuscript

Received: January 24, 2019
Peer-review started: January 25, 2019
First decision: March 9, 2019
Revised: March 17, 2019
Accepted: March 26, 2019
Article in press: March 26, 2019
Published online: May 26, 2019

P-Reviewer: Haneder S, Seo DW, Villanueva MT
S-Editor: Wang JL
L-Editor: Filipodia
E-Editor: Xing YX

hypokalemia or other EAS symptoms. These complex clinical features were the most significant factors to deteriorate a patient's condition. Early diagnosis and treatment from clinicians were essential for the anti-cancer treatment for patients with SCLC.

Key words: Case report; Small cell lung cancer; Diabetes, Ectopic adrenocorticotropic hormone syndrome; Adrenocorticotropic hormone; Diagnosis

Core tip: Small-cell lung cancer (SCLC) is a fatal tumor that is increasing in prevalence. Prognosis of patients with SCLC is closely related to early diagnosis. We report two middle-aged patients who were originally diagnosed with diabetes mellitus with no classical symptoms of lung cancer. Ectopic adrenocorticotropic hormone syndrome symptoms including thyroid dysfunction, hypercortisolism, and glucose intolerance, which are related to elevated adrenocorticotropic hormone and cortisol levels, were all normal after anticancer treatment. Our findings highlight that SCLC might start with diabetes mellitus and increased cortisol level and hypokalemia or other ectopic adrenocorticotropic hormone syndrome symptoms, and it reminds clinicians of the importance of early diagnosis of SCLC with ectopic adrenocorticotropic hormone syndrome.

Citation: Zhou T, Wang Y, Zhao X, Liu Y, Wang YX, Gang XK, Wang GX. Small cell lung cancer starting with diabetes mellitus: Two case reports and literature review. *World J Clin Cases* 2019; 7(10): 1213-1220
URL: https://www.wjgnet.com/2307-8960/full/v7/i10/1213.htm
DOI: https://dx.doi.org/10.12998/wjcc.v7.i10.1213

INTRODUCTION

Lung cancer (LC) is the most commonly diagnosed cancer, and its prognosis has not improved in recent years[1-5]. Small cell lung cancer (SCLC), accounting for 12%–19% of LC cases, is a fatal tumor that is increasing in prevalence[6]. Despite high sensitivity to chemotherapy, SCLC still has a poor long-term outcome due to shortened cell doubling time, frequent relapse and earlier metastasis[7-10]. Thus, to diagnose SCLC as soon as possible is key to its treatment. In order to attain the above goal, it is critical to differentiate early manifestations of SCLC from other related diseases. The majority of SCLCs express a neuroendocrine program, which is related to ectopic adrenocorticotropic hormone (ACTH) syndrome (EAS)[11,12]. EAS is an endogenous ACTH-dependent form of Cushing's syndrome that is associated with markedly increased ACTH and cortisol levels. EAS accounts for 5%–10% of all patients presenting with ACTH-dependent hypercortisolism, while SCLC and neuroendocrine tumors account for the majority of such cases[13]. LC typically displays respiratory symptoms. Beyond that, the features of EAS can help to differentiate SCLC from other tumors to some extent. However, there are few case reports on the other manifes-tations of SCLC as early diagnostic clues, which can help clinicians catch the disease at an early stage.

In this paper, we present two cases of SCLS admitted with newly-onset diabetes mellitus but without the classical symptoms of LC or Cushing's syndrome. Rapid socioeconomic development has led to a dramatic increase in the prevalence of diabetes[14,15]. Thus, diagnosis of diabetes seems to be easier than before. Through the two cases, we draw clinical attention to the fact that diabetes might be an initial symptom of SCLC. Early diagnosis and treatment are critical factors that might influence prognosis of the patients.

CASE PRESENTATION

Case 1

Chief complaints: A 50-year-old man presented with aggravating thirst, diuresis, blurred vision, and significant weight loss for 1 mo.

History of present illness: One month before admission, the patient suffered from aggravating thirst, diuresis, blurred vision, and significant weight loss of 5 kg in 1 mo. No fever and other symptoms were present during onset of the illness.

History of past illness: The patient had a history of hypertension. The patient has been smoking for 20 years at a rate of 15 cigarettes daily. He also had a family history of type 2 diabetes mellitus.

Physical examination: Physical examination found that blood pressure was 200/100 mmHg, heart rate was 86 beats/min, body temperature was 36.3 °C, and body mass index (BMI) was 25.93 kg/m^2. Sporadic chromatosis and mild edema were found in the lower limbs. The rest of the physical examination was normal.

Laboratory testing: The laboratory tests showed elevated hemoglobin A1c (HbA1c) (8.2%), urine glucose (3+), 8-hr ACTH (36.89 pmol/L), 8-hr cortisol (1027.56 nmol/L) and 24-hr urinary free cortisol (12221 nmol). The laboratory results also showed decreased level of serum K^+ (2.18 mmol/L), Na^+ (135 mmol/L), Cl^- (94.9 mmol/L) and Ca^{2+} (1.84 mmol/L). Concentrations of urine Na^+ (339.5 mmol/24 hr) and Cl^- (300 mmol/24 hr) were increased. Thyroid function results showed decreased levels of free tri-iodothyronine (2.4 pmol/L) and free thyroxine (10.21 pmol/L). Dexamethasone-suppression test showed that there was no suppression of ACTH and cortisol secretion. These results are shown in Table 1.

Imaging examination: Findings on laboratory evaluation raised the suspicion of ectopic ACTH secretion that may have originated from SCLC. The conjecture was confirmed by chest X-ray and biopsy (cT2aN3M0). X-rays showed the following: (1) right middle lobe: peripheral LC with lymph node metastasis and distal obstructive pneumonia; and (2) bilateral pleural effusion. Bronchoscopic biopsy showed SCLC. Immunohistochemistry showed: Ki-67 (+ 80%), thyroid transcription factor-1 (+), CD56 (+), Synaptophysin (+). These results are shown in Figure 1. Adrenal gland computed tomography (CT) showed bilateral adrenal stroma, and pituitary magnetic resonance imaging showed nothing abnormal.

Case 2

Chief complaints: A 54-year-old woman presented with elevated blood glucose concentration for 3 d before physical examination.

History of present illness: Three days before admission, the patient showed blood glucose elevation at physical examination without obvious clinical manifestations. Her weight loss was 2 kg in 1 mo and she felt slight weakness.

History of past illness: Hypertension (140/100 mmHg) was found at physical examination. The patient had a family history of diabetes mellitus and was an active smoker of 40 cigarettes daily.

Physical examination: Physical examination showed body temperature was 36.5 °C, blood pressure 130/98 mmHg, heart rate 89 beats/min, and BMI 21.37 kg/m^2. Systemic examination was normal.

Laboratory examination: The laboratory tests showed elevated hemoglobin A1c (9.4%), urine glucose (1 +), fasting glucose (11.2 mmol/L), 8-hr ACTH (167.1 pmol/L), 8-hr cortisol (> 1710.49 nmol/L) and 24-h urinary free cortisol (12762.25 nmol). The laboratory results also showed decreased level of serum K^+ (2.45–3.25 mmol/L) and Ca^{2+} (1.72–1.94 mmol/L). Thyroid function results showed decreased levels of thyroid-stimulating hormone (0.039 μIU/mL), free tri-iodothyronine (2.8 pmol/L) and free thyroxine (11.72 pmol/L). These results are shown in Table 2.

Imaging examination: Pituitary punctate enhanced imaging showed nothing abnormal. Positron emission tomography-computed tomography-CT showed a hypermetabolic nodule in the left lingular lobe. An immunohistochemistry test for antibodies showed the presence of Ki-67, thyroid transcription factor-1, CD56, and Synaptophysin. These results are shown in Table 2 and Figure 2.

FINAL DIAGNOSIS

Case 1

According to the typical symptoms, physical examination, and imaging findings, this patient was diagnosed with SCLC (cT2aN3M0) with EAS.

Table 1 Laboratory examination results in Case 1 (only abnormal results shown)

Items		Test result	Normal range
HbA1c		8.2%	< 6.5%
γ-GT		65.0 U/L	5.0–54.0 U/L
Serum ions	K^+	2.2 mmol/L	3.5–5.5 mmol/L
	Na^+	135.0 mmol/L	137–145 mmol/L
	Cl^+	94.9 mmol/L	98–107 mmol/L
	Ca^{2+}	1.8 mmol/L	2.1–2.55 mmol/L
Urine glucose		3 +	Negative
Thyroid function	TSH	0.6 μIU/mL	0.27–4.2 μIU/mL
	FT3	2.4 pmol/L	3.1–6.8 pmol/L
	FT4	10.2 pmol/L	12.0–22.0 pmol/L
ACTH, 8 hr		36.9 pmol/L	1.6–13.9 pmol/L
Cortisol, 8 hr		1027.6 nmol/L	240–619 nmol/L
24-hr UFC		12221.0 nmol	108–961 nmol/L
Urine	K^+	74.0 mmol/24 hr	51–102 mmol/24 hr
	Na^+	339.5 mmol/24 hr	130–260 mmol/24 hr
	Ca^{2+}	7.5 mmol/24 hr	2.5–7.5 mmol/24 hr
	Cl^-	300.0 mmol/24 hr	100–250 mmol/24 hr
Dexamethasone-suppression test, at overnight, low-dose and high-dose		No suppression	Suppressed

HbA1c: Hemoglobin A1c; γ-GT: Gamma glutamyltransferase; ACTH: Adrenocorticotropic hormone; TSH: Thyroid-stimulating hormone; FT3: Free tri-iodothyronine; FT4: Free thyroxine; UFC: Urinary free cortisol.

Case 2

According to the typical symptoms, physical examination, and imaging findings, the patient was diagnosed with SCLC with EAS.

TREATMENT

Case 1

Antineoplastic treatment was prescribed, comprising six courses of chemotherapy (etoposide + cisplatin) and three courses of biotherapy. Radiotherapy was also admitted to the treatment plan (54 Gy/1.8 Gy/30 fractions).

Case 2

Treatment comprised of diabetic diet, lowering blood glucose, and correcting electrolyte disturbances. Etoposide + cisplatin were given.

OUTCOME AND FOLLOW-UP

Case 1

Thyroid function, cortisol and ACTH were all back to normal range after the second course of chemotherapy. Lung CT revealed that the lesion had reduced by one-third. However, bone metastasis (T2aN3M1b) was found in manubrium sterni and centrum T6 after the fourth course of chemotherapy. Re-examination showed enlargement of the pulmonary lesion. Abdominal CT showed liver metastases. Severe hypokalemia (lowest: 1.85 mmol/L) and hypertension reoccurred, and bone marrow metastasis was found.

Case 2

The thyroid function, cortisol, ACTH, fasting and postprandial glucose, and hemoglobin A1c were back to normal ranges after 3 mo.

DISCUSSION

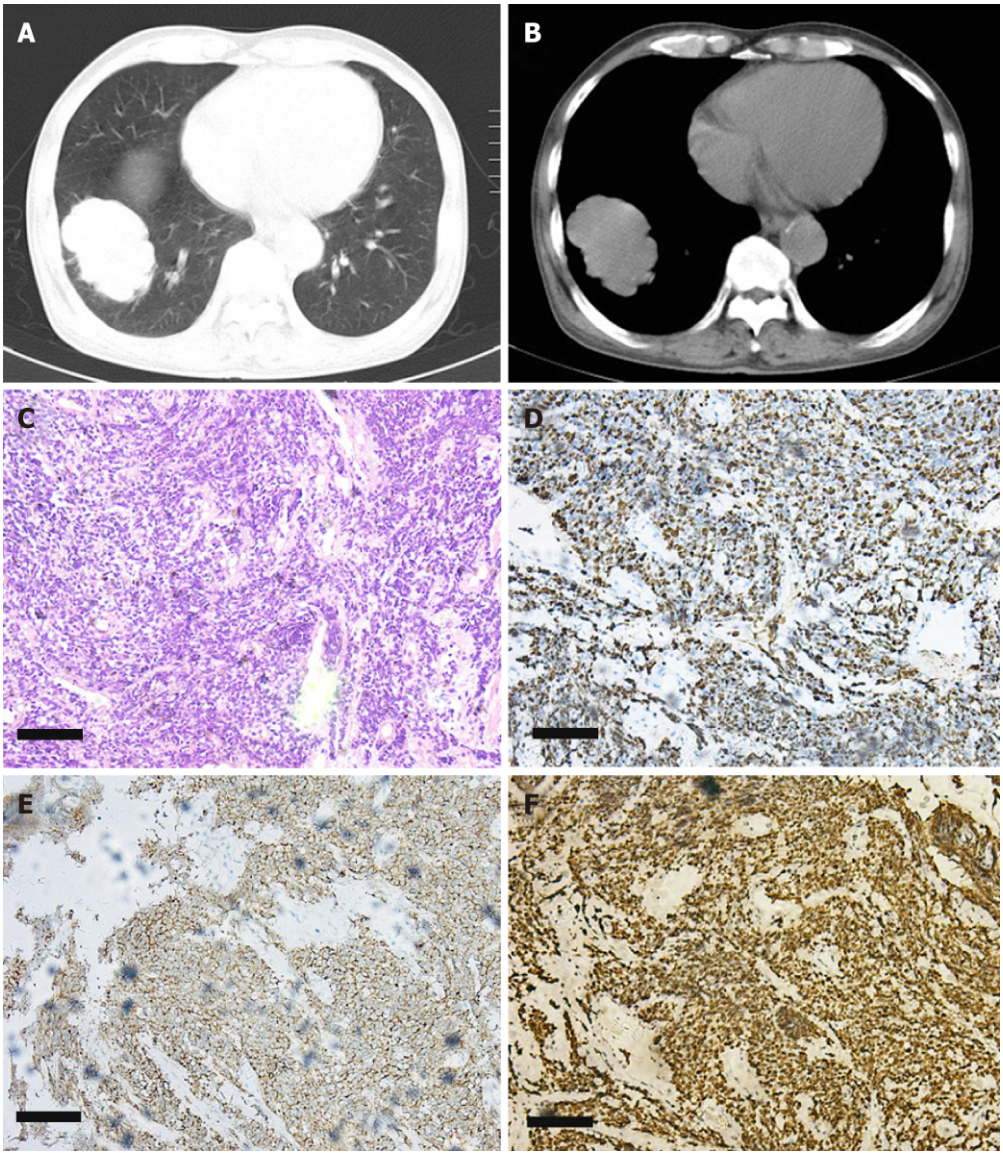

Figure 1 Lung computed tomography and bronchoscopic biopsy of Case 1. A, B: Lung computed tomography of the patient. Right middle lobe: Peripheral lung cancer with lymph node metastasis and distal obstructive pneumonia. Bilateral pleural effusion; C: Hematoxylin and eosin staining of the tissue; D: Ki-67 staining of the tissue; E: Synaptophysin staining of the tissue; F: Thyroid transcription factor-1 staining of the tissue.

Both patients reported here were admitted with diabetes mellitus. They had the following common features: (1) middle age, smoking history and hypokalemia; (2) no significant clinical manifestations of Cushing's syndrome, but increased ACTH and high level of cortisol in serum and urine; and (3) bronchoscopic biopsy confirmed SCLC. Changes in thyroid function in both patients were attributed to inhibition of the pituitary–thyroid axis by excess cortisol[16]. The condition of Patient 1 deteriorated rapidly, losing the best opportunity for treatment, whereas Patient 2 remained healthy for 2 years.

EAS is usually caused by neuroendocrinological carcinoma, mainly SCLC (45%), thymic carcinoma (15%), bronchus carcinoid (10%), pancreas islet-cell carcinoma (10%), chromaffin tumor (2%), and oophoroma (1%), as well as some other rare causes[17-19]. Cushing's syndrome caused by SCLC with ectopic ACTH production is reported to occur in 1.6%–4.5% of patients with SCLC[11]. Qualitative diagnosis of EAS is based on clinical manifestations and hormonal tests[20]. Localization of EAS is based on CT, magnetic resonance imaging and octreotide scan, which is effective in detecting minor lesions[21]. Measurement of ACTH and cortisol concentrations and performance of a high-dose dexamethasone suppression test are useful methods for diagnosis of EAS. CT, positron emission tomography-CT and bronchoscopic biopsy confirmed the diagnosis of SCLC. The median survival time of patients with SCLC with EAS is short[22]. For EAS, surgery remains the optimal treatment in all forms of Cushing's syndrome[23]. Some reports showed that metyrapone, ketoconazole and

Table 2 Laboratory examination results in Case 2 (only abnormal results shown)

Items		Test result	Normal range
HbA1c		9.4%	< 6.5%
Fasting glucose		11.2 mmol/L	3.9–6.1 mmol/L
blood routine	NE %	0.8	0.5–0.7
	RBC	3.97×10^{12}/L	4.0×10^{12}–5.5×10^{12}/L
	HGB	111.0 g/L	120–160 g/L
Urine glucose		1 +	Negative
Thyroid function	TSH	0.04 μIU/mL	0.27–4.2 μIU/mL
	FT3	2.8 pmol/L	3.1–6.8 pmol/L
	FT4	11.7 pmol/L	12.0–22.0 pmol/L
Ion, serum	K^+	2.5–3.3 mmol/L	3.5–5.5 mmol/L
	Ca^{2+}	1.7–1.9 mmol/L	2.1–2.55 mmol/L
ACTH, 8 hr		167.1 pmol/L	1.6–13.9 pmol/L
Cortisol, 8 hr		> 1710.5 nmol/L	240–619 nmol/L
24-h UFC		12762.3 nmol/L	108–961 nmol/L
CEA		5.6 ng/mL	< 5 ng/mL

HbA1c: Hemoglobin A1c; NE: Neutrophil; RBC: Red blood cell; HGB: Hemoglobin; TSH: Thyroid-stimulating hormone; FT3: Free tri-iodothyronine; FT4: Free thyroxine; ACTH: Adrenocorticotropic hormone; UFC: Urinary free cortisol; CEA: Carcinoembryonic antigen.

octreotide are effective but not widely used due to the adverse effects and long onset of action[24-26].

Available evidence on the relationship between SCLC and diabetes is limited. Several studies have confirmed that 8%–18% of cancer patients have diabetes mellitus, and type 2 diabetes mellitus is believed to be a risk factor for several solid tumors[27-30]. Furthermore, clinical studies have indicated that patients with both cancer and diabetes usually have a poor prognosis[31,32]. Xu *et al*[33] reported that treatment of diabetes using metformin can improve prognosis of SCLC based on their results including 79 SCLC patients with diabetes. Thus, diabetes might play an important role in the development and prognosis of cancer[34,35]. Early diagnosis of diabetes might be indicative of the later detection of several cancers such as LC. Unfortunately, the underlying mechanism remains unclear. We think that hypercortisolism induced by EAS might paly a key role in the dysfunction of glucose homeostasis, which provokes hyperglycemia. Thus, high blood glucose level is not simply a reflection of diabetes, but might also be a manifestation of serious disorders that require clinicians to take notice.

CONCLUSION

The conclusion of the current findings is that SCLC might start with diabetes mellitus. High blood glucose level is not simply a reflection of diabetes, and might be a manifestation of serious disorders that requires attention from clinicians. Increased cortisol and hypokalemia were the most significant factors in our patients' conditions, which should be monitored carefully during treatment. Furthermore, early and accurate diagnosis of SCLC patients with diabetes is essential for prognosis.

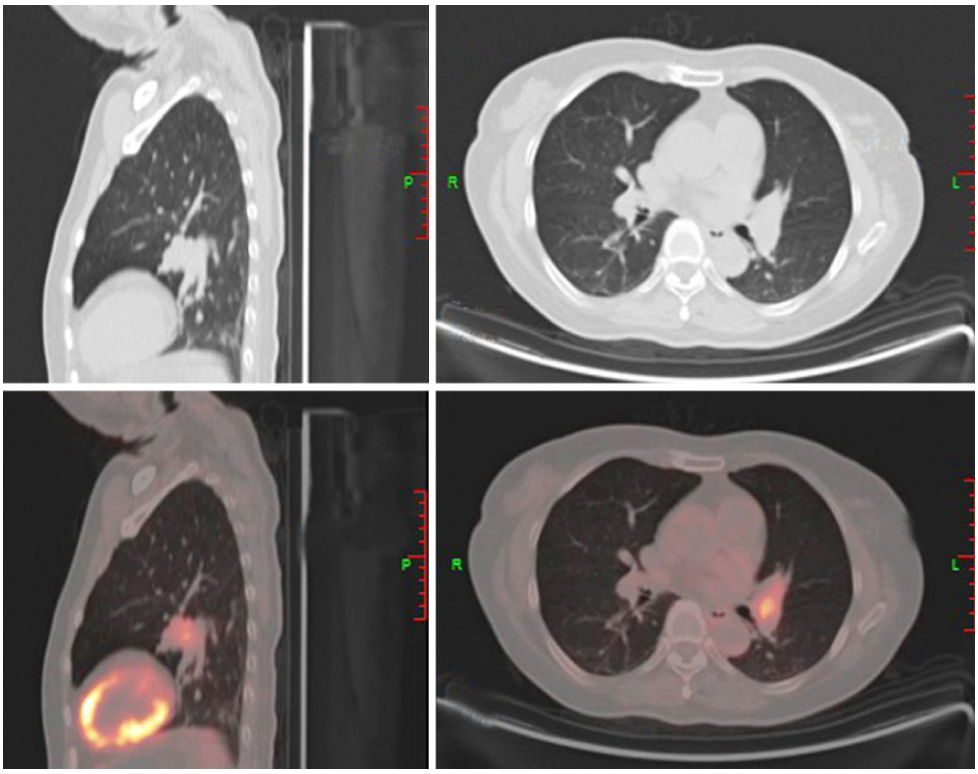

Figure 2 Positron emission tomography-computed tomography of Case 2. A hypermetabolic nodule is visible in the left lingular lobe (central lung cancer).

REFERENCES

1 **Torre LA**, Bray F, Siegel RL, Ferlay J, Lortet-Tieulent J, Jemal A. Global cancer statistics, 2012. *CA Cancer J Clin* 2015; **65**: 87-108 [PMID: 25651787 DOI: 10.3322/caac.21262]

2 **Choi WI**, Choi J, Kim MA, Lee G, Jeong J, Lee CW. Higher Age Puts Lung-Cancer Patients at Risk for Not Receiving Anti-cancer Treatment. *Cancer Res Treat* 2018 [PMID: 30653747 DOI: 10.4143/crt.2018.513]

3 **Wang Y**, Zhou Y, Hu Z. The Functions of Circulating Tumor Cells in Early Diagnosis and Surveillance During Cancer Advancement. *J Transl Int Med* 2017; **5**: 135-138 [PMID: 29085785 DOI: 10.1515/jtim-2017-0029]

4 **Cheng LL**, Liu YY, Su ZQ, Liu J, Chen RC, Ran PX. Clinical characteristics of tobacco smoke-induced versus biomass fuel-induced chronic obstructive pulmonary disease. *J Transl Int Med* 2015; **3**: 126-129 [PMID: 27847900 DOI: 10.1515/jtim-2015-0012]

5 **Grigorescu AC**. Chemotherapy for elderly patients with advanced cancer: A pilot study in Institute of Oncology Bucharest. *J Transl Int Med* 2015; **3**: 24-28 [PMID: 27847881 DOI: 10.4103/2224-4018.154291]

6 **Govindan R**, Page N, Morgensztern D, Read W, Tierney R, Vlahiotis A, Spitznagel EL, Piccirillo J. Changing epidemiology of small-cell lung cancer in the United States over the last 30 years: analysis of the surveillance, epidemiologic, and end results database. *J Clin Oncol* 2006; **24**: 4539-4544 [PMID: 17008692 DOI: 10.1200/JCO.2005.04.4859]

7 **Jung KW**, Won YJ, Kong HJ, Lee ES; Community of Population-Based Regional Cancer Registries. Cancer Statistics in Korea: Incidence, Mortality, Survival, and Prevalence in 2015. *Cancer Res Treat* 2018; **50**: 303-316 [PMID: 29566481 DOI: 10.4143/crt.2018.143]

8 **Li X**, Li B, Zeng H, Wang S, Sun X, Yu Y, Wang L, Yu J. Prognostic value of dynamic albumin-to-alkaline phosphatase ratio in limited stage small-cell lung cancer. *Future Oncol* 2019 [PMID: 30644319 DOI: 10.2217/fon-2018-0818]

9 **Legius B**, Nackaerts K. Severe intestinal ischemia during chemotherapy for small cell lung cancer. *Lung Cancer Manag* 2017; **6**: 87-91 [PMID: 30643574 DOI: 10.2217/lmt-2017-0016]

10 **Üstün F**, Tokuc B, Tastekin E, Durmuş Altun G. Tumor characteristics of lung cancer in predicting axillary lymph node metastases. *Rev Esp Med Nucl Imagen Mol* 2019; **38**: 80-86 [PMID: 30638878 DOI: 10.1016/j.remn.2018.09.010]

11 **Aoki M**, Fujisaka Y, Tokioka S, Hirai A, Henmi Y, Inoue Y, Narabayashi K, Yamano T, Tamura Y, Egashira Y, Higuchi K. Small-cell Lung Cancer in a Young Adult Nonsmoking Patient with Ectopic Adrenocorticotropin (ACTH) Production. *Intern Med* 2016; **55**: 1337-1339 [PMID: 27181543 DOI: 10.2169/internalmedicine.55.6139]

12 **Lin CJ**, Perng WC, Chen CW, Lin CK, Su WL, Chian CF. Small cell lung cancer presenting as ectopic ACTH syndrome with hypothyroidism and hypogonadism. *Onkologie* 2009; **32**: 427-430 [PMID: 19556823 DOI: 10.1159/000219433]

13 **Delisle L**, Boyer MJ, Warr D, Killinger D, Payne D, Yeoh JL, Feld R. Ectopic corticotropin syndrome and small-cell carcinoma of the lung. Clinical features, outcome, and complications. *Arch Intern Med* 1993; **153**: 746-752 [PMID: 8383484 DOI: 10.1001/archinte.1993.00410060054009]

14 **Dehghan M**, Mente A, Zhang X, Swaminathan S, Li W, Mohan V, Iqbal R, Kumar R, Wentzel-Viljoen E,

Rosengren A, Amma LI, Avezum A, Chifamba J, Diaz R, Khatib R, Lear S, Lopez-Jaramillo P, Liu X, Gupta R, Mohammadifard N, Gao N, Oguz A, Ramli AS, Seron P, Sun Y, Szuba A, Tsolekile L, Wielgosz A, Yusuf R, Hussein Yusufali A, Teo KK, Rangarajan S, Dagenais G, Bangdiwala SI, Islam S, Anand SS, Yusuf S; Prospective Urban Rural Epidemiology (PURE) study investigators. Associations of fats and carbohydrate intake with cardiovascular disease and mortality in 18 countries from five continents (PURE): a prospective cohort study. *Lancet* 2017; **390**: 2050-2062 [PMID: 28864332 DOI: 10.1016/S0140-6736(17)32252-3]

15 **Zimmet P**, Alberti KG, Magliano DJ, Bennett PH. Diabetes mellitus statistics on prevalence and mortality: facts and fallacies. *Nat Rev Endocrinol* 2016; **12**: 616-622 [PMID: 27388988 DOI: 10.1038/nrendo.2016.105]

16 **Mazzoccoli G**, Pazienza V, Piepoli A, Muscarella LA, Giuliani F, Sothern RB. Alteration of hypothalamic-pituitary-thyroid axis function in non-small-cell lung cancer patients. *Integr Cancer Ther* 2012; **11**: 327-336 [PMID: 21862518 DOI: 10.1177/1534735411413269]

17 **Wajchenberg BL**, Mendonca BB, Liberman B, Pereira MA, Carneiro PC, Wakamatsu A, Kirschner MA. Ectopic adrenocorticotropic hormone syndrome. *Endocr Rev* 1994; **15**: 752-787 [PMID: 7705280 DOI: 10.1210/edrv-15-6-752]

18 **Aniszewski JP**, Young WF, Thompson GB, Grant CS, van Heerden JA. Cushing syndrome due to ectopic adrenocorticotropic hormone secretion. *World J Surg* 2001; **25**: 934-940 [PMID: 11572035 DOI: 10.1007/s00268-001-0032-5]

19 **Hayes AR**, Grossman AB. The Ectopic Adrenocorticotropic Hormone Syndrome: Rarely Easy, Always Challenging. *Endocrinol Metab Clin North Am* 2018; **47**: 409-425 [PMID: 29754641 DOI: 10.1016/j.ecl.2018.01.005]

20 **Howlett TA**, Drury PL, Perry L, Doniach I, Rees LH, Besser GM. Diagnosis and management of ACTH-dependent Cushing's syndrome: comparison of the features in ectopic and pituitary ACTH production. *Clin Endocrinol (Oxf)* 1986; **24**: 699-713 [PMID: 3024870 DOI: 10.1111/j.1365-2265.1986.tb01667.x]

21 **Santhanam P**, Taieb D, Giovanella L, Treglia G. PET imaging in ectopic Cushing syndrome: a systematic review. *Endocrine* 2015; **50**: 297-305 [PMID: 26206753 DOI: 10.1007/s12020-015-0689-4]

22 **Kim EY**, Kim N, Kim YS, Seo JY, Park I, Ahn HK, Jeong YM, Kim JH. Prognostic Significance of Modified Advanced Lung Cancer Inflammation Index (ALI) in Patients with Small Cell Lung Cancer_ Comparison with Original ALI. *PLoS One* 2016; **11**: e0164056 [PMID: 27706243 DOI: 10.1371/journal.pone.0164056]

23 **Paduraru DN**, Nica A, Carsote M, Valea A. Adrenalectomy for Cushing's syndrome: do's and don'ts. *J Med Life* 2016; **9**: 334-341 [PMID: 27928434]

24 **Ma L**, Yin L, Hu Q. Therapeutic compounds for Cushing's syndrome: a patent review (2012-2016). *Expert Opin Ther Pat* 2016; **26**: 1307-1323 [PMID: 27454103 DOI: 10.1080/13543776.2016.1217331]

25 **Clark AJ**, Forfar R, Hussain M, Jerman J, McIver E, Taylor D, Chan L. ACTH Antagonists. *Front Endocrinol (Lausanne)* 2016; **7**: 101 [PMID: 27547198 DOI: 10.3389/fendo.2016.00101]

26 **Alexandraki KI**, Grossman AB. Therapeutic Strategies for the Treatment of Severe Cushing's Syndrome. *Drugs* 2016; **76**: 447-458 [PMID: 26833215 DOI: 10.1007/s40265-016-0539-6]

27 **Richardson LC**, Pollack LA. Therapy insight: Influence of type 2 diabetes on the development, treatment and outcomes of cancer. *Nat Clin Pract Oncol* 2005; **2**: 48-53 [PMID: 16264856 DOI: 10.1038/ncponc0062]

28 **Wu L**, Rabe KG, Petersen GM. Do variants associated with susceptibility to pancreatic cancer and type 2 diabetes reciprocally affect risk? *PLoS One* 2015; **10**: e0117230 [PMID: 25658847 DOI: 10.1371/journal.pone.0117230]

29 **Gong Y**, Wei B, Yu L, Pan W. Type 2 diabetes mellitus and risk of oral cancer and precancerous lesions: a meta-analysis of observational studies. *Oral Oncol* 2015; **51**: 332-340 [PMID: 25650271 DOI: 10.1016/j.oraloncology.2015.01.003]

30 **Yeo Y**, Ma SH, Hwang Y, Horn-Ross PL, Hsing A, Lee KE, Park YJ, Park DJ, Yoo KY, Park SK. Diabetes mellitus and risk of thyroid cancer: a meta-analysis. *PLoS One* 2014; **9**: e98135 [PMID: 24927125 DOI: 10.1371/journal.pone.0098135]

31 **Sehgal V**, Childress R. Urgent Need to Define Pretreatment Predictors of Immune Check Point Inhibitors Related Endocrinopathies: A Case Report and Review of Literature. *J Transl Int Med* 2017; **5**: 235-239 [PMID: 29340281 DOI: 10.1515/jtim-2017-0039]

32 **St Onge E**, Miller S, Clements E, Celauro L, Barnes K. The Role of Glucagon-like Peptide-1 Receptor Agonists in the Treatment of Type 2 Diabetes. *J Transl Int Med* 2017; **5**: 79-89 [PMID: 28721339 DOI: 10.1515/jtim-2017-0015]

33 **Xu T**, Liang G, Yang L, Zhang F. Prognosis of small cell lung cancer patients with diabetes treated with metformin. *Clin Transl Oncol* 2015; **17**: 819-824 [PMID: 26063645 DOI: 10.1007/s12094-015-1311-1]

34 **Hjartåker A**, Langseth H, Weiderpass E. Obesity and diabetes epidemics: cancer repercussions. *Adv Exp Med Biol* 2008; **630**: 72-93 [PMID: 18637486 DOI: 10.1007/978-0-387-78818-0_6]

35 **Luo J**, Hendryx M, Qi L, Ho GY, Margolis KL. Pre-existing diabetes and lung cancer prognosis. *Br J Cancer* 2016; **115**: 76-79 [PMID: 27195423 DOI: 10.1038/bjc.2016.141]

World Journal of Clinical Cases

Submit a Manuscript: https://www.f6publishing.com

World J Clin Cases 2019 May 26; 7(10): 1221-1229

DOI: 10.12998/wjcc.v7.i10.1221

ISSN 2307-8960 (online)

CASE REPORT

Significant benefits of osimertinib in treating acquired resistance to first-generation EGFR-TKIs in lung squamous cell cancer: A case report

Yan Zhang, Hui-Min Chen, Yong-Mei Liu, Feng Peng, Min Yu, Wei-Ya Wang, Heng Xu, Yong-Sheng Wang, You Lu

ORCID number: Yan Zhang (0000-0003-0148-7773); Hui-Min Chen (0000-0003-0657-7196); Yong-Mei Liu (0000-0002-0346-1158); Feng Peng (0000-0003-4272-5408); Min Yu (0000-0001-8978-892X); Wei-Ya Wang (0000-0003-0719-6387); Heng Xu (0000-0002-9549-0780); Yong-Sheng Wang (0000-0002-9725-4802); You Lu (0000-0003-2133-6833).

Author contributions: Zhang Y and Chen HM contributed equally to this work; all authors contributed to the acquisition of data and writing and revision of this manuscript.

Supported by the National Natural Science Foundation of China, No. 81402561.

Informed consent statement: Informed written consent was obtained from the patient for publication of this report and any accompanying images.

Conflict-of-interest statement: The authors declare that they have no conflicts of interest.

CARE Checklist (2016) statement: The authors have read the CARE Checklist (2013), and the manuscript was prepared and revised according to the CARE Checklist (2016).

Yan Zhang, Hui-Min Chen, Yong-Mei Liu, Feng Peng, Min Yu, Yong-Sheng Wang, You Lu, Department of Thoracic Oncology, Cancer Center, West China Hospital, Sichuan University, Chengdu 610041, Sichuan Province, China

Wei-Ya Wang, Department of Pathology, West China Hospital, Sichuan University, Chengdu 610041, Sichuan Province, China

Heng Xu, Precision Medicine Center, State Key Laboratory of Biotherapy, Precision Medicine Key Laboratory of Sichuan Province, West China Hospital, Sichuan University, Chengdu 610041, Sichuan Province, China

Corresponding author: Yan Zhang, PhD, Doctor, Professor, Department of Thoracic Oncology, Cancer Center, West China Hospital, Sichuan University, 37 Guoxue Lane, Chengdu 610041, Sichuan Province, China. zhang.yan@gmx.com
Telephone: +86-28-85422571
Fax: +86-28-85422571

Abstract

BACKGROUND

Lung squamous cell cancer (LSCC) rarely harbors epidermal growth factor receptor (*EGFR*) mutations, even much rarer for acquired T790M mutation. Although clinical trials of AURA series illustrated that non-small cell lung cancer (NSCLC) with *EGFR* T790M mutation can benefit from osimertinib, only five LSCC patients were enrolled in total; moreover, the efficacy for LSCC was not shown in the results. Therefore, the response of LSCC to osimertinib is still unclear to date.

CASE SUMMARY

We report an LSCC case with T790M-related acquired resistance after treatments with first-generation EGFR-tyrosine kinase inhibitors (EGFR-TKIs) and benefited from osimertinib significantly. A 63-year-old Chinese man was diagnosed with stage IV (cT2N2M1b) LSCC harboring an *EGFR* exon 19-deletion mutation. Following disease progression after gefitinib and multi-line chemotherapy, re-biopsy was conducted. Molecular testing of *EGFR* by amplification refractory mutation system-polymerase chain reaction detected the exon 19-deletion without T790M mutation. Therefore, the patient was given erlotinib, but progression developed only 3 mo later. Then the frozen re-biopsy tissue was

Manuscript source: Unsolicited manuscript

Received: January 2, 2019
Peer-review started: January 4, 2019
First decision: January 27, 2019
Revised: February 19, 2019
Accepted: March 16, 2019
Article in press: March 16, 2019
Published online: May 26, 2019

P-Reviewer: Tsuji T
S-Editor: Gong ZM
L-Editor: Wang TQ
E-Editor: Wu YXJ

tested by next-generation sequencing (NGS), which detected an *EGFR* T790M mutation. However, he was very weak with symptoms of dysphagia and cachexia. Fortunately, osimertinib was started, leading to alleviation from the symptoms. Four months later, normal deglutition was restored and partial response was achieved. Finally, the patient achieved an overall survival time period of 29 mo.

CONCLUSION
Our findings highlight that *EGFR* T790M mutation may also be an important acquired drug resistance mechanism for LSCC and offer direct evidence of the efficacy of osimertinib in LSCC with T790M mutation. NGS and better preservation conditions may contribute to higher sensitivity of *EGFR* T790M detection.

Key words: Lung squamous cell cancer; Lung cancer; Epidermal growth factor receptor mutation; T790M; Osimertinib; Tyrosine kinase inhibitor; Targeted therapy; Case report

Core tip: This is a case report of T790M-related acquired drug resistant lung squamous cell cancer (LSCC) patient with good response to osimertinib, which indicated that T790M is also an important mechanism for acquired resistance in LSCC. In this case, the secondary T790M mutation of epidermal growth factor receptor (*EGFR*) was detected by next-generation sequencing (NGS) for frozen tissue but not detected by amplification refractory mutation system-polymerase chain reaction for formalin-fixed and paraffin-embedded sample, which suggests that NGS and better preservation conditions may contribute to higher sensitivity of *EGFR* T790M detection.

Citation: Zhang Y, Chen HM, Liu YM, Peng F, Yu M, Wang WY, Xu H, Wang YS, Lu Y. Significant benefits of osimertinib in treating acquired resistance to first-generation EGFR-TKIs in lung squamous cell cancer: A case report. *World J Clin Cases* 2019; 7(10): 1221-1229
URL: https://www.wjgnet.com/2307-8960/full/v7/i10/1221.htm
DOI: https://dx.doi.org/10.12998/wjcc.v7.i10.1221

INTRODUCTION

The oncogenic driver profile of lung squamous cell lung cancer (LSCC) is significantly different from that of lung adenocarcinoma[1]. Epidermal growth factor receptor (EGFR) is the most important driver gene in lung adenocarcinoma; therefore, LSCC rarely harbours *EGFR* mutations[2,3].

Although lung adenocarcinoma can benefit from EGFR-tyrosine kinase inhibitors (TKIs) and the acquired resistance mechanism has been widely researched[4], the data for LSCC are very limited due to the rare incidence of *EGFR*-positive LSCC. We previously performed a multicentre retrospective study of *EGFR*-positive LSCC patients treated with EGFR-TKI[5], which showed that the progression-free survival (PFS) for LSCC is only 5.1 mo[6], significantly inferior to lung adenocarcinoma, which is about 9.7 to 13.1 mo[7-9]. This indicates that the *EGFR* signalling pathway in LSCC may not be identical to that in adenocarcinoma.

Osimertinib, an oral, potent, irreversible EGFR-TKI, has been reported to be highly effective in patients with *EGFR* T790M mutation-positive non-small-cell lung cancer (NSCLC) in previous three clinical trials of the AURA series. Although 882 NSCLC patients were enrolled in the three clinical trials, only five LSCC patients were included (3 from AURA, 2 from AURA2, and 0 from AURA3); moreover, the efficacy of osimertinib for LSCC was not shown in the results[10-12]. T790M-positive LSCC is rarely reported. Only 14 additional cases were reported previously in addition to the cases in the AURA series clinical trials; however, none of these patients were treated with osimertinib[13-20]. Although one patient with a T790M mutation was administered with another third-generation EGFR-TKI, rociletinib, this was an LSCC transformation from adenocarcinoma, rather than acquired resistance to first-generation TKIs[20]. The response of LSCC to osimertinib is still unclear to date. More

clinical evidence is needed for the management of LSCC with T790M after treatment with first-generation EGFR-TKIs.

Here, we report an LSCC patient with T790M-related acquired drug resistance after treatments with first-generation EGFR-TKIs who benefited from the third-generation EGFR-TKI osimertinib.

CASE PRESENTATION

Chief complaints

A 62-year-old male patient was initially admitted to our hospital due to cough and sputum for one month and hemoptysis for ten days.

History of present illness

One month ago, the patient developed symptoms of cough, expectorated white phlegm, but did not take any medicine. Then, he began suffering hemoptysis then days ago.

History of past illness

Unremarkable.

Personal and family history

The patient had a long-term history of smoking for about 40 years (10 cigarettes per day) without personal or family history of other diseases.

Physical examination upon admission

At admission, he was conscious with a regular heart rate of 75 bpm and a blood pressure of 128/75 mmHg. He had lost 4 kg weight in the past two months. Left lower lung breath sounds weakened. The other physical examinations were normal.

Laboratory examinations

Results of laboratory routine examinations including complete blood count, fecal occult blood, blood biochemistry, and urine were within normal limits. But his carcinoembryonic antigen was 6.93 ng/mL (reference, <3.4 ng/mL) and cytokeratin 19 fragment antigen 21-1 was 14.63 ng/mL (reference, <3.0 ng/mL).

Imaging examinations

Computed tomography of the chest revealed an occupying lesion in the inferior lobe of the left lung (Figure 1A) with hilar and mediastinal lymphadenectasis (Figure 1B). Magnetic resonance imaging showed abnormal long T1 and T2 signals at the right femoral neck and ischium and radionuclide bone imaging revealed increased bone uptake on TC-99m (Figure 1C-E).

FINAL DIAGNOSIS

Histological examination of a transbronchial lung biopsy and a cytological examination of the bronchus and sputum confirmed LSCC, without adenosquamous carcinoma or mixture of other components. The final diagnosis was stage IV (cT2N2M1b) LSCC. We also tested for EGFR mutations by amplification refractory mutation system-polymerase chain reaction (ARMS-PCR; AmoyDx, Xiamen, China) using a small biopsy specimen. We found that this patient had an *EGFR* exon 19 deletion mutation.

TREATMENT

Systemic treatments were subsequently administered (Figure 2). The patient began initial gefitinib 250 mg per day from November 2013 and had a partial response until June 2014, when CT scans showed disease progression in the left lung and new metastases in the rib and abdominal lymph nodes. He subsequently stopped gefitinib and started combination chemotherapy with gemcitabine and cisplatin for two cycles. Unfortunately, he again developed disease progression in the lung and T11 costotransverse joint. Then, second-line docetaxel and cisplatin were administered for two cycles. After treatment, he complained of headaches, and brain MRI showed disease progression with multiple new lesions in the left cerebellum. Subsequently, he was treated with whole brain radiotherapy (WBRT, 37.5 Gy/2.5 Gy/15 f) and

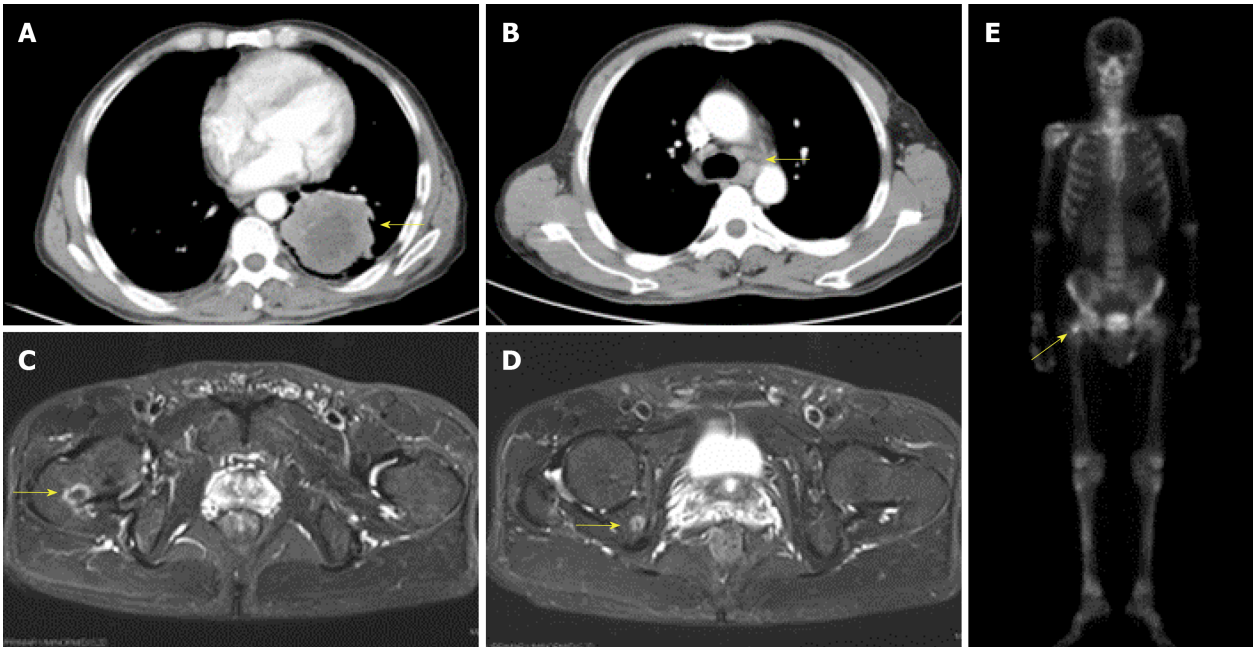

Figure 1 Baseline imaging examinations. Primary cancer in the inferior lobe of the left lung (A, arrow) with metastases to the hilar and mediastinal lymph nodes (B, arrow) and multiple bones (C-E, arrows).

chemotherapy with vinorelbine alone (20 mg/m^2 intravenously days 1, 8, 15, once every 4 wk). However, chemotherapy scheduled on day 15 was discontinued due to severe bone marrow suppression.

The patient underwent re-biopsy of the left lung mass through CT-guided percutaneous puncture, and two specimens were obtained. One specimen was formalin-fixed and paraffin-embedded for pathological and gene alteration tests, and the other was stored in liquid nitrogen. Pathological testing showed identical LSCC (Figure 3), and molecular testing of *EGFR* by ARMS-PCR quantified the exon 19 deletion without the T790M mutation, which remained unchanged from the baseline status (Figure 4A). Then, he began to receive treatment with erlotinib from December 2014. Unfortunately, after 3 mo, the disease progressed to the liver, and the patient developed dysphagia due to compression by enlarged mediastinal lymph nodes. He felt increasingly weak in the following days and developed cachexia.

Then, the frozen tissue was subjected to molecular testing by next-generation sequencing (NGS; NextSeq, Illumina), which confirmed the presence of an *EGFR* T790M mutation (allele frequency of 9.2%) in addition to the baseline exon 19 deletion mutation with an allele frequency of 70.2% (Figure 4B). From March 2015, the patient was administered with osimertinib at 80 mg PO QD. It is comforting that his dysphagia and Eastern Cooperative Oncology Group (ECOG) status gradually improved over the period of two weeks. Four months later, deglutition was restored to normal, and a partial response was achieved based on evaluation by chest computed tomography.

OUTCOME AND FOLLOW-UP

The patient's ECOG status significantly deteriorated from January 2016, and 1 mo later, the patient died from disease progression in February 2016. The PFS was no more than 10 mo and the overall survival time was 29 mo. The patient did not receive CT scan from August 2015 to February 2016.

DISCUSSION

LSCC harbouring activating *EGFR* mutations are rare and even rarer for the coexistence of T790M mutations. This is a rare case of LSCC with coexistence of the *EGFR* exon 19 deletion and T790M mutation. Moreover, the patient benefited from osimertinib with a partial response. The overall survival time was 29 months.

LSCC rarely harbours *EGFR* mutations, not to mention an acquired T790M

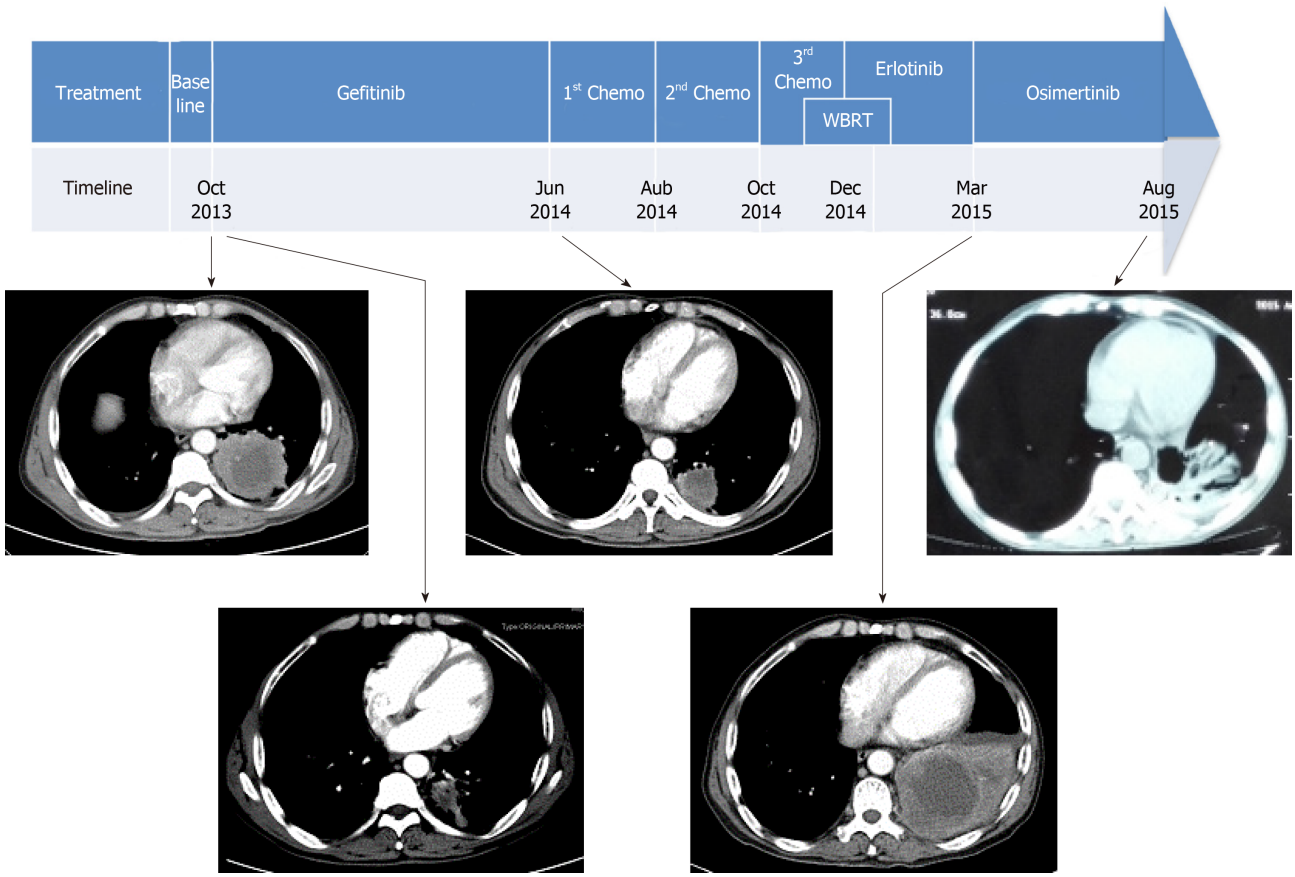

Figure 2 Sequence of anti-cancer treatments across the timeline and imaging evaluation of respective treatment. The primary tumor had a partial response to treatment with osimertinib. WBRT: Whole brain radiotherapy.

mutation. We review the previous literature that reports LSCC harbouring the T790M mutation (Table 1)[13-20]. To date, only 14 patients were reported in addition to the five LSCC patients enrolled in the clinical trials of the AURA series. Detailed TKI treatment information was available for only nine patients, of which five had LSCC transformation from adenocarcinoma[14,15,17,20]. The remaining three patients were acquired resistance cases after first-generation EGFR-TKI, but none were treated with third-generation EGFR-TKI[13,16]. It is worth noting that patient 5 received another third-generation EGFR-TKI, rociletinib[20]. However, this patient had an LSCC transformation derived from adenocarcinoma with *de novo* T790M detected at baseline. Furthermore, osimertinib has been proven by the FDA and is probably more potent than rociletinib[21]. As far as we are aware, this is the first reported T790M-related acquired resistant LSCC case with response to osimertinib, which serves as direct evidence of the effectiveness of osimertinib in LSCC.

In this case of LSCC, we observed a secondary T790M mutation of *EGFR*, contributing to the acquired resistance to first-generation EGFR inhibitors. This means that T790M is also an important mechanism for acquired resistance in LSCC. However, it is a key issue if this was a pure LSCC or not. Sometimes adenosquamous carcinoma or cancer with a mixture of other components may be mistakenly diagnosed as LSCC. It was reported that tests of multiple biopsies are helpful for accurate pathological and molecular diagnosis[22]. In this study, two biopsies of separate sites at different times and subsequent multiple serial sections were examined. Both of the results supported an identical diagnosis of LSCC with an *EGFR* exon 19 deletion mutation (Figure 3). Moreover, diagnosis by cytological examination of the bronchus and sputum also supported the LSCC diagnosis. In addition, imaging characteristics and long-term smoking history also supported this diagnosis. There was no evidence of coexistence with other components in multiple biopsies that were collected at multiple time points using multi-detection methods, so we consider this patient to have pure LSCC.

Previous research has suggested that the *EGFR* pathway in LSCC may be different from that in adenocarcinoma[5]. The PFS of patients receiving first-line gefitinib is about 8 mo. Although it is higher than the median PFS of our previous study, it is still obviously lower than that in adenocarcinoma[9]. Our case suggests that the EGFR

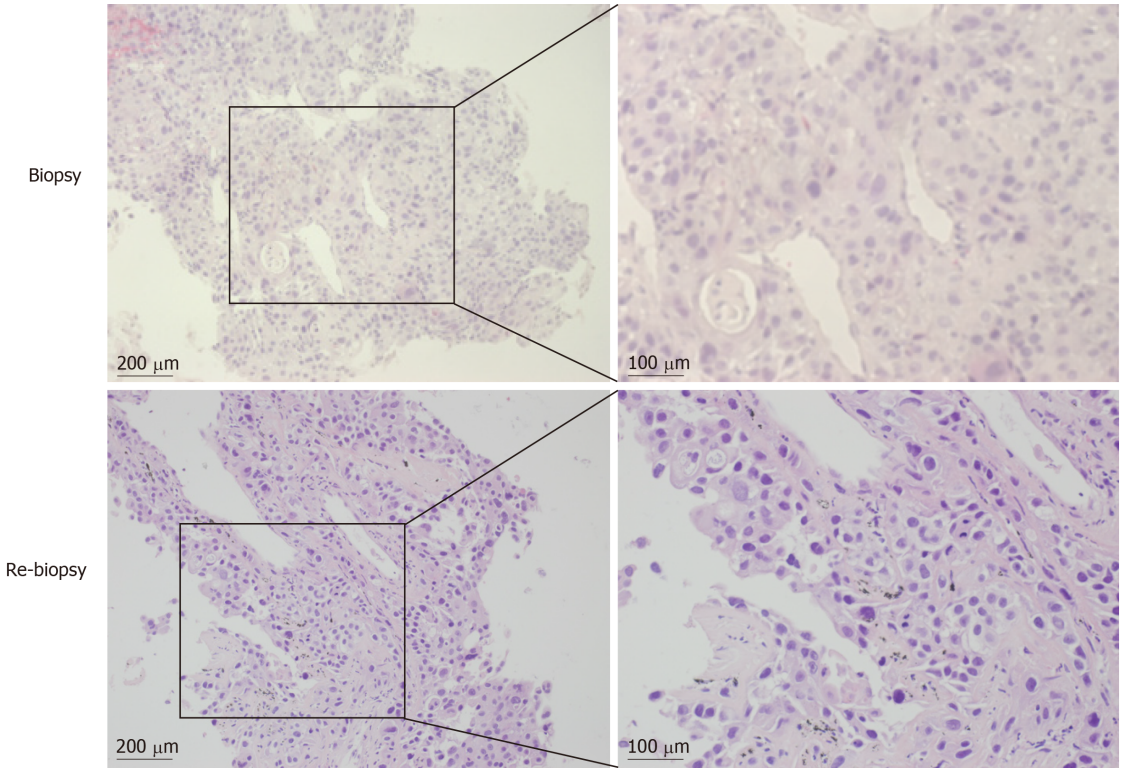

Figure 3 HE staining of specimens from two biopsies (baseline and re-biopsy before osimertinib). Squamous cell carcinoma was diagnosed by both pathological tests.

pathway may be different between lung adenocarcinoma and LSCC. But it still warrants investigation in large clinical trials.

Previous reports revealed that the threshold of ARMS-PCR was at least 1% for detecting a mutant allele fraction, whereas that for NGS was as low as 0.04%[23]. In this case, the second biopsy specimen was analysed for *EGFR* mutation by ARMS-PCR and NGS separately; however, the *EGFR* T790M mutation was only detected by NGS, which was attributed to the higher sensitivity of NGS[24] and lower degradation rate of DNA stored in liquid nitrogen. We foresee that NGS will play a more important role in *EGFR* T790M detection in the future.

CONCLUSION

In summary, our findings highlighted that *EGFR* T790M is also an important mechanism of acquired resistance for LSCC and offered direct evidence of the effectiveness of osimertinib in LSCC patients with the T790M mutation. Novel detection methods, such as NGS and better preservation conditions, hold promise for the more sensitive detection of the *EGFR* T790M mutation.

ACKNOWLEDGMENTS

The authors are very grateful to Dr. Yi-Xi Chen for helpful comments on language editing, and Jing Zhang from Burning Rock Medical Examination Institute Co., Ltd for her technical help with genomics.

Table 1 Summary of the main clinicopathologic and molecular characteristics of squamous cell carcinoma cases with T790M mutation reported in the literature to date[10-17]

Case ID	Baseline							Targeted therapy	Treatment response	Progression						Ref.
	Age / sex	Smoker	Stage	Morphology	Sampling method	Anatomic site	EGFR mutation			Progression time (mo)	Sampling method	Anatomic site	Morphology	EGFR mutation	3rd generation TKI	
1	63/F	Never	IV	ADC	PE	RUL	WT[1]	Erlotinib	PR	22	B	RUL	SCC	L858R + T790M	No	Bugano *et al*[11]
2	NA	NA	IV	SCC	B	NA	Exon 19 deletion	Erlotinib	NA	10	B	NA	SCC	Exon19 - deletion + T790M	NA	Masago *et al*[10]
3	48/F	Never	IV	SCC	B	RUL	p.L747_P753>S	Gefitinib	PD	2	B	RUL	SCC	Exon19 - deletion + T790M	No	Grazia no *et al*[13]
4	70/F	Never	IV	SCC	B	LUL	L858R	Gefitinib	SD / PR[2]	4	B	Liver	SCC	L858R + T790M	No	Grazia no *et al*[13]
5	64/F	Never	IV	ADC	B	RL	L858R+ T790M	Gefitinib	SD	10	B	RL	SCC	L858R + T790M	Rociletinib	Harata ni *et al*[17]
6	74/F	Former	IV	ADC	B	LL	L858R	Gefitinib	PR	10	B	LL	SCC	L858R + T790M	No	Jukna *et al*[14]
7	79/F	Never	IV	ADC	PE	RLL	p.E746_A750del	Gefitinib	PR	15	B	RL	SCC	p.E746_A750del + T790M	No	Jukna *et al*[14]
8	52/M	Former	IA	ADC	EB	LUL	L858R	Gefitinib	SD	12	B	Pleura	SCC	L858R + T790M	No	Ding *et al*[12]
9	53/M	Former	IIIA	SCC	B	NA	T790M	NA	NA	NA	NA	NA	NA	NA	NA	Lai *et al*[15]
10	65/M	Never	IB	SCC	B	NA	T790M	NA	NA	NA	NA	NA	NA	NA	NA	Lai *et al*[15]
11	50/F	Never	IIA	SCC	B	NA	T790M	NA	NA	NA	NA	NA	NA	NA	NA	Lai *et al*[15]
12	71/F	Current	NA	SCC	EB	NA	T790M	NA	NA	NA	NA	NA	NA	NA	NA	Ou *et al*[16]
13	60/F	Current	NA	SCC	EB	NA	T790M	NA	NA	NA	NA	NA	NA	NA	NA	Ou *et al*[16]
14	72/M	Current	NA	SCC	EB	NA	T790M	NA	NA	NA	NA	NA	NA	NA	NA	Ou *et al*[16]
15	63/M	Former	IV	SCC	B	RLL	Exon 19 deletion	Gefitinib /erlotinib	PR / SD[3]	8	B	RLL	SCC	p.E746_A750del + T790M	Osimertinib	Current article

[1]Low cellularity in cytological samples.
[2]SD In the lung and PR in liver metastases.
[3]PR to gefitinib and SD to erlotinib. ADC: Adenocarcinoma; B: Biopsy; EB: Excisional biopsy; LL: Left lobe; LUL: Left upper lobe; NA: Not available; PE: Pleural effusion; PD: Progression disease; PR: Partial response; RL: Right lobe; RLL: Right lower lobe; RUL: Right upper lobe; SD: Stable disease; SCC: Squamous cell carcinoma.

A

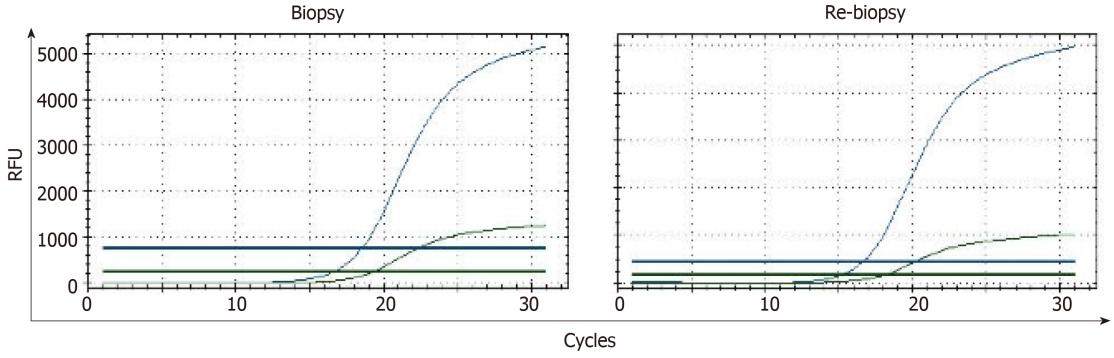

B

	Biopsy (2013 Nov)	Re-biopsy (2014 Nov)
Histology	Squamous cell carcinoma	Squamous cell carcinoma
ARMS-PCR	Exon 19 deletion	Exon 19 deletion
NGS	-	p.E746_A750del & T790M

Figure 4 Pathological and gene alteration analyses of the two biopsies. Amplification refractory mutation system-polymerase chain reaction test only detected exon 19 deletion in both samples (A), whereas next-generation sequencing detected the presence of an *EGFR* T790M mutation in addition to the exon 19-deletion mutation (p.E746_A750del) of the re-biopsy sample (B). NGS: Next-generation sequencing; ARMS-PCR: Amplification refractory mutation system-polymerase chain reaction.

REFERENCES

1 **Gandara DR**, Hammerman PS, Sos ML, Lara PN, Hirsch FR. Squamous cell lung cancer: from tumor genomics to cancer therapeutics. *Clin Cancer Res* 2015; **21**: 2236-2243 [PMID: 25979930 DOI: 10.1158/1078-0432.CCR-14-3039]

2 **Pao W**, Girard N. New driver mutations in non-small-cell lung cancer. *Lancet Oncol* 2011; **12**: 175-180 [PMID: 21277552 DOI: 10.1016/S1470-2045(10)70087-5]

3 **Tang Y**, Wang WY, Zheng K, Jiang L, Zou Y, Su XY, Chen J, Zhang WY, Liu WP. EGFR mutations in non-small cell lung cancer: an audit from West China Hospital. *Expert Rev Mol Diagn* 2016; **16**: 915-919 [PMID: 27348572 DOI: 10.1080/14737159.2016.1199961]

4 **Yu HA**, Arcila ME, Rekhtman N, Sima CS, Zakowski MF, Pao W, Kris MG, Miller VA, Ladanyi M, Riely GJ. Analysis of tumor specimens at the time of acquired resistance to EGFR-TKI therapy in 155 patients with EGFR-mutant lung cancers. *Clin Cancer Res* 2013; **19**: 2240-2247 [PMID: 23470965 DOI: 10.1158/1078-0432.CCR-12-2246]

5 **Liu Y**, Zhang Y, Zhang L, Liu B, Wang Y, Zhou X, Li Y, Zhao Q, Gong Y, Zhou L, Zhu J, Ding Z, Wang J, Peng F, Huang M, Li L, Ren L, Lu Y. Efficacy of epidermal growth factor receptor-tyrosine kinase inhibitors for lung squamous carcinomas harboring EGFR mutation: A multicenter study and pooled analysis of published reports. *Oncotarget* 2017; **8**: 49680-49688 [PMID: 28591695 DOI: 10.18632/oncotarget.17915]

6 **Cross DA**, Ashton SE, Ghiorghiu S, Eberlein C, Nebhan CA, Spitzler PJ, Orme JP, Finlay MR, Ward RA, Mellor MJ, Hughes G, Rahi A, Jacobs VN, Red Brewer M, Ichihara E, Sun J, Jin H, Ballard P, Al-Kadhimi K, Rowlinson R, Klinowska T, Richmond GH, Cantarini M, Kim DW, Ranson MR, Pao W. AZD9291, an irreversible EGFR TKI, overcomes T790M-mediated resistance to EGFR inhibitors in lung cancer. *Cancer Discov* 2014; **4**: 1046-1061 [PMID: 24893891 DOI: 10.1158/2159-8290.CD-14-0337]

7 **Rosell R**, Carcereny E, Gervais R, Vergnenegre A, Massuti B, Felip E, Palmero R, Garcia-Gomez R, Pallares C, Sanchez JM, Porta R, Cobo M, Garrido P, Longo F, Moran T, Insa A, De Marinis F, Corre R, Bover I, Illiano A, Dansin E, de Castro J, Milella M, Reguart N, Altavilla G, Jimenez U, Provencio M, Moreno MA, Terrasa J, Muñoz-Langa J, Valdivia J, Isla D, Domine M, Molinier O, Mazieres J, Baize N, Garcia-Campelo R, Robinet G, Rodriguez-Abreu D, Lopez-Vivanco G, Gebbia V, Ferrera-Delgado L, Bombaron P, Bernabe R, Bearz A, Artal A, Cortesi E, Rolfo C, Sanchez-Ronco M, Drozdowskyj A, Queralt C, de Aguirre I, Ramirez JL, Sanchez JJ, Molina MA, Taron M, Paz-Ares L; Spanish Lung Cancer Group in collaboration with Groupe Français de Pneumo-Cancérologie and Associazione Italiana Oncologia Toracica. Erlotinib versus standard chemotherapy as first-line treatment for European patients with advanced EGFR mutation-positive non-small-cell lung cancer (EURTAC): a multicentre, open-label, randomised phase 3 trial. *Lancet Oncol* 2012; **13**: 239-246 [PMID: 22285168 DOI: 10.1016/S1470-2045(11)70393-X]

8 **Mok TS**, Wu YL, Thongprasert S, Yang CH, Chu DT, Saijo N, Sunpaweravong P, Han B, Margono B, Ichinose Y, Nishiwaki Y, Ohe Y, Yang JJ, Chewaskulyong B, Jiang H, Duffield EL, Watkins CL, Armour AA, Fukuoka M. Gefitinib or carboplatin-paclitaxel in pulmonary adenocarcinoma. *N Engl J Med* 2009; **361**: 947-957 [PMID: 19692680 DOI: 10.1056/NEJMoa0810699]

9 **Zhou C**, Wu YL, Chen G, Feng J, Liu XQ, Wang C, Zhang S, Wang J, Zhou S, Ren S, Lu S, Zhang L, Hu C, Hu C, Luo Y, Chen L, Ye M, Huang J, Zhi X, Zhang Y, Xiu Q, Ma J, Zhang L, You C. Erlotinib versus chemotherapy as first-line treatment for patients with advanced EGFR mutation-positive non-small-cell lung cancer (OPTIMAL, CTONG-0802): a multicentre, open-label, randomised, phase 3 study. *Lancet Oncol* 2011; **12**: 735-742 [PMID: 21783417 DOI: 10.1016/S1470-2045(11)70184-X]

10 **Goss G**, Tsai CM, Shepherd FA, Bazhenova L, Lee JS, Chang GC, Crino L, Satouchi M, Chu Q, Hida T, Han JY, Juan O, Dunphy F, Nishio M, Kang JH, Majem M, Mann H, Cantarini M, Ghiorghiu S,

Mitsudomi T. Osimertinib for pretreated EGFR Thr790Met-positive advanced non-small-cell lung cancer (AURA2): a multicentre, open-label, single-arm, phase 2 study. *Lancet Oncol* 2016; **17**: 1643-1652 [PMID: 27751847 DOI: 10.1016/S1470-2045(16)30508-3]

11 **Jänne PA**, Yang JC, Kim DW, Planchard D, Ohe Y, Ramalingam SS, Ahn MJ, Kim SW, Su WC, Horn L, Haggstrom D, Felip E, Kim JH, Frewer P, Cantarini M, Brown KH, Dickinson PA, Ghiorghiu S, Ranson M. AZD9291 in EGFR inhibitor-resistant non-small-cell lung cancer. *N Engl J Med* 2015; **372**: 1689-1699 [PMID: 25923549 DOI: 10.1056/NEJMoa1411817]

12 **Mok TS**, Wu Y-L, Ahn M-J, Garassino MC, Kim HR, Ramalingam SS, Shepherd FA, He Y, Akamatsu H, Theelen WS, Lee CK, Sebastian M, Templeton A, Mann H, Marotti M, Ghiorghiu S, Papadimitrakopoulou VA; AURA3 Investigators. Osimertinib or Platinum-Pemetrexed in EGFR T790M-Positive Lung Cancer. *N Engl J Med* 2017; **376**: 629-640 [PMID: 27959700 DOI: 10.1056/NEJMoa1612674]

13 **Masago K**, Fujita S, Muraki M, Hata A, Okuda C, Otsuka K, Kaji R, Takeshita J, Kato R, Katakami N, Hirata Y. Next-generation sequencing of tyrosine kinase inhibitor-resistant non-small-cell lung cancers in patients harboring epidermal growth factor-activating mutations. *BMC Cancer* 2015; **15**: 908 [PMID: 26572169 DOI: 10.1186/s12885-015-1925-2]

14 **Bugano DDG**, Kalhor N, Zhang J, Neskey M, William WN. Squamous-cell transformation in a patient with lung adenocarcinoma receiving erlotinib: Co-occurrence with T790M mutation. *Cancer Treat Commun* 2015; **4**: 34-36 [DOI: 10.1016/j.ctrc.2015.03.007]

15 **Ding X**, Wang L, Liu X, Sun X, Yu J, Meng X. Genetic characterization drives personalized therapy for early-stage non-small-cell lung cancer (NSCLC) patients and survivors with metachronous second primary tumor (MST): A case report. *Medicine (Baltimore)* 2017; **96**: e6221 [PMID: 28272214 DOI: 10.1097/MD.0000000000006221]

16 **Graziano P**, de Marinis F, Gori B, Gasbarra R, Migliorino R, De Santis S, Pelosi G, Leone A. EGFR-Driven Behavior and Intrapatient T790M Mutation Heterogeneity of Non-Small-Cell Carcinoma With Squamous Histology. *J Clin Oncol* 2015; **33**: e115-e118 [PMID: 24752053 DOI: 10.1200/JCO.2013.49.5697]

17 **Jukna A**, Montanari G, Mengoli MC, Cavazza A, Covi M, Barbieri F, Bertolini F, Rossi G. Squamous Cell Carcinoma "Transformation" Concurrent with Secondary T790M Mutation in Resistant EGFR-Mutated Adenocarcinomas. *J Thorac Oncol* 2016; **11**: e49-e51 [PMID: 26746366 DOI: 10.1016/j.jtho.2015.12.096]

18 **Lai Y**, Zhang Z, Li J, Sun D, Zhou Y, Jiang T, Han Y, Huang L, Zhu Y, Li X, Yan X. EGFR mutations in surgically resected fresh specimens from 697 consecutive Chinese patients with non-small cell lung cancer and their relationships with clinical features. *Int J Mol Sci* 2013; **14**: 24549-24559 [PMID: 24351833 DOI: 10.3390/ijms141224549]

19 **Oh JE**, An CH, Yoo NJ, Lee SH. Detection of low-level EGFR T790M mutation in lung cancer tissues. *APMIS* 2011; **119**: 403-411 [PMID: 21635547 DOI: 10.1111/j.1600-0463.2011.02738.x]

20 **Haratani K**, Hayashi H, Watanabe S, Kaneda H, Yoshida T, Takeda M, Shimizu T, Nakagawa K. Two cases of EGFR mutation-positive lung adenocarcinoma that transformed into squamous cell carcinoma: successful treatment of one case with rociletinib. *Ann Oncol* 2016; **27**: 200-202 [PMID: 26483048 DOI: 10.1093/annonc/mdv495]

21 **Sequist LV**, Soria JC, Camidge DR. Update to Rociletinib Data with the RECIST Confirmed Response Rate. *N Engl J Med* 2016; **374**: 2296-2297 [PMID: 27195670 DOI: 10.1056/NEJMc1602688]

22 **Paik PK**, Varghese AM, Sima CS, Moreira AL, Ladanyi M, Kris MG, Rekhtman N. Response to erlotinib in patients with EGFR mutant advanced non-small cell lung cancers with a squamous or squamous-like component. *Mol Cancer Ther* 2012; **11**: 2535-2540 [PMID: 22896669 DOI: 10.1158/1535-7163.MCT-12-0163]

23 **Sorber L**, Zwaenepoel K, Deschoolmeester V, Van Schil PE, Van Meerbeeck J, Lardon F, Rolfo C, Pauwels P. Circulating cell-free nucleic acids and platelets as a liquid biopsy in the provision of personalized therapy for lung cancer patients. *Lung Cancer* 2017; **107**: 100-107 [PMID: 27180141 DOI: 10.1016/j.lungcan.2016.04.026]

24 **Tuononen K**, Mäki-Nevala S, Sarhadi VK, Wirtanen A, Rönty M, Salmenkivi K, Andrews JM, Telaranta-Keerie AI, Hannula S, Lagström S, Ellonen P, Knuuttila A, Knuutila S. Comparison of targeted next-generation sequencing (NGS) and real-time PCR in the detection of EGFR, KRAS, and BRAF mutations on formalin-fixed, paraffin-embedded tumor material of non-small cell lung carcinoma-superiority of NGS. *Genes Chromosomes Cancer* 2013; **52**: 503-511 [PMID: 23362162 DOI: 10.1002/gcc.22047]

World Journal of Clinical Cases

Submit a Manuscript: https://www.f6publishing.com

World J Clin Cases 2019 May 26; 7(10): 1230-1233

DOI: 10.12998/wjcc.v7.i10.1230

ISSN 2307-8960 (online)

CASE REPORT

Successful endoscopic extraction of a proximal esophageal foreign body following accurate localization using endoscopic ultrasound: A case report

Xiao-Ming Wang, Shan Yu, Xin Chen

ORCID number: Xiao-Ming Wang (0000-0003-1849-2069); Shan Yu (0000-0002-4528-7207); Xin Chen (0000-0001-7699-8848).

Author contributions: Wang XM designed the research; Wang XM, Yu S, and Chen X performed the research; Wang XM and Yu S wrote the paper.

Informed consent statement: All study participants, or their legal guardian, provided informed written consent prior to study enrollment.

Conflict-of-interest statement: None.

CARE Checklist (2016) statement: The authors have read the CARE Checklist (2016), and the manuscript was prepared and revised according to the CARE Checklist (2016).

Manuscript source: Unsolicited

Xiao-Ming Wang, Shan Yu, Xin Chen, Department of Gastroenterology, Panzhihua Central Hospital, Panzhihua 617067, Sichuan Province, China

Corresponding author: Xiao-Ming Wang, Chief Doctor, Department of Gastroenterology, Panzhihua Central Hospital, No. 34, Yikang Street, Panzhihua 617067, Sichuan Province, China. 18096308792@163.com
Telephone: +86-812-2238131
Fax: +86-812-2222606

Abstract

BACKGROUND

It is rare to find fish bones completely embedded in the wall of the esophagus with endoscopic findings similar to those of submucosal tumors. Most of the patients had the foreign body removed by thoracotomy or thoracoscopy in the past, which resulted in great trauma.

CASE SUMMARY

We report a 58-year-old woman who experienced dysphagia for 6 d after eating fish. Cervical computed tomography (CT) and endoscopic ultrasonography (EUS) indicated a fish bone completely embedded in the wall of the esophagus with endoscopic findings similar to those of submucosal tumors. The results of CT reconstruction and EUS suggested that the fish bone was parallel to the longitudinal axis of the esophagus. We performed a longitudinal mucosal incision from the highest point of the uplift by using an Olympus dual knife to find the fish bone. Unfortunately, no fish bone was found, so we extended the incision and endoscopic submucosal dissection (ESD) technique was used to detect and remove the fish bone entirety.

CONCLUSION

The extraction of fish bone *via* ESD immediately after the injection of methylene blue into the submucous membrane under EUS guidance to obtain accurate localization of the foreign body may be the best treatment for such patients.

Key words: Fish bone; Endoscopic mucosal dissection; Upper esophageal wall; Case report

manuscript

Received: January 29, 2019
Peer-review started: January 29, 2019
First decision: February 21, 2019
Revised: March 14, 2019
Accepted: May 10, 2019
Article in press: May 11, 2019
Published online: May 26, 2019

P-Reviewer: Lazăr DC, Viswanath YKS
S-Editor: Ji FF
L-Editor: Wang TQ
E-Editor: Wu YXJ

Core tip: It is rare to find the fish bone completely embedded in the wall of the esophagus with endoscopic findings similar to those of submucosal tumors. We report a fish bone that is fully embedded and migrated through the esophageal wall. During the operation, it was found that the fish bone was not directly below the highest point of the mass protuberance. Therefore, it is suggested that submucous injection of methylene blue under endoscopic ultrasonographic guidance can be used to locate the foreign body accurately and reduce the injury of treatment.

Citation: Wang XM, Yu S, Chen X. Successful endoscopic extraction of a proximal esophageal foreign body following accurate localization using endoscopic ultrasound: A case report. *World J Clin Cases* 2019; 7(10): 1230-1233
URL: https://www.wjgnet.com/2307-8960/full/v7/i10/1230.htm
DOI: https://dx.doi.org/10.12998/wjcc.v7.i10.1230

INTRODUCTION

Fish bones are one of the most common foreign bodies found in the digestive tract. Esophageal foreign bodies are mostly embedded in the narrow part of the esophagus. If not treated in time, sharp foreign bodies may puncture the esophagus and cause serious complications. Patients may have symptoms of odynophagia, dysphagia, hemoptysis, fever, chest pain, and other discomfort. Gastroscopy, computed tomography (CT), X-ray, and other examinations can reveal esophageal foreign bodies. Foreign bodies can be moved by esophageal peristalsis, swallowing food, and normal pleural pressure. A fish bone completely embedded into the esophageal wall which results in a submucosal mass is rare. Therefore, for patients who feel uncomfortable after eating fish and endoscopic examination suggests a submucosal bulge, the possibility of a fish bone granuloma should be considered. It has been reported in the past that fish bones were often removed from the esophageal wall by thoracoscopy. In this case, we chose endoscopic submucosal dissection (ESD) to remove a fish bone, which was less invasive.

CASE PRESENTATION

Chief complaints

Dysphagia for 6 d.

History of present illness

A 58-year-old woman who experienced dysphagia for 6 d after eating fish was admitted to a local hospital. Endoscopic indication of mucosal damage at the entrance of the pharynx and esophagus was observed, but no fish bone was found in the stomach or esophagus. The patient received anti-inflammatory treatment, but the dysphagia continued without fever, vomiting, or hematemesis. Then the patient presented to our hospital.

History of past illness

The patient denied history of hypertension, diabetes mellitus, viral hepatitis, or tuberculosis. She had no known drug or food allergies. She also denied history of operation, trauma, or blood transfusion.

Personal and family history

The patient denied history of drinking and smoking or any family history.

Physical examination upon admission

Her temperature was 36.6 °C, heart rate was 61 beats/min with normal rhythm, respiratory rate was 20 breaths/min, and blood pressure was 120/70 mmHg. She had facies dolorosa, but the color of whole body skin and mucous membrane was normal. Rales were not heard in bilateral lungs. No extra or abnormal heart sound, murmurs, or pericardium friction sound was noted. The abdomen was flat and soft, and there was no marked pitting edema in lower extremities.

Laboratory examinations

Routine blood, urine, stool, coagulation, and blood biochemistry tests were all normal.

Imaging examinations

Gastroscopic examination suggested that the upper esophageal segment exhibited a strip-shaped submucous bulge of approximately 8 mm × 40 mm (Figure 1A). CT suggested that the upper esophageal segment contained a high-density band in the right wall, with a diameter of approximately 35 mm (Figure 1B). Endoscopic ultrasonography (EUS) revealed that the upper submucosa of the esophagus exhibited a striped hyperechoic mass, with a rear weak echo, and the muscularis propria was involved (Figure 1C).

FINAL DIAGNOSIS

A foreign body embed in the submucosa of the upper esophageal wall.

TREATMENT

The results of CT reconstruction and EUS suggested that the fish bone was parallel to the longitudinal axis of the esophagus. Considering the age of patient and surgical operation may make much injury, we chose minimally invasive surgery performed by endoscopy to remove the fish bone. We performed a longitudinal mucosal incision from the highest point of the uplift by using an Olympus dual knife to find the fish bone. We did not find the fish bone in a longitudinal incision longer than 50 mm, and we therefore used ESD to remove the entire lump in the mucous membrane. However, no fish bone was found despite the small amount of mucosal tissue that remained. We continued to extend the incision in the anal direction, and found a fish bone embedded in the submucous layer when the incision length reached 70 mm. This location suggested that the fish bone had migrated into the submucous layer of the esophageal wall. We used a snare to slowly extract the fish bone out of the patient's mouth (Figure 1D and E). The wound was sutured using a Nanjing minimally invasive soft tissue clamp.

OUTCOME AND FOLLOW-UP

The patient was treated with antibiotics for 3 d. She was discharged from the hospital without complaints of fever, chest pain, hematemesis, or melaena.

DISCUSSION

Fish bones are one of the most common foreign bodies found in the digestive tract, but it is rare to find fish bones completely embedded in the wall of the esophagus with endoscopic findings similar to those of submucosal tumors. Therefore, if the patient is uncomfortable after eating fish, and endoscopic examination suggests submucous bulging, a fish bone granuloma should be suspected. The fish bone was not located directly below the bulging mass in the present case but had migrated into the esophageal wall. It is very important to locate the fish bone position accurately to reduce the size of the incision and wound. Cao *et al*[1] reported that methylene blue injection into the submucous layer labeled the foreign body position under the guidance of an ultrasound endoscope, and a thoracoscope was used to remove the fish bone. Therefore, we suggest the extraction of fish bone *via* ESD immediately after the injection of methylene blue into the submucous membrane under ultrasonographic guidance to obtain accurate localization of the foreign body and thereby reduce the wound size, bleeding, and perforation in endoscopic surgery and avoid additional surgery. This approach may be a better method to treat this condition.

CONCLUSION

The extraction of fish bone *via* ESD immediately after the injection of methylene blue into the submucous membrane under ultrasonographic guidance to obtain accurate localization of the foreign body may be the best way for such patients. It can help us to reduce the wound size, bleeding, and perforation in endoscopic surgery and avoid

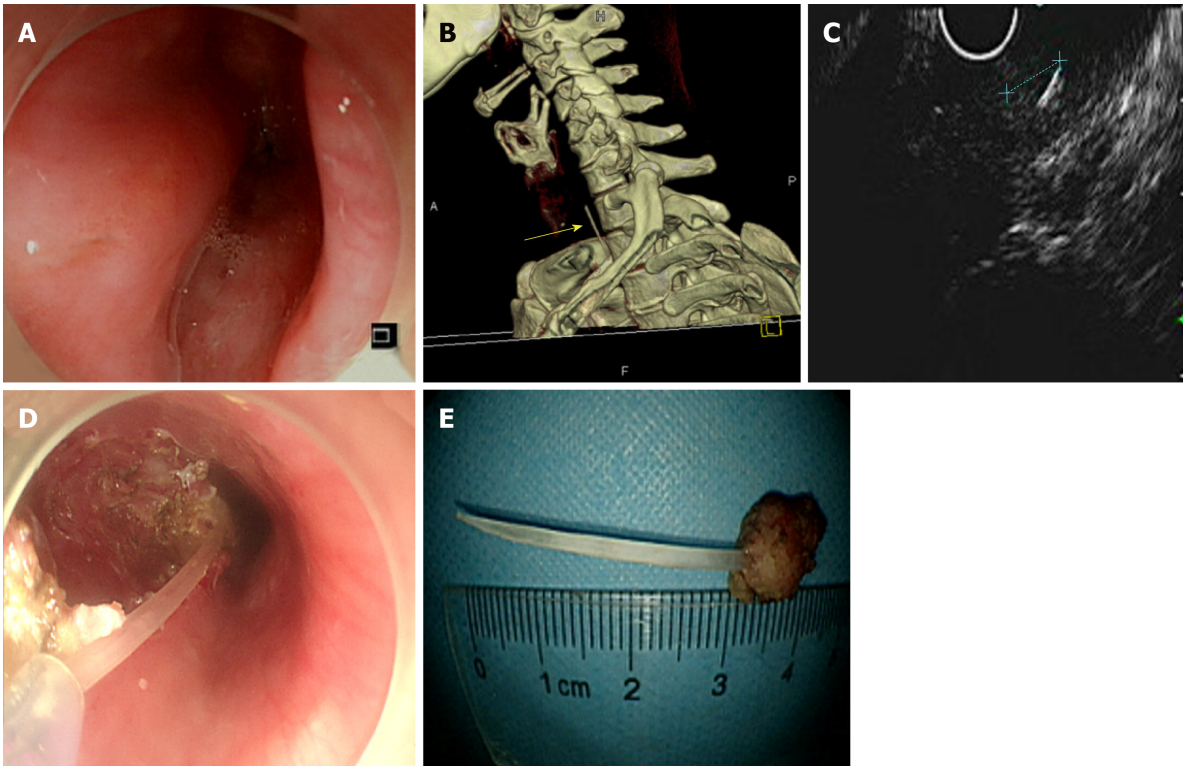

Figure 1 Fish bone removal by endoscopy. A: Gastroscopic examination suggested that the upper esophageal segment exhibited a strip-shaped submucous bulge; B: Computed tomography suggested that the upper esophageal segment contained a high-density band in the right wall; C: Endoscopic ultrasonography revealed that the upper submucosa of the esophagus exhibited a striped hyperechoic mass; D: Removal of the fish bone by endoscopic submucosal dissection (ESD); E: The fish bone removed by ESD.

additional surgery.

REFERENCES

1 **Cao L**, Chen N, Chen Y, Zhang M, Guo Q, Chen Q, Cheng B. Foreign body embedded in the lower esophageal wall located by endoscopic ultrasonography: A case report. *Medicine (Baltimore)* 2018; **97**: e11275 [PMID: 29953004 DOI: 10.1097/MD.0000000000011275]

World Journal of Clinical Cases

Submit a Manuscript: https://www.f6publishing.com

World J Clin Cases 2019 May 26; 7(10): 1234-1241

DOI: 10.12998/wjcc.v7.i10.1234

ISSN 2307-8960 (online)

CASE REPORT

Minimally invasive endoscopic maxillary sinus lifting and immediate implant placement: A case report

Mahmoud Mudalal, Xiao-Lin Sun, Xue Li, Jiao Fang, Man-Lin Qi, Jia Wang, Liu-Yi Du, Yan-Min Zhou

ORCID number: Mahmoud Mudalal (0000-0001-5551-6053); Xiao-Lin Sun (0000-0003-2659-2537); Xue Li (0000-0002-5389-2992); Jiao Fang (0000-0002-9884-5882); Man-Lin Qi (0000-0003-2453-7614); Jia Wang (0000-0002-9757-1437); Liu-Yi Du (0000-0002-7472-8649); Yan-Min Zhou (0000-0002-4173-6765).

Author contributions: Zhou YM and Mudalal M contributed to study conception and design, reviewed the article, and contributed to manuscript writing and drafting; Sun XL and Li X reviewed the literature and contributed to manuscript drafting; Fang J and Du LY analyzed and interpreted the imaging findings; Qi ML was responsible for the revision of the manuscript for important intellectual content; all authors issued final approval of the version to be submitted.

Supported by Jilin Provincial Science and Technological Projects-International Cooperation, No. 20180414030GH; Jilin Provincial Sanitation and Health-Technical Innovation Fund, No. 2018J074.

Informed consent statement: Informed written consent was obtained from the patient for publication of this report and any accompanying images.

Conflict-of-interest statement: The authors declare that they have no conflict of interest.

CARE Checklist (2016) statement: The authors have read the CARE Checklist (2016), and the manuscript was prepared and revised according to the CARE

Mahmoud Mudalal, Xiao-Lin Sun, Xue Li, Jiao Fang, Man-Lin Qi, Jia Wang, Liu-Yi Du, Yan-Min Zhou, Department of Dental Implantology, School and Hospital of Stomatology, Jilin University, Changchun 130021, Jilin Province, China

Corresponding author: Yan-Min Zhou, DDS, PhD, Chairman, Chief Doctor, Full Professor, Department of Dental Implantology, School and Hospital of Stomatology, Jilin University, 1500 Qinghua Rd, Chaoyang District, Changchun 130021, Jilin Province, China.
zhouym62@126.com
Telephone: +86-431-88958006

Abstract

BACKGROUND

This case report discusses a modified approach for maxillary sinus augmentation, in which platelet-rich fibrin, endoscope, simultaneous implant placement, and sinus floor elevation (PESS) were applied for a maxillary sinus floor lift in a 40-year-old patient.

CASE SUMMARY

A 40-year-old woman suffered missing upper right first molar. Implant stability quotient and cone-beam computed tomography (CBCT) were used to evaluate the diagnosis. CBCT showed insufficient posterior maxillary bone with a mean residual alveolar bone height of only 3.5 mm. The patient underwent a minimally invasive sinus floor elevation endoscopically. The sinus membrane was elevated in two stages, and a 12-mm implant was placed immediately. At 3 mo postoperatively, the final impressions were accomplished, and a full-ceramic crown was fit-placed. A 6-mo follow-up demonstrated satisfactory aesthetic and functional results.

CONCLUSION

This is the first report to use an endoscope for maxillary sinus floor lifting in cases with severe and insufficient bone height. This case report demonstrates the advantages of the PESS technique, which include minimal invasiveness with high precision, being applicable in cases with a residual alveolar bone height < 4 mm with a promising result, and a shortened treatment period from 12 to 3 mo.

Key words: Maxillary sinus augmentation; Platelet-rich fibrin; Endoscope; Internal sinus floor elevation; Case report

Checklist (2016).

Manuscript source: Unsolicited manuscript

Received: January 29, 2019
Peer-review started: January 29, 2019
First decision: March 9, 2019
Revised: March 20, 2019
Accepted: March 26, 2019
Article in press: March 26, 2019
Published online: May 26, 2019

P-Reviewer: Mattos B, Munhoz EA
S-Editor: Ji FF
L-Editor: Wang TQ
E-Editor: Wu YXJ

Core tip: The advantages of the modified approach for maxillary sinus augmentation, in which platelet-rich fibrin, endoscope, simultaneous implant placement, and sinus floor elevation (PESS) are combined, include: (1) Being applicable in cases with a residual alveolar bone height < 4 mm; (2) Shortened treatment period from 12 to 3 mo; and (3) Minimally invasive procedure with high precision.

Citation: Mudalal M, Sun XL, Li X, Fang J, Qi ML, Wang J, Du LY, Zhou YM. Minimally invasive endoscopic maxillary sinus lifting and immediate implant placement: A case report. *World J Clin Cases* 2019; 7(10): 1234-1241
URL: https://www.wjgnet.com/2307-8960/full/v7/i10/1234.htm
DOI: https://dx.doi.org/10.12998/wjcc.v7.i10.1234

INTRODUCTION

Sufficient bone is an essential requirement in the field of implantology. The maxillary posterior area is a difficult location for implant placement in comparison with the other areas of the mouth[1-3]. The process of maxillary sinus enlargement due to bone loss after maxillary posterior tooth extraction is known as pneumatization of the maxillary sinus. Moreover, this area of maxilla tuberosity has the lowest bone density. Maxillary sinus augmentation is a surgical procedure to increase the vertical height of the alveolar bone followed by immediate or second stage dental implant placement[4]. There are many approaches and bio-materials used for this procedure. Tatum first developed the procedure in 1977, and Boyne and James were the first to publish research regarding this technique in 1980[5].

Traditionally, a residual alveolar bone width of 5 mm would require maxillary sinus augmentation. This was conducted using the lateral window technique that involved a grafting material and simultaneous or delayed implant placement[6]. However, the invasion of microorganisms in the oral cavity often causes infections, leading to a high failure rate[7]. In the early 1990s, an endoscopic technique to lift the sinus membrane was introduced. However, studies on endoscope-controlled sinus elevation showed that lower complication rates were only observed when a residual alveolar bone height in the posterior area of the maxilla was > 4 mm and the mean elevated height was < 4 mm[8,9].

The use of bio-materials as grafts in sinus floor elevation surgeries is gradually gaining grounds with increasing evidence showing that grafted sinus floor elevation showed better Osseo integration than graft-free sinus floor elevation[10]. Commonly used bio-materials included platelet-rich concentrates with anabolic factors that are derived from platelets as well as catabolic factors produced by leukocytes that promote tissue healing. Studies investigating growth factor concentration and release kinetics reported platelet-rich fibrin (PRF) to be superior over other platelet concentrates. PRF contains fibrin, an important adjunct molecule that serves as an ideal delivery vehicle in tissue reengineering, thus giving it a therapeutic advantage over traditional platelet-rich plasma[11,12]. Platelet-rich fibrin + Endoscope + Simultaneous implant placement + Sinus floor elevation (PESS) technique is a promising solution in cases with a < 4 mm residual alveolar crest height[13]. By combining endoscopic-guided trans-crestal sinus floor elevation with PRF and simultaneous dental implant installation, final prosthesis can be fitted within 3 mo, a much shorter period than 12 mo if we followed the traditional treatment.

This aim of this report is to illustrate a modified approach for the enhancement of the atrophic posterior maxilla with dental implants. It also aims to present the minimally invasive option available for the increment of the vertical alveolar bone height for oral rehabilitation surgeries. Moreover, the PESS technique is a promising solution in cases which have a < 4 mm residual alveolar crest height.

CASE PRESENTATION

Chief complaint

A 40-year-old female non-smoker, who was medically fit and had no bruxism, consulted the Department of Oral Implantology with a complaint of a missing upper molar. The tooth was extracted several years ago due to a periodontal problem.

History of present illness

Missing upper molar with adequate dimensions and keratinized gingiva in #16 area were found for further prosthetic restoration.

History of past illness

She had no significant medical history.

Imaging examinations

Cone-beam computed tomography (CBCT) showed a severe vertical bone loss with a mean residual bone height (RBH) of 3.53 mm (Figure 1A and B).

FINAL DIAGNOSIS

The final diagnosis was severe vertical bone loss with an RBH less than 4 mm.

TREATMENT

Before the surgery, the patient signed an informed consent form in accordance with the bio-ethical guidelines of the hospital. The treatment plan developed based on the patient's condition was discussed with the patient and is shown in Figure 1C. The procedure began by patient rinsing her mouth with 0.12% chlorhexidine mouthwash 3 min per time, for 3 times. Articaine with adrenaline 1:100000 was used as local anesthesia. Instead of vertical release incision on the flap and mucoperiosteum, a punch incision was established to gain access to the bone crest using a motor-driven circular tissue bur (29630, Nobel Biocare, Sweden) with the same diameter of the selected implant (Figure 2A and B).

A precise preparation for an implant bed was established with various osteotomes. The pilot drill was used at a speed of 800 rpm in combination with the bur's width and depth, leaving approximately 1 mm gap from the maxillary sinus floor boundary. This step was done with special care in order not to perforate the Schneiderian membrane, a thin bilaminar mucoperiosteal membrane that lines the maxillary sinuses. After that, the cortical bone of the sinus floor was up-fractured carefully with a rounded and blunted 4.3 mm osteotome (KOHLER, Germany) to elevate the maxillary sinus membrane to a height of 7 mm (Figure 2C). During the elevation procedure, an endoscope (POLYDIAGNOST, Germany) was used to monitor the integrity of the sinus floor membrane (Figure 2D).

Using the standard protocol, a total of three PRF were established (three whole blood samples were taken in three glass-coated 10 mL plastic tubes without any anticoagulant and immediately centrifuged at 3000 rpm for 10 min). Following that, PRF clots were pressed into the membranes with a sterile dry gauze to fill up the elevated sinus (Figure 3A and B). The maxillary sinus membrane was elevated another time to obtain a total height of 12 mm (Figure 3C). Real-time observation was made endoscopically on the movements of PRF-filled membranes and the maxillary sinus floor membrane during the nasal inspiration and exhalation exercises. It revealed an intact maxillary sinus membrane, in which the entire maxillary sinus and PRF membranes moved together (Figure 3D). Implant installation was implemented properly (4.8 mm × 12 mm, Straumann, Switzerland) with a torque of 30 N/cm (Figure 3E), followed by healing cap placement (Figure 3F). All procedures were performed under an assessment with 0.9% saline irrigation and suctioning.

Postoperatively, the patient was prescribed with a 3-d course of antibiotics (oral metronidazole 300 mg TID and amoxicillin 500 mg TID) and 0.12% chlorhexidine mouthwash twice a day for 7 d.

OUTCOME AND FOLLOW-UP

After 2 and 3 mo of the implant placement, CBCT and implant stability quotient (ISQ) measurements were performed using the resonance frequency analysis. The ISQ values were obtained in five directions (mesial, distal, lingual, buccal, and occlusal) of the implant three times. CBCT at 2 mo post-surgery revealed a good level of healing. Results also demonstrated good bone-implant osseointegration during the first 8 wk (Figure 4).

At 3-mo follow-up, the mean ISQ value increased to 67.4 (Figure 5). An impression for the upper arch and a wax-bite registration were made according to standard procedures for implant-level impression techniques (Figure 6). The prosthetic

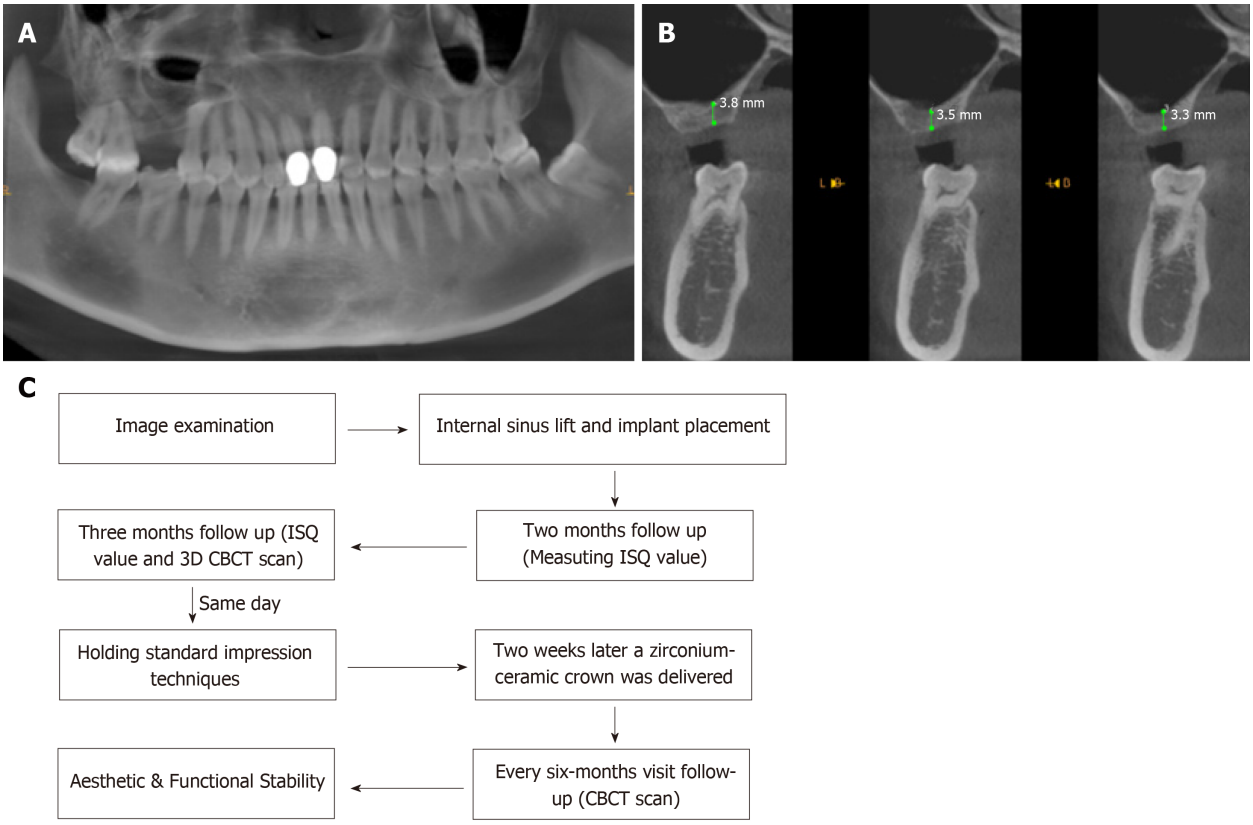

Figure 1 Preoperative cone-beam computed tomography. A: Sagittal cone-beam computed tomography (CBCT) image showing the mesio-distal dimensions; B: Coronal CBCT image showing a 3.5 mm height of #16; C: Flow chart timeline of the treatment plan. CBCT: Cone-beam computed tomography; ISQ: Implant stability quotient.

restoration was able to address the main concern of providing proper occlusion, margins, and embrasures during the fabrication process. Two weeks later, a zirconium-ceramic crown was applied, and fine tuning was conducted at the same visit (Figure 7). The final results were highly satisfactory. Six-month follow-up showed that the bone height remained stable. The mean ISQ value was 71.0 (Figure 8).

DISCUSSION

In patients with insufficient maxilla, it is important to innovate various methods for maxillary sinus floor elevations in order to achieve better clinical results. Moreover, it is vital to compensate any vertical alveolar bone loss to support proper implant placement and to ensure its viability[14,15]. Our case report illustrates a modified approach in a 40-year-old woman in need of a maxillary sinus augmentation.

In order to restore vertical alveolar bone loss, various surgical modalities have been proposed for the insertion of dental implants in the maxillary posterior part, showing a high implant survival rate with a low failure incidence. However, the indication for the any mentioned surgical techniques is not strictly equivalent and the treatment choice should be based on a careful evaluation of the individual case. The residual alveolar bone height and the ability to establish implant stability are fundamental in deciding which augmentation modality should be used to obtain a sufficient bone height for dental implant installation.

Traditionally, lateral window techniques were used to augment the maxillary sinus in cases with an alveolar height < 5 mm. However, this approach often results in postoperative complications such as discomfort, swelling, bleeding, infection, exposure of the covering membrane, and occasionally nasal bleeding[16,17]. As a result, minimally invasive surgical procedures were devised to shorten the treatment period and to optimize the maxillary posterior edentulous area for implantation. In this paper, a modified technique is reported for maxillary sinus floor elevation, achieving a maximum height of 12 mm. The use of endoscope provided a good visualization of the surgical site, thus improving the outcomes of the procedure.

The usage of PRF delivered multiple advantages at different phases. At the initial

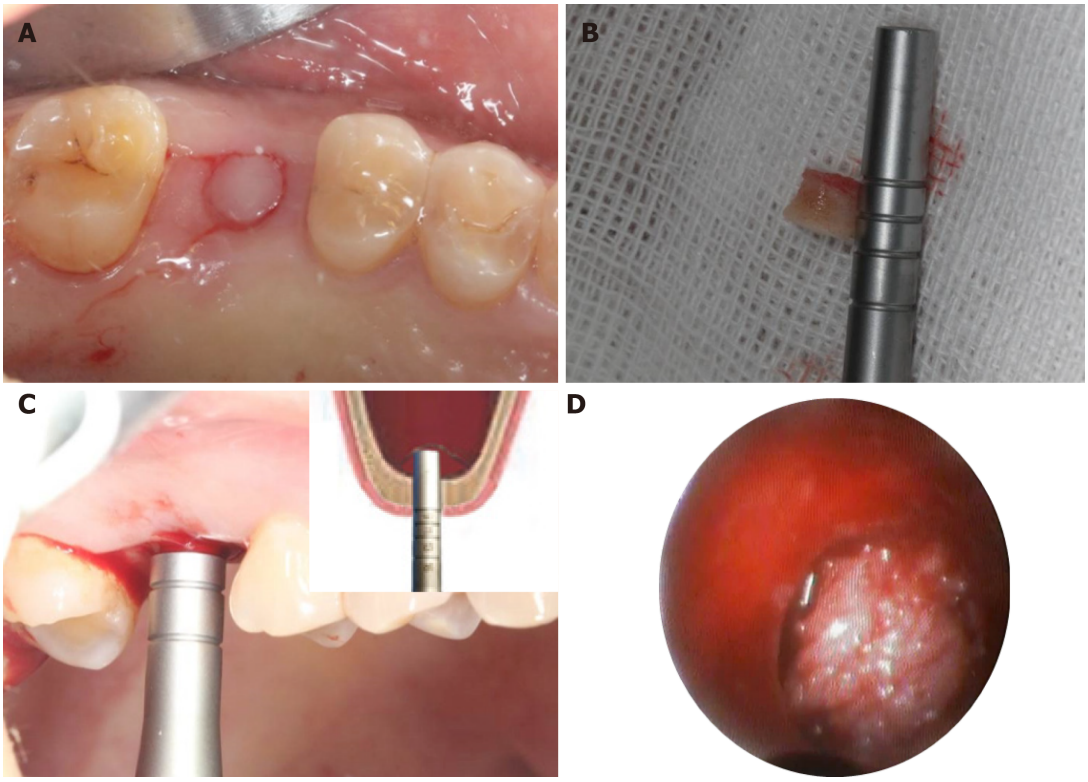

Figure 2 Intraoperative illustrations to explain each step of the surgery. A: Establishment of a punch incision; B: Full-thickness keratinized gingival punch removal; C: Gentle elevation of the Schneiderian membrane till approximately 7 mm; D: An endoscope was used to monitor the maxillary sinus membrane.

stage, it was a good cushioning material because of its flexibility. This could decrease the risk of perforation of the Schneider membrane. Due to the blind nature of this procedure, in the unfortunate event that membrane perforation was observed, PRF membrane would also act as an ideal sealant to patch the perforated membrane. In our case, no perforation was monitored during the procedure. Furthermore, PRF is a perfect biomedical additive and could reduce the healing period by half[18].

There were no postoperative complications. Minimally invasive endoscopic techniques are often associated with a high success rate, as shown in our case. CBCT indicated an increase in the bone formation around the implant. The calculated ISQ values represented a significant increase of implant-bone osseointegration. Clinically successful (aesthetically and functionally) crown delivery within 14 wk of surgery represented a great satisfactory result for both the patient and the clinician.

CONCLUSION

Our case report demonstrated that the PESS technique had promising short and long-term clinical results. It can be used in patients with a residual alveolar bone height < 4 mm. Furthermore, endoscopic-guided trans-crestal sinus floor elevation combined with PRF and simultaneous dental implant installation could be followed by final prosthesis within 3 mo. This represents a perfect solution for similar situations in which traditional treatment would require 12 mo of treatment. In conclusion, minimally invasive endoscopic maxillary sinus lift with immediate implant installation is a reliable approach in oral rehabilitation of atrophic posterior maxilla with an RBH < 4 mm. This case illustrates the advantages of minimally invasive surgical procedures in terms of reduced postoperative discomfort, swelling, and pain as compared to lateral approach techniques, and enhanced healing by adding PRF. This technique can be further expanded in view of the successful outcomes. To the end, endoscopic-guided trans-crestal sinus floor elevation combined with PRF and simultaneous dental implant installation, followed by final prosthesis within 3 mo, is a perfect solution for such a situation which needs 12 mo of treatment if we follow the traditional ways.

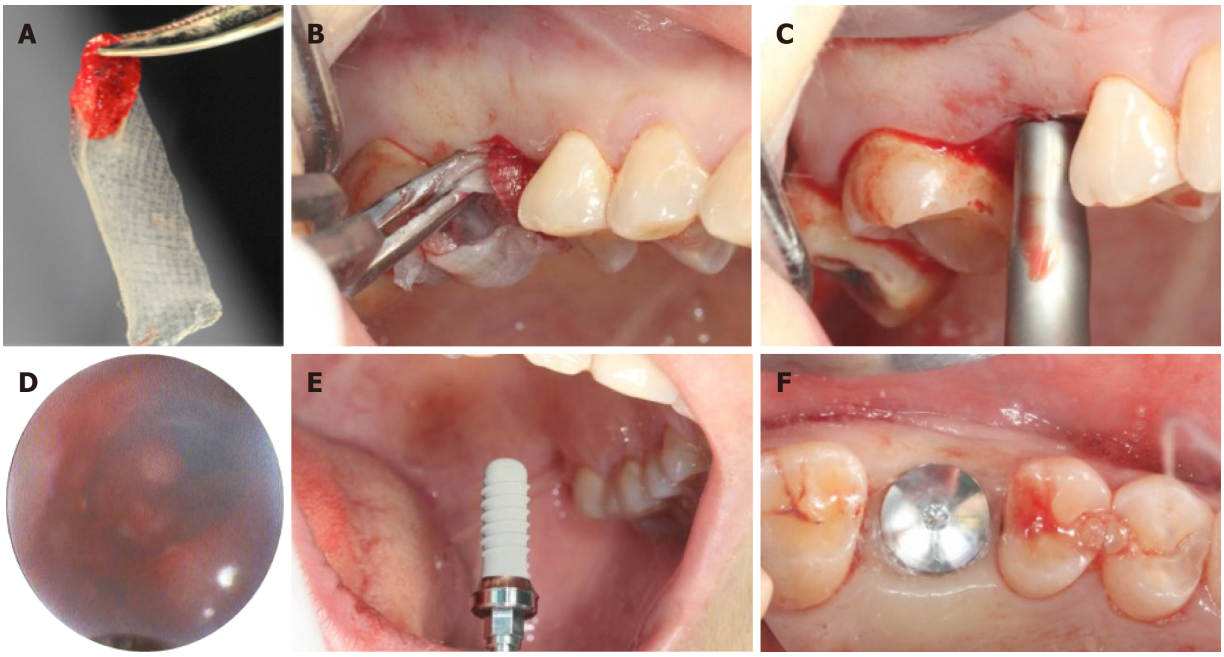

Figure 3 Methodological illustration of platelet-rich fibrin establishment. A: Three platelet-rich fibrin (PRF) clots were compressed between sterile dry gauze; B: Established PRF membranes were filled into the primary elevated sinus floor; C: The sinus membrane was secondary up-elevated to reach a 12 mm total height; D: Endoscopic evaluation on PRF and sinus floor membranes by nasal breathing exercises; E: Installation of an implant (4.8 mm × 12 mm, Straumann, Switzerland); F: Placement of a suitable healing cap.

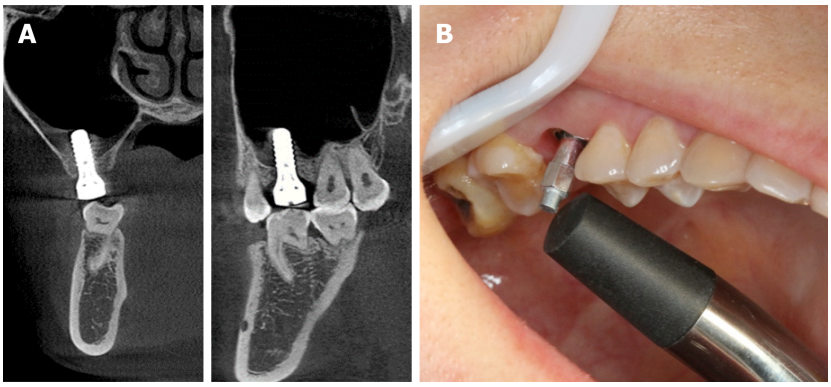

Figure 4 Assessments at 2 mo after surgery. A: Coronal and sagittal cone-beam computed tomography images showing the uneventful osseointegration around the implant; B: Mean implant stability quotient value was 57.8.

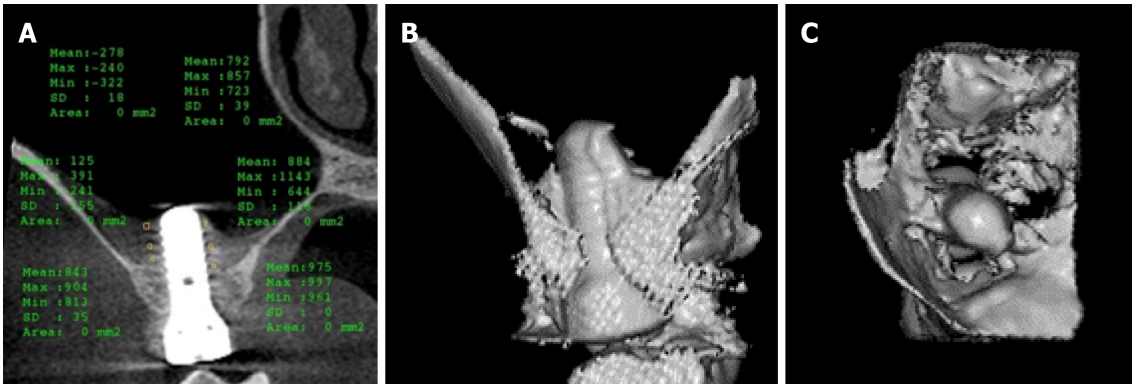

Figure 5 Cone-beam computed tomography images obtained at the 3-mo follow-up. A: Coronal cone-beam computed tomography (CBCT) image showing the gained bone height around the implant; B: 3D CBCT image showing the gained bone from the buccal side; C: Another intra-maxillary 3D CBCT image showing the bone formation level at the same time.

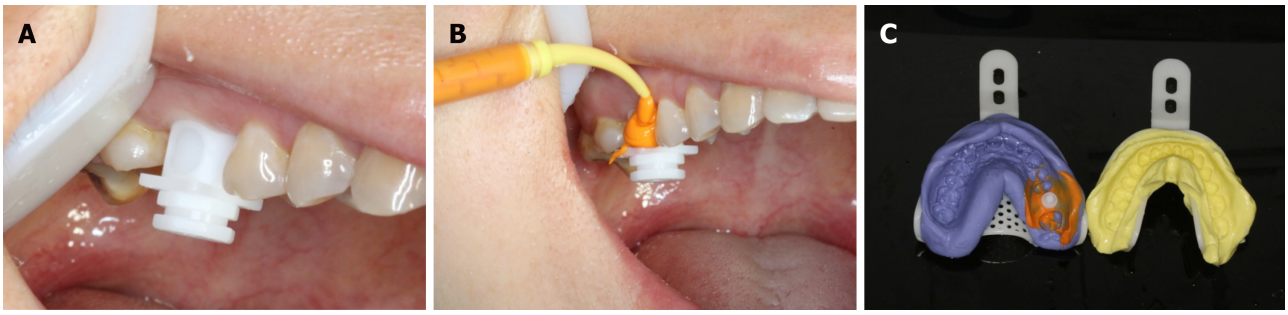

Figure 6 Intraoral photos to illustrate the standard impression techniques. A: Suitable abutment was fitted; B: Impression cap and liners were positioned for accurate impression results; C: Final impression with analog in place for the following cast procedures.

Figure 7 A zirconium-ceramic crown was delivered. Final result was satisfactory. A: A painless 35 N torque was added to put the abutment in place; B: Occlusal view of the final prosthesis in place; C: Buccal view of the final prosthesis in place.

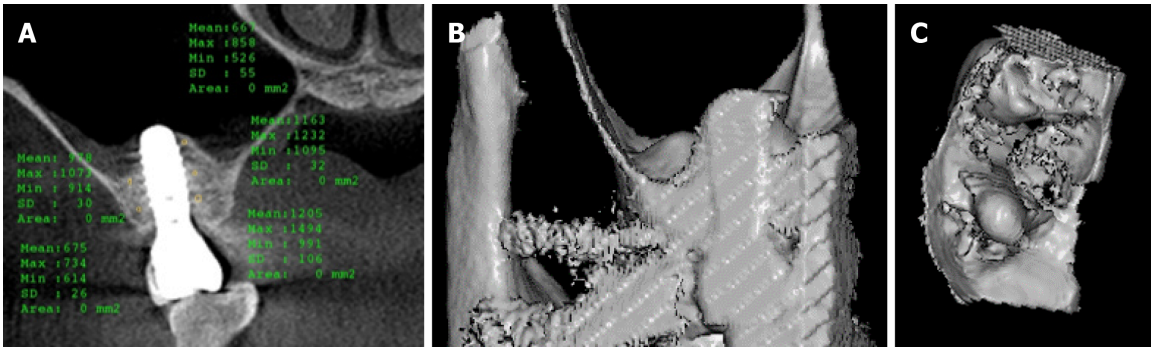

Figure 8 Cone-beam computed tomography images obtained at the 6-mo follow-up. A: Increased bone level and implant stability quotient values were gained around the implant; B: 3D cone-beam computed tomography image showing positive and successful results; C: Intra-maxillary bone formation showed stable and promising future results.

REFERENCES

1 **Agamy EM**, Niedermeier W. Indirect sinus floor elevation for osseointegrated prostheses. A 10-year prospective study. *J Oral Implantol* 2010; **36**: 113-121 [PMID: 20426588 DOI: 10.1563/AAID-JOI-D-09-00085]

2 **Esposito M**, Grusovin MG, Rees J, Karasoulos D, Felice P, Alissa R, Worthington H, Coulthard P. Effectiveness of sinus lift procedures for dental implant rehabilitation: a Cochrane systematic review. *Eur J Oral Implantol* 2010; **3**: 7-26 [PMID: 20467595 DOI: 10.1259/dmfr/23060413]

3 **Lundgren S**, Cricchio G, Hallman M, Jungner M, Rasmusson L, Sennerby L. Sinus floor elevation procedures to enable implant placement and integration: techniques, biological aspects and clinical outcomes. *Periodontol 2000* 2017; **73**: 103-120 [PMID: 28000271 DOI: 10.1111/prd.12165]

4 **Mohan N**, Wolf J, Dym H. Maxillary sinus augmentation. *Dent Clin North Am* 2015; **59**: 375-388 [PMID: 25835800 DOI: 10.1016/j.cden.2014.10.001]

5 **Boyne PJ**, James RA. Grafting of the maxillary sinus floor with autogenous marrow and bone. *J Oral Surg* 1980; **38**: 613-616 [PMID: 6993637 DOI: 10.1111/j.1365-2842.1980.tb00468.x]

6 **Fugazzotto PA**. Augmentation of the posterior maxilla: a proposed hierarchy of treatment selection. *J Periodontol* 2003; **74**: 1682-1691 [PMID: 14682667 DOI: 10.1902/jop.2003.74.11.1682]

7 **Petersen PE**, Bourgeois D, Bratthall D, Ogawa H. Oral health information systems--towards measuring

progress in oral health promotion and disease prevention. *Bull World Health Organ* 2005; **83**: 686-693 [PMID: 16211160]
8 **Wiltfang J**, Schultze-Mosgau S, Merten HA, Kessler P, Ludwig A, Engelke W. Endoscopic and ultrasonographic evaluation of the maxillary sinus after combined sinus floor augmentation and implant insertion. *Oral Surg Oral Med Oral Pathol Oral Radiol Endod* 2000; **89**: 288-291 [PMID: 10710451 DOI: 10.1016/S1079-2104(00)70090-4]
9 **Engelke W**, Deckwer I. Endoscopically controlled sinus floor augmentation. A preliminary report. *Clin Oral Implants Res* 1997; **8**: 527-531 [PMID: 9555210]
10 **Nedir R**, Nurdin N, Khoury P, Perneger T, Hage ME, Bernard JP, Bischof M. Osteotome sinus floor elevation with and without grafting material in the severely atrophic maxilla. A 1-year prospective randomized controlled study. *Clin Oral Implants Res* 2013; **24**: 1257-1264 [PMID: 22925088 DOI: 10.1111/j.1600-0501.2012.02569.x]
11 **Castillo TN**, Pouliot MA, Kim HJ, Dragoo JL. Comparison of growth factor and platelet concentration from commercial platelet-rich plasma separation systems. *Am J Sports Med* 2011; **39**: 266-271 [PMID: 21051428 DOI: 10.1177/0363546510387517]
12 **Mudalal M**, Zhou YM. Biological Additives and Platelet Concentrates for Tissue Engineering on Regenerative Dentistry Basic Science and Concise Review. *Asian J Pharm* 2017; **11**: 255-263
13 **Toscano NJ**, Holtzclaw D, Rosen PS. The effect of piezoelectric use on open sinus lift perforation: a retrospective evaluation of 56 consecutively treated cases from private practices. *J Periodontol* 2010; **81**: 167-171 [PMID: 20059429 DOI: 10.1902/jop.2009.090190]
14 **Starch-Jensen T**, Aludden H, Hallman M, Dahlin C, Christensen AE, Mordenfeld A. A systematic review and meta-analysis of long-term studies (five or more years) assessing maxillary sinus floor augmentation. *Int J Oral Maxillofac Surg* 2018; **47**: 103-116 [PMID: 28545806 DOI: 10.1016/j.ijom.2017.05.001]
15 **Ting M**, Rice JG, Braid SM, Lee CYS, Suzuki JB. Maxillary Sinus Augmentation for Dental Implant Rehabilitation of the Edentulous Ridge: A Comprehensive Overview of Systematic Reviews. *Implant Dent* 2017; **26**: 438-464 [PMID: 28520572 DOI: 10.1097/ID.0000000000000606]
16 **Duan DH**, Fu JH, Qi W, Du Y, Pan J, Wang HL. Graft-Free Maxillary Sinus Floor Elevation: A Systematic Review and Meta-Analysis. *J Periodontol* 2017; **88**: 550-564 [PMID: 28168901 DOI: 10.1902/jop.2017.160665]
17 **Silva LD**, de Lima VN, Faverani LP, de Mendonça MR, Okamoto R, Pellizzer EP. Maxillary sinus lift surgery-with or without graft material? A systematic review. *Int J Oral Maxillofac Surg* 2016; **45**: 1570-1576 [PMID: 27765427 DOI: 10.1016/j.ijom.2016.09.023]
18 **Choukroun J**, Diss A, Simonpieri A, Girard MO, Schoeffler C, Dohan SL, Dohan AJ, Mouhyi J, Dohan DM. Platelet-rich fibrin (PRF): a second-generation platelet concentrate. Part V: histologic evaluations of PRF effects on bone allograft maturation in sinus lift. *Oral Surg Oral Med Oral Pathol Oral Radiol Endod* 2006; **101**: 299-303 [PMID: 16504861 DOI: 10.1016/j.tripleo.2005.07.012]

Published By Baishideng Publishing Group Inc
7041 Koll Center Parkway, Suite 160, Pleasanton, CA 94566, USA
Telephone: +1-925-2238242
Fax: +1-925-2238243
E-mail: bpgoffice@wjgnet.com
Help Desk:https://www.f6publishing.com/helpdesk
https://www.wjgnet.com